A RISING STAR

A comprehensive approach to *Akkermansia muciniphila* ecosystems, interactions and applications

SHARON Y. GEERLINGS

Propositions

1. Exopolysaccharide production is a key function of *Akkermansia muciniphila*.
   (this thesis)

2. *A. muciniphila* is a prevalent resident in the gastrointestinal tract of humans and animals throughout the mammalian kingdom.
   (this thesis)

3. Scientists, who are also musicians, benefit from making music by conducting more creative research.

4. Better guidelines should be developed for the classification of novel bacterial species.

5. The practice of cooking translates into laboratory skills.

6. With the current level of human knowledge, collaboration is a must to remove boundaries.

7. Horror games are scarier than horror movies.

Propositions belonging to the thesis, entitled

A rising star: A comprehensive approach to *Akkermansia muciniphila* ecosystems, interactions and applications

Sharon Y. Geerlings,
Wageningen, 18 January 2023

A rising star: A comprehensive approach to *Akkermansia muciniphila* ecosystems, interactions and applications.

Sharon Y. Geerlings

Thesis committee

Promotors
Prof. Dr W.M. de Vos
Professor of Microbiology
Wageningen University & Research

Prof. Dr M.C.M. van Loosdrecht
Professor of Environmental Biotechnology
Delft University of Technology

Co-promotor
Dr C. Belzer
Associate professor at the Laboratory of Microbiology
Wageningen University & Research

Other members
Prof. Dr K. Schroen, Wageningen University & Research
Dr N. Ottman, Bacthera, Hørsholm, Denmark
Dr R. Kleerebezem, Delft University of Technology
Prof. Dr R. Kort, VU Amsterdam

This research was conducted under the auspices of the Graduate School VLAG (Advanced studies in Food Technology, Agrobiotechnology, Nutrition and Health Sciences)

A rising star: A comprehensive approach to *Akkermansia muciniphila* ecosystems, interactions and applications.

Sharon Y. Geerlings

Thesis

submitted in fulfilment of the requirements for the degree of doctor
at Wageningen University
by the authority of the Rector Magnificus,
Prof. Dr A.P.J. Mol,
in the presence of the
Thesis Committee appointed by the Academic Board
to be defended in public
on Wednesday 18 January 2023
at 4 p.m. in the Omnia Auditorium.

Sharon Y. Geerlings
A rising star: A comprehensive approach to *Akkermansia muciniphila* ecosystems, interactions and applications.
334 Pages
PhD thesis, Wageningen University, Wageningen, the Netherlands (2023)
With references, with summary in English
ISBN: 978-94-6447-507-4
DOI: 10.18174/581871

Table of contents

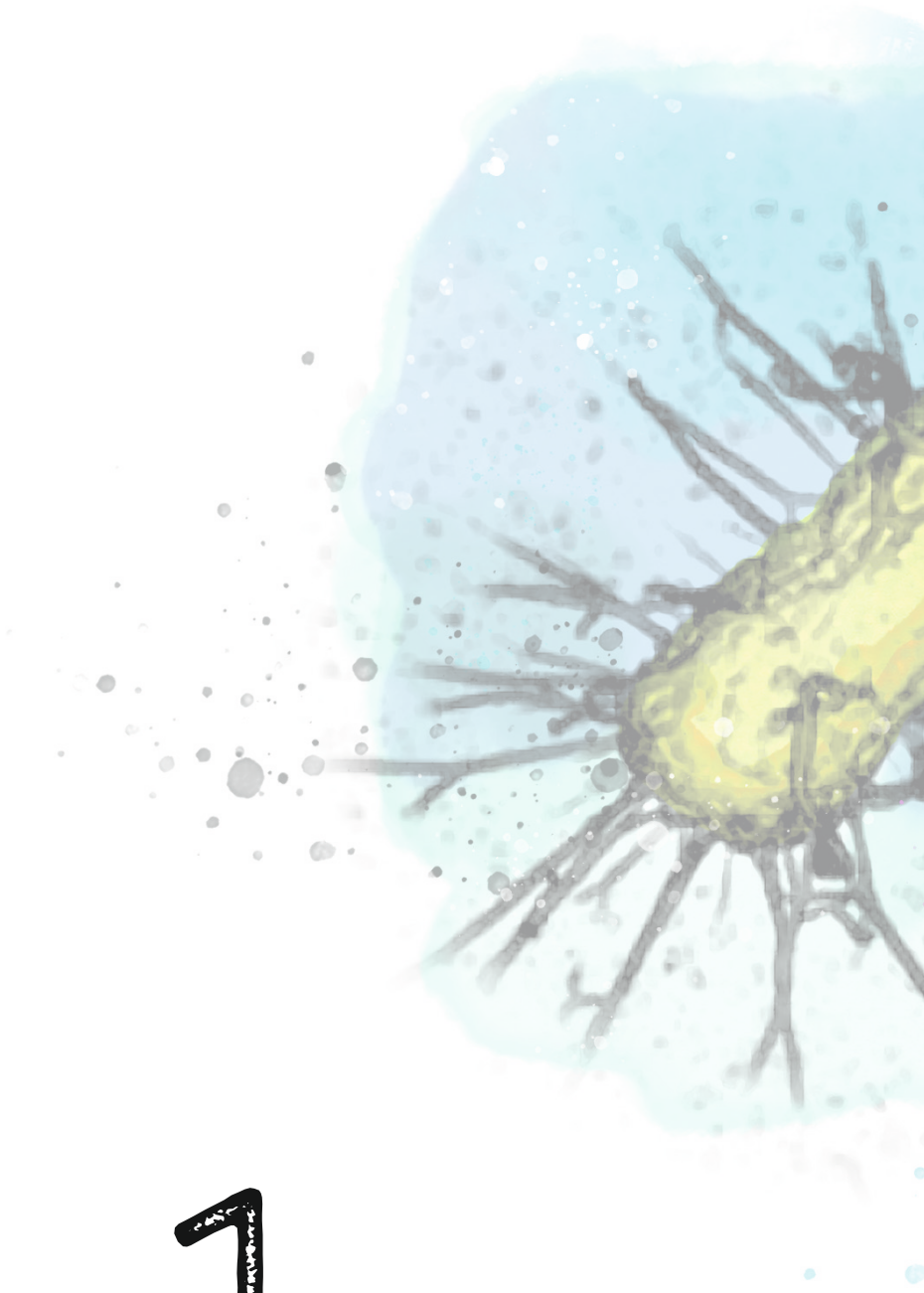

Chapter 1

General introduction and thesis outline

Akkermansia muciniphila is a fascinating intestinal symbiont, which has received considerable attention over the last two decades due to its mechanisms of action to improve host health. In this thesis, *A. muciniphila* plays a main role in all the chapters. *A. muciniphila* Muc^T was isolated in 2004 at the laboratory of Microbiology at Wageningen University (Derrien et al. 2004). It is a Gram-negative bacterium belonging to the Verrucomicrobiota (formerly Verrucomicrobia) phylum. In the human gut, *A. muciniphila* is currently the only representative of this phylum and present in high numbers with an abundance ranging from 0.5-5% (Cani and de Vos 2017). The name *A. muciniphila* was derived from Dr. Antoon Akkermans, who was leading the Microbial Ecology group within the Laboratory of Microbiology at the time of isolation, shortly before his retirement. The isolation was performed on the fecal sample of a healthy individual using purified mucin as the sole source of carbon, nitrogen, and energy (Derrien et al. 2004, Cani et al. 2022, Belzer and de Vos 2012). The genome of *A. muciniphila* Muc^T is composed of one circular chromosome of 2.7 Mbp coding for 2,176 protein-coding genes and is in terms of function mainly dedicated to mucus degradation (van Passel et al. 2011). Here an introduction is provided into the role of *A. muciniphila* in host health and other functions of this bacterium. In addition, we will introduce different models that may be used to study its performance.

A. muciniphila involvement in human health

Extensive studies have been performed on the correlation between the gut microbiota and health and disease (de Vos et al. 2022). The gut microbiota composition was found to be strongly correlated to several diseases, including pre-diabetes, type 2 diabetes, obesity, non-alcoholic fatty liver disease and liver cirrhosis (Tims et al. 2013, Le Chatelier et al. 2013, Allin et al. 2018, Zhong et al. 2019, Jiang et al. 2015, Qin et al. 2014). The results from the use of fecal microbiota transplantations in various inflammatory and metabolic diseases, caused an emerging interest to develop interventions aiming to alter the gut microbiota (Hanssen et al. 2021, Fan and Pedersen 2021). In turn this has led to the increasing interest in the development of interventions using specific gut bacteria, called next-generation beneficial microbes (Cani and de Vos 2017, Bui and de Vos 2021).

Inverse correlation with disease states

Considerable interest in *A. muciniphila* derived from human association studies, showing inverse correlations to several disease states (Cani et al. 2022). However, it should be noted that a few exceptions have been reported, likely due to confounding factors (Cani and de Vos 2017). A reverse correlation of the abundance of *A. muciniphila* and disease states was found in several metabolic diseases, such as obesity,

prediabetes and type 2 diabetes (T2D) (Santacruz et al. 2010, Dao et al. 2016, Karlsson et al. 2012, Zhang et al. 2013). In turn, in adults a higher abundance of *A. muciniphila* is associated with a healthier metabolic status (Dao et al. 2016). Furthermore, individuals with a high baseline of *A. muciniphila* showed to have improved clinical outcomes after calorie restriction. Interestingly, the negative correlation of *A. muciniphila* with obesity was also observed in children (Karlsson et al. 2012). In addition to metabolic diseases, *A. muciniphila* was also found to be reversely correlated to intestinal disorders, including IBD and appendicitis (Png et al. 2010, Rajilic-Stojanovic et al. 2013, Swidsinski et al. 2011). For example, the abundance of *A. muciniphila* in mucosal biopsies was strongly reduced in ulcerative colitis (non-inflamed 92-fold and inflamed 172-fold) and Crohn's disease patients (14.8-fold) (Png et al. 2010). Finally, children with autism, a neurological and developmental disorder, were found to have lower relative abundances of *A. muciniphila* as well (Wang et al. 2011).

Direct evidence for the role of *A. muciniphila* on host health

Many studies have collected valuable information on the effect of administration of *A. muciniphila* Muc^T on host health using mice models and a clinical study (Everard et al. 2013, Plovier et al. 2017, Sheng et al. 2018, Depommier et al. 2020, Raftar et al. 2021, Zhai et al. 2019). The administration of *A. muciniphila* Muc^T in mice models has been studied in both alive and pasteurized form, as well as the administration of its extracellular vesicles (EVs) and specific proteins (**Figure 1**).

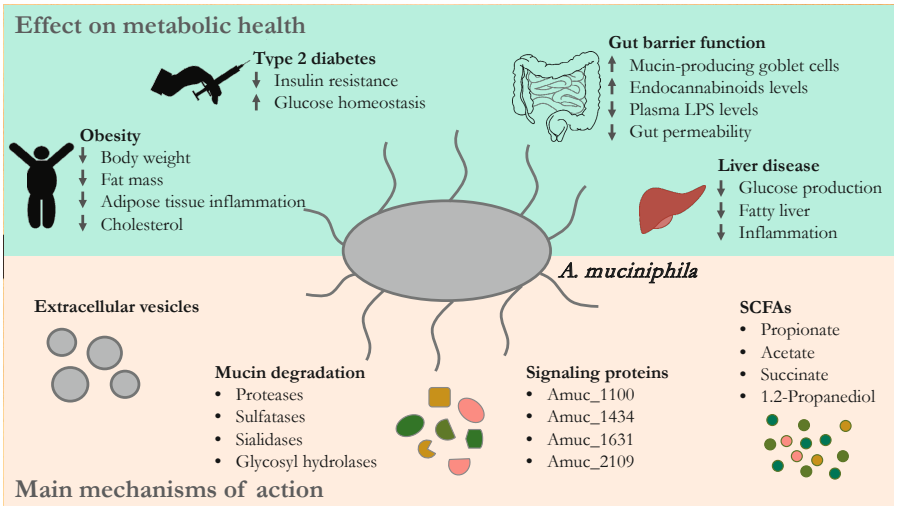

Figure 1: Overview of the effect of *A. muciniphila* on metabolic health and its main mechanisms of action studied in humans and mice. Detailed explanations of the effect of *A. muciniphila* on metabolic health (green) and its mechanisms of action (orange) can be found in the main text of this section.

As mentioned earlier, the abundance of *A. muciniphila* is negatively correlated to obesity. Studies using mice models showed an effect of the administration of both live and pasteurized *A. muciniphila* Muc^T cells. Germ-free mice colonized by *A. muciniphila* showed an altered mucosal gene expression profile, with increased expression of genes involved in immune responses and cell fate determination (Derrien et al. 2011). Another study using live *A. muciniphila* cells reversed high-fat diet induced metabolic disorders, including fat mass gain, metabolic endotoxemia, adipose tissue inflammation and insulin resistance (Everard et al. 2013). However, a follow-up study using pasteurized cells grown on synthetic medium showed even stronger effects than live *A. muciniphila* cells on body weight gain, fat mass gain and glucose intolerance (Plovier et al. 2017). After this finding, more experiments in mice models were performed to further research the effect of *A. muciniphila* on obesity (Sheng et al. 2018, Depommier et al. 2020, Choi et al. 2021). These studies also reported alleviating effects on obesity, including reduced body weight, a decrease in adipogenesis, lipogenesis and total cholesterol levels, as well as an improvement in glucose homeostasis and suppression of inflammatory insults (Sheng et al. 2018, Depommier et al. 2020, Choi et al. 2021). Next to obesity, mice studies showed that *A. muciniphila* may alleviate liver diseases, such as liver fibrosis, fatty liver disease and alcoholic liver disease (Raftar et al. 2021, Kim et al. 2020, Grander et al. 2018). Furthermore, studies showed *A. muciniphila* administration improved both dextran sulfate sodium (DSS)-induced colitis and chronic colitis in mice (Zhai et al. 2019, Bian et al. 2019). In both cases, *A. muciniphila* exerted anti-inflammatory effects. Interestingly, not only the cells but also the administration of *A. muciniphila* EVs improved DSS-induced colitis in mice (Kang et al. 2013). However, considering the doses of EVs that were used, it is important to note that more research is needed to determine the amount of EVs produced by a certain amount of *A. muciniphila* cells. For example, how many cells are needed to produce an effective amount of EVs for therapeutic purposes, as opposed to the use of pasteurized cells. Lastly, *A. muciniphila* administration may also protect against infection by influenza virus in mice (Hu et al. 2020).

Even though mice studies have resulted in the identification of potential effects of *A. muciniphila* on host health, clinical trials are needed to confirm these results in humans. A recent clinical trial confirmed the capacity of pasteurized *A. muciniphila* Muc^T cells to be at least as effective as live cells (Depommier et al. 2019). In this study, the administration of *A. muciniphila* in patients with obesity and metabolic syndrome showed an improved insulin sensitivity, reduced insulinemia and plasma total cholesterol. In addition, a reduction of body weight was observed including reduced fat mass and hip circumference. These studies, whether using live or pasteurized *A. muciniphila* Muc^T cells, demonstrate a role in alleviating several disease states, as well as the potential to use *A. muciniphila* derived products, such as EVs. Altogether,

these studies raised interest for the use of *A. muciniphila* as a therapeutic microbe. Recently, on September 5th 2022, The Akkermansia Company launched the first food supplement containing pasteurized *Akkermansia*, focusing on weight management and control of blood sugar.

A. muciniphila improves gut barrier function

Next to the direct effects of *A. muciniphila* cells in different disease states, several studies have identified another positive effect of this bacterium on host health, namely strengthening of the gut barrier function (Everard et al. 2013, Ottman et al. 2017, Shin et al. 2014, Chelakkot et al. 2018). *A. muciniphila* administration was found to be associated to an increased number of mucin-producing goblet cells, as well as an increase in the intestinal endocannabinoids levels that control gut peptide secretion, inflammation, and the gut barrier in mice. (Shin et al. 2014, Everard et al. 2013). In addition, *A. muciniphila* also showed its ability to strengthen an impaired gut barrier by strengthening the enterocyte monolayer integrity *in vitro* (Reunanen et al. 2015). Furthermore, administration of *A. muciniphila* reversed elevated plasma LPS levels, which can be linked to an impaired gut barrier, through the inhibition of cannabinoid receptor 1 (Wu et al. 2017). Furthermore, strengthening of the intestinal barrier was observed by the enhanced expression of Occludin and Tight junction protein-1. However, not only the administration of *A. muciniphila* was found to influence the gut barrier function, but also the administration of its EVs and outer membrane protein Amuc_1100 in mice (Chelakkot et al. 2018, Ottman et al. 2017, Plovier et al. 2017). Amuc_1100 was shown to activate toll-like receptor 2 (TLR2), which can regulate various tight-junction proteins (Ottman et al. 2017, Plovier et al. 2017). It was shown that both Amuc_1100 and EVs derived from *A. muciniphila* decreased gut permeability of Caco-2 cells (Chelakkot et al. 2018, Ottman et al. 2017). An impaired gut barrier is associated with several diseases, including IBD and causally obesity (Mennigen and Bruewer 2009, Wu et al. 2017). Therefore, improvement of the gut barrier function may be one of the modes of action for *A. muciniphila* and its derived products to improve disease states such as IBD.

The role of signaling molecules in host health

An increasing number of signaling proteins produced by *A. muciniphila* Muc^T, which are interacting with the host, have been identified over the past years (**Figure 1**) (Cani et al. 2022, de Vos et al. 2022). The outer membrane protein Amuc_1100 is well-known due to its interaction with the host (Ottman et al. 2016). This protein is part of a gene cluster involved in pili-production which also includes Amuc_1098, encoding for the secretin PilQ. Amuc_1098 is responsible for the exposure of type 4 pili to the environment and was found to be the most abundantly produced outer membrane protein of *A. muciniphila* (Ottman et al. 2016). Administration of Amuc_1100 showed

a similar effect as live and pasteurized cells in protection against diet-induced obesity in mice (Plovier et al. 2017). In addition, this protein is stable at pasteurization temperatures and activates TLR2, which regulates multiple tight-junction proteins (Plovier et al. 2017, Ottman et al. 2017). Recently, several other proteins were identified that have been implicated in host signaling, including Amuc_1631. This protein is also known as P9 and improved glucose homeostasis and ameliorated metabolic disease in mice (Yoon et al. 2021). Furthermore, Amuc_1434, an aspartic protease, inhibited human colorectal cancer LS174T cell viability through the tumor-necrosis-factor-related apoptosis-inducing ligand (TRAIL)-Mediated Apoptosis Pathway (Meng et al. 2020). Lastly, Amuc_2109, a β-N-acetylhexosaminidase, has been identified to protect against DSS-induced colitis in mice through enhancement of the intestinal barrier and gut microbiota modulation (Qian et al. 2022). However, whereas the location, production and stability have been studied for Amuc_1100 and Amuc_1098, this has not yet been studied for the newly identified host signaling proteins Amuc_1434, Amuc_1631 and Amuc_2109.

Cultivation of beneficial microbe *A. muciniphila*

A. muciniphila Muc^T is often cultivated on mucin-based medium prior to studying its effect on host health (Everard et al. 2013, Wang et al. 2022, Qu et al. 2021, Bian et al. 2019, Yaghoubfar et al. 2020, Wu et al. 2020). However, it should be taken into consideration that animal-derived mucus fractions are not free from residues of other bacteria and possibly animal cell fractions, which may bias the experiment. For commercialization the production of *A. muciniphila* needs to be executed on industrial scale. The medium that is used for cultivation should in turn be food-grade, preferably plant based, non-allergenic, free of mucin derived from slaughterhouses and support growth of *A. muciniphila* to high densities. Lastly, the signaling molecules known to interact with the host, for example Amuc_1100, should be produced sufficiently in this medium.

The development of a metabolic model predicted that *A. muciniphila* Muc^T can synthesize all the essential amino acids except threonine (Ottman et al. 2017). Later, a necessity for N-Acetylglucosamine (GlcNAc) was also identified (van der Ark et al. 2018). Both threonine and GlcNAc are abundantly present in mucus. Therefore, it is most likely that *A, muciniphila* lost the capacity to synthesize threonine and GlcNAc due to mucin adaptation (Ottman et al. 2017, van der Ark et al. 2018). This information resulted in the development of a synthetic medium, where mucus could be substituted by threonine, glucose and GlcNAc or GlcNAc alone, and peptone (Ottman et al. 2017, van der Ark et al. 2018). Since then, synthetic media have been used in a series of mechanistic studies in diabetic and obese mice and in a clinical trial where beneficial effects of *A. muciniphila* were shown (Plovier et al. 2017, Depommier et al. 2019).

A. muciniphila new strains & genomics

A. muciniphila strains and genomics in the human host

A. muciniphila is present in the intestinal tract throughout different stages of life and detected in many different geographical locations (Geerlings et al. 2018). In the healthy human colon, *A. muciniphila* is a highly abundant member (approximately 3%) of the gut microbiota (de Vos 2017). However, higher abundances up to ~15% have also been detected, depending on the individual and the detection method (Momozawa et al. 2011). *A. muciniphila* was even found to represent 44 to 85% of the reads in patients under heavy antibiotic treatment (Dubourg et al. 2013). Interestingly, humans are not only colonized by one strain of *A. muciniphila*, but potentially by different *Akkermansia* strains (van Passel et al. 2011, Ouwerkerk et al. 2022). One of the first metagenomic studies focusing on the presence of different *Akkermansia* strains suggested colonization by at least eight different strains. Although, it is important to note that these sequences were derived from short Illumina reads. Therefore, mis-assembly or other technical biases may have affected this finding. Since this initial finding, more studies started to focus on the presence of multiple *A. muciniphila* strains in the human gut (Guo et al. 2017, Kim et al. 2022, Becken et al. 2021). To date, *A. muciniphila* is the only representative of Verrucomicrobiota in the gut. However, genomic analysis of *Akkermansia* in the human gut suggests the presence of multiple *Akkermansia* species (Guo et al. 2017, Karcher et al. 2021, Kumar et al. 2022). All these strains appear to have highly similar 16S rRNA sequences with >98 % identity to that of the type strain Muc^T. One newly isolated *Akkermansia* strain DSM 33459 was found to have only 87.5% average nucleotide identity compared to the type strain and showed differences in its fatty acid profile and carbon utilization (Kumar et al. 2022). However, the identity of 16S rRNA between *Akkermansia* DSM 33459 and *A. muciniphila* Muc^T was high, namely 99.2%.

Phylogenetic analysis and genome comparisons of *Akkermansia* spp. have also been performed on larger scales (Guo et al. 2017, Becken et al. 2021, Karcher et al. 2021). A study focusing on isolating and analyzing new *A. muciniphila* strains in China found 33 new *A. muciniphila* strains isolated from human feces (Guo et al. 2017). These were analyzed together with six strains isolated from mice. Maximum likelihood (ML) phylogenetic analysis based on core genome single nucleotide polymorphisms (SNPs) identified three phylogroups, named AmI, AmII and AmII. The three phylogroups contain a high genome-wide nucleotide diversity and distinct metabolism and function profiles. Furthermore, the average nucleotide identity between phylogroups was below 96%, which is the threshold used for prokaryotic species definition (Richter and Rossello-Mora 2009). In contrast, the phylogroups do share consistent phenotypic characteristics, habitat and conserved 16S rRNA genes (similarities >99%) (Guo et al.

2017). In addition, a recent study isolated and characterized 71 new *A. muciniphila* strains from children and adolescents undergoing treatment for obesity (Becken et al. 2021). Using a higher number of isolates than the previous study and including previously found isolates in their phylogenetic analysis as control led to the identification of four phylogroups (AmI until AmIV). Even though AmI strains were most prominent among children and adolescents, AmII and AmIV strains outcompeted AmI strains when supplemented to antibiotic-treated mice. In addition, phylogroup-specific phenotypes were detected, including oxygen tolerance, adherence to epithelial cells, iron and sulfur metabolism, and bacterial aggregation.

A large-scale population genomics analysis of the *Akkermansia* genus including 2420 *Akkermansia* genomes revealed that the *Akkermansia* strains in the human gut can be grouped into five distinct candidate species (Karcher et al. 2021). These candidate species exhibit ecological co-exclusion, different functional capabilities and distinct body mass association patterns. In line with the previously performed smaller scale study (Guo et al. 2017), whole genome divergence was detected (whole genome similarity <90%) even though the 16S rRNA sequences were highly similar (>98%) (Karcher et al. 2021). The genomic characteristics found in several *Akkermansia* studies are unusual considering most bacterial species that are below 95% genome similarity have over 3% divergence of the 16S rRNA gene (Karcher et al. 2021). This may explain why the diversity has not been detected previously with 16S rRNA amplicon sequencing analysis.

The novel human-associated *Akkermansia* strains exert strain specific effects in several functions (Liu et al. 2021, Luna et al. 2022, Kirmiz et al. 2020, Kumar et al. 2022, Zhai et al. 2019). For example, *Akkermansia* strains showed strain-dependent utilization efficiencies of human milk oligosaccharides (HMOs), which are likely related to differences in copy numbers and enzyme activity of α-fucosidases, α-sialidases, and β-galactosidases (Luna et al. 2022). In addition, differences in vitamin B_{12} biosynthesis by *Akkermansia* strains were also reported, resulting in different fermentation profiles possibly affecting interaction with the human host and other gut bacteria (Kirmiz et al. 2020). Strain-specific effects were also detected in mice studies focusing on DSS-induced ulcerative colitis and chronic colitis, including differences in anti-inflammatory properties, improvement of gut permeability and body weight restoration (Zhai et al. 2019, Liu et al. 2021). Lastly, compared to the type-strain, newly isolated *Akkermansia* strain DSM 33459 was found to have more pronounced health effects using live cells in the used mouse model, with live cells more effective than pasteurized cells (Kumar et al. 2022). However, it is unclear how reproducible and robust this effect is in different experimental setups and the physiological growth conditions of the used *Akkermansia* strains. Moreover, the observed effect should be studied in humans.

The possible differences observed in *Akkermansia* strains emphasizes the need to carefully characterize new strains to assess which strain may be most effective to use as therapeutic microbe in different situations. Lastly, it is important to note that only one other *Akkermansia* species has been identified to date, which is *Akkermansia glycaniphila* (average nucleotide identity of 79.9% compared to *A. muciniphila* Muc^T) isolated from python feces (Ouwerkerk et al. 2016).

A. muciniphila colonization in other hosts

Next to the presence of *Akkermansia* spp. in humans, its presence is also widely spread in the gut throughout the animal kingdom. *Akkermansia* spp. have been detected in mammals and other vertebrates (Ley et al. 2008, Sommer et al. 2016, Carey et al. 2013, Sonoyama et al. 2009, Costello et al. 2010, Ouwerkerk et al. 2016, Belzer and de Vos 2012, Green et al. 2013). Mammals harboring *Akkermansia* spp. include the brown bear, ground squirrel and the Syrian hamster (Sommer et al. 2016, Carey et al. 2013, Sonoyama et al. 2009). Furthermore, *Akkermansia* spp. were detected in other vertebrates including python, zebra fish, chicken and salmon (Costello et al. 2010, Ouwerkerk et al. 2016, Belzer and de Vos 2012, Green et al. 2013). In contrast, *Akkermansia* spp. were not detected in invertebrates, whereas some invertebrates were found to harbor Verrucomicrobiota species such as, termites, ants, earthworms and nematodes (Isanapong et al. 2013, Sanders et al. 2014, Wust et al. 2011, Vandekerckhove et al. 2002). Only few *Akkermansia* spp. and Verrucomicrobiota were isolated from the gut environment of these different hosts. *A. glycaniphila* was isolated from python feces (Ouwerkerk et al. 2016). Furthermore, another species within the Verrucomicrobiota phylum named *Diplosphaera colotermitum* was isolated from the gut of a termite (Ouwerkerk et al. 2016, Wertz et al. 2012). Recently, two novel candidate *Akkermansia* spp. were proposed namely, *Candidatus* Akkermansia intestinavium isolated from the gut of birds and *Candidatus* Akkermansia intestinigallinarum isolated from the gut of hens (Gilroy et al. 2021).

Altogether, *Akkermansia* spp. and Verrucomicrobiota are detected in the gut throughout the animal kingdom, despite the environmental differences including GI tract anatomy, diet, host physiology and body temperature. The distribution of these bacteria suggests co-evolution of this organisms with its host. However, *Akkermansia* spp. throughout the gut in the animal kingdom has not been as extensively studied as the *Akkermansia* spp. found in human hosts. Therefore, genomic and phylogenetic analysis may provide us with more information about the evolution of this species within different hosts, as well as possible differences in functions between hosts within the animal kingdom.

Adaptation of *A. muciniphila* to the gut environment

A. muciniphila resides in the mucosal layer which covers the epithelial cells in the large intestine (Derrien et al. 2004). Mucus is being continuously produced by the host epithelial cells. By creating a barrier between the epithelial cells and luminal content, the mucosal layer protects the epithelial cells from direct contact with microorganisms (Johansson et al. 2011). Further protection is obtained from the production of antimicrobial peptides and IgA. In addition, the mucosal layer provides nutrients to mucolytic bacteria in the gut. The mucosal layer can be divided into two segments: the inner layer which is firmly attached to the epithelial cells and devoid of bacteria and the outer layer where microbes can colonize due to its higher permeability (Johansson et al. 2008). Even though the layers have different densities, they are both mainly composed of gel-forming mucin MUC2, which consists of large polymers formed by N-terminal trimerization and C-terminal dimerization (Ambort et al. 2012). After production, the mucus layer expands upon release from goblet cell secretory granulae due to an increase in pH from 5.2 to 7.2, and decreased calcium concentrations. Decreased calcium concentrations weaken the N-terminal interactions causing the expansion of MUC2 mucin into flat mucin sheets, as water binds to the mucin domain glycans (Johansson and Hansson 2016). Afterwards, the density of the outer layer further decreases due to endogenous proteases, promoting microbe colonization in the mucus layer (Johansson et al. 2008).

MUC2 proteins are rich in proline, serine and threonine (PTS) domains which are densely glycosylated (Johansson et al. 2011, Johansson et al. 2008). Furthermore, MUC2 contains multiple sugars such as GlcNAc, N-acetylgalactosamine (GalNAc), galactose and fucose (**Figure 2**) (Tailford et al. 2015). Finally, most MUC2 glycans also contain sialic acid (Tailford et al. 2015). *A. muciniphila* utilizes mucin as the sole carbon, nitrogen and energy source (Derrien et al. 2004). The genome of *A. muciniphila* Muc^T is mainly dedicated to mucus degradation considering it has 61 proteins involved in mucin-degradation including proteases, sulfatases, sialidases and glycosyl hydrolases (GHs) such as β-galactosidases, β-N-acetylhexosaminidases, exo-α-sialidases, α-L-fucosidases, and α-N-acetylglucosaminidases (van Passel et al. 2011, Ottman et al. 2017). The predicted proteome of *A. muciniphila* Muc^T contains proteins belonging to different glycosyl hydrolase families, including: GH2, GH3, GH13, GH16, GH18, GH20, GH27, GH29, GH31, GH33, GH35, GH36, GH43, GH57, GH63, GH77, GH84, GH89, GH95, GH97, GH105, GH109, GH110 and GH123 (Drula et al. 2022).

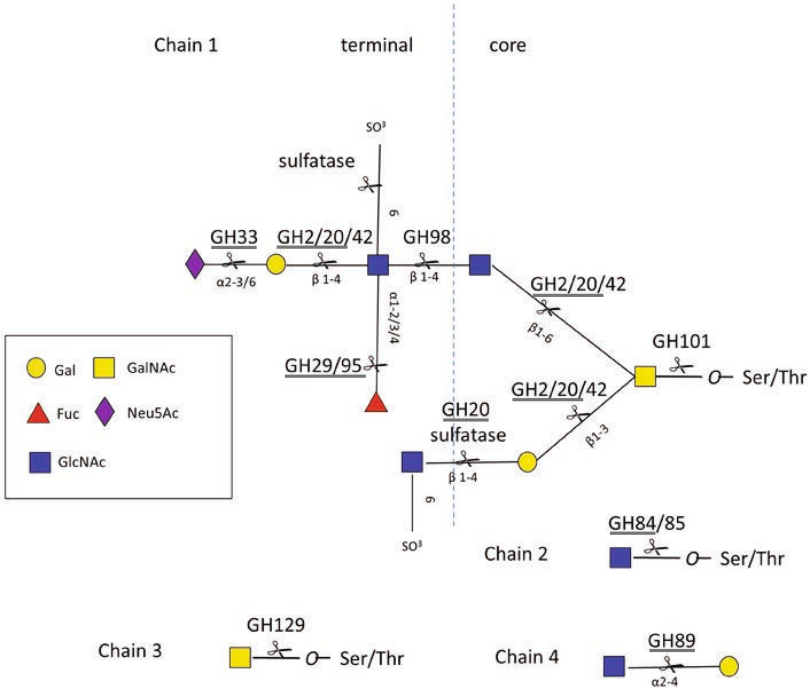

Figure 2: Schematic overview of O-glycan chains showing sites of action of GHs and sulfatases. (adapted from Tailford et al. 2015). GH families present in the genome of *A. muciniphila* Muc^T are underlined.

It is known that *A. muciniphila* has the enzymatic capacity to degrade and utilize mucin glycans (Derrien et al. 2004, Derrien 2007, Derrien et al. 2010). However, even though *A. muciniphila* degrades mucin forming a protective layer of the epithelial cells, at the same time its administration increases mucus production as confirmed in mice studies (Kim et al. 2021). The fermentation of glycans and non-digestible carbohydrates results in the production of short chain fatty acids (SCFAs) which in turn induce health effects (den Besten et al. 2013). *A. muciniphila* can produce acetate, propionate, and to a lesser extent succinate and 1,2-propanediol by mucus utilization (Derrien et al. 2004, Ottman et al. 2017). In the gut, acetate, propionate and butyrate are the most abundantly produced SCFAs (den Besten et al. 2013). All three SCFAs induce beneficial effects to the host epithelial cells and immune cells through the activation of intracellular and extracellular processes (Parada Venegas et al. 2019). Acetate, propionate and butyrate beneficially affect host energy and substrate metabolism through the secretion of gut hormones, including peptide YY and glucagon-like peptide-1, affecting appetite, slowing gastric emptying, enhancing

insulin secretion and inhibiting glucagon secretion (Hernandez et al. 2019, Bridgeman et al. 2020, Hosseini et al. 2011). Furthermore, butyrate has epigenetic effects through inhibition of histone deacetylases and was found to confer numerous health benefits in animal models, including reduced serum triglycerides, total cholesterol and glucose, and reduced weight gain (Bridgeman et al. 2020). In addition, propionate was found to be an efficient substrate for glucose production in the liver (de Vadder and Mithieux 2018). Lastly, evidence suggests both butyrate and propionate exert an antiproliferative effect on colon cancer cells (Hosseini et al. 2011).

To survive or adapt in the mucosal layer, there are several environmental parameters to consider. For instance, the presence of oxygen near the epithelial cells of the gut is an important parameter to take into account. The gut together with its microbiota create the steepest oxygen gradient in the human body (Espey 2013). This oxygen gradient changes from 80-100 mmHg in the submucosa to near anoxia at the midpoint of the lumen. However, it is important to note that the oxygen gradients are not static but vary with every meal. This controls redox effectors produced by both the host and the gut microbiota including nitric oxide, hydrogen sulfide, and reactive oxygen species. This indicates that the bacteria residing in the mucosal layer, need to be able to tolerate low concentrations of oxygen present in the environment. Interestingly, *A. muciniphila* Muc^T was found to be able to tolerate exposure to an oxic environment for 1 hour, after which 90% of the cells was still alive (Reunanen et al. 2015). Later, the oxygen tolerance of *A. muciniphila* Muc^T was studied in more depth focusing on its response to oxygen exposure and reduction capacities (Ouwerkerk et al. 2016). Here, *A. muciniphila* did not only significantly reduce oxygen, but it was also found to thrive in terms of growth rate and yield in the presence of nanomolar amounts of oxygen. Upon exposure to oxygen, transcriptome analysis of *A. muciniphila* revealed its oxygen stress response after which respiration was activated through the cytochrome bd complex, which functions as a terminal oxidase. Furthermore, superoxide dismutase (Amuc_1592) and catalase HPII (Amuc_2017) were upregulated upon oxygen exposure to scavenge reactive oxygen species (ROS). Using these mechanisms, *A. muciniphila* can cope with low oxygen concentrations as well as ROS present in the mucosal layer.

Another environmental parameter to consider in the large intestine is the presence of bile acids. Interestingly, the abundance of *A. muciniphila* was positively correlated to circulating primary bile acids in mice (Pierre et al. 2016, Juárez-Fernández et al. 2021). Furthermore, an in vitro study showed increased growth of *A. muciniphila* Muc^T in medium containing 0.1%, 0.5% and 1% porcine bile extract, when compared to medium that did not contain bile (van der Ark et al. 2017). However, the addition of purified bile salts inhibited the growth of *A. muciniphila* at a concentration of 0.5% or higher (van der Ark 2018). In another study, individual bile salts were found

to have differential effects on the growth of *A. muciniphila* Muc^T (Hagi et al. 2020). A putative bile acid transporter gene (Amuc_0139) is annotated in the genome of *A. muciniphila*. Using this protein, *A. muciniphila* could reduce bile acids inside of the cell, thereby reducing its effects. However, transcriptome analysis did not show a difference in gene expression of this gene in the presence of bile salts (Hagi et al. 2020). Instead, membrane transporters and the squalene-associated membrane structure were identified as possible major bile response systems in *A. muciniphila.* Another mechanism, as also used by other bacteria such as *Bifidobacterium* spp., is the production of exopolysaccharides (EPS) to protect the cell wall against bile acids (Fanning et al. 2012, Ruas-Madiedo et al. 2009).

Bacterial exopolysaccharide production

A wide range of microorganisms produce extracellular polymeric substances, such as bacteria, microalgae, yeasts and fungi (Costa et al. 2018). These highly hydrated polymers are composed of polysaccharides, structural proteins, enzymes, nucleic acids, lipids and humic acids. Polysaccharides comprise a major fraction of the extracellular polymeric substance matrix. Bacterial EPS, which are high molecular weight carbohydrate biopolymers, are an essential group of compounds secreted by bacteria (Mohd Nadzir et al. 2021). They consist of sugar units connected by glycosidic linkages that can vary from linear to heavily branched (1,2). Bacteria can either produce capsular EPS which is loosely bound to the cell or fully secreted EPS. Furthermore, the polymers can consist of a single type of monosaccharide called homopolysaccharides (HoPs) or multiple types of monosaccharides namely heteropolysaccharides (HePs). EPS may exert different functions for bacterial cells, including cell aggregation, biofilm formation, cell-cell communication, water retention, nutrient source, sorption of organic and inorganic components, enzymatic activity, surface adhesion and protective barrier (Shukla et al. 2019). Furthermore, EPS may protect the cell against cell desiccation, starvation, predation by protozoa, phagocytosis, oxidizing biocides, antibiotics, UV radiation and environmental stress such as temperature, extreme pH, toxic substances and disinfectant.

Different probiotic strains can express health promoting effects through the production of EPS. The definition of probiotics is: "Live microorganisms that, when administered in adequate amounts, confer a health benefit on the host". Well-known bacteria widely studied for their EPS production and its properties are lactic acid bacteria. The EPS of several *Lactobacillus* species and strains were found to exert different health benefits including anti-tumor, anti-diabetic, immunomodulatory and antioxidant activities and in-vivo dermal wound healing properties (Sungur et al. 2017, Ayyash et al. 2020, Górska et al. 2010, Adesulu-Dahunsi et al. 2018, Trabelsi et al. 2017). In addition, EPS produced by *Bifidobacterium* spp. were also found to exert health benefits. For example, EPS

of *Bifidobacterium* spp. was shown to reduce cholesterol levels in diet-induced obese mice and exerted immunomodulatory activity (Salazar et al. 2019, Wu et al. 2010). Where many studies have focused on EPS production by lactic acid bacteria and *Bifidobacterium* spp., less is known about EPS production by *A. muciniphila*. EPS production and structural analysis of this bacterium has not been studied in detail. However, several studies have indicated that *A. muciniphila* may be able to produce EPS under different cultivation conditions (Ouwerkerk et al. 2016, Rodriguez-Daza 2020). Transcriptome data showed *A. muciniphila* may use EPS production as a protective mechanism against oxygen presence (Ouwerkerk et al. 2016). In addition, two genes, Amuc_1470 (exopolysaccharides locus protein-H) and Amuc_1413 (capsular exopolysaccharide biosynthesis protein), possibly involved in EPS production by *A. muciniphila*, were upregulated in *A. muciniphila* cultures exposed to products containing cranberry extract, flavan-3-ols-rich fraction and microbial polyphenolic metabolite urolithin A (Rodriguez-Daza 2020). Considering the health benefits *A. muciniphila* exerts to its host, and the health benefits of EPS produced by other probiotic bacteria, it would be of interest to study EPS production by *A. muciniphila*.

In vitro and *in vivo* ecosystems to study *A. muciniphila* and other members of the gut microbiota

The ecosystem in the human gut is a niche with extremely complex and dynamic interactions (Sung et al. 2017). Many different types of interactions take place in a microbial ecosystem as complex as the human gut, leading to both symbiotic and competitive relationships. Gaining insight in the complex interactions present in the human gut at community and individual taxa level is pivotal for the development of effective microbiome modulation strategies (Shetty et al. 2017, Costello et al. 2012, Gilbert and Lynch 2019). Complex dietary fibers and mucus glycans are important factors in the metabolic activity of the gut microbiota (Salonen and de Vos 2014, Berkhout et al. 2022). The species capable of degrading complex dietary fibers and mucus are therefore key players in the community. Several steps are involved in the degradation of carbon sources which are executed by different bacteria (Scott et al. 2014, Flint et al. 2012). For example, degradation of dietary fibers and mucus glycans by specialists releases simple carbohydrates available to use by other members of the gut microbiota. This interaction is referred to as cross-feeding. In contrast, functional redundancy is also observed in the gut microbiota, for example among butyrate producers using acetate or monosaccharides (Clark et al. 2021). This functional redundancy leads to competition within the gut microbiota.

Many different approaches exist to study microbe-microbe interactions in the gut, varying from *in silico* methods leading to predictions of microbe-microbe interactions, *in vivo* studies mainly using mice as hosts for defined or undefined communities, as well as *in vitro* studies in batch or continuous cultures. One example often used to study interactions in the gut microbiota is by inoculating chemostats mimicking the human gut using human feces. Well-known *in vitro* intestinal models are the Simulator of the Human Intestinal Microbial Ecosystem (SHIME) or mucosal SHIME (M-SHIME) and the TNO Intestinal Model 2 (TIM-2) (Van de Wiele et al. 2015, Venema 2015). Currently, the assembly of synthetic communities using host-derived strains is receiving considerable attention. Species selection for synthetic communities are based on their function and prevalence, among other criteria. Synthetic microbial communities of the human gut can be studied under controlled conditions either *in vivo* using animal models, or *in vitro* e.g. using chemostats (Desai et al. 2016, Kovatcheva-Datchary et al. 2019, Oliphant et al. 2019, D'Hoe et al. 2018, Venturelli et al. 2018). Recently, a defined 14-species synthetic community representing the five dominant phyla possessing important core metabolic capabilities was established *in vivo* using germ-free mice (Desai et al. 2016). Here, the interactions between gut microbes, dietary fibers and the colonic mucus barrier were studied. Similarly, two human fecal-derived defined microbial communities were cultured in bioreactors (Oliphant et al. 2019). The first synthetic community was derived from a single fecal donor, whereas the second community was constructed using species each from a unique donor fecal sample. Using this experimental setup, the influence of coadaptation of strains within a host on community dynamics was studied. As opposed to *in vivo* animal models, *in vitro* models are standardized providing highly reproducible results and allow for frequent sampling (Venema and van den Abbeele 2013). Therefore, combining *in vitro* intestinal models with defined microbial communities may contribute considerably to the understanding of community assembly and structure, compositional and functional dynamics. It is important to note that all mentioned *in vitro* models do not include host cells that are present in the gut. To overcome this limitation, studies are focusing on the development of a gut-on-a-chip, taking host cells into account. One study successfully cultivated gut bacteria on their device, in the form of single cultivation and an eight-species community (Kim et al. 2012, Kim et al. 2016). This gut-on-a-chip consists of two channels simulating the gut lumen and a blood vessel, which are separated by a membrane coated with extracellular matrix and Caco-2 cells. However, growth of anaerobic bacteria on the chip has not been reported (Elzinga et al. 2019). Therefore, further research should focus on the optimization of cultivating anaerobic gut bacteria alone or in a community on the gut-on-a-chip.

Interactions between *A. muciniphila* and other members of the gut microbiota

Several studies have investigated competitive and cross-feeding interactions between *A. muciniphila* and other members of the gut microbiota (Belzer et al. 2017, Segura Munoz et al. 2022, Kostopoulos et al. 2021, Chia et al. 2018). A metabolic interaction network was established between *A. muciniphila* and three butyrate producers, *Anaerostipes caccae, Eubacterium hallii* (now re-classified as *Anaerobutyricum soehngenii*), and *Faecalibacterium prausnitzii* resulting in syntrophic growth and butyrate production on mucus (Belzer et al. 2017). Interestingly, the interaction was bi-directional due to the production of pseudovitamin B_{12} by *E. hallii*, leading to the production of propionate by *A. muciniphila*. A follow-up study showed that *A. muciniphila* increases the expression of mucolytic enzymes upon the presence of a community member, in this case *A. caccae*, thereby increasing the availability of simple sugars for other members in the community (Chia et al. 2018). In contrast, a different response was found when *A. muciniphila* was co-cultured with mucin degrading generalist *Bacteroides thetaiotaomicron* (Kostopoulos et al. 2021). Upon co-cultivation *B. thetaiotaomicron* showed a more general glycan degrading profile, while the profile of *A. muciniphila* remained unaltered as compared to the monoculture. Instead, *A. muciniphila* coped with the competition through the upregulation of defense related genes. Next to competition with other bacteria, strict competitive exclusion between *A. muciniphila* strains has also been demonstrated (Segura Munoz et al. 2022, Schmidt et al. 2022). Altogether, these examples indicate a key role of *A. muciniphila* in the human gut as a mucin degrading specialist.

Research aims and thesis outline

The research projects in this thesis aim to assess the functions of *A. muciniphila* in the human body and other hosts as well as in *in vitro* and *in vivo* models. Therefore, we aimed to use bioinformatics and phylogenetic analysis to identify newly isolated *Akkermansia* strains from the human body and different mammalian hosts. Furthermore, we aimed to study the functions of *A. muciniphila* in several *in vitro* and *in vivo* models to elucidate the stability of these functions in food-grade media, co-cultivations and a synthetic community. Lastly, in this thesis we aim to gain further insight on one of the physiological characteristics of *A. muciniphila*, namely exopolysaccharide production, of which the genetic machinery, structure and potential health benefits are still unknown.

This thesis consists of eight chapters including the general introduction and thesis outline, a review, research papers and the general discussion.

Chapter 2 explores the presence of *Akkermansia*-like spp. based on its 16S rRNA sequence and metagenomic signatures in the human body to understand its colonization pattern in time and space. The presence of *Akkermansia*-like sequences (including Verrucomicrobia phylum and/or *Akkermansia* spp. sequences found in the literature) was detected in several locations apart from the colon, including the oral cavity, human milk, the pancreas, the biliary system, the small intestine, and the appendix. In this review we propose hypothetical functions of *A. muciniphila* in these anatomical sites.

Chapter 3 provides an overview of the presence of *A. muciniphila* in different mammalian hosts. *Akkermansia* spp. are widely spread in the gut throughout the animal kingdom which may be indicating co-evolution with its host. Therefore, we studied the presence and genomic divergence of Verrucomicrobiota and *Akkermansia* spp. within different mammalian hosts. This was done by phylogenetic analysis, detecting and isolating new *A. muciniphila* strains from different mammalian orders to compare their genomic traits and assess their functionality in mucin degradation.

Chapter 4 assesses the use of a newly developed food-grade and plant-based media with varying carbon sources. For human interventions, cultivation medium is needed, free of animal-derived components, food-grade and non-allergenic that also allows for efficient growth to high densities. The growth of *A. muciniphila* on this newly developed food-grade and plant-based medium was compared to its growth on mucin-containing medium using a multi-omics approach.

Chapter 5 describes EPS produced by *A. muciniphila* to confirm the EPS composition and identify through which pathway *A. muciniphila* produces EPS. Revealing information regarding the structure of EPS may lead to uncovering mechanisms involved in microbe-microbe and host-microbe interactions and its therapeutic and food applications. We used food-grade medium to assess EPS production by *A. muciniphila*. Furthermore, we studied the genetic machinery *A. muciniphila* employs for EPS production using bioinformatics and transcriptome analysis.

Chapter 6 shows the assembly of a synthetic gut microbiota community in bioreactors consisting of 16 different species including *A. muciniphila*. We aimed to investigate microbe-microbe interactions in this synthetic community. The bioreactors were continuously supplied with mucus, while a mixture of dietary fibers was added three times a day to mimic a dietary regimen. Both transcriptome and 16S rRNA sequencing were used to evaluate the microbe-to-microbe and metabolic interactions between key bacteria in the human gut microbiota. In all three fermentors, *A. muciniphila* was one of the most abundant species.

Chapter 7 describes the transcriptional landscape of *A. muciniphila* in different environmental conditions, including complexity of the community, diet, medium composition and experimental design. Considering that *A. muciniphila* is studied in a variety of experimental setups, we aimed to assess the main functions of *A. muciniphila* throughout these frequently used experimental setups. We focused on the transcriptional response of *A. muciniphila* in these *in vitro* and *in vivo* ecosystems and assessed genes associated with its key functions across all ecosystems.

Chapter 8 summarizes and discusses the findings of the research projects described in this thesis. In addition, this chapter will provide future perspectives for research of *A. muciniphila* and its functions.

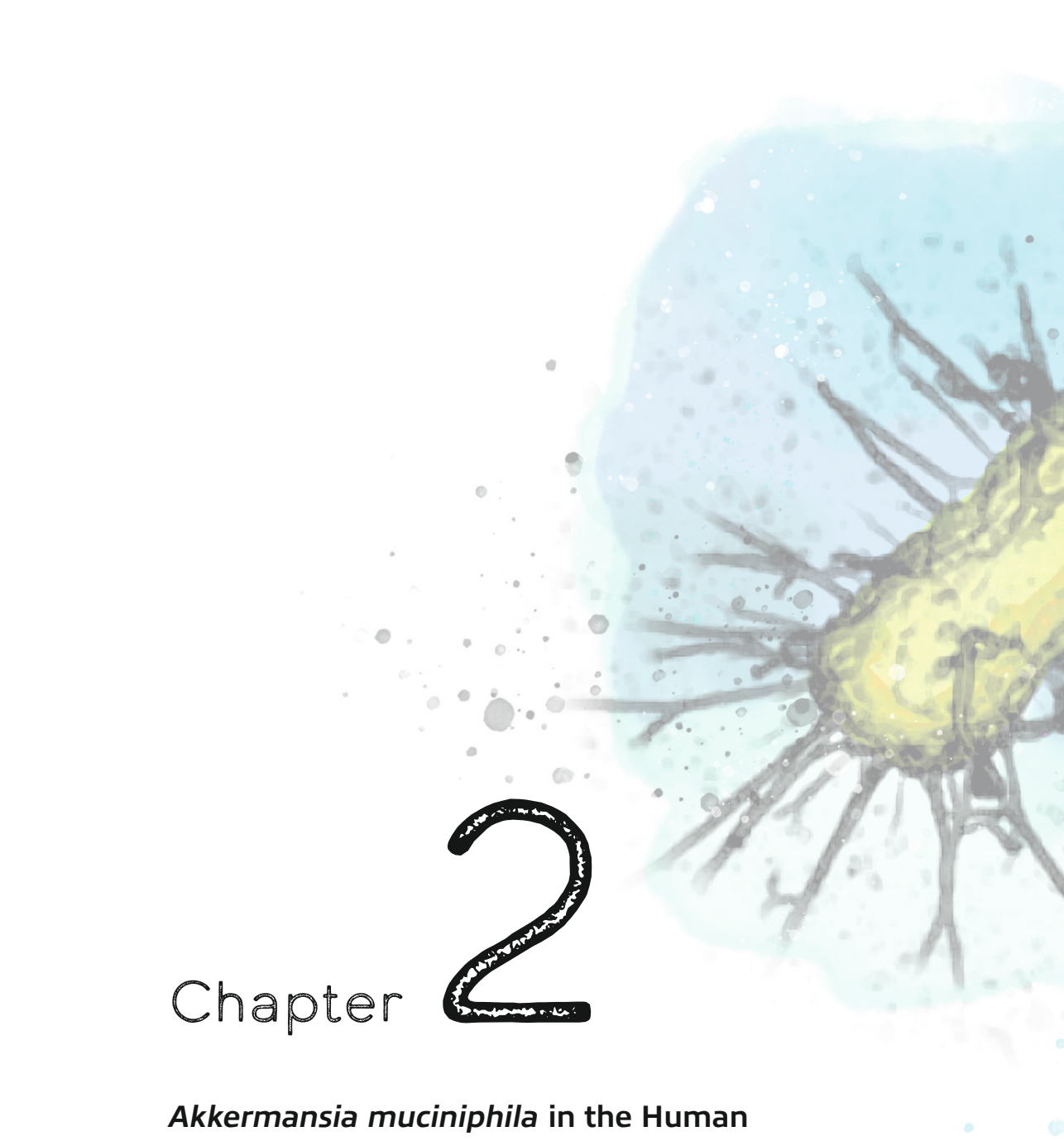

Chapter 2

Akkermansia muciniphila in the Human Gastrointestinal Tract: When, Where, and How?

Sharon Y. Geerlings, Ioannis Kostopoulos, Willem M. de Vos and Clara Belzer

Microorganisms doi:10.3390/microorganisms6030075

Abstract

Akkermansia muciniphila is a mucin-degrading bacterium of the phylum Verrucomicrobia. Its abundance in the human intestinal tract is inversely correlated to several disease states. *A. muciniphila* resides in the mucus layer of the large intestine, where it is involved in maintaining intestinal integrity. We explore the presence of *Akkermansia*-like spp. based on its 16S rRNA sequence and metagenomic signatures in the human body so as to understand its colonization pattern in time and space. *A. muciniphila* signatures were detected in colonic samples as early as a few weeks after birth and likely could be maintained throughout life. The sites where *Akkermansia*-like sequences (including Verrucomicrobia phylum and/or *Akkermansia* spp. sequences found in the literature) were detected apart from the colon included human milk, the oral cavity, the pancreas, the biliary system, the small intestine, and the appendix. The function of *Akkermansia*-like spp. in these sites may differ from that in the mucosal layer of the colon. *A. muciniphila* present in the appendix or in human milk could play a role in the re-colonization of the colon or breast-fed infants, respectively. In conclusion, even though *A. muciniphila* is most abundantly present in the colon, the presence of *Akkermansia*-like spp. along the digestive tract indicates that this bacterium might have more functions than those currently known.

Introduction

The microbial community in the human gut plays a role in the balance between health and disease. The gut microbiota has recently emerged as an important factor in human physiology, both under homeostatic and pathological conditions (Blaser 2014). Characterization of the gut microbiota may identify gut-related abnormalities and play an important role in establishing functional linkages to health status (Verdu et al. 2015). Some gut disorders with associated microbiota imbalance include celiac disease (Verdu et al. 2015), irritable bowel syndrome (IBS) (Distrutti et al. 2016, Lopez-Siles et al. 2014), inflammatory bowel disease (IBD) (Sheehan et al. 2015, Png et al. 2010, Rajilic-Stojanovic et al. 2013), and type 2 diabetes (T2D) (Zhang et al. 2013, Schneeberger et al. 2015, Everard et al. 2013).

The *A. muciniphila*-type strain Muc^T of the phylum Verrucomicrobia was first described in 2004 (Derrien et al. 2004). This bacterium was isolated from the fecal sample of a healthy individual using purified mucin as the sole source of carbon, nitrogen, and energy for growth. *A. muciniphila* has only a few similarities to other representatives of Verrucomicrobia (van Passel et al. 2011). Interestingly, *Akkermansia* is the only genus of the Verrucomicrobia phylum found in gut samples. Large differences were observed between verrucomicrobial genomes, in terms of the GC content and genome sizes. In contrast, similarities were observed within the Verrucomicrobia phylum as a large proportion of the proteins in verrucomicrobial proteomes were found to contain signal peptides (26.1% for *A. muciniphila*). In the colon of a healthy human being, *A. muciniphila* is present in high levels with an abundance of approximately 3% (Png et al. 2010, de Vos 2017). The core activity of *A. muciniphila* is to degrade mucus using the many mucolytic enzymes encoded in its genome (Png et al. 2010, van Passel et al. 2011).

The presence of *A. muciniphila* has been associated with healthy gut and its abundance has been inversely correlated to several disease states (Png et al. 2010, Rajilic-Stojanovic et al. 2013, Zhang et al. 2013, Swidsinski et al. 2011, Karlsson et al. 2012, Dao et al. 2016). For example, in cases of IBD (patients with ulcerative colitis and Crohn's disease), the abundance of *A. muciniphila* was found to be decreased (Png et al. 2010, Rajilic-Stojanovic et al. 2013). Also, individuals with acute appendicitis were found to harbor a decreased amount of *A. muciniphila* (Swidsinski et al. 2011). In this case, the abundance of *A. muciniphila* was inversely related to the severity of the appendicitis. Furthermore, obese children were shown to have a significant reduction in *A. muciniphila*-like bacteria (Karlsson et al. 2012). In a comprehensive study of infants in daycare, *A. muciniphila*-based sequences were found to be reduced in children that had received multiple antibiotic courses and were at risk for later

life obesity (Korpela et al. 2016). In concordance with these studies, another reported the association of *A. muciniphila* with a healthier metabolic status in obese and overweight individuals (Dao et al. 2016). Moreover, the genus *Akkermansia* and its metabolic pathways were found to be enriched in athletes with a low body mass index (Clarke et al. 2014, Barton et al. 2018). Lastly, the abundance of Verrucomicrobiae was significantly reduced in pre-diabetes and T2D (Zhang et al. 2013). It is important to note that these diseases may have an effect on the integrity or thickness of the mucus layer, and thereby effect the abundance of *A. muciniphila*. To confirm this, studies taking both the microbial composition and mucus layer integrity into account should be performed. Altogether, these studies indicate the correlation of *A. muciniphila* to a healthy status and indicate the possible use of *Akkermansia* spp. as a biomarker for disease.

Interactions between the host and *A. muciniphila* have been studied in mice (Everard et al. 2013, Derrien et al. 2011). Colonization by *A. muciniphila* resulted in transcriptional changes, leading to an increase in the expression of genes associated with immune responses (Derrien et al. 2011). Furthermore, *A. muciniphila* was found to strengthen the gut barrier function in mice (Everard et al. 2013). By doing so, *A. muciniphila* played a role in normalizing metabolic endotoxemia and adipose tissue metabolism. These findings have been supported by another study showing that *A. muciniphila* affects genes involved in cellular lipid metabolism (Lukovac et al. 2014). The effect of a fiber-free diet was studied in mice colonized with a synthetic community consisting of 14 species, including *A. muciniphila* (Desai et al. 2016). Feeding these mice a fiber-free diet was found to damage the mucus barrier. The changes in microbial community included an increased abundance of *A. muciniphila* and a switch in metabolism of gut microbiota species from fiber degradation to mucus glycan degradation (Desai et al. 2016, Makki et al. 2018). An in vitro study using human colonic cell lines (Caco-2 and HT-29) demonstrated the adherence of *A. muciniphila* to the intestinal epithelium, thereby strengthening the epithelial integrity rather than causing a pro-inflammatory reaction (Reunanen et al. 2015). Lastly, outer membrane proteins of *A. muciniphila* were found to have a role in the modulation of immune responses (Ottman et al. 2016). Recently, one of the outer membrane proteins was identified (Amuc_1100) (Ottman et al. 2017). This study demonstrated that the outer membrane pili-like protein is involved in immune regulation and the enhancement of trans-epithelial resistance.

Several studies have purposely or unintentionally revealed the presence of *Akkermansia*-like spp. in segments of the human body other than the colon, where *A. muciniphila* might also have important functions. In this review, we will discuss the presence of Verrucomicrobia and *Akkermansia*-like spp. in different anatomic regions of the digestive tract. The physiology and environmental parameters of these anatomic

regions will be taken into account to assess the possibility of *A. muciniphila* to colonize and be active at these niches.

Prevalence of *Akkermansia muciniphila* through Geography and Age in the Human Gut

Akkermansia muciniphila is present in the intestinal tract throughout different stages of life (Collado et al. 2007, Derrien et al. 2008). This was determined using fecal samples from healthy subjects divided into groups based on their age, analyzed using fluorescence in situ hybridization (FISH) and quantitative PCR (qPCR). The number of bacteria related to *A. muciniphila* significantly increased from early life to adult subjects (Collado et al. 2007, Derrien et al. 2008). When focusing on the prevalence of bacteria related to *A. muciniphila*, 16% of one-month old infants in this study were found to harbor *Akkermansia* in their intestinal tracts (Collado et al. 2007). At this very young age, the concentration of *A. muciniphila* ranged between 2.05 and 4.36 log cells per gram of feces. Subsequently, at 6 months of age the percentage of infants where *A. muciniphila* could be detected increased to 72%, with a further increase to 90% in 12-month-old infants. The concentrations were in the ranges of 2.50–7.30 and 2.80–9.50 log cells per gram of feces in 6-month-old and 12-month-old infants, respectively. However, in this study no correlation was made between the *A. muciniphila* abundance and the feeding mode of the infant (breast and/or formula feeding). Other studies not primarily focusing on the presence of *A. muciniphila* have also shown the presence of *Akkermansia*-like spp. or the Verrucomicrobia phylum in the infant's gut at different geographical locations, such as Finland, Germany, and Malawi (Grzeskowiak et al. 2012, Grzeskowiak et al. 2012, de Weerth et al. 2013). The presence of *A. muciniphila* in the infant's gut could be considered as a marker for gut microbiota development and diversity (Grzeskowiak et al. 2012). Next to infants, adults (25–35 years old) were found to harbor 5–8.8 log cells per gram of feces of *A. muciniphila*, while a significant decrease was noted in elderly subjects (80–82 years old) namely, 95.5% (Collado et al. 2007). These outcomes differed in another study, where young adults harbored significantly less *Akkermansia* spp. than the elderly both in terms of prevalence and abundance (Biagi et al. 2010). In addition, centenarians were found to harbor a higher concentration of *Akkermansia* spp. Also, semi-supercentenarians (individuals with an age of 105 or higher) had a higher concentration of *Akkermansia*-like spp. than other (younger) age groups in the study (Biagi et al. 2016). *A. muciniphila* is proposed to have a role in the immunological and metabolic health of semi-supercentenarians, rendering it a biomarker for healthy aging. In contrast to age, gender does not play a role considering the amount of *A. muciniphila* (Derrien et al. 2008).

The genome of *A. muciniphila* (ATCC BAA-835) was sequenced and annotated (van Passel et al. 2011). These sequences were used to mine 37 reported gut metagenomes derived from adults belonging to six nationalities to evaluate the presence and genetic diversity of *Akkermansia* spp. in the human gut. The prevalence of *Akkermansia* spp. in these metagenomes was found to be 30%, using a cutoff of >95% identity to 16S rRNA. When queried with the *Akkermansia* genome (identity > 90%), 62% of the metagenomic libraries were shown to be *Akkermansia* carriers, which is comparable to earlier findings of a Finnish cohort (Collado et al. 2007). The relative abundances of *Akkermansia* spp. DNA in these libraries varied from <0.01% to almost 4% (van Passel et al. 2011). However, higher abundances of Verrucomicrobia in the GIT have also been reported, for example in biopsy samples (up to ~15% depending on the method and individual) (Momozawa et al. 2011). The analysis of fecal samples from the Metagenomics of the Human Intestinal Tract (MetaHit) project, derived from Danish and Chinese individuals, revealed country-specific differences in gut microbiota (Li et al. 2014). In terms of *Akkermansia*-like spp., the mean relative abundance of Danish individuals (0.0137) was higher than that of Chinese individuals (0.0015). Moreover, a recent study showed that Verrucomicrobia sequences were found to be enriched in the guts of industrialized regions compared to the guts of traditional populations ($p < 2 \times 10^{-16}$), such as the traditional Hadza hunter-gatherers (Smits et al. 2017). However, as with many comparative microbiota analyses, confounding factors related to sample processing, DNA extraction, and subsequent processing cannot be ruled out (Costea et al. 2017). A study performed in China showed that the frequency of *A. muciniphila* is lower in southern Chinese than in European populations (Guo et al. 2016). The frequency in southern China was found to be 51.71%, which is significantly lower than the ~75% found in European populations (Collado et al. 2007, Guo et al. 2016). Interestingly, in southern China the highest frequencies were detected among the elderly, while in European populations a significant decrease was noted for the elderly. This observed difference may be due to external factors affecting the microbiota composition, including geographic location, diet, and age.

The human gut may be colonized by different *Akkermansia*-like spp. (van Passel et al. 2011). The 16S rRNA sequences detected in metagenomic datasets suggested colonization by at least eight different *Akkermansia*-like spp. However, as these sequences derived from short Illumina reads, mis-assembly and other technical biases may have affected this conclusion. Moreover, it is also possible that simultaneous colonization by different species occurs. Recently, 39 *A. muciniphila* strains were isolated from human and mouse feces and subsequently analyzed for their 16S rRNA sequences and draft genomes (Guo et al. 2016, Guo et al. 2017). All 16S rRNA sequences from these strains shared over 97% sequence identity with that of the type strain *A. muciniphila* Muc^T isolated from Europe, suggesting that they represent isolates

from the same species. Using these isolates, three phylogroups (AmI, AmII, and AmIII) were identified based on core genome single nucleotide polymorphisms (SNPs). We constructed a maximum likelihood tree based on the available 16S sequences of the Chinese *A. muciniphila* strains in the National Center for Biotechnology Information (NCBI) sequence database and all other 16S rRNA *Akkermansia*-like sequences derived from colonic and ileal biopsy samples derived from the SILVA small subunit Reference 132 dataset (**Figure 1**a and Supplementary **Figure S1**). In this tree, the newly isolated Chinese *A. muciniphila* strains fall into two out of three distinct clades (clades one and two) that, however, have only minimal differences. In comparison with the type strain, the first clade has 99–100% identity, the second clade 98–99%, and the third clade 98%. Interestingly, the Chinese *A. muciniphila* strains have reportedly distinct metabolic and functional features (Guo et al. 2017). However, unlike *A. muciniphila*-type strain Muc^T, complete closed genomes of these Chinese *A. muciniphila* strains have not been reported. Furthermore, functional analysis of the Chinese *A. muciniphila* strains has not been performed, but the strains are able to grow on mucus (Guo et al. 2017). Next to *A. muciniphila*, only one other *Akkermansia*-like sp. has been validly described, namely *Akkermansia glycaniphila* strain Pyt^T isolated from reticulated python feces (included in the phylogenetic tree shown in **Figure 1**a) (Ouwerkerk et al. 2016, Ouwerkerk et al. 2017). The closest relative of *A. glycaniphila* is *A. muciniphila* Muc^T, sharing 94.4% 16S rRNA sequence similarity (Ouwerkerk et al. 2016). The average nucleotide identity between the *A. glycaniphila* Pyt^T genome and the genome of *A. muciniphila* Muc^T was found to be 79.7%. Compared to *A. muciniphila*, *A. glycaniphila* is also able to use mucin as a sole carbon, energy, and nitrogen source. However, the relatedness between these two species, determined by DNA-DNA hybridization, is low, namely 28.3%. To be able to compare functional differences between Chinese *A. muciniphila* strains, the *Akkermansia*-like sequences found in biopsies of the ileum and large intestine (included in the tree), and *A. muciniphila* Muc^T, enclosed genomes and functional analyses are needed.

Altogether, *A. muciniphila*'s presence varies among individuals. Its abundance varies not only from person to person but also from age group to age group. On top of that, other factors such as geographical location may also play an important role in the presence and richness of *Akkermansia*-like spp. in the human GIT.

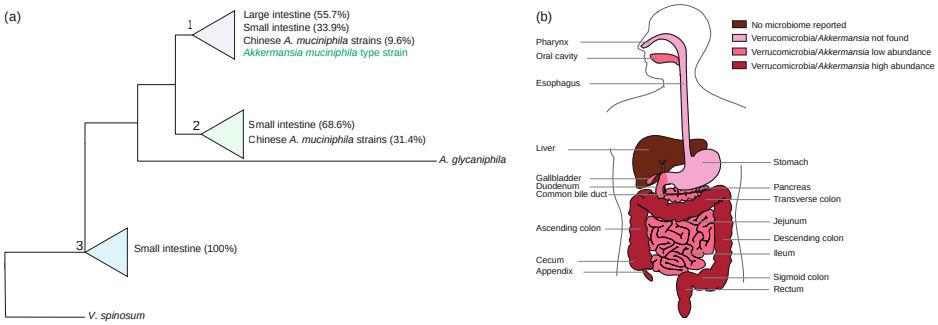

Figure 1. (**a**) *Akkermansia* is not only present in the large intestine, but also in other anatomic regions of the digestive tract. A schematic overview of the positioning of 16S rRNA clones in the small and large intestines and the available sequences of the Chinese *A. muciniphila* strains towards the *A. muciniphila*-type strain Muc^T and *A. glycaniphila* Pyt^T. The percentages indicate the compositions of the clades. The tree was generated using the randomized axelerated maximum likelihood (RAxML) method version 7.0.3 in ARB using a 40% positional conservatory filter (Ludwig et al. 2004). The original detailed maximum likelihood tree is shown in Supplementary Figure S1. Similar groups were observed using the neighbor joining method (Supplementary Figure S2). (**b**) Overview of Verrucomicrobia/*Akkermansia* sequences in the human digestive tract.

Physiologic Adaptation of *Akkermansia muciniphila* to the Human GIT

A. muciniphila is an oval shaped, anaerobic Gram-negative bacterium that was first described by Derrien et al. (Derrien et al. 2004). Transmission electron microscopy revealed the presence of filamentous structures on Muc^T cells when grown on mucin medium. On top of this, strain Muc^T is able to exclude Indian ink, suggesting that the filamentous structures are capsular polymers. More recently, outer membrane proteins of *A. muciniphila* were analyzed, which resulted in the identification of pili proteins (de Vos 2017, Ottman et al. 2016, Ottman et al. 2017).

When focusing on the growth parameters of *A. muciniphila*, it is known that growth was observed between temperatures of 20 and 40 °C and pH values of 5.5–8.0 (**Figure 2**) (Derrien et al. 2004). However, the optimum growth temperature and pH are 37 °C and 6.5, respectively. *A. muciniphila* is an obligate chemoorganotroph, utilizing mucus as a sole carbon, nitrogen, and energy source (Derrien et al. 2004). Consequently, the short chain fatty acids (SCFAs) acetate, propionate, and to smaller extent 1,2-propanediol and succinate are produced (Derrien et al. 2004, Ottman et al. 2017). Another factor that influences the growth of *A. muciniphila* is the presence of oxygen. *A. muciniphila*

was found to be able to tolerate and even benefit from nanomolar concentrations of oxygen in liquid medium (Ouwerkerk et al. 2016). Upon the presence of oxygen, there is a change of acetate to propionate production by *A. muciniphila*. This results in an increased production of ATP and NADH, which enhances the growth of *A. muciniphila*.

To compose a minimal medium for *A. muciniphila*, a genome-scale metabolic model was constructed (Ottman et al. 2017). This model predicts the degradation of mucin-derived monosaccharides. The model showed that *A. muciniphila* is able to synthesize all essential amino acids, except for l-threonine, was not present in the pathway. Furthermore, growth experiments revealed that *A. muciniphila* can degrade a variety of sugars such as glucose, *N*-Acetylglucosamine (GlcNAc), *N*-Acetylgalactosamine (GalNAc), and fucose. However, to obtain growth large amounts of casein tryptone, mucin or a rich medium was required. Hereafter, another study showed that *A. muciniphila* does not code for GlmS, which mediates the conversion of fructose-6-phosphate to glucosamine-6-phosphate (van der Ark et al. 2018). This reaction is essential for peptidoglycan formation. Therefore, the degradation of glucose does not lead to biomass production. *A. muciniphila* does code for NagB, which catalyzes the reverse reaction, indicating that the addition of GlcNAc is essential for growth of *A. muciniphila*. Altogether, this information led to the development of a defined minimal medium for *A. muciniphila,* in which l-threonine and GlcNAc or GalNAc are essential components for growth (van der Ark et al. 2018).

Recently, the growth of *A. muciniphila* in the presence of bile has been studied (van der Ark et al. 2017). Interestingly, the *A. muciniphila* abundance was positively correlated to circulating primary bile acids in mice (Pierre et al. 2016). The addition of 0.1%, 0.5%, and 1% porcine bile extract resulted in increased growth of *A. muciniphila* in comparison to the medium that did not contain bile (van der Ark et al. 2017). In contrast, purified bile salts addition of 0.5% or higher resulted in inhibited growth of *A. muciniphila*, whereas the addition of 0.1% purified bile salts did not inhibit growth (van der Ark 2018). Moreover, the survival of *A. muciniphila* in gastric juice was found to be very low (van der Ark et al. 2017).

Several studies have described the antibiotic resistance of *A. muciniphila* (Dubourg et al. 2013, Dubourg et al. 2017). The type strain of *A. muciniphila* (Muc^T) was found to be susceptible to imipenem, piperacillin/tazobactam, and doxycycline, while resistance was noted for vancomycin, metronidazole, and penicillin G (Dubourg et al. 2013). Another *A. muciniphila* strain was resistant against vancomycin and ofloxacin, but susceptible to penicillin, amoxicillin, ceftriaxone, and imipenem (Dubourg et al. 2017). *A. muciniphila* MucT has potential beta-lactamase genes and may code for a 5-nitroimidazole antibiotic resistance protein (van Passel et al. 2011). The in

silico prediction of a strain directly sequenced from stool (*A. muciniphila* strain Urmite) predicted the presence of antibiotic resistance genes for the classes beta-lactamases, glycopeptides, MLS (macrolides, lincosamides, streptogramines), phenicol, sulphonamide, tetracycline, and trimethoprim (Caputo et al. 2015). Guo et al. described the presence of three antibiotic resistance genes in *A. muciniphila* strain GP36, which originated from plasmid pRSF1010 (8684 bp) of *Salmonella enterica* (Guo et al. 2017). This indicates that *A. muciniphila* might acquire antibiotic resistance genes through lateral gene transfer.

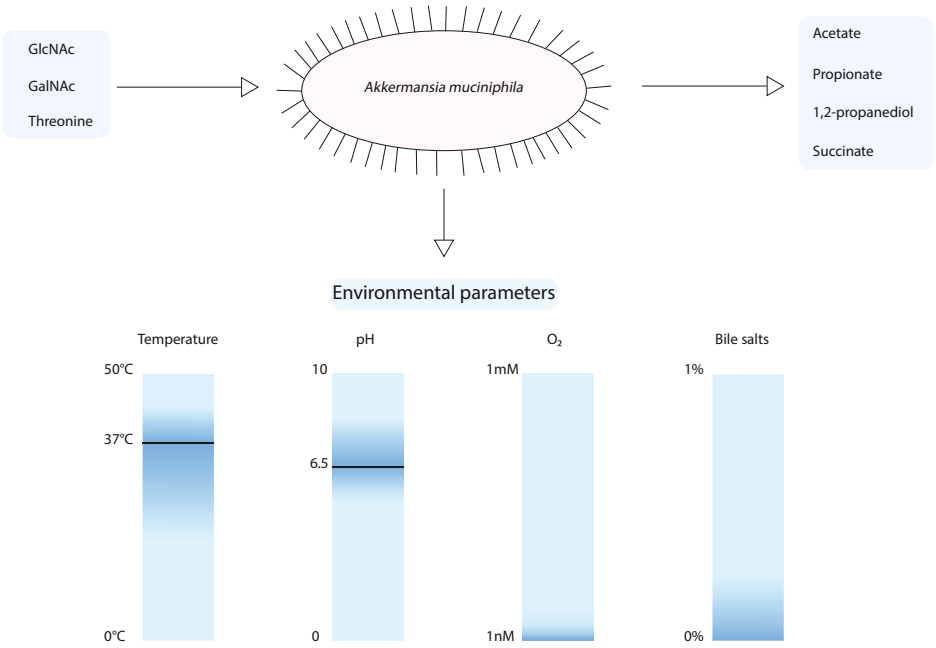

Figure 2. Schematic overview of the growth parameters of *A. muciniphila*. The optimum growth temperature and pH are 37 °C and 6.5, respectively. In addition, *A. muciniphila* is able to tolerate nM concentrations of oxygen and is able to grow in the presence of 0.1% purified bile salts.

The growth parameters of *A. muciniphila* described above coincide with the environmental parameters found in the large intestine. The oxygen concentration in the gut follows a steep gradient from the intestinal submucosa to the lumen, where the oxygen concentrations decrease to near anoxia (Espey 2013). *A. muciniphila* may take advantage of this oxygen concentration in the mucus layer, enhancing its growth. The mucosal layer of the large intestines serves as a carbon, nitrogen, and energy

source for the use of *A. muciniphila*. The mucin backbone is rich in threonine (among other amino acids) and contains many sugar groups, including GlcNAc and GalNAc (Johansson et al. 2011). As mentioned earlier, these are among the minimal growth requirements of *A. muciniphila*. Although the mucus layer in the large intestine is thought to be the optimal niche for *A. muciniphila*, mucus is also present at other locations of the GIT. Several conditions may vary in the GIT, such as type of mucin that is secreted, pH, oxygen concentration, and concentration of bile acids. The ability of *A. muciniphila* to cope with these conditions will be discussed below.

Akkermansia muciniphila along the Human Gastrointestinal Tract

Akkermansia-like spp. were found to be present in different anatomical regions of the digestive tract, including the oral cavity, breast milk, pancreas, biliary system, small and large intestines, and appendix (**Figure 1**b). Next to the aforementioned regions, *Akkermansia*-like sequences were also detected in human blood (Dubourg et al. 2017, Santiago et al. 2016, Traykova et al. 2017). However, the presence of *Akkermansia*-like sequences was only detected in subjects with diseases as septicemia and cirrhosis. In a mice study, *A. muciniphila* was detected in the oral cavity, stomach, small intestine, and large intestine the upon administration of breast milk and formula milk (Gomez-Gallego et al. 2014). However, in this review we will mainly focus on the presence of *Akkermansia*-like spp. in the human body.

Oral Cavity

The oral cavity is a moist environment with a relatively constant temperature between 34 and 36 °C (Marcotte and Lavoie 1998). There are several ecological niches in the oral cavity that mostly have a neutral pH. The mean pH of the mucosal sites was found to be 6.78 ± 0.04 (Aframian et al. 2006). Examples of different sites in the oral cavity are the tongue, soft and hard palates, tooth surfaces, and tonsils (Marcotte and Lavoie 1998). In terms of temperature and pH, the oral cavity can support the growth of a wide variety of microorganisms. Therefore, the microbial community of the oral cavity is site-specific and highly diverse (Aas et al. 2005).

Several studies found a high abundance of the phyla Firmicutes, Proteobacteria, Bacteroidetes, and Actinobacteria, with *Streptococcus* (belonging to the phylum Firmicutes) being the most abundant genus (Shaw et al. 2017, Bik et al. 2010). The presence of Verrucomicrobia in the oral cavity is often not described (Shaw et al. 2017, Bik et al. 2010, Nasidze et al. 2009, Sarkar et al. 2017, Leake et al. 2016). However, the presence of *Akkermansia*-like sequences was found in the oral cavity

of a choledocholithiasis patient (Ye et al. 2016). The salivary samples were taken by gargling with 20 mL of sterile saline water. Thus, the microorganisms in these samples originate from multiple niches in the oral cavity.

The relative abundance of *Akkermansia*-like spp. in this sample was low, namely 0.02% (Ye et al. 2016). In addition, these sequences were only found in one out of six patients included in this study. In terms of pH and temperature, *Akkermansia* spp. could be able to survive in the oral cavity (Derrien et al. 2004). Furthermore, Gram-negative and obligate anaerobes with proteolytic lifestyles are present in healthy gingival crevice biofilms (Marsh et al. 2015). As discussed before, *A. muciniphila* has a mucin-degrading lifestyle (Derrien et al. 2004). The mucins found in the oral cavity are MUC5B, MUC7, MUC19, MUC1, and MUC4 (Linden et al. 2008). Of these mucin structures, MUC5B is the most abundant gel-forming mucin in the oral cavity (Nielsen et al. 1997, Thornton et al. 1999). As *A. muciniphila* has mucin-degrading enzymes similar to those found in oral *Streptococcus* spp., *A. muciniphila* might be able to use the mucin structures in the oral cavity as a substrate for growth (van der Hoeven et al. 1990, Derrien et al. 2010). However, further research is needed to confirm this hypothesis.

Mucin oligosaccharides are able to bind microbes and in some cases exert functions in antimicrobial activity or carry antimicrobial proteins (Linden et al. 2008). For example, MUC7 and MUC5B both bind statherin and histatin-1. By binding these molecules, mucins exert a protective function in the oral cavity. The potential role of *Akkermansia* spp. in the oral cavity is unknown. However, one could hypothesize that its capability to stimulate the mucus production of the epithelial cells enhances their protection e.g., against pathogens. Another possibility could be that *Akkermansia* spp. produces compounds in mucin degradation that could be useful for other bacteria in the oral microbial community. Lastly, *Akkermansia* spp. might be involved in the modulation of the host response. Altogether, more studies should be conducted to confirm the presence of *Akkermansia* spp. and its function in the oral cavity.

Pancreas

The pancreas is a complex organ comprised of both exocrine glands (secreting digestive enzymes into the intestinal lumen) and endocrine glands, called the islets of Langerhans, which secrete hormones directly into the bloodstream (Tan 2014). The pancreas plays a central role in human metabolism, allowing ingested food to be converted and used as fuel by cells throughout the body. The pancreas may be affected by devastating diseases, such as pancreatitis, pancreatic adenocarcinoma (PAC), and diabetes mellitus (DM), which generally results in a wide metabolic imbalance (Leal-Lopes et al. 2015). Nutrient metabolism in pancreatic cells is not only essential for providing energy for the cell, but also serves as a mechanism to

sense and react to circulating levels of macronutrients. This gives the pancreas a central role in metabolism regulating the whole-body energy homeostasis. Efficient energy metabolism in pancreatic endocrine cells of the islets is required to permit the secretion of many hormones, mainly insulin and glucagon, that regulate glucose and lipid utilization throughout the body. The pancreas is thought to be devoid of bacteria. However, microbial translocation as a result of disease states has led to measurements of microbes in pancreatic tissue. Because it is dangerous and impossible to take biopsies of pancreatic tissue, due to the risk of leakage of pancreatic fluid, pancreatic samples can only be obtained via surgery. As such, samples of healthy individuals are not yet reported. Healthy controls are usually healthy tissue surrounding a pathologic site. Recent research has shown that disruption of pancreatic metabolism is often a consequence of disruptions in the gut microbiome (Jouvet and Estall 2017). Another study has shown that the pH in the pancreas drops significantly (p-value < 0.05) in patients with painful chronic pancreatitis (7.02 ± 0.06) compared to healthy individuals (7.25 ± 0.04) (Patel et al. 1995). That pH change in patients with chronic pancreatitis might be one of the reasons why the bacterial barrier in the pancreas is ruptured and the abundance of bacterial phyla and species is elevated (Memba et al. 2017).

A. muciniphila plays an important role in the maintenance of the gut barrier function (Dao et al. 2016). A few studies have shown the association of *A. muciniphila* with the pancreas and its health. A recent study with patients undergoing pancreatic fluid pancreaticoduodenectomy (PD) revealed that the mean relative abundances of the Verrucomicrobia phylum and *Akkermansia* genus, respectively, were 0.0005 and 0.0004 in the pancreas of these patients (Rogers et al. 2017). The study also highlighted that in the pancreas tissue of the patients, other commensal bacteria were found to be present. The Proteobacteria phylum and *Klebsiella* genus were the most abundant, with mean relative abundances of 0.5410 and 0.2011, respectively. *Faecalibacterium*, *Bacteroides*, and *Prevotella* were also detected in the pancreas of PD patients. The presence of other gut microbes in the pancreas apart from *Akkermansia* may indicate trophic interactions between them.

Interestingly, it was found that mice treated with pancreatic enzyme replacement therapy (PERT), had a significant, 58-fold increase of *A. muciniphila* sequences compared to the control samples (mice treated with tap water) (Nishiyama et al. 2018). Furthermore, it is stated that pancrealipase diminishes pancreatic exocrine insufficiency-associated symptoms by inducing the colonization of *A. muciniphila* followed by the normalization of the intestinal barrier. Therefore, it is hard to speculate on the role of *Akkermansia* species and/or *A. muciniphila* in the pancreas.

The *Akkermansia* genus is detected in the pancreas, mainly in conditions of pathology. The significant change of pH of the pancreatic fluid in patients with chronic pancreatitis (7.02 ± 0.06) might be a reason why *Akkermansia* was detected in pathological conditions. Thus far, there is not any evidence showing that the pancreas is colonized by bacteria in healthy individuals or that it is a bacteria-free organ. In all of the studies that have been described so far, the bacterial colonization of the pancreas is inextricably linked to the cause of pancreatic disease. The higher abundance of bacteria in patients with pancreatic diseases could be associated with an overall higher abundance of microbiota members in these states of disease due to bacterial overgrowth and translocation. Decreased gut barrier function in both acute and chronic pancreatitis increases bacterial translocation. This bacterial translocation could have significant impact on the nutrient absorption and therefore on the availability of nutrients for intestinal microorganisms, and the microbial composition of the gut.

Bile Ducts and Gallbladder

Bile is a complex aqueous solution secreted by the liver (Boyer 1986). Both gallbladder bile and common bile duct bile of patients undergoing cholecystectomy were found to have an alkaline pH in the ranges of 6.8–7.65 and 7.5–8.05, respectively (Sutor and Wilkie 1976). In most animal/mammal species, bile contains less than 5% solid contents (Boyer 1986). The most abundant organic substances in bile are bile salts (Boyer 2013). The primary bile salts in the mammalian liver are cholic acid and chenodeoxycholic acid (CDCA). They are produced from cholesterol in the liver and are then excreted into the duodenum (Islam et al. 2011). Bile salts exert several functions. For example, they were found to have a role in antimicrobial defense, promoting lipid absorption and protein digestion and assimilation (Inagaki et al. 2006, Gass et al. 2007). Conjugation of these bile salts occurs at the side chain, where either taurine or glycine is added, leading to the formation of stronger acids (Boyer 2013). Intestinal bacteria are able to convert the stronger acids producing secondary bile acids by deconjugating them. Large amounts of bile salts are secreted into the gut; however, only limited amounts are excreted from the human body (Hofmann 1976). More than 95% of the bile salts are reabsorbed in the ileum and redirected to the liver for recirculation. According to this enterohepatic circulation mechanism, each bile salt is recirculated approximately 20 times.

Interestingly, the bile duct was first considered to be generally sterile (Csendes et al. 1975). However, more recently several studies have focused on the microbial community present in bile (Ye et al. 2016, Rogers et al. 2017, Shen et al. 2015, Wu et al. 2013, Pereira et al. 2017, Scheithauer et al. 2009). The phyla Firmicutes, Fusobacteria, Proteobacteria, Actinobacteria, and Bacteroidetes (among others), have been identified in bile samples (Ye et al. 2016, Rogers et al. 2017, Wu et al. 2013, Pereira et

al. 2017). These phyla are all commonly found in the human gut (Stearns et al. 2011). Subsequently, the bacteria found in the biliary tract are likely to originate from the human duodenum (Ye et al. 2016). The most common genera in bile samples were found to be *Prevotella*, *Streptococcus*, *Veillonella*, *Fusobacterium*, and *Haemophilus* (Pereira et al. 2017).

To study the function of the biliary microbiota, predictive functional profiles were constructed using Phylogenetic Investigation of Communities by Reconstruction of Unobserved States (PICRUSt) (Ye et al. 2016). This method revealed that biliary bacteria have significantly enriched pathways, in comparison to the upper digestive tract microbiota, related to environmental information processing, cell motility, carbohydrate metabolism, amino acid metabolism, and lipid metabolism. Furthermore, several studies have focused on the role of the biliary microbiota in the development of diseases such as gallstone disease and biliary neoplasia in primary sclerosing cholangitis (PSC) (Wu et al. 2013, Pereira et al. 2017, Belzer et al. 2006, Saltykova et al. 2016). However, to explore the exact role of the microbiota in gallstone formation, more research needs to be conducted. In addition, PSC was not associated with changes in the microbial community of the biliary system (Pereira et al. 2017). However, *Streptococcus* species were found to be positively correlated to disease progression and might therefore have a pathogenic role in the progression of PSC.

Although the presence of Verrucomicrobia and/or *Akkermansia*-like sequences has not been described in all studies involving the biliary microbiota, they have been found to be present in a proportion of studies including bile samples (Ye et al. 2016, Rogers et al. 2017, Wu et al. 2013, Pereira et al. 2017). In a study describing the bacterial community in bile and gallstone samples, *Akkermansia*-like sequences were detected (Wu et al. 2013). The relative abundance of *Akkermansia*-like sequences in 12 out of 26 bile samples ranged between 0.03 and 0.4%. In addition, 10 out of 29 gallstone samples contained *Akkermansia* spp. with a relative abundance ranging between 0.02% and 0.3%. *Akkermansia*-like sequences were also detected by another study in the bile sample of one out of six gallstone patients, revealed using V3-4 Illumina sequencing (Ye et al. 2016). The relative abundance of *Akkermansia*-like sequences in this sample was low, namely 0.153%. In addition, the mean relative abundances of Verrucomicrobia and *Akkermansia* spp. were determined to be 0.05% and 0.04%, respectively, in bile samples from 50 patients undergoing pancreaticoduodenectomy (Rogers et al. 2017). Furthermore, bile samples of subjects with opisthorchiasis (bile duct infection by *Opisthorchis felineus* (Fedorova et al. 2018)) contained higher amounts of Verrucomicrobia (among other phyla) than subjects with gallstone disease without infection of *O. felineus* (Saltykova et al. 2016). The presence of Verrucomicrobia was not specific to the *Akkermansia* genus and the exact relative abundance of

Verrucomicrobia was not provided. Even though five phyla including Verrucomicrobia were found to be more abundant in infected subjects than non-infected subjects, there were no functional differences between these groups based on analysis using PICRUSt. The studies described in this section were properly controlled for contaminants.

The pH values of gallbladder bile and common bile duct bile are both within the growth range of *A. muciniphila*. However, for *Akkermansia* spp. to be able to remain in bile, they are expected to harbor a mechanism for protection against bile. A putative bile acid transporter gene (Amuc_0139) is annotated in the genome of *A. muciniphila*, which might function to export bile acids from the cell (van der Ark 2018). This process could reduce the effects of bile acids inside the cells of *A. muciniphila*. Another possible mechanism, as identified in *Bifidobacterium* spp., is the protection of the cell wall against bile acids by the production of exopolysaccharides (Fanning et al. 2012, Ruas-Madiedo et al. 2009). However, this mechanism has not been identified for *Akkermansia muciniphila.*

Several mucins have been identified in the biliary tract, specifically in the gallbladder. The mucins that are expressed in the gallbladder are MUC3, MUC5B, MUC5AC, and MUC6 (Gum et al. 1997, Pigny et al. 1996, Keates et al. 1997, Yoo et al. 2016). Even though colonic mucin consists mainly of MUC2, *A. muciniphila* might be able to use the mucins in the gallbladder as a substrate. Next to *Akkermansia* spp. other bacteria with mucin-degrading capacities in the GI tract have been identified in the biliary system. As such, *Streptococcus anginosus* (Saltykova et al. 2016) and bacteria with operational taxonomic unit (OTU) IDs with 99% identity matching that of *Bacteroides vulgatus* (Wu et al. 2013) were found to be present in bile samples. Although the function of *Akkermansia* spp. in the biliary system is unknown, it might have a role in the strengthening of the mucosal barrier. In this way, the mucosal layer may provide increased protection against pathogens. This could explain the increase of Verrucomicrobia during infection of *Opisthorchis felineus,* since it might function to strengthen the mucosal barrier and thereby provide protection during infection.

Small Intestine

The GIT supplies the human body with energy and essential nutrients (Zoetendal et al. 2012). This is achieved by the conversion and absorption of food components reaching the small intestine. The small intestine can be divided into three segments: duodenum, jejunum, and ileum (Savage 1977). The transit time of the small intestine was found to be between 30 min and 4.5 h (Hung et al. 2006). Once the gastric content enters the duodenum, it is neutralized by bicarbonate derived from the pancreas, liver, and duodenal mucosa, causing pH fluctuations (Ovesen et al. 1986). More recent investigations of pH profiles revealed that pH values increased from 5.9–6.3 in the

proximal part of the small intestine (duodenum) (Koziolek et al. 2015). In the distal parts, pH values were found to increase to pH 7.4–7.8.

The epithelial cells within the small intestine are covered with mucus. In contrast to the mucosal layer in the stomach and the colon, the mucosal layer in the small intestine is thinner and less dense (Atuma et al. 2001). In addition, this layer is not firmly attached to the epithelial surface and forms a soluble mucus gel (Atuma et al. 2001, Johansson et al. 2008). The mucus gel layers observed in the duodenum and jejunum are similar in thickness, although no loose/sloppy mucus was found in the jejunum (Atuma et al. 2001). In contrast to the duodenum and jejunum, the mucus layer in the ileum is significantly thicker. The accumulation rates were similar throughout the different segments of the small intestine.

The fast transit time, in comparison to the large intestine, contributes to limited microbial growth in the small intestine (Savage 1977). In addition, the secretion of digestive enzymes and bile into the small intestine creates a harsh environment in terms of microbial growth (Zoetendal et al. 2012). The bacterial concentration in the duodenum and jejunum is only 10^3–10^4 bacteria/mL content (Sender et al. 2016). This concentration increases in the ileum, where the bacterial concentration is 10^8 bacteria/mL content. Due to the challenging conditions for microbial growth in the small intestine (acidity and higher oxygen levels than in the colon), the microbial community is dominated by bacteria that are facultative anaerobic, able to grow quickly, and able to tolerate bile acids and antimicrobials (Donaldson et al. 2016). At the same time, these bacteria are also competing with the host and other microorganisms for simple sugars in the small intestine. Interestingly, phagocytes in the small intestine are thought to play a role in immune surveillance of the small intestinal mucosa (Morikawa et al. 2016). This means that phagocytes are able to selectively take up bacteria, which might be linked to maintaining immune homeostasis.

The location of the small intestine in the human body causes difficulties in sampling, in comparison to, for example, the oral and fecal microbiota. Therefore, fewer studies have been performed describing the microbiota in the small intestine (Zoetendal et al. 2012, Sundin et al. 2017). In the duodenum, the phyla Firmicutes and Actinobacteria were found to be predominant in the duodenal fluid of both obese and healthy groups (n = 5 for each group) (Angelakis et al. 2015). Other (less abundant) phyla detected in the duodenum were Proteobacteria, Fusobacteria, TM7, Bacteroidetes, and Tenericutes. However, an inter-individual variability in the taxonomic composition between these samples was observed. Even though the duodenum was found to have fewer OTUs than mouth, colon, and stool samples, it does harbor most phyla observed in the other sites (Stearns et al. 2011). The mucosa-associated microbiota

of the duodenum was found to be dominated by the phylum Firmicutes and genus *Streptococcus* (Shanahan et al. 2016). The genera *Prevotella, Veillonella*, and *Neisseria* were also found to be present in the mucosal layer. Interestingly, the duodenal mucosa-associated microbiota found in this study overlaps in broader levels of classification with that of the oral cavity and saliva. Further down the small intestine, the most dominant phyla in jejunal fluid were found to be Firmicutes, Proteobacteria, and Bacteroidetes (Sundin et al. 2017). Less abundant phyla (5–10%) were Actinobacteria and Fusobacteria. In comparison to the findings of the microbiota composition in the duodenum, the abundance of Proteobacteria and Bacteroidetes were found to be dominant over Actinobacteria in the jejunum (Sundin et al. 2017). When comparing the microbiota composition found in samples obtained after the washing procedure and mucosal biopsies, these compositions were highly similar. The last part of the small intestine (ileum) was found to be dominated by the phyla Bacteroidetes, *Clostridium* cluster XIVa, and Proteobacteria (Zoetendal et al. 2012, Li et al. 2012).

Several studies have focused on the small intestinal microbiota in disease states, such as IBS, Crohn's disease, and liver cirrhosis (Hartman et al. 2009, Haberman et al. 2014, Dlugosz et al. 2015, Chen et al. 2016, Assa et al. 2016). A study focused on IBS showed that the small intestinal microbiota of IBS patients and healthy individuals did not differ in terms of major phyla or genera (Dlugosz et al. 2015). In contrast, the duodenal mucosal microbiota of cirrhotic patients were surprisingly different to that of healthy controls (Chen et al. 2016). The dysbiosis observed in duodenal samples of cirrhotic patients might be associated with an altered oral microbiota or an altered environment of the duodenum.

Even though the phylum Verrucomicrobia is not included in the dominant microbial compositions described above, Verrucomicrobia and *Akkermansia*-like spp. have been detected in all segments of the small intestinal tract. In duodenal fluid, Verrucomicrobia and *Akkermansia*-like spp. were found in three out of six subjects (with relative abundances of 0.17%, 0.012%, and 0.013%) using V3-4 Illumina sequencing (Ye et al. 2016). In addition, Verrucomicrobia (not specified to *Akkermansia*) were detected in duodenal biopsies (0.0688%) and mucus (0.0387%) using 454/Roche GS FLX sequencing (Li et al. 2015). Jejunal contents have also been shown to harbor *Akkermansia*-like spp., with a mean relative abundance of 0.01% (n = 17) (Rogers et al. 2017). Analysis of swabs from jejunal contents were performed using Illumina MiSeq. Another study detected *Akkermansia*-like spp. in four out of 20 subjects with concentrations ranging from three to 90 hits, equaling to 0 to 0.029% of total hits, also using Illumina MiSeq (Rogers et al. 2017). Furthermore, Verrucomicrobia were found in the distal ileum using direct cloning and sequencing, making up 5% of the detected microbial community (Wang et al. 2005). Lastly, *Akkermansia*-like sequences were detected in the ileocecal biopsies of

patients with PSC and ulcerative colitis, as well as non-inflammatory controls (relative abundances of 0.49% ± 0.52%, 0.37% ± 0.37%, and 0.36% ± 0.31%, respectively) (Rossen et al. 2015). In the schematic tree in **Figure 1**a, the *A. muciniphila* sequences derived from ileum biopsies are clustered together. This occurs in particular in the third clade, which is made up entirely of *Akkermansia*-like sequences derived from the ileum, with a 16S rRNA sequence identity of 98% in comparison to *A. muciniphila* Muc^T. The isolation of *Akkermansia*-like species in the ileum is needed to study possible differences between the strains found in the small intestine and the strains in the large intestine. Considering the pH in the small intestine, the *Akkermansia*-like spp. found in the ileum and other parts of the small intestine could have a different optimum pH for growth.

The function of the small intestinal microbiota was also studied using comparative metagenomics and RNAseq (Zoetendal et al. 2012). This study, in which *A. muciniphila* was not detected, revealed that the metabolic focus small intestinal microbiota lies within carbohydrate uptake and metabolism. In more detail, simple carbohydrate transport phosphotransferase systems, fermentation, central metabolism, the metabolism of amino acids, and the production of cofactors were enriched. A more recent study emphasized that the ileum mucosal microbiota might have a role in plant cell wall polysaccharide (PCW) degradation (Patrascu et al. 2017). A large portion of the glycans that reach the small intestine are PCW polysaccharides. These polysaccharides cannot be degraded by humans, whereas the ileal microbiota associated with the mucus layer was found to have the enzymatic potential to break down PCW polysaccharides. The exact role of *A. muciniphila* in the small intestine remains unknown, but *Akkermansia*-like spp. could have a role in immune signaling in this part of the GIT. In mice, the addition of *A. muciniphila* in comparison with germ-free mice resulted in more significant modulation in the ileum of PPARα-RXRα activation, tryptophan metabolism, serotonin receptor signaling, and dopamine receptor signaling, among others (Derrien et al. 2011). The number of differentially expressed genes in the ileum of *A. muciniphila* mono-associated mice was 253 (144 upregulated and 99 downregulated genes). The administration of *A. muciniphila* resulted in an increase of Reg3g expression under the control diet and a decrease of Lyz1 expression in the ileum (Everard et al. 2013). Another study also showed a decrease in Cnr1 expression and increase of Cldn3 expression in the ileum upon the administration of *A. muciniphila* in mice (Plovier et al. 2017). As discussed before, the mucus layer in the small intestine is thinner and less dense than that of the colon (Atuma et al. 2001). This allows closer contact between the microbial community and host cells, promoting immune signaling in this region of the gut. The presence of *Akkermansia*-like spp. in the ileum might contribute to immune health.

Large Intestine

The large intestine specializes in digestion and consists of several different segments, namely the cecum, ascending colon, transverse colon, descending colon, rectum, and anus (Macfarlane and Macfarlane 2007). The colonic transit time of healthy individuals is longer than the transit time of the small intestine, ranging between 9 and 46 h (mean 28 h) (Madsen 1992). In healthy individuals, a decrease in luminal pH is observed in the cecum in almost all subjects (pH ranging from 5.5–7.5) (Nugent et al. 2001). This drop in pH is due to the fermentation of carbohydrates by colonic bacteria, leading to the production of SCFAs. Then, the pH increases along the large intestines to pH values ranging between 6.1 and 7.5. The mucosal pH of the large intestine parallels the luminal pH (McDougall et al. 1993). However, the mucosal pH is less acidic than the luminal pH in all anatomic regions of the large intestine.

The epithelial cells along the large intestine are covered by the mucosal layer (Johansson et al. 2011). As such, the mucosal layer protects the epithelial cells from direct contact with microorganisms. On top of this, the mucosal layer also contains antimicrobial proteins such as IgA. The mucosal layer can be divided into two parts: the inner and outer mucus layers. The inner mucus layer is firmly attached to the epithelial cells and devoid of bacteria, whereas microbes are capable of colonizing the outer layer due to its higher permeability (Johansson et al. 2008). Both layers are mainly composed of the gel-forming mucin MUC2, consisting of large polymers that are formed by N-terminal trimerization and C-terminal dimerization (Ambort et al. 2012). The expansion of the mucus layer occurs due to increased pH and decreased calcium (Ca^{2+}) levels. N-terminal interactions are weakened by the decreased calcium concentrations. Therefore, water is able to bind to the mucin domain glycans, leading to the formation of flat mucin sheets. Furthermore, the less dense outer layer is the result of endogenous proteases, promoting the possibility of microbes to colonize the mucus layer (Johansson et al. 2008). The degradation of these mucins by mucin-degrading bacteria of the colon microbiota affects the host cells e.g., by producing SCFAs (Johansson and Hansson 2016).

The gut microbiota is mainly studied using fecal samples, since these samples can be obtained without colonoscopies. However, microbial communities detected in fecal samples mainly reflect the luminal microbiota in the distal large intestine. Therefore, the microbial communities in biopsies can differ distinctly from that in fecal samples (Stearns et al. 2011). Several studies have confirmed that the microbial communities in biopsy samples of different anatomic regions of the colon show similarities, focusing on the major phylogenetic groups (Stearns et al. 2011, Wang et al. 2005, Zhang et al. 2014). Along the intestinal tract, Firmicutes and Bacteroidetes were predominant, with lower proportions of Proteobacteria and Fusobacteria observed in biopsy

samples (Stearns et al. 2011, Zhang et al. 2014). The sequencing of fecal samples of 22 individuals from four different European countries revealed the presence of three robust clusters, called enterotypes (Arumugam et al. 2011). These enterotypes are either enriched in (1) *Bacteroides*; (2) *Prevotella* and co-occurring *Desulvibrio*; or (3) *Ruminococcus* and co-occurring *Akkermansia*. Recently, a method of restricting enterotyping space was proposed to increase the ability to detect samples outside of these enterotyping spaces (Costea et al. 2018). Overall, the dominant phyla in fecal samples derived from healthy individuals were found to be Firmicutes, Bacteroidetes, and Actinobacteria. Less abundant phyla were Proteobacteria and Verrucomicrobia (Arumugam et al. 2011).

In addition to studies on the role of the gut microbiota in health, the gut microbiota has also been studied in diseases such as IBD, IBS, obesity, and type-2 diabetes. A shift in microbiota composition was observed in IBD patients and may have a role in the onset, maintenance, and severity of the disease, although this shift could also partly be due to the disturbed gut environment (Walker et al. 2011). In IBS patients, a decrease in bacterial diversity was observed (Codling et al. 2010, Carroll et al. 2012). However, a consistent gut microbiota pattern in IBS patients is lacking (Tap et al. 2017). In obesity, inconsistent findings have been reported. For example, one study reported an increase of Firmicutes and a decrease of Bacteroidetes, while another reported the opposite (Ley et al. 2005, Schwiertz et al. 2010). Lastly, a decrease in canonical butyrate-producing bacteria was found in patients with T2D (Qin et al. 2012). A decrease in butyrate-producing bacteria was associated with an increase in opportunistic pathogens, mainly Proteobacteria. Taken together, the studies on the gut microbiota in individual diseases are not all uniform, highlighting the difficulties in appointing markers for disease.

The gut microbiota plays an important role in the metabolism of host nutrients and the health maintenance of the host. Carbohydrates (mainly polysaccharides) that have not been hydrolyzed in the small intestine become available for the microbial community in the colon (Cummings and Macfarlane 1991). The main substrates entering the colon are resistant starch and polysaccharides derived from plant cell walls. The major end products produced by the gut microbiota are SCFAs (e.g., acetate, propionate, and butyrate) and gases (e.g., H_2 and CO_2) using the available substrates. Of these, butyrate is used as an energy source by colonic epithelial cells (Clausen and Mortensen 1995). Furthermore, propionate is able to signal to the host through the GPR41 and GPR43 receptors (Le Poul et al. 2003). Interestingly, SCFAs activate free fatty acid (FFA) receptor 2 and FFA3 in the gut (Le Poul et al. 2003, Brown et al. 2003, Nilsson et al. 2003). These receptors control peptides (peptide YY and glucagon-like peptide 1) involved in appetite regulation (Flint et al. 2012). Therefore, SCFA production

in the gut may be associated with food intake. Next to dietary carbohydrates, the colonic microbiota also has a role in the degradation of host-derived glycans (mucin), xenobiotics, and drugs (Cummings and Macfarlane 1991, Possemiers et al. 2011). The gut microbiota is also able to stimulate host immunity in order to protect the host against pathogens (Kamada et al. 2013). In this way, the gut microbiota enhances the innate immune response and has a role in increasing the gut barrier function. One of the microbial species in the gut involved in immune regulation and increasing gut barrier function is *A. muciniphila* (Everard et al. 2013, Ottman et al. 2017).

A recent study revealed the presence of Verrucomicrobiae in all anatomical regions of the large intestine by sequencing the V2 region (Momozawa et al. 2011). The concentrations of Verrucomicrobiae (in two individuals) ranged between 0.3% and 15.8%. Interestingly, one individual harbored only low concentrations, ranging between 0.3% and 1.4%, while concentrations in another individual ranged between 9.8% and 15.8% throughout the anatomic regions. Notably, the individual with higher Verrucomicrobiae concentrations was a Crohn's disease patient. Differences were not only observed between individuals, but also between the experimental designs. The use of another DNA extraction method resulted in lower amounts of Verrucomicrobiae with concentrations in the range of 0.3–7.3% in both individuals. Next to this study, there are more studies identifying the Verrucomicrobia phylum and/or *Akkermansia*-like spp. focusing on several anatomic regions of the large intestine (Stearns et al. 2011, Wang et al. 2005, McHardy et al. 2013, Lyra et al. 2012, Hong et al. 2011, Sanapareddy et al. 2012). Verrucomicrobia were identified in the cecum by another study, although quantities were not shown (McHardy et al. 2013). Even though the pH is lower in the cecum (pH 5.5–7.5), it is still within the growth range of *A. muciniphila*. In the ascending colon, Verrucomicrobia were identified with a concentration of 6% in the large intestine of a healthy volunteer (Wang et al. 2005). Using a qPCR approach within the same region, a concentration of 4.17 ± 0.6 log 10 genomes per gram of a sample of *Akkermansia*-like spp. was described (Lyra et al. 2012). Furthermore, the transverse colon of two out of four included subjects showed the presence of Verrucomicrobia, with 563 and 7771 sequence counts of this phylum in each sample (Stearns et al. 2011). In the sigmoid colon, compared to the transverse colon, the same study reported a decrease in one of the subjects (from 563 to 64 sequence counts), whereas an increase was noted in another subject (from 7771 to 11,941 sequence counts). The qPCR approach resulted in a similar concentration to that found in the ascending colon, namely 4.16 ± 0.56 log 10 genomes per gram of a sample (Lyra et al. 2012). Several studies have also described the presence of *Akkermansia*-like sequences in the rectum (Hong et al. 2011, Stearns et al. 2011, Wang et al. 2005). Where one study reported a higher concentration in the rectum (9%) than in the ascending colon, another reported a rapid decrease in sequence counts from 64 and 11,941 in the

sigmoid colon, to sequence counts of 1 and 2, respectively (Wang et al. 2005, Stearns et al. 2011). In conclusion, based on these studies, the presence and abundance of *A. muciniphila* in the large intestine is subject-specific.

To compare the 16S rRNA *Akkermansia*-like sequences in biopsies to fecal samples, a maximum likelihood tree was constructed (**Figure S3**). Interestingly, the majority of the *Akkermansia*-like sequences derived from biopsies were clustered together. This cluster contains a low amount of *Akkermansia*-like sequences derived from fecal samples. Therefore, one could hypothesize that sub-populations of *Akkermansia* spp. exist within the large intestine. However, it should be noted that complete *Akkermansia* spp. genomes derived from biopsies and lumen are needed to support this hypothesis.

In contrast to the presence of *A. muciniphila* in other regions of the GIT, its function has been more explored in its ecological niche. *A. muciniphila* was found to be correlated to health and inversely correlated to several disease states (as explained in the introduction). However, besides its presence in health and disease, *A. muciniphila* was also found to be involved in syntrophic interactions (Belzer et al. 2017). For example, co-cultivations of *A. muciniphila* with butyrate-producing bacteria (*Anaerostipes caccae, Eubacterium hallii*, and *Faecalibacterium prausnitzii*) resulted in butyrate production. Therefore, it is suggested that the mucus-degrading capacity of *A. muciniphila* stimulates intestinal metabolite pool and specifically butyrate levels, which is beneficial for the host. Another example is the release of sulfate during mucin degradation. This sulfate might be used by sulfate-reducing bacteria in the colon, producing hydrogen sulfide (Derrien 2007, Willis et al. 1996). In turn, *A. muciniphila* predictively harbors genes involved in l-cysteine biosynthesis using hydrogen sulfide, suggesting that *A. muciniphila* might have a role in the detoxification of hydrogen sulfide in the gut (Ottman et al. 2017).

As mentioned earlier, the colonization of *A. muciniphila* in mice led to an increased expression of genes associated with immune responses and the strengthening of the gut barrier function (Everard et al. 2013, Derrien et al. 2011). In addition, the outer membrane protein (Amuc_1100) was found to be involved in immune regulation and the enhancement of trans-epithelial resistance (Ottman et al. 2017). Altogether, these studies suggest an important role of *A. muciniphila* in the microbial community of the large intestine in addition to its role in host interactions, promoting the use of this bacterium as a therapeutic agent for intestinal disorders.

Appendix

The human appendix extends from the cecum and is 5–10 cm long and 0.5–1 cm wide (Randal Bollinger et al. 2007). The function of the appendix has been up for debate for

quite some time. Charles Darwin described the lack of function of the appendix and noted that the appendix is a remainder from primate ancestors that ingested leaves, in which the appendix functioned to ferment plant material (Darwin 1871, Smith et al. 2013). The appendix is covered in gut-associated lymphoid tissue, suggesting its involvement in immune function (Berry 1900). An apparent function of the human appendix was described, suggesting that the appendix functions as a "safe house" for beneficial bacteria (Randal Bollinger et al. 2007). This same study revealed a higher abundance of microbial biofilms in the appendix than other areas of the human colon. To our knowledge, a description of the pH in the human appendix is lacking. However, the rabbit appendix was found to have a pH ranging between 6.2 and 6.7 (Merchant et al. 2011). Secretions of the rabbit appendix are rich in bicarbonate and occur spontaneously and at a relatively rapid rate (1–12 mL/h). Therefore, it has been suggested that in rabbits, the appendix may have a major role in the regulation of pH in the cecum. However, similar data is not available for the human appendix.

Considering the difficulty of obtaining samples of the human appendix, there are few studies describing the microbiota of the appendix. These studies mainly focus on the microbiota in appendicitis in comparison to healthy controls (Zhong et al. 2014, Jackson et al. 2014, Salo et al. 2017). In healthy controls, the taxa *Fusibacter*, *Selenomonas,* and *Peptostreptococcus* were increased in comparison to the rectal microbiota (Jackson et al. 2014). This finding indicates that the human appendix harbors a distinct microbiota. A wide variation of abundances in phylum, genus, and species levels was detected within groups divided by health and severity of inflammation (Salo et al. 2017). In healthy controls, Firmicutes and Bacteroidetes were found to be the most abundant phyla. Other abundant phyla detected in these samples were Fusobacteria, Actinobacteria, and Proteobacteria. Phyla with lesser abundances (<2%) were Spirochaetes, Cyanobacteria, Synergistetes, Tenericutes, and Verrucomicrobia.

While some studies found significant differences between the microbiota of appendicitis patients and healthy controls (Zhong et al. 2014, Jackson et al. 2014) or between severity of inflammation (Guinane et al. 2013), another did not (Salo et al. 2017). One of the genera linked to appendicitis is *Fusobacterium* (Zhong et al. 2014, Guinane et al. 2013). Increased abundances of this genus were observed in appendicitis patients in comparison to healthy controls (Zhong et al. 2014), and the presence of *Fusobacterium* could be linked to the severity of inflammation (Guinane et al. 2013). In contrast, the presence of *A. muciniphila* was found to be inversely correlated to the severity of appendicitis (Swidsinski et al. 2011). Using fluorescence in situ hybridization (FISH), the mean proportion of single bacterial groups for *A. muciniphila* was found

to be 4.0 ± 4.6, 1.0 ± 2.1, and 0.2 ± –0.6 for no appendicitis, catarrhal appendicitis, and suppurative appendicitis, respectively.

The mucus layer of the appendix was found to contain a more concentrated biofilm than other parts of the large bowel (Randal Bollinger et al. 2007). Therefore, the appendix might be a favorable niche for mucin-degrading bacteria, including *A. muciniphila*. Although the role of *A. muciniphila* in the appendix is not specified, one could hypothesize that, being part of the appendiceal microbiota, *A. muciniphila* might have a role in re-colonizing the colon after an infection or colonic dysfunction. Thereby, *A. muciniphila* could function in the maintenance of a healthy gut microbiota by restoring the mucus barrier function subsequent to infection/inflammation.

Human Breast Milk and Early Life Intestine

In breast-fed infants, the main source of glycans are human milk oligosaccharides (HMOs) (Bode 2012). Human milk consists of a mixture of nutrients for infants, conveying immunologic and other health benefits (Flint et al. 2012). Human milk contains 5–15 g/L HMOs, and over 200 different HMO structures exist. The major monosaccharides present in HMOs are d-glucose, d-galactose, *N*-acetyl-glucosamine, l-fucose, and *N*-acetylneuraminic acid (sialic acid) (Zivkovic et al. 2011). HMOs in the infant gut act as substrates for specific bacteria in the gut, functioning as natural prebiotics by stimulating the growth of beneficial intestinal bacteria such as bifidobacteria and lactobacilli (Zivkovic et al. 2011, Bidart et al. 2014). It is remarkable to mention that milk oligosaccharides and glycoconjugates are able to prevent the development of pathogens and toxins, inhibiting their binding on the surface of the epithelial cells (Jost et al. 2015). The structure of HMOs has chemical similarities to mucus glycans (Newburg 2000).

A. muciniphila has been identified in human milk samples immediately after delivery (colostrum), and at 1 and 6 months (Collado et al. 2012). *A. muciniphila* cell counts in breast milk were measured after conducting qPCR, revealing that *A. muciniphila* was higher in abundance in overweight than normal weight mothers, with mean concentrations of 1.25, 1.09, and 1.20 log number of gene copies/mL in colostrum samples and breast milk samples. Furthermore, *A. muciniphila* was observed to be present in colostrum samples that were collected from 11 women after elective caesarean with a median counts number of 0.9 (interquartile range from 0.0 to 1.5) analyzed by qPCR (Aakko et al. 2017). In turn, in samples from human breast tissue from 43 women (aged 18 to 90 years), the presence of *Akkermansia*-like species was found using 16S rRNA sequencing (Urbaniak et al. 2014).

As mentioned earlier, *A. muciniphila* is also present in infants' intestines from the first months of life (Collado et al. 2007, Grzeskowiak et al. 2012, Grzeskowiak et al. 2012). The structures in HMOs can also be found in mucus glycans (Koropatkin et al. 2012, Tailford et al. 2015). *A. muciniphila* was able to break down structures of HMOs into simpler sugars, releasing SCFAs (acetate and propionate) in the media. *A. muciniphila* expressed enzymes that were involved in carbohydrate and glycan degradation, such as α-l-fucosidases, exo-α-sialidases, β-galactosidases, and β-hexosaminidases (Ottman 2015). This indicates that *A. muciniphila* might be able to use HMOs, using human milk as a sole energy, carbon, and nitrogen source, which could also explain its presence in breast milk and the breast tissue of lactating woman.

To confirm this, further research should be conducted to gain more insight in the mucolytic activities and the function of *A. muciniphila* in human milk. The presence of *Akkermansia* spp. and *A. muciniphila* specific in human milk may benefit the maturation of the infant's microbiota establishment and immune maturation, as its outer protein was found to be involved in immune regulation (Ottman et al. 2017). Last but not least, *A. muciniphila* glycan degradation ability might be proved to play an important role in the initial colonization of the infant's gut, thus having a major impact on later life.

Akkermansia muciniphila in *In Vitro* Gut Models

In contrast to invasive sampling of the human body, in vitro models have also been introduced to study the spatial organization of the human gut microbiota. Multiple in vitro models are available for this purpose, such as the Gastro-Intestinal Model (TIM-1 and TIM-2) and the Simulator of Human Intestinal Microbial Ecosystem (SHIME). The small intestinal model TIM-1 consists of four compartments representing the stomach, duodenum, jejunum, and ileum (Mateo Anson et al. 2009), while TIM-2 simulates the large intestine (Rajilic-Stojanovic et al. 2010). The SHIME was developed in 1993 (Molly et al. 1993). This model simulates five compartments of the digestive tract, namely the stomach, small intestine, and the ascending, transverse, and descending colon. In addition, a variation on SHIME was developed, named the mucosal SHIME (M-SHIME) (Van den Abbeele et al. 2012). The M-SHIME has a mucosal compartment, developed to study the microbial colonization of the mucus layer.

Most of the studies including *A. muciniphila* used the SHIME model. The presence of *A. muciniphila* in different compartments of in vitro models has also been evaluated (Van den Abbeele et al. 2010, Van Herreweghen et al. 2017). In SHIME, *Akkermansia* spp. are more abundantly present in the transverse and descending colon compartments

than in the proximal compartments (ascending colon) of this model (Van den Abbeele et al. 2010, Van Herreweghen et al. 2017, Kemperman et al. 2013, Garcia-Villalba et al. 2017). This is not in concordance with findings using biopsy samples, where no clear depletion of Verrucomicrobiae was observed in the ascending colon (Momozawa et al. 2011). Another SHIME experiment also described the distal location of *Akkermansia* spp. (Kemperman et al. 2013). In addition, in this model the growth of *Akkermansia*-like spp. was stimulated by black tea and red wine grape extract. Interestingly, in M-SHIME, *A. muciniphila* did not reach high densities as was observed in the distal compartments in the SHIME setup (Van den Abbeele et al. 2013). This might be due to the setup of the M-SHIME model, which is lacking distal colon compartments, where *Akkermansia*-like spp. reached the highest densities (Kemperman et al. 2013, Van den Abbeele et al. 2010, Garcia-Villalba et al. 2017). Recently, a study using the SHIME model demonstrated that *A. muciniphila* is pH- and mucin-dependent (Van Herreweghen et al. 2017). An increase of *A. muciniphila* was observed upon the addition of mucin. When the pH in the distal colon was lowered, a decrease in *A. muciniphila* was observed in comparison to the same compartment with a higher pH. Altogether, these studies suggest that these models can be used to study the effect of environmental parameters and diet on the human gut microbiota in health and disease states.

Conclusions

To date, the presence of *A. muciniphila* has mainly been associated with the mucus layer of the colon. However, in this review we collected results from other studies and showed that *Akkermansia*-like sequences have also been found to be present in other anatomical regions of the digestive tract and human breast milk. In short, these regions are the oral cavity, pancreas, bile ducts and gallbladder, small intestine, large intestine, and appendix (**Figure 1**b). The environmental parameters (e.g., pH, oxygen and nutrient availability) differ among anatomic regions of the human body, affecting the growth of *A. muciniphila*. As the aforementioned organs have different functions, the function of *A. muciniphila* might also differ in different regions of the digestive tract. In this review, we proposed hypothetical functions of *A. muciniphila* in these regions; however, further research is needed to confirm its role among the different regions of the digestive tract. Altogether, the presence of *Akkermansia*-like spp. along the digestive tract indicates that this bacterium might have more functions than those known so far. Still, as can be concluded from abundance of *Akkermansia*-like spp., its optimal ecological niche remains the mucus layer in the colon.

Acknowledgments

We would like to thank Asimenia Gavriilidou and Daan van Vliet, who provided insight and expertise in the phylogenetic analysis.

Supplementary Materials

Figure S1: Detailed maximum likelihood phylogenetic tree (RAxML) including *Akkermansia*-like sequences derived from large intestine and ileum biopsies and Chinese *A. muciniphila* strains. This content is available online (doi:10.3390/microorganisms6030075).

Figure S2: Detailed Neighbor Joining phylogenetic tree including *Akkermansia*-like sequences derived from large intestine and ileum biopsies and Chinese *A. muciniphila* strains. This content is available online (doi:10.3390/microorganisms6030075).

Figure S3: Detailed maximum likelihood phylogenetic tree (RAxML) including *Akkermansia*-like sequences derived from fecal samples, large intestine, and ileum biopsies and Chinese *A. muciniphila* strains. This content is available online (doi:10.3390/microorganisms6030075).

Chapter 3

Genomic convergence between *Akkermansia muciniphila* in different mammalian hosts

Sharon Y. Geerlings*, Janneke P. Ouwerkerk*, Jasper J. Koehorst, Jarmo Ritari, Steven Aalvink, Bärbel Stecher, Peter J. Schaap, Lars Paulin, Willem M. de Vos, Clara Belzer

* These authors contributed equally.

BMC Microbiology doi: 10.1186/s12866-021-02360-6

Abstract

Akkermansia muciniphila is a member of the human gut microbiota where it resides in the mucus layer and uses mucin as the sole carbon, nitrogen and energy source. *A. muciniphila* is the only representative of the Verrucomicrobia phylum in the human gut. However, *A. muciniphila* 16S rRNA gene sequences have also been found in the gut of many vertebrates. We detected *A. muciniphila*-like bacteria in the gut of animals belonging to 15 out of 16 mammalian orders. In addition, other species belonging to the Verrucomicrobia phylum were detected in fecal samples. We isolated 10 new *A. muciniphila* strains from the feces of chimpanzee, siamang, mouse, pig, reindeer, horse and elephant. The physiology and genome of these strains were highly similar in comparison to the type strain *A. muciniphila* Muc^T. Overall, the genomes of the new strains showed high average nucleotide identity (93.9% to 99.7%). In these genomes, we detected considerable conservation of at least 75 of the 78 mucin degradation genes that were previously detected in the genome of the type strain Muc^T. The low genomic divergence observed in the new strains may indicate that *A. muciniphila* favors mucosal colonization independent of the differences in hosts. In addition, the conserved mucus degradation capability points towards a similar beneficial role of the new strains in regulating host metabolic health.

Introduction

The gut of vertebrates is colonized with a dense and diverse microbiota (Ley et al. 2008). Several factors affect the gut microbiota composition of vertebrates including diet, host phylogeny and gut morphology (Ley et al. 2008). The microbiota has had a large influence on animal evolution, and can be seen as an obligate and beneficial symbiont (McFall-Ngai et al. 2013). The main phyla representing the gut microbiota in mammals are Firmicutes, Bacteroidetes, Proteobacteria, Actinobacteria, and Verrucomicrobia (Ley et al. 2008). The gut microbiota produces short chain fatty acids from degradation of otherwise indigestible components providing the host with the ability to digest a wider variety of available foods (Ley et al. 2008, Muegge et al. 2011). The gut microbiota also produces vitamins and other beneficial substances that the host cannot synthesize (Rajilic-Stojanovic et al. 2013).

Some microbiota members can flourish within the mucus layer, a glycan-rich and anaerobic environment offered by its host (Van den Abbeele et al. 2011), including mucus-degrading specialist *Akkermansia muciniphila* (Derrien et al. 2004). *A. muciniphila* is the only representative of the Verrucomicrobia phylum in the human gut. Mucin utilization by *A. muciniphila* has been shown i) *in vitro*, where it grows on mucin as sole carbon and nitrogen source (Derrien et al. 2004), ii) *in vivo*, where it scavenges mucin efficiently (Berry et al. 2013) and iii) *in silico* using a genome-scale model and omics analysis (Ottman et al. 2017). Recent mouse and human studies have demonstrated that intake of *A. muciniphila* has a series of health benefits, including improved barrier function, increased insulin sensitivity and reduction of obesity (Plovier et al. 2017, Depommier et al. 2019). Of interest, mouse experiments have shown that while *A. muciniphila* can degrade mucin, its presence increases mucus production, mucus layer thickness and tight junction protein production (Plovier et al. 2017, Everard et al. 2013, van der Lugt et al. 2019).

A. muciniphila is abundantly present in the human intestinal tract, varying from 1 to 4 % of the bacterial population in the colon (Collado et al. 2007). Its abundance was found to be linked to a healthy status in humans (Cani and de Vos 2017). Interestingly, *A. muciniphila* has also been detected in other mammals, such as the brown bear (Sommer et al. 2016). Furthermore, *A. muciniphila* has been detected in several small animals, such as the ground squirrel and Syrian hamster (Carey et al. 2013, Sonoyama et al. 2009). In addition, *Akkermansia* spp. are widely spread in the gut throughout the animal kingdom including mammals (Ley et al. 2008) and other vertebrates such as python (Costello et al. 2010, Ouwerkerk et al. 2016), zebra fish (Belzer and de Vos 2012), chicken (Belzer and de Vos 2012), and salmon (Green et al. 2013). Next to bacteria belonging to the genus *Akkermansia*, other Verrucomicrobia are detected in the animal

gut of invertebrates including termites (Isanapong et al. 2013), ants (Sanders et al. 2014), earthworm (Wust et al. 2011) and nematodes (Vandekerckhove et al. 2002). A few examples of Verrucomicrobia isolates from the gut environment are *A. muciniphila* (Derrien et al. 2004), python isolate *A. glycaniphila* (Ouwerkerk et al. 2016), and termite gut isolate *Diplosphaera colotermitum* (Wertz et al. 2012).

A. muciniphila is able to colonize a broad range of hosts, despite differences in GI tract anatomy (simple, foregut, hindgut), diet (carnivore, omnivore, herbivore), host physiology and body temperature. This distribution might be an indication of co-evolution of this organism with its host. Therefore, we explored the presence and genomic divergence of Verrucomicrobia and *Akkermansia* spp. within different mammalian hosts.

Results

A. muciniphila and other Verrucomicrobia within the gut of different mammals

Detailed analysis of Verrucomicrobia 16S rRNA gene sequences derived from SILVA database 138 (Quast et al. 2013) (>1100 bp, pintail >75) revealed that *A. muciniphila* is not the sole representative species of the Verrucomicrobia phylum in the gut of mammals. The phylogenetic tree was constructed using both the neighbor joining method and RAxML. Both trees showed similar output and the Verrucomicrobia-derived sequences could be grouped into 12 clades of which 9 clades contained samples obtained from the mammalian gut (**Figure 1** and **Figure S1**).

The first clade contains 1352 *A. muciniphila* like 16S rRNA sequences, not solely mammalian. In this clade, eight mammalian orders were detected: Proboscidea (African elephant), primates (human, gorilla, lemur, chimpanzee, pygmy loris), Carnivora (cheetah), Sirenia (Dugong), Cingulata (armadillo), Rodentia (rat, mice and thirteen-lined ground squirrel), Artiodactyla (eland, pig, cow (rumen fluid)), Perissodactyla (horse). The non-mammalian sequence present in this clade was derived from a chicken. In addition, the 16S rRNA sequences of *A. muciniphila* strains isolated in this study were positioned in clade 1 (**Figure 1**).

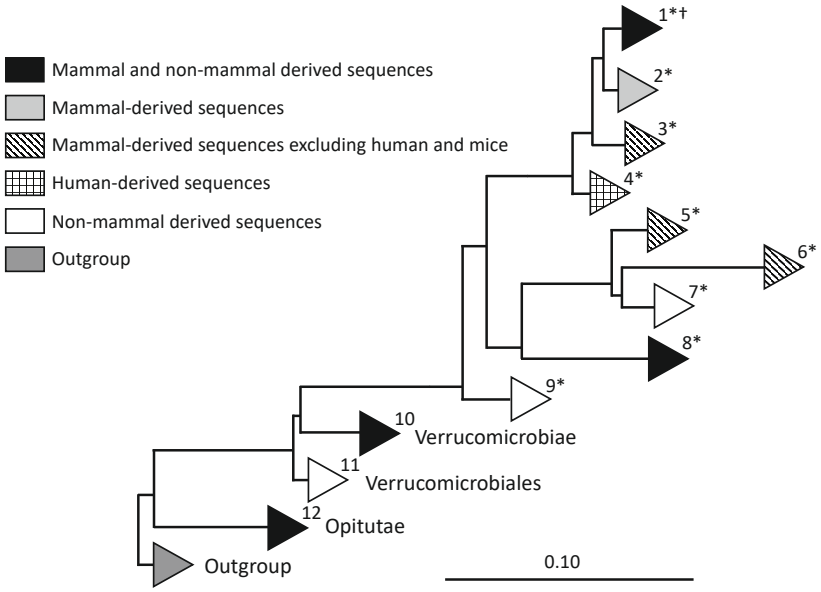

Figure 1 – Verrucomicrobia diversity within samples from the gut. Schematic representation of all clades within the Verrucomicrobia that contain intestinal obtained sequences based on the phylogenetic tree. (*) Clades containing *Akkermansia* sequences. (†) All newly isolated *A. muciniphila* strains are positioned in clade 1.

Five clades solely contained mammalian sequences, including clade 2, 3, 4, 5 and 6. Clade two contains 277 sequences, mainly derived from primates (human) and Rodentia (mice) and one sequence derived from Sirenia (dugong). Interestingly, sequences derived from the snub-nosed monkey formed a separate clade (3) within the phylogenetic tree, as well as 57 human-derived sequences in clade 4. Other clades solely consisting of mammalian derived sequences were clade 5 and 6. Clade 5 contained 201 sequences derived from 6 mammalian orders, including Proboscidea (African elephant), Artiodactyla (cow, okapi, buffalo, babirusa, warty pig, gazelle, takin, giraffe, przewalskii gazelle, springbok), Diprotodontia (kangaroo), Rodentia (capybara, Prevost's squirrel), Perissodactyla (horse, wild ass, rhinoceros, zebra), Chiroptera (flying fox). Clade 6 contained 20 sequences from mammalian orders Lagomorpha (rabbit) and Proboscidea (elephant). Sequences derived from animals both living in captivity and in the wild were represented in all animal-containing clades excluding mice. To be able to compare the similarity (%) of type strain *A. muciniphila* Muc^T to the different clades, *A. muciniphila* Muc^T was compared to representative sequences of each clade. The similarities and amount of representatives per clade are shown in table 1.

Table 1 –Gut obtained Verrucomicrobia sequences of clades 1-12 corresponding to Figure 1.

Clade	Total amount of sequences in clade	Taxonomy	Host	Similarity (%) to Muc^T lower limit	Similarity (%) to Muc^T upper limit	Amount representative sequences
1	1352	Genus: Akkermansia	Human (786), other primates (89), Proboscidea (17), Carnivora (4), Sirenia (2), Cingulata (2), rodentia (440), Artiodactyla (6), Perissodactyla (3) and Galliformes (3)	91.91	100	15
2	277	Genus: Akkermansia	Human (111), Rodentia (165) and Sirenia (1).	95.66	99.09	10
3	4	Genus: Akkermansia	Primates (4)	98.30	98.84	4
4	57	Genus: Akkermansia	Human (57)	94.18	98.41	5
5	201	Genus: Akkermansia	Proboscidea (1), Artiodactyla (142), Diprotodontia (30), Rodentia (3), Perissodactyla (24) and Chiroptera (1)	85.15	90.69	17
6	20	Genus: Akkermansia	Rodentia (19) and Proboscidea (1)	86.25	89.22	4
7	12	Genus: Akkermansia	Fish gut sequences (12)	89.41	90.22	3
8	5	Genus: Akkermansia	Squamata (4) and Sirenia (1)	94.03	94.11	2
9	7	Genus: Akkermansia	Invertebrates (7)	92.74	93.06	2
10	45	Order: Chtoniobacterales, Methylacidiphales and Verrucomicrobiales	Human (UC patients) (2), moth larvae (1), earthworm (37), termite (1), grass carp (2) and ascidian (2).	82.12	86.52	7
11	63	Order: Verrucomicrobiales	earthworm (24), ascidian sea squirt (29), sea cucumber (1), sea horse (1), olive flounder (1), small abalone (2), brown surgeonfish (1), black surgeonfish (1) and grass carp (1), squat lobster (2)	83.37	87.20	8

Table 1 *(Continued)*

Clade	Total amount of sequences in clade	Taxonomy	Host	Similarity (%) to Muc^T lower limit	Similarity (%) to Muc^T upper limit	Amount representative sequences
12	89	Order: Opitutales	Termites (11), ants (6), black millipede (1), cockroaches (2), ascidian (43), olive flounder (1), royal panaque (1), flying fox (2), baboon (2), eastern black and white colobus (12), Sumatran orang-utan (3), red kangaroo (3), capybara (1) and European rabbit (1).	77.95	82.35	10

Other mammalian gut derived sequences that belonged to the Verrucomicrobia phylum were found within clade 8, 10 and 12. Clade 8 consisted of only five sequences in total, four derived from a python (*A. glycaniphila*) and one sequence from the mammalian order Sirenia (Dugong). Clade 10 contained two sequences that belong to the Prosthecobacter genus obtained from intestinal samples of UC patients (**Figure 1** and **Table 1**). Furthermore clade 12 contained sequences from mammalian orders Chiroptera (flying fox) and primates (hamadryas baboon and eastern black and white colobus and Sumatran orangutan), Diprotodontia (red kangaroo), Rodentia (capybara) and Lagomorpha (European rabbit) belonging to the class Opitutae. The remaining Verrucomicrobia clades (7, 9 and 11) solely contained 16S rRNA gene sequences derived from the non-mammal Animalia gut (**Figure 1** and **Table 1**).

Verrucomicrobia prevalence in fecal samples of different mammals

Fecal samples of 108 different animals belonging to 47 species of 16 mammalian orders were collected. The prevalence of *A. muciniphila* was determined by quantitative PCR (qPCR) on all samples. Amplicons were generated with *A. muciniphila*-specific primers in 50 out of 108 samples, with abundances up to 4% (**Figure 2**). In addition, 16S rRNA gene sequencing of Verrucomicrobia resulted in Verrucomicrobia sequences derived from the Caribbean manatee, echidna, Western gorilla and otter. These sequences were added to the phylogenetic tree shown in **Figure 1**, in which they were positioned in clade 1 (Caribbean manatee), clade 5 (Western gorilla and echidna) and clade 10 (otter).

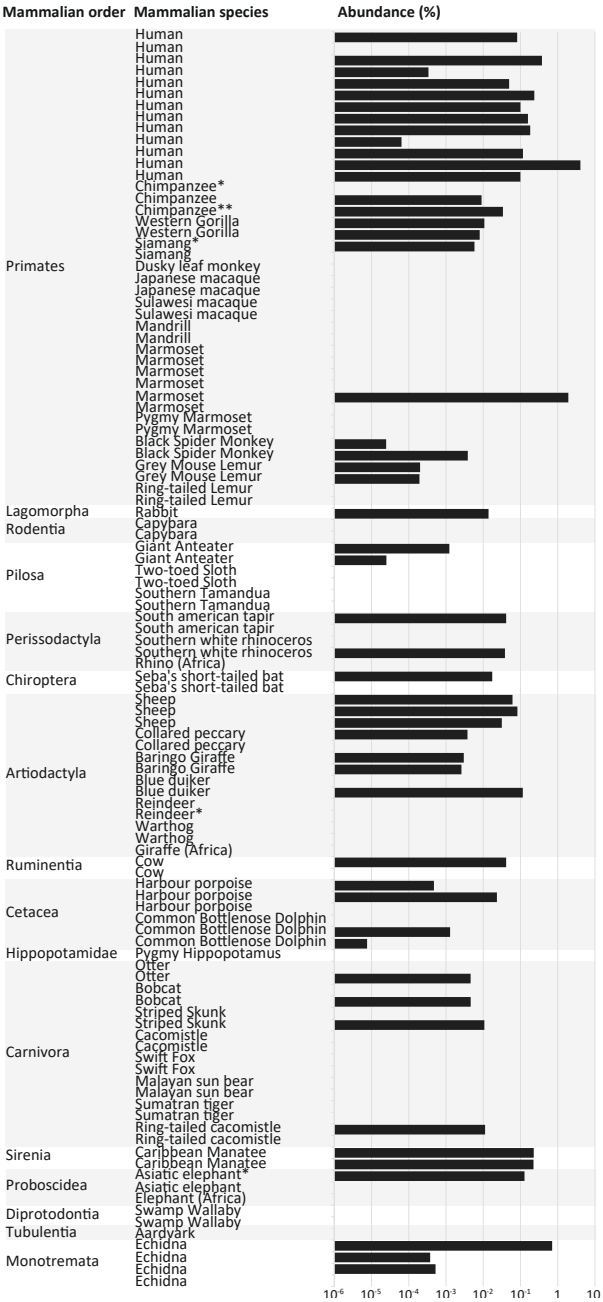

Figure 2 – Prevalence, abundance and phylogeny of *A. muciniphila*. Orders are depicted on the vertical axis following the phylogeny of mammals (for primates (Perelman et al. 2011)). (*) Samples from which pure isolates were obtained. Abundance of the *Akkermansia* genus was determined using qPCR.

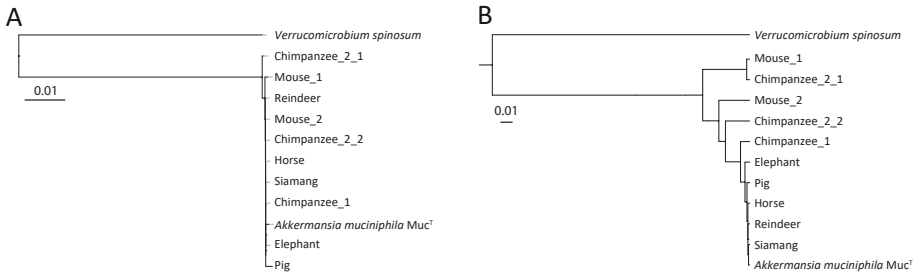

Figure 3 – phylogeny of the new isolates. (A) Phylogeny of the new isolates based on 16S rRNA gene sequence, aligned in ARB using NJ. Bar represents 1% sequence divergence. (B) Phylogeny of the new isolates based on the presence of domains in the draft genomes. Bar represents 1% sequence divergence. *A. muciniphila* Muc^T, and *V. spinosum* DSM 4136 are used as reference.

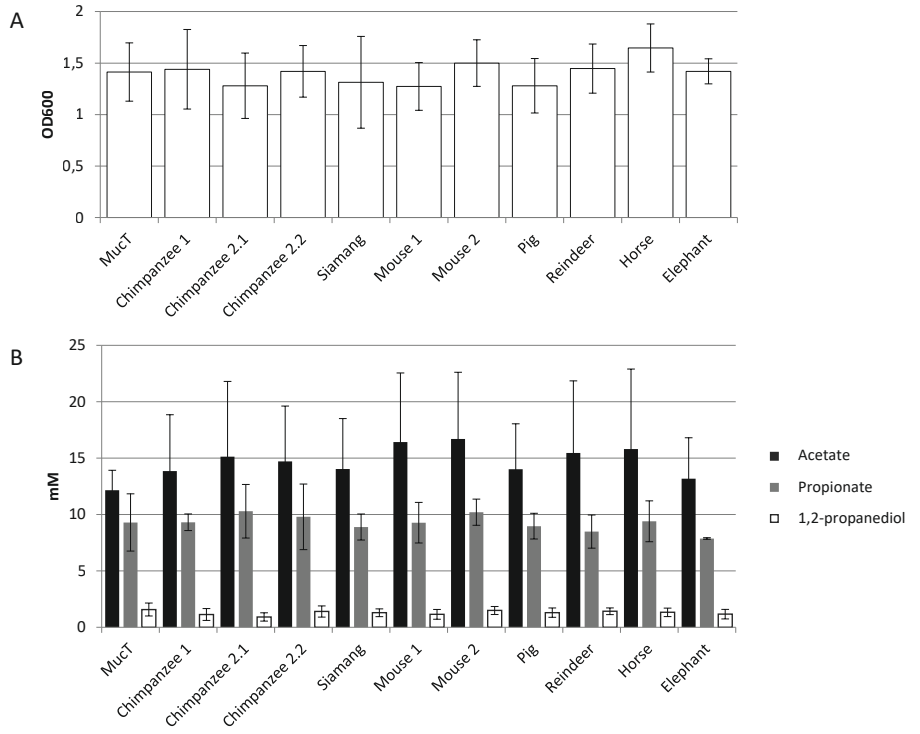

Figure 4 – Physiology on mucin-based medium. (A) Maximum OD600 reached when grown on a mucin-based medium. (B) The SCFA profile when grown on a mucin based medium.

New *A. muciniphila* isolates show low physiologic divergence

Ten new *A. muciniphila* isolates were obtained from fecal samples of the chimpanzee, siamang, mouse, pig, reindeer, horse, and elephant. The 16S rRNA gene sequence of these ten isolates was determined, and showed high similarity (>99.9%) to the 16S rRNA gene sequence *A. muciniphila* Muc^T (**Figure 3**A). All new *A. muciniphila* strains had small and oval shaped cells of approximately 700 nm in length, as described previously for the type strain (Derrien et al. 2004). All cells stained Gram-negative, grew in single cells, doublets, and aggregates in mucin medium. The cell growth (determined by OD600) and short chain fatty acid (SCFA) production (determined by high performance liquid chromatography (HPLC)) in a mucin-based medium was similar to the type strain *A. muciniphila* Muc^T (**Figure 4**). In addition, the strains had similar growth rates, and produced similar amounts of acetate, propionate and 1,2-propanediol. Taking into consideration the morphologic, physiologic and 16S rRNA gene sequence similarity, all strains should belong to *A. muciniphila* species.

Low genomic divergence between 10 new *A. muciniphila* isolates

The genomic DNA of all newly obtained isolates were sequenced and assembled into draft genomes (**Table 2**) consisting of 25-215 contigs. Isolates had genome sizes in the range of *A. muciniphila* Muc^T (2.7 Mb), although the genomes of Chimpanzee 2_1, Chimpanzee 2_2, and Mouse 1 were slightly larger (2.9 Mb) (**Table 2**). This was also reflected in the total predicted gene count (**Table 2**). All isolates had comparable GC content ranging from 55.2 to 55.9 (**Table 2**). The average nucleotide identity (ANI) was >99.7% for 7 isolates (from chimpanzee 1, siamang, mouse 1, pig, reindeer, horse, and elephant). The ANI was lower for the isolates from chimpanzee 2_1 (93.9%), chimpanzee 2_2 (97.4%), and mouse 2 (93.9%). The BLAST similarity and the number of SNPs of these three genomes were also in line with these results. This indicates that these three isolates are phylogenetically more distant. The ANI BLAST between all new isolates is shown in **Table S1**. The phylogeny based on the domain presence in the genomes was constructed and reflected the 16S rRNA gene phylogeny (**Figure 3**B and **Table S2**). In addition, the pan-genome has been determined as shown in **Figure S2**.

Table 2 – General genome characteristics.

Strain	Coverage	Contigs	Genome size (Mbp)	GC content (%)	Total gene count	Comparison with *A. muciniphila* Muc^T		
						ANI (%)	BLAST similarity (>5 kb) (%)	SNP
Chimpanzee 1	222	77	2.6	55.7	2233	99.98	99.99	0
Chimpanzee 2_1	150	185	2.9	55.9	2629	93.87	94.39	82
Chimpanzee 2_2	208	120	2.9	55.2	2524	97.38	97.83	124644
Siamang	212	110	2.7	55.8	2291	99.94	99.99	53418
Mouse 1	179	215	2.9	55.8	2585	93.85	93.49	128793
Mouse 2	120	25	2.7	55.5	2330	99.85	98.91	25020
Pig	185	70	2.8	55.8	2384	99.98	99.99	8
Reindeer	127	104	2.7	55.7	2303	99.94	99.99	14
Horse	271	90	2.8	55.7	2369	99.95	99.99	13
Elephant	193	188	2.7	55.7	2361	99.99	99.99	15

Comparing all draft genomes of the new isolates to the complete genome of *A. muciniphila* Muc^T using BLAST Ring Image Generator (BRIG) showed the low genomic divergence (**Figure 5**). Several potential phage remnants were identified that showed different GC content or GC skew and were not conserved among all isolates. Moreover, on 3 points in the draft genome there was a gap, likely because of the presence of one of the 3 rRNA operons that interfered with the draft genome sequence assembly.

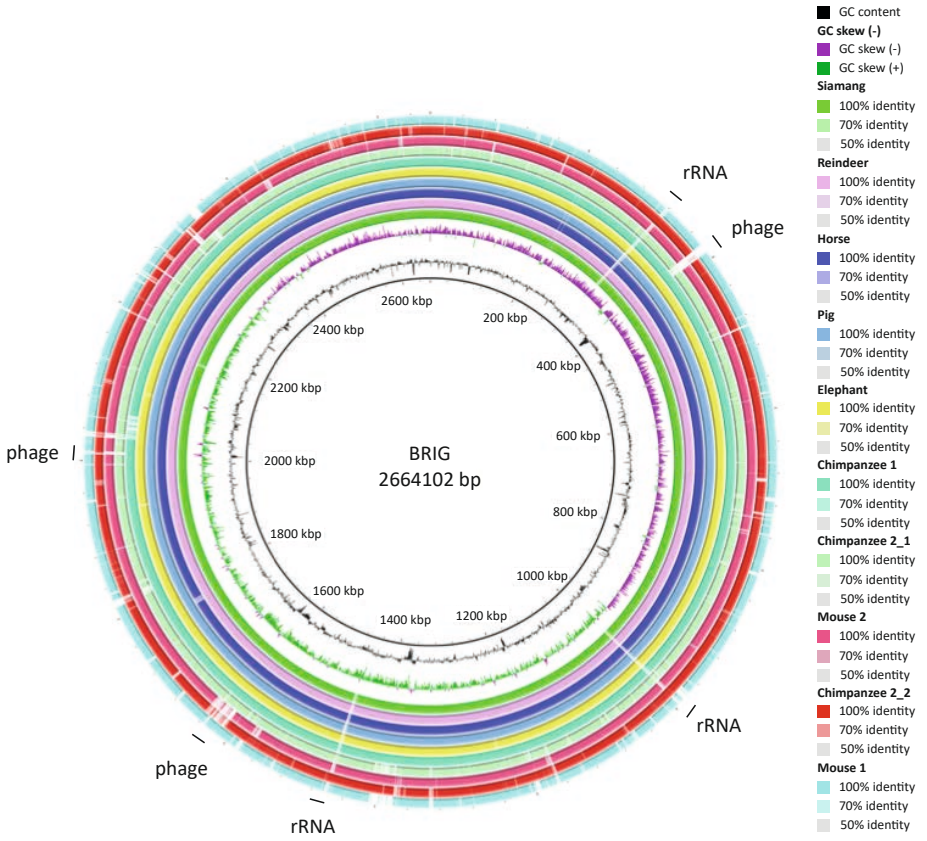

Figure 5 – BRIG genome comparison of draft genomes of new isolates to *A. muciniphila* Muc^T. Genome comparison to the type strain *A. muciniphila* Muc^T as reference based on sequence similarity. From inside to outside: the first ring describes the GC content, the second ring describes the GC skew, the next ten rings describe the similarity of the represented genomes to *A. muciniphila* Muc^T as explained in the legend. On the outside both the rRNA operons and the phage remnants are indicated.

Mucin degradation and utilization proteins of all isolates were individually analyzed for sequence divergence. In addition to the 61 mucin-degrading proteins predicted to be excreted (van Passel et al. 2011), 18 other genes were predicted to be involved in mucin degradation and utilization. The seven isolates (from chimpanzee 1, siamang, mouse 1, pig, reindeer, horse, and elephant) that had the highest sequence similarity compared to strain Muc^T harbored the same 78 mucin degradation and utilization proteins (Additional table S3), though the draft genome isolate obtained from a horse lacked one α-L-fucosidase (Amuc_1699). In comparison with the complete genome of the type strain Muc^T, we found that the draft genome of chimpanzee strain 2_2 lacked genes for two glycosyl hydrolases (Amuc_1637 and Amuc_1120) and the PfkB (Amuc_0075), which is annotated to be involved in fructose degradation. In comparison with the complete genome of the type strain Muc^T, we found that the draft genome of chimpanzee strain 2_1 lacked genes for two glycosyl hydrolases (Amuc_1120 and Amuc_0824) and one α-N-acetylglucosaminidase (Amuc_1220) as compared to the type strain. In comparison with the complete genome of the type strain Muc^T, we found that the draft genome of mouse strain 2 solely lacked the gene for one glycosyl hydrolase (Amuc_1637).

Discussion

Akkermansia muciniphila is an abundant member of the healthy human gut, and colonizes the mucus layer that lines the intestinal epithelial cells. Apart from human, *Akkermansia* 16S rRNA gene sequences can be detected in intestinal samples of many vertebrates. *A. muciniphila* is the only cultured representative of the Verrucomicrobia obtained from the human gut and was isolated from a fecal sample of a healthy adult. We determined the prevalence of Verrucomicrobia using the SILVA database, the clone libraries of Verrucomicrobia specific amplicons, and performed qPCR on 108 fecal samples collected for this study. In addition, we obtained ten new *A. muciniphila* isolates from non-human mammals that were characterized by determining their draft genome.

Our results indicate that *A. muciniphila* is not the sole species belonging to the phyla of the Verrucomicrobia that colonizes the gut of mammals. Clade 5 and 6, that contained sequences derived from fecal samples of a wide variety of mammals excluding human and mice, were found to be closely related to *A. muciniphila* Muc^T. The 16S rRNA gene sequence similarities compared to Muc^T ranged between 85.15-90.69% and 86.25-89.22% for clade 5 and 6, respectively. In addition, more distantly related Verrucomicrobia sequences were detected in fecal samples. Verrucomicrobia sequences belonging to the Prosthecobacter family (85% similarity) were detected in

gut samples of UC patients. Furthermore, Verrucomicrobia sequences belonging to the Opitutae class have been detected in the following mammals: flying fox, European rabbit, capybara, red kangaroo, Sumatran orangutan, hamadryas baboon and, eastern black and white colobus.

Clade 5 and 6 contain only non-human mammal sequences. Our isolation effort did not result in any of these *Akkermansia* species. This could mean that mucin is not the main nutritional source for these organisms or that there are differences in host mucin and therefore in mucus degradation by *Akkermansia*. However, more research is needed to investigate the type of mucins produced and secreted in the gut of different mammals to confirm this hypothesis. Recently, co-colonization with multiple *A. muciniphila* strains has been described to be possible for two *A. muciniphila* strains groups obtained from healthy human individuals (Guo et al. 2016). It would be of interest to investigate whether *A. muciniphila* and a species from clade 5 or 6 could co-colonize in a mucin-dominated environment within the gut

Our results confirm earlier reports that *A. muciniphila* is widely spread throughout mammals (Belzer and de Vos 2012). Moreover, we provide a comparative genomic analysis of new *A. muciniphila* isolates. By combining 16S rRNA gene database sequences and quantitative PCR, we could detect *Akkermansia* in animals that belong to 15 out of 16 mammalian orders included in this study. The *Akkermansia* 16S rRNA gene sequences present within different animals were highly similar. This suggests that *Akkermansia* is highly conserved and only minor changes upon co-evolution with its different host species occurred.

The qPCR analysis did not confirm the presence of *A. muciniphila* in two of the samples from which new *A. muciniphila* isolates were obtained (chimpanzee 1 and reindeer). The Verrucomicrobia PCR did confirm the presence of Verrucomicrobia in these samples. Possible inhibition of qPCR amplification might be the reason that *A. muciniphila* was not detected in these samples.

Although for some orders only few animals were tested, there does not seem to be a correlation between the abundance of *Akkermansia spp.* and the host phylogeny. A possible explanation for this high degree of conservation could be horizontal spread of the microorganism among animals in captivity due to close contact with humans as most samples were taken in the Dutch zoos. However, we could confirm that *Akkermansia spp.* and other Verrucomicrobia can also be detected in fecal samples of animals that live in the wild, both from our and a previous study (Ley et al. 2008). The spread of *Akkermansia spp.* is not restricted to any geographical location, since highly similar 16S rRNA gene sequences were found in fecal samples taken from different

parts of the world, more specific in rural Africa (Ley et al. 2008), rural Australia (this study), North-America (Ley et al. 2008, Eckburg et al. 2005, Turnbaugh et al. 2009) Asia (Li et al. 2008) and Europe (this study)(Derrien et al. 2004). Based on the observation that highly similar 16S rRNA gene sequences were found to be present within the different animals, we hypothesize that *Akkermansia spp.* are highly conserved within its different hosts. Potentially because only minor changes upon co-evolution with its different host species are needed to colonize the mucosal niche.

The presence of *A. muciniphila* in the mammalian gut has also been assessed by reconstructing metagenome assembled genomes from datasets of human, mouse and pig gut microbiomes (Guo et al. 2017). In line with our findings, the presence of *A. muciniphila* in the mammalian gut was found to be globally distributed. In this study, we used culturing techniques to isolate new *A. muciniphila* strains from the mammalian gut. However, metagenome assembled genomes of *Akkermansia* spp. that could not be obtained by culturing techniques in this study, may give more insight into the function of these strains and their ability to degrade mucus in the mammalian gut.

Mucin proteins are conserved among mammals, and even within the chordate phylum. Mucin glycoproteins are rich in proline, threonine and serine and are highly glycosylated (Moran et al. 2011). These properties enable *A. muciniphila* to use mucin as both nitrogen and carbon source (Ottman 2015). It is not known how the mucin proteins are glycosylated in the numerous vertebrates, but regardless of the potential glycosylation patterns the genomes of the *A. muciniphila* isolates encode many enzymes that can cleave a wide variety of glycan chains. Differences in the presence of mucus degradation genes in comparison to the type strain were only detected in three out of ten isolates. The genes lacking in these genomes may not directly have an effect on the mucus degrading capability, since other glycosyl hydrolases, α-L-fucosidases and N-acetylglucosaminidases are also present in the genome of *A. muciniphila*. Furthermore, it is important to note that the genomes of the new isolates were not closed. Therefore, it is a possibility that these genes are present in the genome but not detected in our analysis. Overall, this data suggests that *A. muciniphila* is a mucin-degrading specialist that has the potential to colonize different mammals regardless of their potential differences in mucin structure.

We did not observe indications for animal-species specific colonization when connecting the sequences of the *Akkermansia* clades with the hosts of origin. This contrasts what has been described for *H. pylori*, a well-studied mucosal pathogen that is mainly found in human and in very narrow range of other hosts (Lee et al. 1993). Testifying for the adaptation of *H. pylori* to the human host is the observation that its genome can be linked to human migration over our planet (Falush et al. 2003).

Conclusions

Our findings indicate that *A. muciniphila* is frequently colonizing the gut of mammals. In this study, we isolated 10 new *A. muciniphila* strains from feces of chimpanzee, siamang, mouse, pig, reindeer, horse and elephant. All new *A. muciniphila* isolates grew on mucin as sole carbon and nitrogen source suggesting that representatives of this species colonize the mucus layer of its host and therefore seem not be affected by the host diet or physiology. The low genomic divergence observed in the new strains may indicate that *A. muciniphila* favors mucosal colonization independent of the differences in hosts. In addition, the conserved mucus degradation capability points towards a similar beneficial role of the new strains in regulating host metabolic health.

Acknowledgements

We thank Nicolette Snijders (NAM), Paulien Bunskoek (DF), Simone Kools (BZ), Plankendael for fecal sample collections, and Hans Heilig, Aylin Oymaci, Marloes Witte, Eline Stroobach for technical assistance. The authors gratefully appreciate Prof. Bert 't Hart (Rijswijk, the Netherlands) and Prof. Jon Lamans (Erasmus University) for availability of marmoset fecal samples, Prof. Els Urbanus for the gift of the initial fecal sample of which Mouse 1 was isolated, Tom van den Bogert for the gift of the cow rumen sample and Jing Zhang for the gift of the pig fecal samples. We are grateful to our colleagues at the laboratory of Microbiology for stimulating discussions.

Methods

Sample collection

Fecal samples from animals were obtained at three Dutch zoo's: Burgers Zoo (Arnhem, The Netherlands), Dolfinarium (Hardewijk, The Netherlands), Natura Artis Magistra (Amsterdam, The Netherlands), Plankendael (Antwerp, Belgium), animal facilities of Wageningen UR (Wageningen, The Netherlands), animal facilities of Erasmus MC (Rotterdam, The Netherlands), animal facility of the Institute of Microbiology, (ETH Zurich, Switzerland), Animal facilities of Leiden University Medical Centre (Leiden, The Netherlands), from pets living at Dutch homes, but also from wild animals that live in either rural Africa or rural Australia. Mouse 2 has been deposited under the name *A. muciniphila* YL44, DSM26127 (https://www.dsmz.de/catalogues/dzif-sammlung-der-dsmz/maus-mikrobiomliste.html). Additional information about the samples can be found in **Table S4**.

Isolation and growth conditions

Approximately 0.2 g of fecal sample was taken and dissolved in anaerobic PBS (pH7) containing 0.5 g/l of cysteine-HCL within 24 hours of defecation. A fraction of all samples was used to prepare a glycerol (25%v/v) stock and stored at -80°C. The other fraction of all samples were 10-fold diluted in anaerobic mucin medium, composed of a bicarbonate-buffered basal medium (Derrien et al. 2004) with a pH of 6.5-7.0, supplemented with 0.5% (vol/vol) purified and dialyzed hog gastric mucin (Type III, Sigma) as sole carbon and nitrogen source as described previously (Miller and Hoskins 1981). All incubations were performed until growth was observed at 37°C in 30 ml serum bottles, containing 10 ml mucin media, sealed with butyl rubber stoppers under anaerobic conditions provided by a gas phase of 1.5 atm N2/CO2 (80:20 vol/vol). Enrichment was achieved by repeated serial dilutions. After this primary enrichment, the strains were purified by repeated plating of single colonies onto anaerobic mucin medium agar (0.8% (w/v) agar (Bacto Agar, BD), only selecting *Akkermansia*-like colonies based on previously described morphology (Derrien et al. 2004) and of which an *Akkermansia*-specific PCR (Collado et al. 2007) was found positive. The Short-chain fatty acids in cultures containing the purified strains were measured using a Thermo Electron spectrasystem HPLC equipped with an Agilent Metacarb 67H column. Purified strains were stored in mucin medium containing glycerol (25% v/v) at -80°C. DNA was extracted using the Masterpure™ Gram Positive DNA Purification Kit (Epicentre®)

A. muciniphila 16S rRNA gene abundance

Quantitative PCR amplification was performed as previously described (Collado et al. 2007) with minor modifications: samples were analyzed in a total volume of 10 µl consisting of 1 x iQ SYBR Green Supermix (BioRad), 200 nM forward primer AM1: CAGCACGTGAAGGTGGGGC (Collado et al. 2007) or 1369F: CGGTGAATACGTTCYCGG (Suzuki et al. 2000), 200 nM reverse primer AM2: CCTTGCGGTTGGCTTCAGAT (Collado et al. 2007) or 1492R: CGGCTACCTTGTTACGAC (Weisburg et al. 1991), 1 x VisiBlue Master Mix colorant (Tataabiocenter), and 0.2 ng/µl sample DNA, Nuclease-Free Water (Promega) was added to 10 µl. The primerset including AM1 and AM2 specifically amplifies *A. muciniphila* DNA and the primerset including 1369F and 1492R is a general 16S rRNA primerset to determine the total abundance. All reactions were performed in triplicates in a BioRad CFX-384 device (Veenendaal, The Netherlands). Standard curves of 16S rRNA from *A. muciniphila* cloned into pGMTeasy vector (Promega) were prepared, corresponding to a range from 10^8 to 10^0 cells. The quality of the standard curves were assessed using qPCR. The abundance of *A. muciniphila* 16S rRNA genes was determined by dividing the amount of *Akkermansia* 16S rRNA gene amplicon by that obtained from total 16S after correcting for the 16S rRNA gene copy of *A. muciniphila* (3 copies), and the average number of 16S rRNA genes (4.1

copies) in intestinal bacteria (Case et al. 2007). The starting quantity (SQ) values used for the calculations are available in **Table S5**.

16S rRNA gene sequencing of Verrucomicrobia

DNA obtained from the fecal samples was amplified in a final volume of 25 µl consisting of 1 x Green GoTaq reaction buffer (Promega), 200nM of each dNTPs (Promega), 200 nM forward primer VER_37: TGGCGGCGTGGWTAAGA (Ranjan 2010), 200 nM of reverse primer VER_673: TGCTACACCGWGAATTC (Ranjan 2010), 1U GoTaq DNA polymerase (Promega), Nuclease-Free Water (Promega) was added to obtain a total volume of 25 µl. Samples were amplified with a Dinxperlo BV G Storm thermocycler (Somerton Biotechnology) with the following program: Denaturation at 95°C for 5 min, followed by 35 cycles of denaturation at 95°C for 30 sec, annealing at 50°C for 30 sec, extension at 72°C for 1 min, and a final extension step at 72°C for 10 min. The amplicons were purified using a High pure PCR Cleanup micro kit following the manufacturer's protocol (Roche, Woerden, the Netherlands). Ligation of these amplicons in pGEMTeasy vector system as described by the manufacturer (Promega) and subsequent transformation into E. coli XL1-blue competent cells (Agilent Technologies). Inserts were sequenced at GATC (Biotech, Konstanz, Germany) using the flanking binding sites for T7: TATTTAGGTGACACTATAG and SP6: TAATACGACTCACTATAGGG. Vector, primers and low quality ends of the sequences were trimmed using DNA-baser v.354. 16S rRNA gene sequences were aligned using the SINA online alignment services (Pruesse et al. 2012) and subsequently imported into ARB (Ludwig et al. 2004).

16S rRNA gene database mining and phylogenetic tree construction

All intestinal Verrucomicrobia sequences >1100 bp, with pintails >75 were downloaded from the SILVA database version 138. The isolation source and host organism, if lacking, were retrieved from the original publications if possible and added to the designated fields in the database. All analysis concerning 16S rRNA gene sequences used for data mining performed on this dataset. The selected outgroup for the phylogenetic analysis consisted of 13 sequences from three phyla: Lentisphaerae, Omnitrophica and Chlamydiae. All 16S rRNA based phylogenetic analysis were performed with a single trimmed alignment file. The phylogenetic tree was constructed in ARB (version 5.3-org-8209) using a randomized axelerated maximum likelihood (RAxML) method (version 7.0.3) and a 40% positional conservatory filter (Ludwig et al. 2004). Depending on the amount of sequences in each clade, up until 20 representatives of each clade were selected for sequence similarity comparisons of each clade to *A. muciniphila* Muc^T.

DNA isolation and genome sequencing

High molecular weight genomic DNA was extracted from overnight-grown cultures as previously described (Douillard et al. 2013). DNA quality and concentrations were

determined by spectrophotometric analysis using NanoDrop equipment (Thermo Scientific) and by electrophoresis on a 1% agarose gel. DNA was stored at -20°C until subsequent sequencing.

Genome sequencing was carried out at the Institute of Biotechnology, University of Helsinki (Finland). A MiSeq library was generated and sequenced on an Illumina MiSeq Personal Sequencer with 250 bp paired-end reads and an insert size of 500 bp. Reads were assembled using Ray (k-mer 101)(Boisvert et al. 2012).

Genome annotation

Annotation was carried out with an in-house pipeline consisting of Prodigal v2.5 for prediction of protein coding DNA sequences (Hyatt et al. 2010), InterProScan 5RC7 for protein annotation (Hunter et al. 2012), tRNAscan-SE v1.3.1 for prediction of tRNAs (Lowe and Eddy 1997) and RNAmmer v1.2 for prediction of rRNAs (Lagesen et al. 2007). Additional protein function predictions were derived via BLAST identifications against the UniRef50 (Suzek et al. 2007) and Swissprot (UniProt, 2014) databases (download August 2013). Subsequently, the annotation was further enhanced by adding EC numbers via PRIAM version 2013-03-06 (Claudel-Renard et al. 2003). Non-coding RNAs were identified using rfam_scan.pl v1.04, on release 11.0 of the RFAM database (Burge et al. 2013). CRISPRs were annotated using CRISPR Recognition Tool v1.1 (Bland et al. 2007). A further step of automatic curation was performed by weighing the annotation of the different associated domains, penalizing uninformative functions (e.g. "Domain of unknown function"), and prioritizing functions of interest (e.g. domains containing "virus", "bacteriophage", "integrase" for bacteriophage related elements; similar procedure for different other functions).

Pan-genome analysis

To determine the pan-genome, the genomes were annotated using Prokka (Seemann 2014). Subsequently, Roary was used to obtain the core-genome alignment (Page et al. 2015). Based on this information, a maximum likelihood phylogenetic tree was constructed. The phylogenetic tree and the core-genome alignment were combined in Phandango to visualize the results (Hadfield et al. 2018).

16S rRNA gene sequence retrieval

For each organism the 16S rRNA reads were retrieved by filtering the FASTQ file through sortmeRNA using default settings while only using the 16S SILVA 118 database (Kopylova et al. 2012). The obtained reads where then assembled using IDBA_UD into a 16S rRNA gene contig and used for further analysis (Peng et al. 2012).

Supplementary information

Figure S1.pdf – Original detailed randomized axelerated maximum likelihood (RAxML) tree. This content is available online (doi: 10.1186/s12866-021-02360-6)

Table S1 – ANI BLAST and aligned percentage between all new *A. muciniphila* isolates. This content is available online (doi: 10.1186/s12866-021-02360-6)

Table S2.xlsx – Overview of the functional domains of the type strain and all new *A. muciniphila* isolates. This content is available online (doi: 10.1186/s12866-021-02360-6)

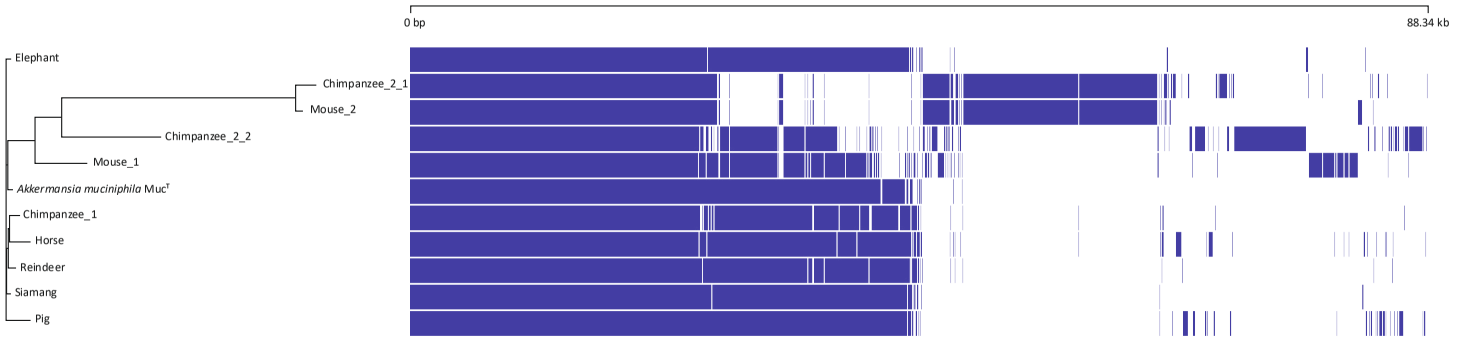

Figure S2: Pan genome of the type strain and all new *A. muciniphila* isolates visualized using Phandango

Figure S2 – Pan-genome of the type strain and all new *A. muciniphila* isolates visualized using Phandango.

Table S3 – Mucin degradation and utilization genes. Depicted are the sequence similarities of the genes from the newly obtained strains compared to the genes of strain Muc^T.

Locus tag	Annotation	Chimpanzee_1	Elephant	Horse	Pig	Reindeer	Siamang	Chimpanzee_2_2	Mouse_2_MG	Chimpanzee_2_1	Mouse_1_M89
Amuc_1671	phosphofructokinase	1,00	1,00	1,00	1,00	1,00	1,00	1,00	1,00	0,94	0,94
Amuc_1481	6-phosphofructokinase	1,00	1,00	1,00	1,00	1,00	1,00	0,99	1,00	0,96	0,96
Amuc_0721	fructose-bisphosphate [Upper glycolysis]	1,00	1,00	1,00	1,00	1,00	1,00	0,99	0,99	0,98	0,98
Amuc_0562	Triose-phosphate [Upper glycolysis]	1,00	1,00	1,00	1,00	1,00	1,00	0,99	1,00	0,97	0,97
Amuc_0210	6-phosphofructokinase	1,00	1,00	1,00	1,00	1,00	1,00	0,99	1,00	0,94	0,94
Amuc_2164	glycoside [Glycosyl hydrolase]	1,00	1,00	1,00	1,00	1,00	1,00	1,00	0,99	0,96	0,96
Amuc_2148	Beta-N-acetylhexosaminidase [Glycosyl hydrolase]	1,00	1,00	1,00	1,00	1,00	1,00	0,98	0,99	0,95	0,95
Amuc_2136	Glycoside [Glycosyl hydrolase]	1,00	1,00	1,00	1,00	1,00	1,00	0,98	1,00	0,99	0,99
Amuc_2109	Beta-N-acetylhexosaminidase [Glycosyl hydrolase]	1,00	1,00	1,00	1,00	1,00	1,00	0,97	0,99	0,92	0,92
Amuc_2108	glycoside [Glycosyl hydrolase]	1,00	1,00	1,00	1,00	1,00	1,00	1,00	1,00	0,99	0,99
Amuc_2019	Beta-N-acetylhexosaminidase [Glycosyl hydrolase]	1,00	1,00	1,00	1,00	1,00	1,00	0,99	1,00	1,00	1,00
Amuc_2018	Beta-N-acetylhexosaminidase [Glycosyl hydrolase]	1,00	1,00	1,00	1,00	1,00	1,00	0,99	1,00	0,99	0,99
Amuc_1924	Beta-N-acetylhexosaminidase [Glycosyl hydrolase]	1,00	1,00	1,00	1,00	1,00	1,00	1,00	1,00	1,00	1,00
Amuc_1870	Alpha-glucosidase [Glycosyl hydrolase]	1,00	1,00	1,00	1,00	1,00	1,00	0,99	0,97	0,92	0,92
Amuc_1868	glycoside [Glycosyl hydrolase]	1,00	1,00	1,00	1,00	1,00	1,00	0,98	1,00	0,99	0,99
Amuc_1835	Exo-alpha-sialidase [Glycosyl hydrolase]	1,00	1,00	1,00	1,00	1,00	1,00	0,98	0,99	0,99	0,99
Amuc_1815	Beta-N-acetylhexosaminidase [Glycosyl hydrolase]	1,00	1,00	1,00	1,00	1,00	1,00	1,00	1,00	1,00	1,00
Amuc_1812	alpha [Glycosyl hydrolase]	1,00	1,00	1,00	1,00	1,00	1,00	0,99	0,99	0,99	0,99

Table S3 *(Continued)*

Locus tag	Annotation	Chimpanzee_1	Elephant	Horse	Pig	Reindeer	Siamang	Chimpanzee_2_2	Mouse_2_MG	Chimpanzee_2_1	Mouse_1_M89
Amuc_1686	Beta-galactosidase [Glycosyl hydrolase]	1,00	1,00	1,00	1,00	1,00	1,00	0,98	0,99	0,96	0,96
Amuc_1669	Beta-N-acetylhexosaminidase [Glycosyl hydrolase]	1,00	1,00	1,00	1,00	1,00	1,00	1,00	1,00	0,98	0,98
Amuc_1667	glycoside [Glycosyl hydrolase]	1,00	1,00	1,00	1,00	1,00	1,00	0,97	1,00	0,97	0,97
Amuc_1666	glycoside [Glycosyl hydrolase]	1,00	1,00	1,00	1,00	1,00	1,00	0,99	0,95	0,95	0,95
Amuc_1637	alpha [Glycosyl hydrolase]	1,00	1,00	1,00	1,00	1,00	1,00	0,00	0,00	0,95	0,95
Amuc_1621	4-alpha-glucanotransferase [Glycosyl hydrolase]	1,00	1,00	1,00	1,00	1,00	1,00	0,97	0,97	0,98	0,98
Amuc_1547	conserved [Glycosyl hydrolase]	1,00	1,00	1,00	1,00	1,00	1,00	0,98	1,00	0,96	0,96
Amuc_1463	hypothetical [Glycosyl hydrolase]	1,00	1,00	1,00	1,00	1,00	1,00	1,00	1,00	0,97	0,97
Amuc_1420	conserved [Glycosyl hydrolase]	1,00	1,00	1,00	1,00	1,00	1,00	0,97	0,99	0,93	0,93
Amuc_1260	glycoside [Glycosyl hydrolase]	1,00	1,00	1,00	1,00	1,00	1,00	0,98	1,00	0,97	0,97
Amuc_1220	Alpha-N-acetylglucosaminidase [Glycosyl hydrolase]	1,00	1,00	1,00	1,00	1,00	1,00	0,99	0,99	0,00	0,00
Amuc_1216	oxidoreductase [Glycosyl hydrolase]	1,00	1,00	1,00	1,00	1,00	1,00	0,93	0,99	0,92	0,92
Amuc_1187	Alpha-galactosidase [Glycosyl hydrolase]	1,00	1,00	1,00	1,00	1,00	1,00	0,96	0,99	0,95	0,95
Amuc_1120	conserved [Glycosyl hydrolase]	1,00	1,00	1,00	1,00	1,00	1,00	0,00	0,99	0,00	0,00
Amuc_1032	Beta-N-acetylhexosaminidase [Glycosyl hydrolase]	1,00	1,00	1,00	1,00	1,00	1,00	0,98	0,99	0,96	0,96
Amuc_1008	glycoside [Glycosyl hydrolase]	1,00	1,00	1,00	1,00	1,00	1,00	0,87	1,00	0,95	0,95
Amuc_0920	oxidoreductase [Glycosyl hydrolase]	1,00	1,00	1,00	1,00	1,00	1,00	0,95	1,00	0,80	0,80
Amuc_0875	glycoside [Glycosyl hydrolase]	1,00	1,00	1,00	1,00	1,00	1,00	1,00	1,00	0,97	0,97
Amuc_0868	Beta-N-acetylhexosaminidase [Glycosyl hydrolase]	1,00	1,00	1,00	1,00	1,00	1,00	1,00	0,99	0,98	0,98

Table S3 *(Continued)*

Locus tag	Annotation	Chimpanzee_1	Elephant	Horse	Pig	Reindeer	Siamang	Chimpanzee_2_2	Mouse_2_MG	Chimpanzee_2_1	Mouse_1_M89
Amuc_0863	glycosyl [Glycosyl hydrolase]	1,00	1,00	1,00	1,00	1,00	1,00	0,99	1,00	0,97	0,97
Amuc_0855	glycoside [Glycosyl hydrolase]	1,00	1,00	1,00	1,00	1,00	1,00	0,96	1,00	0,43	0,43
Amuc_0846	coagulation [Glycosyl hydrolase]	1,00	1,00	1,00	1,00	1,00	1,00	0,95	0,98	0,95	0,95
Amuc_0824	glycoside [Glycosyl hydrolase]	1,00	1,00	1,00	1,00	1,00	1,00	1,00	0,99	0,00	0,00
Amuc_0771	Beta-galactosidase [Glycosyl hydrolase]	1,00	1,00	1,00	1,00	1,00	1,00	0,89	0,99	0,88	0,88
Amuc_0724	Glucan [Glycosyl hydrolase]	1,00	1,00	1,00	1,00	1,00	1,00	0,99	0,98	0,96	0,96
Amuc_0698	beta-glucanase [Glycosyl hydrolase]	1,00	1,00	1,00	1,00	1,00	1,00	1,00	0,99	0,96	0,96
Amuc_0697	beta-glucanase [Glycosyl hydrolase]	1,00	1,00	1,00	1,00	1,00	1,00	0,97	1,00	0,95	0,95
Amuc_0625	Exo-alpha-sialidase [Glycosyl hydrolase]	1,00	1,00	1,00	1,00	1,00	1,00	1,00	1,00	0,99	0,99
Amuc_0623	glycosyl [Glycosyl hydrolase]	1,00	1,00	1,00	1,00	1,00	1,00	0,99	0,99	0,98	0,98
Amuc_0539	glycoside [Glycosyl hydrolase]	1,00	1,00	1,00	1,00	1,00	1,00	0,99	0,99	0,96	0,96
Amuc_0517	raffinose [Glycosyl hydrolase]	1,00	1,00	1,00	1,00	1,00	1,00	0,97	0,99	0,92	0,92
Amuc_0397	Beta-N-acetylhexosaminidase [Glycosyl hydrolase]	1,00	1,00	1,00	1,00	1,00	1,00	0,94	0,99	0,92	0,92
Amuc_0392	coagulation [Glycosyl hydrolase]	1,00	1,00	1,00	1,00	1,00	1,00	0,93	0,99	0,88	0,88
Amuc_0369	Beta-N-acetylhexosaminidase [Glycosyl hydrolase]	1,00	1,00	1,00	1,00	1,00	1,00	0,88	0,75	0,89	0,89
Amuc_0290	glycoside [Glycosyl hydrolase]	1,00	1,00	1,00	1,00	1,00	1,00	0,97	1,00	0,96	0,96
Amuc_0216	hypothetical [Glycosyl hydrolase]	1,00	1,00	1,00	1,00	1,00	1,00	0,97	0,99	0,97	0,97
Amuc_0186	glycoside [Glycosyl hydrolase]	1,00	1,00	1,00	1,00	1,00	1,00	0,99	1,00	0,98	0,98
Amuc_0146	Alpha-L-fucosidase [Glycosyl hydrolase]	1,00	1,00	1,00	1,00	1,00	1,00	0,99	1,00	0,98	0,98

Table S3 *(Continued)*

Locus tag	Annotation	Chimpanzee_1	Elephant	Horse	Pig	Reindeer	Siamang	Chimpanzee_2_2	Mouse_2_MG	Chimpanzee_2_1	Mouse_1_M89
Amuc_0060	Alpha-N-acetylglucosaminidase [Glycosyl hydrolase]	1,00	1,00	1,00	1,00	1,00	1,00	0,99	1,00	0,96	0,96
Amuc_0052	Hyaluronon glucosaminidase [Glycosyl hydrolase]	1,00	1,00	1,00	1,00	1,00	1,00	0,99	0,99	0,94	0,94
Amuc_0017	oxidoreductase [Glycosyl hydrolase]	1,00	1,00	1,00	1,00	1,00	1,00	0,97	0,99	0,53	0,53
Amuc_0010	Alpha-L-fucosidase [Glycosyl hydrolase]	0,00	1,00	1,00	1,00	1,00	1,00	0,99	1,00	0,98	0,98
Amuc_1822	glucosamine-6-phosphate [N-Acetylgalactosamine]	1,00	1,00	1,00	1,00	1,00	1,00	1,00	1,00	0,94	0,94
Amuc_0948	N-acetylglucosamine-6-phosphate [N-Acetylgalactosamine]	1,00	1,00	1,00	1,00	1,00	1,00	0,99	1,00	0,97	0,97
Amuc_0097	ROK [N-Acetylgalactosamine]	1,00	1,00	1,00	1,00	1,00	1,00	0,99	0,99	0,93	0,93
Amuc_1309	Aldose [Galactose degradation]	1,00	1,00	1,00	1,00	1,00	1,00	1,00	1,00	0,98	0,98
Amuc_1261	Aldose [Galactose degradation]	1,00	1,00	1,00	1,00	1,00	1,00	0,99	0,99	0,96	0,96
Amuc_1125	UDP-glucose [Galactose degradation]	1,00	1,00	1,00	1,00	1,00	1,00	0,99	0,99	0,88	0,88
Amuc_0969	galactokinase	1,00	1,00	1,00	1,00	1,00	1,00	0,94	0,99	0,89	0,89
Amuc_0029	NAD-dependent [Galactose degradation]	1,00	1,00	1,00	1,00	1,00	1,00	0,97	0,98	0,92	0,92
Amuc_1832	L-fucose [Fucose degradation]	1,00	1,00	1,00	1,00	1,00	1,00	0,97	0,99	0,94	0,95
Amuc_1830	L-fuculokinase	1,00	1,00	1,00	1,00	1,00	1,00	0,96	0,99	0,94	0,94
Amuc_1829	class [Fucose degradation]	1,00	1,00	1,00	1,00	1,00	1,00	1,00	1,00	0,96	0,96
Amuc_1245	Mannose-6-phosphate [Fructose degradation]	1,00	1,00	1,00	1,00	1,00	1,00	0,94	0,98	0,95	0,95
Amuc_0075	PfkB [Fructose degradation]	1,00	1,00	1,00	1,00	1,00	1,00	0,00	0,99	0,92	0,92
Amuc_2100	aminoglycoside [Carbohydrate transport]	1,00	1,00	1,00	1,00	1,00	1,00	1,00	1,00	0,99	0,99

Table S3 *(Continued)*

Locus tag	Annotation	Chimpanzee_1	Elephant	Horse	Pig	Reindeer	Siamang	Chimpanzee_2_2	Mouse_2_MG	Chimpanzee_2_1	Mouse_1_M89
Amuc_1833	L-fucose [Carbohydrate transport]	1,00	1,00	1,00	1,00	1,00	1,00	0,98	1,00	0,98	0,98
Amuc_1757	Phosphotransferase [Carbohydrate transport]	1,00	1,00	1,00	1,00	1,00	1,00	1,00	1,00	1,00	1,00
Amuc_1699	aminoglycoside [Carbohydrate transport]	1,00	1,00	0,00	1,00	1,00	1,00	1,00	0,99	0,98	0,98
Amuc_0729	aminoglycoside [Carbohydrate transport]	1,00	1,00	1,00	1,00	1,00	1,00	0,99	1,00	0,96	0,96
Average similarity to MucT		1,00	1,00	1,00	1,00	1,00	1,00	0,99	1,00	0,98	0,98

Table S4 – Metadata of obtained fecal samples and isolates.

Sample name	Name	Order	Diet	Zoo
CON 001	Human	Primates	Omnivore	Wageningen UR
CON 005	Human	Primates	Omnivore	Wageningen UR
CON 008	Human	Primates	Omnivore	Wageningen UR
CON 010	Human	Primates	Omnivore	Wageningen UR
CON 011	Human	Primates	Omnivore	Wageningen UR
CON 014	Human	Primates	Omnivore	Wageningen UR
CON 16.0	Human	Primates	Omnivore	Wageningen UR
CON 21.0	Human	Primates	Omnivore	Wageningen UR
CON 22.0	Human	Primates	Omnivore	Wageningen UR
CON 23.0	Human	Primates	Omnivore	Wageningen UR
C	Human	Primates	Omnivore	Wageningen UR
1_1	Human	Primates	Omnivore	Wageningen UR
2_1	Human	Primates	Omnivore	Wageningen UR
A1	Chimpanzee	Primates	Omnivore	Burgers Zoo, Arnhem
A2	Chimpanzee	Primates	Omnivore	Burgers Zoo, Arnhem
A5	Chimpanzee	Primates	Omnivore	Burgers Zoo, Arnhem
A6	Western Gorilla	Primates	Herbivore	Burgers Zoo, Arnhem
A7	Western Gorilla	Primates	Herbivore	Burgers Zoo, Arnhem
A11	Siamang	Primates	Herbivore	Burgers Zoo, Arnhem
A12	Siamang	Primates	Herbivore	Burgers Zoo, Arnhem
A10	Dusky leaf monkey	Primates	Herbivore	Burgers Zoo, Arnhem
54A	Japanese macaqua	Primates	Herbivore/Insectivore	Natura Artis Magistra, Amsterdam
54B	Japanese macaqua	Primates	Herbivore/Insectivore	Natura Artis Magistra, Amsterdam
59A	Sulawesi macaque	Primates	Omnivore	Natura Artis Magistra, Amsterdam

Table S4 *(Continued)*

Sample name	Name	Order	Diet	Zoo
59B	Sulawesi macaque	Primates	Omnivore	Natura Artis Magistra, Amsterdam
55A	Mandrill	Primates	Omnivore	Natura Artis Magistra, Amsterdam
55B	Mandrill	Primates	Omnivore	Natura Artis Magistra, Amsterdam
1_31	Marmoset	Primates	Herbivore/insectivore	Animal facility of Erasmus University, Rotterdam
1_32	Marmoset	Primates	Herbivore/insectivore	Animal facility of Erasmus University, Rotterdam
1_33	Marmoset	Primates	Herbivore/insectivore	Animal facility of Erasmus University, Rotterdam
1_34	Marmoset	Primates	Herbivore/insectivore	Animal facility of Erasmus University, Rotterdam
1_35	Marmoset	Primates	Herbivore/insectivore	Animal facility of Erasmus University, Rotterdam
1_36	Marmoset	Primates	Herbivore/insectivore	Animal facility of Erasmus University, Rotterdam
52A	Pygmy Marmoset	Primates	Herbivore	Natura Artis Magistra, Amsterdam
52B	Pygmy Marmoset	Primates	Herbivore	Natura Artis Magistra, Amsterdam
60A	Black Spider Monkey	Primates	Herbivore	Natura Artis Magistra, Amsterdam
60B	Black Spider Monkey	Primates	Herbivore	Natura Artis Magistra, Amsterdam
51A	Grey Mouse Lemur	Primates	Insectivore/Omnivore	Natura Artis Magistra, Amsterdam
51B	Grey Mouse Lemur	Primates	Insectivore/Omnivore	Natura Artis Magistra, Amsterdam
56A	Ring-tailed Lemur	Primates	Herbivore/Insectivore	Natura Artis Magistra, Amsterdam
56B	Ring-tailed Lemur	Primates	Herbivore/Insectivore	Natura Artis Magistra, Amsterdam
A24	Rabbit	Lagomorpha	Herbivore	Pet animal, Wageningen
M89	Mouse 1	Rodentia	Omnivore	Animal facility of Leiden University, Leiden

Table S4 *(Continued)*

Sample name	Name	Order	Diet	Zoo
MG	Mouse 2	Rodentia	Omnivore	Animal facility of the Institute of Microbiology, ETH Zürich, Switzerland
49A	Capybara	Rodentia	Herbivore	Burgers Zoo, Arnhem
49B	Capybara	Rodentia	Herbivore	Burgers Zoo, Arnhem
53A	Giant Anteater	Pilosa	Insectivore	Natura Artis Magistra, Amsterdam
53B	Giant Anteater	Pilosa	Insectivore	Natura Artis Magistra, Amsterdam
57A	Two-toed Sloth	Pilosa	Herbivore	Natura Artis Magistra, Amsterdam
57B	Two-toed Sloth	Pilosa	Herbivore	Natura Artis Magistra, Amsterdam
58A	Southern Tamandua	Pilosa	Insectivore	Natura Artis Magistra, Amsterdam
58B	Southern Tamandua	Pilosa	Insectivore	Natura Artis Magistra, Amsterdam
34A	South american tapir	Perissodactyla	Herbivore	Burgers Zoo, Arnhem
34B	South american tapir	Perissodactyla	Herbivore	Burgers Zoo, Arnhem
36A	Southern white rhinoceros	Perissodactyla	Herbivore	Burgers Zoo, Arnhem
36B	Southern white rhinoceros	Perissodactyla	Herbivore	Burgers Zoo, Arnhem
35	Rhinoceros	Perissodactyla	Herbivore	Africa
45A	Seba's short-tailed bat	Chiroptera	Herbivore	Burgers Zoo, Arnhem
45B	Seba's short-tailed bat	Chiroptera	Herbivore	Burgers Zoo, Arnhem
40A	California bighorn sheep	Artiodactyla	Herbivore	Burgers Zoo, Arnhem
40B	California bighorn sheep	Artiodactyla	Herbivore	Burgers Zoo, Arnhem
40C	California bighorn sheep	Artiodactyla	Herbivore	Burgers Zoo, Arnhem
42A	Collared peccary	Artiodactyla	Omnivore	Burgers Zoo, Arnhem
42B	Collared peccary	Artiodactyla	Omnivore	Burgers Zoo, Arnhem
A3	Baringo Giraffe	Artiodactyla	Herbivore	Burgers Zoo, Arnhem
A4	Baringo Giraffe	Artiodactyla	Herbivore	Burgers Zoo, Arnhem

Table S4 *(Continued)*

Sample name	Name	Order	Diet	Zoo
30A	Blue duiker	Artiodactyla	Herbivore	Burgers Zoo, Arnhem
30B	Blue duiker	Artiodactyla	Herbivore	Burgers Zoo, Arnhem
A15	European forest reindeer	Artiodactyla	Herbivore	Burgers Zoo, Arnhem
A16	European forest reindeer	Artiodactyla	Herbivore	Burgers Zoo, Arnhem
A20	Warthog	Artiodactyla	Omnivore	Burgers Zoo, Arnhem
A21	Warthog	Artiodactyla	Omnivore	Burgers Zoo, Arnhem
34	Giraffe	Artiodactyla	Omnivore	Africa
horse	Horse	Artiodactyla	Herbivore	The Netherlands
Cow 1	Cow (rumen)	Ruminentia	Herbivore	Animal facility of Wageningen University
Cow 2	Cow (rumen)	Ruminentia	Herbivore	Animal facility of Wageningen University
61A	Harbour porpoise	Cetacea	Carnivore	Dolfinarium, Harderwijk
61B	Harbour porpoise	Cetacea	Carnivore	Dolfinarium, Harderwijk
61C	Harbour porpoise	Cetacea	Carnivore	Dolfinarium, Harderwijk
62A	Common Bottlenose Dolphin	Cetacea	Carnivore	Dolfinarium, Harderwijk
62B	Common Bottlenose Dolphin	Cetacea	Carnivore	Dolfinarium, Harderwijk
62C	Common Bottlenose Dolphin	Cetacea	Carnivore	Dolfinarium, Harderwijk
pig	Pig	Suidea	Omnivore	Animal facility of Wageningen University
35	Pygmy Hippopotamus	Hippopotamidae	Herbivore	Burgers Zoo, Arnhem
50A	Oriental small-clawed otter	Carnivora	Carnivore	Burgers Zoo, Arnhem
50B	Oriental small-clawed otter	Carnivora	Carnivore	Burgers Zoo, Arnhem
39A	Bobcat	Carnivora	Carnivore	Burgers Zoo, Arnhem
39B	Bobcat	Carnivora	Carnivore	Burgers Zoo, Arnhem
41A	Striped Skunk	Carnivora	Carnivore	Burgers Zoo, Arnhem
41B	Striped Skunk	Carnivora	Carnivore	Burgers Zoo, Arnhem

Table S4 *(Continued)*

Sample name	Name	Order	Diet	Zoo
43A	Ring-tailed cacomistle	Carnivora	Carnivore	Burgers Zoo, Arnhem
43B	Ring-tailed cacomistle	Carnivora	Carnivore	Burgers Zoo, Arnhem
44A	Swift Fox	Carnivora	Carnivore	Burgers Zoo, Arnhem
44B	Swift Fox	Carnivora	Carnivore	Burgers Zoo, Arnhem
31AI	Malayan sun bear	Carnivora	Carnivore	Burgers Zoo, Arnhem
31BI	Malayan sun bear	Carnivora	Carnivore	Burgers Zoo, Arnhem
32A	Sumatran tiger	Carnivora	Carnivore	Burgers Zoo, Arnhem
32B	Sumatran tiger	Carnivora	Carnivore	Burgers Zoo, Arnhem
33A	Ring-tailed cacomistle	Carnivora	Carnivore	Burgers Zoo, Arnhem
33B	Ring-tailed cacomistle	Carnivora	Carnivore	Burgers Zoo, Arnhem
63A	Walrus	Carnivora	Carnivore	Dolfinarium, Harderwijk
38A	Caribbean Manatee	Sirenia	Herbivore	Burgers Zoo, Arnhem
38B	Caribbean Manatee	Sirenia	Herbivore	Burgers Zoo, Arnhem
A8	Asiatic elephant	Proboscidea	Herbivore	Burgers Zoo, Arnhem
A9	Asiatic elephant	Proboscidea	Herbivore	Burgers Zoo, Arnhem
33	Elephant	Proboscidea	Herbivore	Africa
37A	Swamp Wallaby	Diprotodontia	Herbivore	Burgers Zoo, Arnhem
37B	Swamp Wallaby	Diprotodontia	Herbivore	Burgers Zoo, Arnhem
48	Aardvark	Tubilidenta	Insectivore	Burgers Zoo, Arnhem
16	Echidna	Monotremata	Herbivore \ Insectivore	Australia
17	Echidna	Monotremata	Herbivore \ Insectivore	Australia
18	Echidna	Monotremata	Herbivore \ Insectivore	Australia
19	Echidna	Monotremata	Herbivore \ Insectivore	ZOO Planckendael, Mechelen, Belgium

Table S5 – Starting quantity (SQ) values of both *Akkermansia* and the general 16S rRNA qPCR runs.

Sample number	Animal	Average SQ general	Average SQ Akkermansia
A1	Chimpanzee	2.00E+04	0.00E+00
A2	Chimpanzee	1.62E+04	6.60E+00
A5	Chimpanzee	2.16E+04	3.30E+01
A6	Western Gorilla	6.36E+04	3.08E+01
A7	Western Gorilla	4.09E+04	1.48E+01
48	Aardvark	3.70E+04	0.00E+00
49A	Capybara	3.63E+04	0.00E+00
49B	Capybara	2.77E+04	0.00E+00
50AI	Otter	4.52E+04	0.00E+00
50BI	Otter	1.93E+04	3.98E+00
38A	Caribbean Manatee	1.00E+05	1.03E+03
38B	Caribbean Manatee	4.78E+04	4.82E+02
39A	Bobcat	1.54E+05	0.00E+00
39B	Bobcat	1.69E+05	3.52E+01
40A	Sheep	2.52E+04	6.95E+01
40B	Sheep	4.47E+04	1.67E+02
40C	Sheep	5.27E+04	7.49E+01
41A	Striped Skunk	1.53E+05	0.00E+00
41B	Striped Skunk	7.31E+04	3.54E+01
42A	Collared peccary	3.27E+04	5.56E+00
42B	Collared peccary	3.96E+04	0.00E+00
43A	Cacomistle	3.44E+04	0.00E+00
43B	Cacomistle	4.98E+04	0.00E+00
44A	Swift Fox	8.89E+04	0.00E+00
44B	Swift Fox	1.33E+05	0.00E+00
A3	Baringo Giraffe	5.27E+04	7.13E+00
A4	Baringo Giraffe	3.91E+04	4.58E+00
A8	Asiatic elephant	5.35E+03	3.10E+01
A9	Asiatic elephant	1.20E+04	0.00E+00
30A	Blue duiker	1.80E+04	0.00E+00
30B	Blue duiker	3.59E+04	1.87E+02
A15	Reindeer	1.73E+04	0.00E+00
A16	Reindeer	4.70E+04	0.00E+00
A10	Dusky leaf monkey	4.96E+04	0.00E+00
31AI	Malayan sun bear	1.90E+05	0.00E+00
31BI	Malayan sun bear	7.07E+04	0.00E+00
A11	Siamang	1.36E+05	3.57E+01

Table S5 *(Continued)*

Sample number	Animal	Average SQ general	Average SQ Akkermansia
A12	Siamang	2.36E+00	0.00E+00
32A	Sumatran tiger	6.45E+04	0.00E+00
32B	Sumatran tiger	8.46E+04	0.00E+00
A20	Warthog	3.57E+04	0.00E+00
A21 I	Warthog	2.67E+04	0.00E+00
45A	Seba's short-tailed bat	4.45E+04	3.52E+01
45B	Seba's short-tailed bat	6.94E+04	0.00E+00
33A	Ring-tailed cacomistle	7.03E+04	3.56E+01
33B	Ring-tailed cacomistle	7.97E+04	0.00E+00
34A	South american tapir	1.90E+04	3.54E+01
34B	South american tapir	1.72E+04	0.00E+00
35	Pygmy Hippopotamus	5.80E+04	0.00E+00
36A	Southern white rhinoceros	2.02E+04	0.00E+00
36B	Southern white rhinoceros	2.02E+04	3.48E+01
37A	Swamp Wallaby	6.93E+03	0.00E+00
37B	Swamp Wallaby	1.86E+04	0.00E+00
16	Echidna	9.28E+02	2.97E+01
17	Echidna	1.44E+05	2.45E+00
18	Echidna	1.72E+05	4.07E+00
19	Echidna	5.37E+02	0.00E+00
A24	Rabbit	2.43E+04	1.53E+01
C	Human	8.29E+03	3.06E+01
33	Elephant(Africa)	3.75E+02	0.00E+00
34	Giraffe (Africa)	3.24E+03	0.00E+00
35	Rhino (Africa)	4.26E+02	0.00E+00
1_1	Human	1.72E+04	0.00E+00
2_1	Human	2.17E+04	3.70E+02
1_31	Marmoset	1.46E+03	0.00E+00
1_32	Marmoset	1.31E+03	0.00E+00
1_33	Marmoset	1.86E+03	0.00E+00
1_34	Marmoset	2.81E+03	0.00E+00
1_35	Marmoset	4.02E+02	3.50E+01
1_36	Marmoset	3.35E+03	0.00E+00
CON 001	Human	2.38E+05	3.64E+00
CON 005	Human	7.65E+04	1.72E+02
CON 008	Human	9.49E+04	1.01E+03
CON 010	Human	7.66E+04	3.46E+02
CON 011	Human	1.44E+05	1.04E+03

Table S5 *(Continued)*

Sample number	Animal	Average SQ general	Average SQ Akkermansia
CON 014	Human	2.09E+05	1.72E+03
CON 16.0	Human	7.27E+05	2.10E+00
CON 21.0	Human	2.70E+04	1.42E+02
CON 22.0	Human	1.86E+04	3.40E+03
CON 23.0	Human	8.03E+03	3.61E+01
Cow 1	Cow	1.90E+04	3.55E+01
Cow 2	Cow	1.03E+04	0.00E+00
51A	Grey Mouse Lemur	4.38E+03	2.81E-02
51B	Grey Mouse Lemur	4.56E+03	2.81E-02
52A	Pygmy Marmoset	9.09E+03	0.00E+00
52B	Pygmy Marmoset	4.93E+03	0.00E+00
53A	Giant Anteater	4.62E+03	1.81E-01
53B	Giant Anteater	1.45E+04	1.16E-02
54A	Japanese macaque	9.51E+04	0.00E+00
54B	Japanese macaque	4.17E+04	0.00E+00
55A	Mandrill	1.34E+05	0.00E+00
55B	Mandrill	7.80E+04	0.00E+00
56A	Ring-tailed Lemur	2.38E+04	0.00E+00
56B	Ring-tailed Lemur	2.45E+04	0.00E+00
57A	Two-toed Sloth	9.18E+03	0.00E+00
57B	Two-toed Sloth	4.38E+03	0.00E+00
58A	Southern Tamandua	2.92E+04	0.00E+00
58B	Southern Tamandua	5.84E+04	0.00E+00
59A	Sulawesi macaque	1.86E+04	0.00E+00
59B	Sulawesi macaque	3.17E+04	0.00E+00
60A	Black Spider Monkey	3.86E+04	3.04E-02
60B	Black Spider Monkey	6.30E+03	7.72E-01
61A	Harbour porpoise	2.03E+03	3.07E-02
61B	Harbour porpoise	1.40E+01	1.04E-02
61C	Harbour porpoise	3.17E+01	0.00E+00
62A	Common Bottlenose Dolphin	6.12E+04	0.00E+00
62B	Common Bottlenose Dolphin	1.33E+02	5.47E-03
62C	Common Bottlenose Dolphin	2.40E+04	5.81E-03

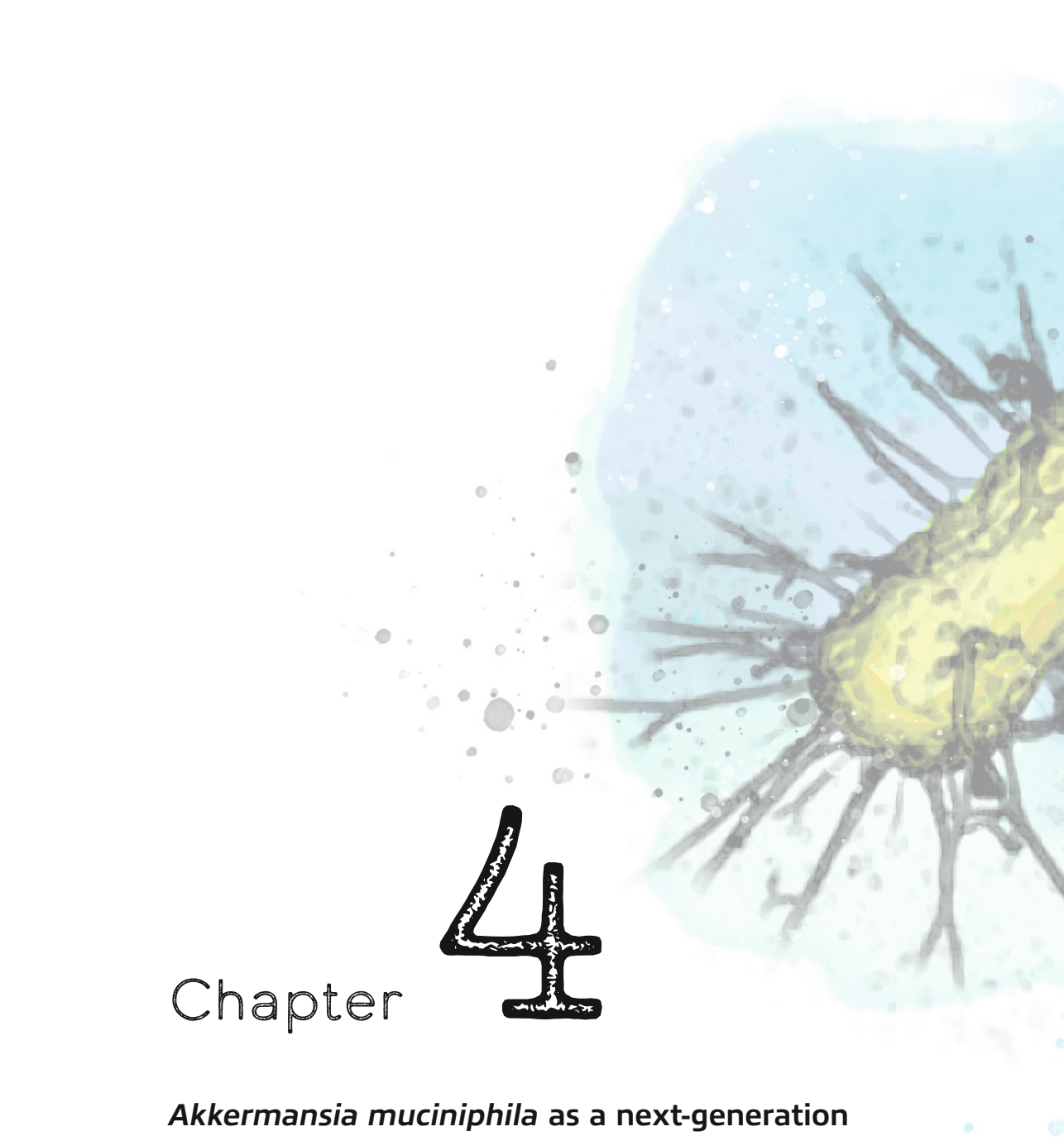

Chapter 4

Akkermansia muciniphila as a next-generation beneficial microbe: Efficient cultivation in food-grade media and its characterization by transcriptomics and proteomics

Sharon Y. Geerlings, Kees van der Ark, Bart Nijsse, Sjef Boeren, Martin Pabst, Mark van Loosdrecht, Clara Belzer and Willem M. de Vos

Abstract

Over the past years, the gut microbiota and its correlation to health and disease has been studied extensively. In terms of beneficial microbes, an increased interest in *Akkermansia muciniphila* has been observed since its discovery. Direct evidence for the role of *A. muciniphila* in host health has been provided in both mice and human studies. However, for human interventions with *A. muciniphila* cells industrial-scale fermentations are needed and hence the used cultivation media should be free of animal-derived components, food-grade, non-allergenic and allow for efficient growth to high densities as to provide cost-effective production platforms. In this study we assessed the growth and performance of *A. muciniphila* in batch bioreactors using newly developed plant-based media with varying carbon sources, including different ratios of GlcNAc and glucose. Comparisons between growth on these media and that on mucin revealed differences on both transcriptome and proteome levels, including differences in the expression of glycosyltransferases, signaling proteins and genes involved in stress-response. Furthermore, differences in cell morphology and OD_{600} values were observed. In conclusion, our data suggests that the food-grade medium composition described here could be used to produce *A. muciniphila* in high yields for therapeutic purposes.

Introduction

Over the past years, the gut microbiota and its correlation to health and disease has been studied extensively (de Vos et al. 2022). Notably, strong correlations have been made between the gut microbiota composition and diseases, such as obesity (Tims et al. 2013, Le Chatelier et al. 2013), pre-diabetes (Allin et al. 2018, Zhong et al. 2019), type 2 diabetes, non-alcoholic fatty liver disease (Jiang et al. 2015) and liver cirrhosis (Qin et al. 2014). Moreover, a causal involvement of gut microbiota by fecal microbiota transplantation has been demonstrated in various inflammatory and metabolic diseases (Hanssen et al. 2021). This is increasing the interest in the development of interventions aiming to alter the gut microbiota, including those with specific gut bacteria also termed next-generation beneficial microbes (Fan and Pedersen 2021, Cani and de Vos 2017, Bui and de Vos 2021).

While most gut bacteria inhabit the lumen of the colon and thrive on dietary leftovers, *Akkermansia muciniphila* is an abundant gut symbiont feeding on the colonic mucosa (Derrien et al. 2004, Geerlings et al. 2018, Cani et al. 2022). *A. muciniphila* is a Gram-negative bacterium belonging to the Verrucomicrobia phylum, found to be present in the mucosal layer and specialized in the use of mucin as single carbon, nitrogen and energy source (Derrien et al. 2004, Belzer and de Vos 2012). Considerable interest in *A. muciniphila* derives from human association studies showing an inverse correlation to diabetes and obesity and its correlations with a healthy metabolic status, as recently reviewed (Cani et al. 2022). These results were initially found with deep metagenomic analyses, later expanded with species-targeted quantifications, and recently supported by linking thousands of *A. muciniphila* metagenomes to host characteristics (Le Chatelier et al. 2013, Dao et al. 2016, Karcher et al. 2021).

Direct evidence for the role of *A. muciniphila* was provided in a series of mouse models where administration of its cells was found to prevent diet-induced obesity (Everard et al. 2013). This hallmark study was followed by many reports showing beneficial effects of *A. muciniphila* administration in a variety of mouse models (Wang et al. 2022, Qu et al. 2021, Bian et al. 2019, Yaghoubfar et al. 2020, Wu et al. 2020). However, all these studies have been using mucin-based media to cultivate *A. muciniphila,* providing a potential bias since this animal-derived glycoprotein is not free from remnants of other bacteria. A breakthrough came with the development of metabolic models that showed the dependency of *A. muciniphila* on exogenously added threonine, resulting in synthetic media that obviated the use of mucin (Ottman et al. 2017). A key finding was the fact that *A. muciniphila* does not have the capacity to synthesize N-acetylglucosamine (GlcNAc) from glucose, most likely as a consequence of its adaptation to mucin that contains this and other nitrogen-sugars (van der Ark et al.

2018). In the resulting synthetic media, mucin was substituted by L-threonine, glucose and GlcNAc as well as peptone (van der Ark et al. 2018, Ottman et al. 2017). These were used in a series of mechanistic studies in diabetic and obese mice demonstrating that pasteurized *A. muciniphila* cells recapitulated the beneficial effects of live cells grown in mucin-free media in diabetic and obese mice (Plovier et al. 2017). The capacity of pasteurized *A. muciniphila* cells to be at least as effective as live cells was confirmed in a recent clinical trial where their administration to metabolic syndrome subjects resulted in improved insulin sensitivity, reduced insulinemia and plasma total cholesterol as well as reduction of body weight, including reduced fat mass and hip circumference (Depommier et al. 2019).

Several studies have been focusing on the cultivation, storage and delivery methods of either pasteurized or alive *A. muciniphila* for therapeutic purposes (Plovier et al. 2017, van der Ark 2018, Chang et al. 2020, Marcial-Coba et al. 2018, Marcial-Coba et al. 2019). Moreover, the environmental conditions in which *A. muciniphila* survives have been studied in detail as it is sensitive to low pH, oxygen and bile salts (Derrien et al. 2004, Ouwerkerk et al. 2016, Hagi et al. 2020). This information may be useful for the delivery of alive *A. muciniphila* for therapeutic purposes. Along with the development of synthetic media, the growth characteristics and the physiology of *A. muciniphila* have been characterized comparing mucin growth to that in media containing single sugars, such as glucose and GlcNAc. This is of importance as *A. muciniphila* exerts its health benefits while using mucin as a carbon, nitrogen and energy source and hence several studies addressed its transcriptome and proteome under these conditions (Ottman et al. 2017, Ouwerkerk et al. 2016). Recent years has seen an increasing number of signaling molecules that *A. muciniphila* is producing, which interact with the host (de Vos et al. 2022, Cani et al. 2022). These include the protein Amuc_1100 that is known to be part of a set of outer membrane proteins encoded by a gene cluster, which also encodes the secretin PilQ (Amuc_1098) that allows type 4 pili to be exposed to the environment (Ottman et al. 2016). Preclinical data has shown that the heat-stable Amuc_1100 protein can reproduce the effects of live and pasteurized cells in protection from diet-induced obesity and is an efficient ligand for signal transduction to Toll-like receptor 2 (TLR2) (Plovier et al. 2017, Ottman et al. 2017). Other recently identified proteins that have been implicated in host signaling include Amuc_1631 (also known as P9), Amuc_1434, and Amuc_2109 but the location and production of these have not yet been studied (Yoon et al. 2021, Meng et al. 2020, Qian et al. 2022).

For human interventions or supplementation with *A. muciniphila* cells, industrial-scale fermentations are needed and hence the used cultivation media should not only be free from mucin derived from animals but also food-grade, non-allergenic and allow efficient growth to high densities as to provide cost-effective production

platforms. Moreover, addressing present consumer needs, plant-based rather than animal-derived components are to be used. Finally, in these conditions there should be sufficient production of signaling molecules that have been identified as interacting with the host. It is furthermore of importance to assess the safety of *A. muciniphila* in the development trajectory for its use in therapeutic applications. A recent study demonstrated the safety of pasteurized *A. muciniphila* cells in variety of in vitro models and a 90 day rat trial (Druart et al. 2021). This and other information was used by the European Food Safety Authority (EFSA) to approve the use of pasteurized *A. muciniphila* cells as a novel food (Turck et al. 2021). This all supports the interest in the fermentation optimization of this next generation beneficial microbe and in this study we assessed the growth and performance of *A. muciniphila* in newly developed food-grade and plant-based media with varying carbon sources using a multi-omics approach in comparison with its growth on mucin-containing media.

Results

Growth characteristics and metabolic activity

In a first series of experiments, we built on the metabolic modeling data that predicted *A. muciniphila* Muc^T to grow efficiently (growth rate of 0.13 h^{-1}) on an equimolar mixture of glucose and GlcNAc in a minimal medium with threonine (Ottman et al. 2017, van der Ark et al. 2018). To increase cell yield, a food-grade and plant-based protein source was added to the minimal medium in the form of 16 g/L soy protein hydrolysate that resulted in a medium (soy medium) yielding a high growth rate of 0.53 h^{-1} exceeding that of *A. muciniphila* on mucin, which is approximately 0.41 h^{-1} (Derrien et al. 2004, Ottman et al. 2017). The cell densities in the soy peptone medium as measured by absorption at OD600 were above 5, whereas mucin medium supported growth to an OD of 2-2.5 (Ottman et al. 2017). Even higher cell yields could be obtained by using pea peptone at a level of 32 g/L which led to high densities of OD600 values above 10. Since the soy protein hydrolysate is derived from a plant source, it is an acceptable food-grade nitrogen source and applicable on a large scale. Moreover, as the growth rate on soy medium was higher than that on mucin and relatively high cell densities were obtained, we decided to further characterize *A. muciniphila* cells grown on this food-grade medium, the more so as these were highly active in protecting mice from diet-induced obesity (Plovier et al. 2017). A few observations were noted in the first series of experiments, that needed to be further addressed. First, phase-contrast and scanning electron microscopy of cells grown on soy medium showed a significantly (p-value < 0.01) elongated shape with a length of 1.3 (±0.80) µm versus 0.8 (±0.25) µm when grown in mucin medium (based on analysis of 251 and 160 cells, respectively) (**Figure S1**). Also, the acetate/propionate ratio in the soy medium was 0.92 while that

of cells grown in mucin was 1.2 (±0.13) (Ouwerkerk et al. 2016). This can be explained by the fact that the GlcNAc, which is present in equal amounts as glucose in the soy medium generates an extra acetate after deamination.

To further address the global differences between *A. muciniphila* cells grown in soy medium and mucin medium, transcriptome analysis was performed to reveal initial transcriptional changes between mucin and soy medium. The main differences were found to be in the increased expression in soy medium of genes encoding transporters such as Major Facilitator Superfamily (MFS), biopolymer, anion and amino acid transporters (Amuc_1331, Amuc_0546, Amuc_0221 and Amuc_0037) as well as peptide, aliphatic sulfonate, nitrate/sulfonate/bicarbonate, cobalt and manganese ABC transporters (Amuc_0672, AMUC_1297, Amuc_0408, Amuc_1198, Amuc_1199, Amuc_0056, Amuc_1380 and Amuc_1186) with an increase >5-fold. In addition, genes involved in oxygen stress-response were found to be higher in soy medium including rubrerythrin (Amuc_2055 and Amuc_2056), peroxidase (Amuc_1321) and catalase (Amuc_2070). In mucin medium, genes involved in cell shape (Amuc_0540) and division (Amuc_0348) and mucin degradation genes such as alpha-N-acetylglucosaminidase (Amuc_0060), beta-glucanase (Amuc_0875) and sulfatases (Amuc_0491 and Amuc_0451) were found to have an >5-fold increase.

High biomass yield reached on food-grade medium

Because of the apparent effect of equimolar amounts of glucose and GlcNAc on the morphology, viscosity and gene expression of *A. muciniphila* cells, we further explored the effect of different carbon source ratios on the growth and physiology of *A. muciniphila*. For this purpose, we decided to use pea peptone (32 g/L) as additional food-grade nitrogen source rather than soy peptone to avoid potential issues associated with phytoestrogens present in soy. Hence, *A. muciniphila* was grown in the pea peptone medium with varying ratios of glucose to GlcNAc in a fermentor system with controlled temperature, pH and gas phase. A total of four fermentations were characterized in detail, with three different glucose to GlcNAc carbon source ratios 3:1 (Condition A), 10:1 (Condition B) and 20:1 (Condition C) and one control, which was supplemented with mucin (Condition D). Interestingly, while the mucin medium allowed a rapid initiation of growth, an increase in the duration of the lag phase was observed along the decreasing concentrations of GlcNAc in the fermentors (**Figure 1**). It is important to note that the pre-cultures were grown on pea peptone medium supplemented with equimolar concentrations of glucose and GlcNAc, which is most similar to condition A in terms of glucose to GlcNAc ratio. However, up to four transfers in food-grade medium supplemented with glucose and GlcNAc in a ratio of 20:1 was found to lead to growth adaptation of *A. muciniphila* and rapid initiation of growth (**Figure S2**). Microscopy results showed the formation of elongated cells in conditions

A-C as compared to mucin (condition D) (**Figure S3**). The number of cells and increased cell length observed in these cultures reflect with a higher biomass production. The decreasing concentration of GlcNAc also led to lower biomass concentrations at the end of the 72-hour fermentation period as determined by the OD600. Condition A was found to have the fastest growth and highest biomass concentration as deduced from the OD600 measurements.

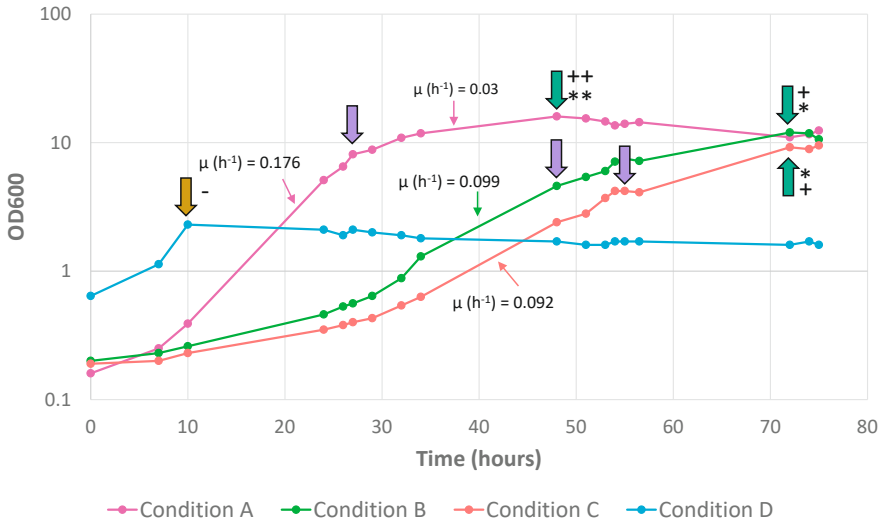

Figure 1: Exponential growth of *A. muciniphila* as a function of glucose to GlcNAc ratios. Fermentors at pH 7.0 were run with glucose to GlcNAc carbon source ratios of 3:1 (Condition A), 10:1 (Condition B) and 20:1 (Condition C) or on mucin (Condition D). Purple arrows indicate mid-log sampling, turquoise arrows indicate end-log sampling, and the brown arrow indicates sampling of condition D. The growth rate is indicated in the graph for conditions A-C. Asterisks at the arrows indicate either glucose and GlcNAc were depleted (**) or only GlcNAc was depleted (*). Observed viscosity in the cultures is indicated with (++) meaning high viscosity, (+) meaning medium viscosity or (-) no viscosity observed.

Transcriptome response in exponential and stationary phase

The growth curve of condition A showed two different growing phases, the first one until approximately 27 hours with a high growth rate (0.176 h^{-1}) and the second phase from 27 to 48 hours (0.03 h^{-1}), the time at which the glucose and GlcNAc were depleted (see **Figure 1**) This observation was also supported by the transcriptome data that showed dozens of genes to be significantly higher expressed in the first compared to the second growth phase (**Figure 2**). The genes with the highest upregulation (>5-

fold) at the end of the first phase included several gene clusters with two or more juxtaposed genes, such as the metabolic gene cluster encoding a glutaminase and a likely glutamine-GABA antiporter (Amuc_0037-0038), as well as several stress proteins (Amuc_1406-1408, coding for DnaK, GroES and GroEL). In addition, the expression of single genes was upregulated for other stress proteins such as Skp (Amuc_0405) and HtpG (Amuc_2002), as well as genes involved in oxygen and other stress responses, such as catalase (Amuc_2070), glutamate decarboxylase (Amuc_0372) and NAD(P)-dependent oxidoreductase (Amuc_0777). Many of the genes observed to be upregulated in the end-log phase of this condition had no known function and were annotated as hypothetical. Genes that were upregulated and annotated with a function included genes involved in transport systems for iron (Amuc_1929-1931), potassium (Amuc_0830-0831 and Amuc_1151-1153) and phosphate (Amuc_1302-1307) as well as phage production (such as Amuc_1355, Amuc_1936 and Amuc_1335). A notable exception was the highly (14.8-fold) upregulated gene for a predicted lactoylglutathione lyase (Amuc_1878) that has shown in *Salmonella* to be involved in the detoxification of methylglyoxal, known to be produced in the gut but also in fermentors with peptones (Chakraborty et al. 2015).

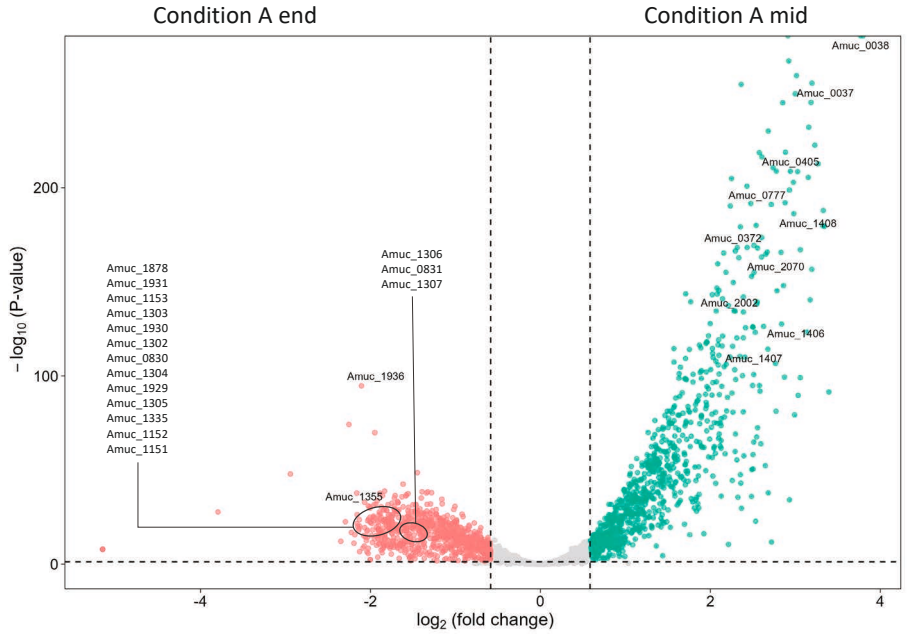

Figure 2: Volcano plot comparing the transcriptional response of *A. muciniphila* in fermentations of the mid-log phase and end-log phase of condition A. Only the differentially expressed genes mentioned in the text are labelled here.

In addition to the transcriptional activity, also the catabolism of *A. muciniphila* in the food-grade medium was assessed as to determine the depletion of the glucose and GlcNAc (**Figure 1** and **Figure S4**). In all conditions, the main fermentation products included acetate, propionate and succinate. As shown previously, the propionate:acetate ratio may differ depending on the cultivation conditions used to grow *A. muciniphila* (van der Ark et al. 2018). In the conditions tested in this study, the ratio of propionate:acetate varied between the different carbon source ratios used for cultivation (**Figure S5**). Comparing the final stages of the fermentors, the lowest propionate:acetate ratio was found in condition D with a ratio of 0.88, followed by condition A with a ratio of 1.06, while the ratios in condition B and C were 1.25 and 1.23, respectively, coinciding with the ratios found in the initial experiments. The carbon balances of the fermentations with glucose and various amounts of GlcNAc were calculated and amounted to approximately 72% (**Figure S6**).

The global proteome is more conserved than the global transcriptome during different growth conditions

We also compared the overall gene expression of *A. muciniphila* in pea peptone medium with different ratios of glucose and GlcNAc (both early and late growth samples were analyzed for each condition– see **Figure 1**) to that of cells grown on mucin using transcriptomics in triplicate (**Figure S7**). In total, 2317 genes were detected in the complete dataset (including 63 tRNAs). The number of differentially expressed genes (DEGs) for all comparisons is shown in **Table S1**. Principal Component Analysis (PCA) showed that condition D and A_end both form separate clusters in comparison to the other samples in this dataset (**Figure 3**). This coincides with the large number of DEGs comparing these two samples with the remaining samples. In addition to gene expression, we also assessed protein production by *A. muciniphila* in all conditions using proteomics of duplicated samples. With this technique, 1648 proteins were detected in the complete dataset. The PCA based on the proteome data did not show separation between A_end and the other samples, indicating that on the proteome level these samples are more similar than observed on the transcriptome level.

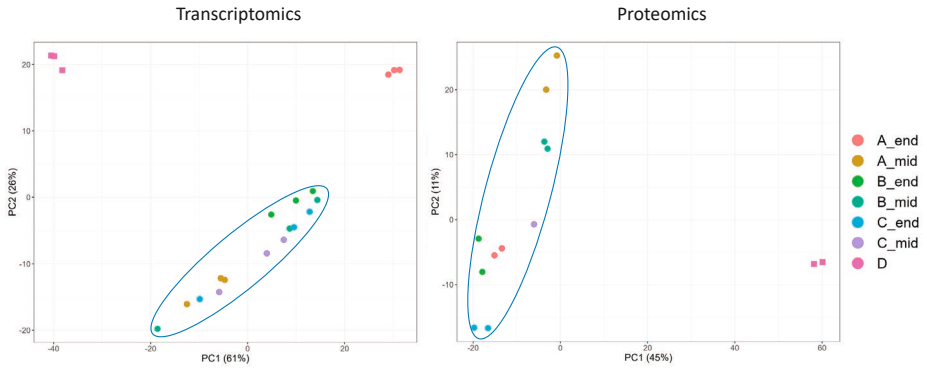

Figure 3: **PCA analysis of fermentor conditions A-D over time, for transcriptomics n=3 and proteomics n=2.** The main clusters are highlighted for clarity; squares represent the results with mucin grown cells.

KEGG metabolic pathway predictions were used to assess the differences in the metabolic pathways operating in various fermentor conditions (**Figure S8**). Overall, the metabolic pathway with the highest abundance across all conditions was found to be the carbohydrate metabolism pathway, with abundances ranging between 3.4% and 5.5% for transcriptomics and between 3.7% and 4.4% for proteomics. The metabolism pathway with the second highest abundance on transcriptome level was the amino acid metabolism pathway, with abundances ranging from 2.6% to 3.7%. However, an exception was noted for the mid-log phase of condition A, where the metabolism of other amino acids has the second highest abundance of 2.93%. In contrast, the proteome showed a higher abundance of proteins involved in the metabolism of other amino acids (2.7%-3.9%) as opposed to the findings in the transcriptomics data. Apart from condition D, where the abundance of proteins involved in the metabolism of other amino acids was only 0.72%, statistical analysis revealed no significant differences between fermentor conditions within the different metabolisms.

GlcNAc concentration affects expression of glycosyltransferases and stress-response genes

A limited number of genes were found to be differentially expressed between the mid-log phases of conditions with different GlcNAc concentrations. Due to the small number of differentially expressed genes between the mid-log phases of condition B and C (two significant differentially expressed genes, Amuc_1139 and Amuc_1140 which are both part of a glycosyltransferase cluster), here we only compare condition A (high GlcNAc) and condition C (low GlcNAc) (252 differentially expressed genes) (**Figure 4**).

A higher concentration of GlcNAc showed significantly higher expression of a glycosyltransferase cluster (Amuc_1139 until Amuc_1142) and genes possibly involved in exopolysaccharide or capsular polysaccharide production (Amuc_2077 until Amuc_2079). Furthermore, a higher concentration of GlcNAc led to overexpression of genes involved in stress-response, including an anaerobic ribonucleoside triphosphate reductase cluster (Amuc_0860 until Amuc_0862), NAD(P)-dependent oxidoreductase (Amuc_0777), rubrerythrin (Amuc_2056), catalase (Amuc_2070), glutamate decarboxylase (Amuc_0372), molecular chaperones DnaK (Amuc_1406), HtpG (Amuc_2002) and GroES (Amuc_1407). In low GlcNAc many genes encoding hypothetical proteins were found among the upregulated genes. However, lactoylglutathione lyase (Amuc_1878), glutamate dehydrogenase (Amuc_2051) and phosphate ABC transporter permease protein PstA (Amuc_1304) were significantly upregulated in this condition as compared to high GlcNAc.

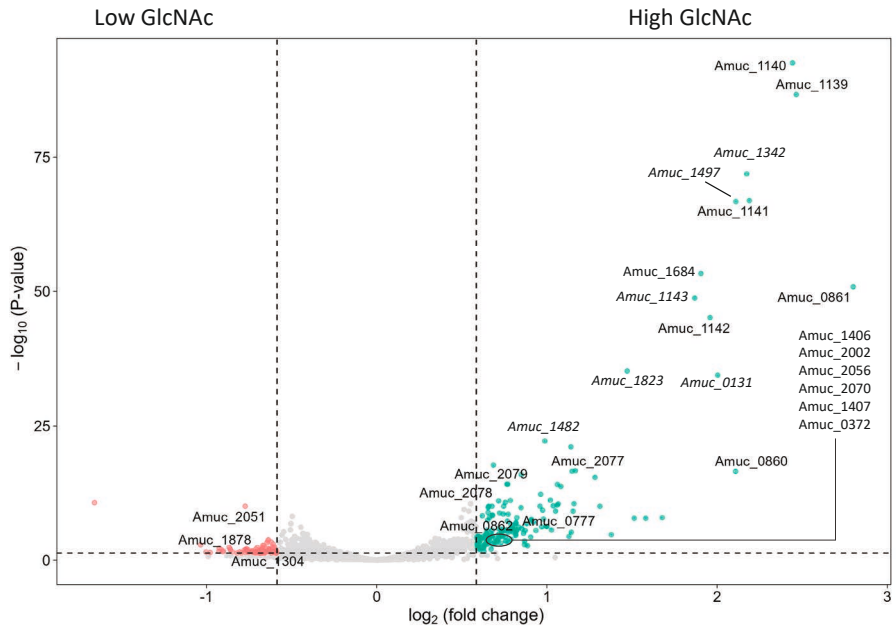

Figure 4: Volcano plot comparing the transcriptional response of *A. muciniphila* in fermentations containing a high concentration of GlcNAc (mid-log condition A) and a low concentration of GlcNAc (mid-log condition C). The differentially expressed genes mentioned in the text are labelled here as well as highly differentiated genes annotated as hypothetical proteins in italics.

Proteomic and transcriptomic response of *A. muciniphila* in glucose/GlcNAc versus mucin

Cultivating *A. muciniphila* in food-grade medium where mucin is substituted for a mixture of glucose and GlcNAc may induce transcriptional and translational changes that affect its physiology. Using the proteome data, we compared mid-log condition A (high GlcNAc) and condition D (mucin). In total, 116 proteins were identified to have a protein abundance ratio higher than 10. The protein abundance ratios indicate that in the mucin condition, mostly proteins involved in mucin degradation were upregulated. In contrast, in high GlcNAc medium the proteins that were upregulated in comparison to mucin were mainly stress-related proteins and glycosyl transferases, in line with the observations related to the transcriptional response.

In the following sections we focus mainly on the transcriptome data these revealed a higher number of differentially expressed genes than that found in the proteomics data. This suggests that cells responded to differences in medium composition by adapting its regulations over its functional aspect, possibly minimizing differences in overall cell composition. Over 1500 genes were found to be significantly differentially expressed between the mid-log conditions containing GlcNAc and mucin (**Table S1**). Multiple gene clusters were identified that were upregulated in either high GlcNAc medium (condition A) and low GlcNAc (Condition C) or mucin medium, growth conditions that showed the most similar growth rates (see **Figure 1**). In the following sections, we compared the transcriptional response of exponentially growing cells (mid-log) on high GlcNAc or low GlcNAc and mucin.

High GlcNAc induces stress-response as compared to mucin

In medium containing high GlcNAc (Condition A) several genes and complete gene clusters related to stress responses were found to be significantly upregulated as compared to the mucin condition (**Figure 5**). This includes a gene cluster encoding for an ABC transporter and phosphate ABC transporter (Amuc_1294-1308), a gene cluster involved in the production of exopolysaccharides (Amuc_2077-Amuc_2096) and an additional glycosyl transferase cluster was significantly upregulated (Amuc_1139-1142), a gene cluster containing multiple aldo/keto reductases (Amuc_1796-1809) and the gene for anaerobic ribonucleoside-triphosphate reductase activating protein (Amuc_0860). Moreover, additional complete gene clusters related to stress responses were found to be significantly upregulated in both high-GlcNAc and low-GlcNAc conditions, as compared to mucin, including a gene cluster encoding ribosomal proteins (Amuc_0294-0308), an iron transport cluster (Amuc_1930 until Amuc_1934) and a potential flavin biosynthesis gene cluster (Amuc_0421-0426). Other genes that may be involved in stress-response, but that were not part of a gene cluster were also identified to be upregulated in both GlcNAc conditions. This includes genes for

rubrerythrin (Amuc_2055-2056), catalase (Amuc_2070), oxidoreductases (Amuc_0116, Amuc_0777, Amuc_1072, Amuc_1176 and Amuc_1389), ribonucleoside-triphosphate reductase (Amuc_0862) and glutamate decarboxylase (Amuc_0372).

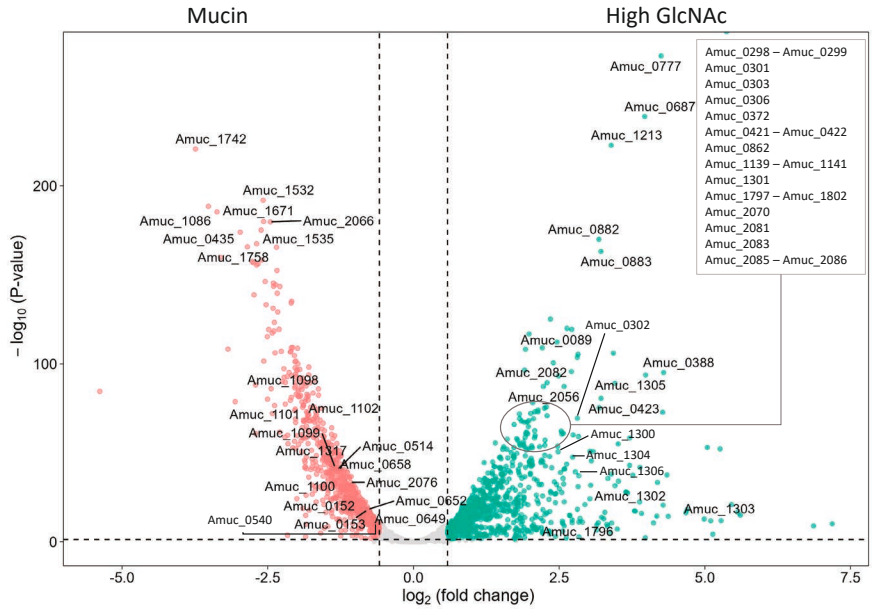

Figure 5: **Volcano plot comparing the transcriptional response of *A. muciniphila* in fermentations containing a high concentration of GlcNAc (mid-log condition A) and mucin (condition D).** Due to the high number of genes upregulated in high-GlcNAc, genes with a -log10 p-value < $1*10^{-50}$ and a log2 fold change < 2.5 that are mentioned in the text are not shown in this figure. All other differentially expressed genes mentioned in the text are labelled here.

Next to the transcriptomic stress response, elongated cells were observed in the fermentors containing glucose and GlcNAc in comparison to the small oval shaped cells visible when *A. muciniphila* was cultivated on mucin (**Figure S3**). Elongated cells were also observed in the previously mentioned soy medium cultures (**Figure S1**), together with an increased expression of Amuc_0540 encoding cell shape-determining protein MreB in mucin as compared to soy medium. Following this observation, we performed a more in-depth analysis of the expression of genes involved in cell elongation and division. At mid exponential phase Amuc_1052 (cell division trigger factor), Amuc_1176 (cell division inhibitor), Amuc_1558 (implicated in cell division based on FtsL cleavage) and Amuc_0348 (cell division protein FtsH) were overexpressed in all fermentors containing glucose and GlcNAc compared to

mucin, of which Amuc_1052 and Amuc_0348 significantly in all mid-exponential conditions (**Table 1**). In contrast, eight genes involved in cell division were significantly overexpressed in the condition containing mucin compared to all mid conditions containing glucose and GlcNAc, namely Amuc_0152 (Tubulin/FtsZ GTPase), Amuc_0153 (cell division protein FtsA), Amuc_0514 (peptidoglycan glycosyltransferase), Amuc_0540 (cell shape-determining protein MreB), Amuc_0649 (transcriptional regulator MraZ), Amuc_0658 (cell cycle protein), Amuc_1317 (integral membrane protein CcmA involved in cell shape determination) and Amuc_2076 (cell division FtsK) (**Table 1**). Overall, the transcriptomic stress-response and elongated cells observed in the cultures grown in synthetic medium without mucin indicates that a stress-response is triggered in the absence of mucin in this medium.

Table 1: Differential expression of genes involved in cell division comparing high-GlcNAc to the mucin condition. Asterisks indicate genes that were also upregulated in the preliminary transcriptome data comparing soy medium to mucin medium.

Genes	Description	High-GlcNAc vs mucin		
		Fold change	p value	
Amuc_1176	Cell division inhibitor	3.07	6.57E-48	Upregulated in high GlcNAc
Amuc_0348	Cell division protein FtsH	2.34	4.32E-36	
Amuc_1052	Cell division trigger factor	2.29	7.41E-31	
Amuc_1558	RIP metalloprotease RseP	1.39	1.63E-06	
Amuc_0662	Polypeptide-transport-associated domain-containing protein FtsQ-type	1.47	4.58E-08	Upregulated in mucin
Amuc_0540	Cell shape-determining protein MreB*	1.59	6.6E-11	
Amuc_0652	Peptidoglycan glycosyltransferase	1.71	4.79E-19	
Amuc_0649	Transcriptional regulator MraZ	1.73	3.34E-17	
Amuc_0153	Cell division protein FtsA	1.74	1.97E-18	
Amuc_0152	Tubulin/FtsZ GTPase	1.92	1.24E-26	
Amuc_2076	Cell division FtsK	2.11	3.66E-34	
Amuc_0658	Cell cycle protein	2.34	3.38E-41	
Amuc_0514	Peptidoglycan glycosyltransferase	2.45	1.26E-41	
Amuc_1317	Integral membrane protein CcmA involved in cell shape determination	2.69	2.88E-46	

A. muciniphila functions involved in host interactions

An important host-signaling protein of *A. muciniphila* was identified to be the protein Amuc_1100. This protein is part of a gene cluster encoded by Amuc_1098-Amuc_1102, involved in pili production (Ottman et al. 2017). Interestingly, transcriptome data showed that this gene cluster was approximately 2.5 to 4-fold upregulated during

growth in mucin (condition D) as compared to both GlcNAc conditions. Other recently identified proteins that have been implicated in host signaling include Amuc_1631 (also known as P9), Amuc_1434, and Amuc_2109, but the location and production of these has not been studied. The expression of all potential signaling proteins overall was found to be slightly higher in mucin, except for Amuc_1434. Since transcription data only provide relative data, we also addressed the proteome data as to identify the real production of the potential host signaling proteins. The LFQ intensities of host signaling proteins Amuc_1100, Amuc_1631 and Amuc_2109 were all found to be slightly higher in the mucin condition, as compared to the high and low GlcNAc conditions (**Table 2**). However, considering the high biomass obtained with high-GlcNAc and low-GlcNAc conditions, the final yield of these proteins in the cultures is expected to be higher in both GlcNAc conditions as compared to mucin. Furthermore, it is important to note that the LFQ intensity of Amuc_2109 is low in comparison to those of Amuc_1100 and Amuc_1631, even when corrected for the protein sizes. The exact location of Amuc_2109 in the cell is unknown, but its location may influence the detection levels of this protein. The potential host signaling protein Amuc_1434 was not detected in our proteome data.

Table 2: LFQ intensities and protein ratios between mucin and GlcNAc conditions of host signaling proteins Amuc_1100, Amuc_1434, Amuc_1631 and Amuc_2109. ND indicates the protein was not detected in the proteome data (LFQ < 1.4E+06).

	Size (kDa)	High GlcNAc	Low GlcNAc	Mucin	Mucin/High GlcNAc	Mucin/Low GlcNAc
Amuc_1100	32	1.46E+09	2.01E+09	1.89E+09	1.3	1.88
Amuc_1434	50	ND	ND	ND	ND	ND
Amuc_1631	87	3.06E+09	2.99E+09	3.12E+09	1.02	2.09
Amuc_2109	38	1.60E+07	1.37E+07	2.39E+07	1.5	3.49

One of the main functions of *A. muciniphila* in the gut is mucin degradation. We assessed the regulation of 65 genes involved in mucin degradation in mucin and GlcNAc conditions (**Table S2** and **Table S3**). Interestingly, when comparing mucin with the high GlcNAc condition, 21 genes out of 65 were significantly upregulated in mucin, while 19 genes were significantly downregulated. In comparison to the low GlcNAc condition, 22 genes were significantly upregulated in mucin, while 26 genes were significantly downregulated. This indicates that these genes also play an important role in sugar metabolism when mucin is not present in the medium. Furthermore, a gene cluster containing genes encoding tryptophan synthases (Amuc_1535 and Amuc_1536) was significantly (6-fold) upregulated in the mucin condition as compared

to high and low GlcNAc. This could correlate to the use of serine in mucin for the biosynthesis of L-tryptophan.

Furthermore, 15 (high GlcNAc) and 16 (low GlcNAc) out of 23 genes encoding PEP-CTERM domain proteins were significantly upregulated (1.5to 4-fold) in mucin compared to the high and low GlcNAc conditions as well as EpsH encoded by Amuc_1470 (2.6-fold and 2-fold, respectively). The combination of PEP-CTERM domain proteins and EpsH was previously suggested to form a protein export sorting system (Haft et al. 2006). Furthermore, a cluster encoding the type II secretion system (Amuc_1584 until Amuc_1586) involved in the secretion of proteins, was also significantly upregulated (2.4 to 4-fold) in mucin conditions. This indicates that in mucin conditions, the emphasis on protein secretion is higher than in conditions without mucin.

Discussion

In this study we assessed the cultivation of *A. muciniphila* food-grade pea-peptone medium with different concentrations of carbon sources as to be able to produce cells to be used in therapeutic applications. The use of food-grade synthetic and non-allergenic medium supplemented with glucose and GlcNAc resulted in high cell yields and fast growth of *A. muciniphila*. Furthermore, we gained detailed insight in the physiology by a combination of biochemical analysis as well as transcriptional and proteomic analysis. In addition, we compared the use of the food-grade synthetic medium to mucin medium, which has been used in many studies to grow *A. muciniphila* cells for animal studies (Everard et al. 2013, Wang et al. 2022, Qu et al. 2021, Bian et al. 2019, Yaghoubfar et al. 2020, Wu et al. 2020).

The highest growth rate and final optical density was reached in food-grade medium containing the highest concentration of GlcNAc. In the GlcNAc conditions, the cells were observed to be elongated, possibly affecting the optical density in these cultivations. Furthermore, PCA analysis showed that in both the proteome and transcriptome data, the mucin condition clusters separately from the conditions containing GlcNAc, whereas in the transcriptome data alone the end-log phase of condition A also clusters separately from the other conditions and timepoints. However, the KEGG metabolism did not reveal significant differences between fermentor conditions within the different metabolisms. Overall, the metabolic pathway with the highest abundance across all conditions was found to be the carbohydrate metabolism pathway. Assessing the transcriptome and proteome data in more detail revealed the upregulation of proteins

and genes involved in stress-response in GlcNAc conditions and the pili-associated system, mucin degradation and protein sorting systems in mucin conditions.

A shift in propionate to acetate production was observed between the condition containing mucin and the condition containing glucose and GlcNAc, as well as between the different glucose and GlcNAc conditions. At the end of the fermentation in mucin a propionate to acetate ratio of 0.88 was observed. However, with the decreasing concentration of GlcNAc in the other conditions, the ratio shifted towards more propionate production. In condition A the ratio was 1:1, which was similar to previous findings where a 50:50 ratio of glucose and GlcNAc was used as a carbon source (van der Ark et al. 2018). The shift towards a higher propionate:acetate ratio in condition B and C is in line with the degradation reactions that were predicted using the genome-scale model of *A. muciniphila* (Ottman et al. 2017). Therefore, it is important to note that using a lower GlcNAc concentration in the cultivation of *A. muciniphila* causes a shift in the propionate to acetate ratio, resulting in an altered short-chain fatty acid profile.

The carbon recovery values indicated a gap between the carbon sources that were consumed and the energy and carbon sources that were produced. The carbon recovery values were ranging between 70-73%, excluding biomass and amino acid formation. Previously, a carbon recovery of 80-90% has been described for *A. muciniphila* cultivated using either GlcNAc, glucose or N-Acetylgalactosamine (GalNAc) as carbon sources (Ottman et al. 2017). Due to the high amount of pea peptone in this medium, the exact biomass could not be measured. Therefore, we hypothesize that including a theoretical portion for biomass, our carbon recoveries may be in the range of the previously observed carbon recoveries for *A. muciniphila*. In addition, considering the elongated cells and the production of EPS, as our transcriptome data indicates, a portion of the initial carbon concentration available in the medium may be used for cell wall and EPS production. Next to the transcriptome data, the observed viscosity in the cultures containing GlcNAc and glucose suggests EPS may be produced in these conditions. Therefore, we further investigated EPS production by *A. muciniphila* in **Chapter 5**.

Cell elongation was observed in the fermentations without mucin. As described previously, the cells of *A. muciniphila* when cultivated on mucin medium are oval-shaped and 640 nm in diameter and 690 nm in length (Derrien et al. 2004). While, in our first series of experiments in synthetic medium supplemented with soy peptone, phase-contrast and scanning electron microscopy of cells grown on soy medium showed a significantly (p-value < 0.01) elongated shape with a length of 1.3 (±0.80) compared to mucin medium. The transcriptome data showed an upregulation

of cell division genes in the condition containing mucin compared to synthetic media, including the genes encoding cell division proteins FtsK (Amuc_2076), FtsZ (Amuc_0152), FtsQ (Amuc_0662) and FtsA (Amuc_0153). The initiation of cell division starts with the formation of the Z-ring, which consists of FtsZ proteins (Harry et al. 2006). After the formation of the Z-ring, subsequent division proteins localize to the Z-ring forming a protein complex named the divisome. These subsequent division proteins also include FtsK, FtsQ and FtsA. In synthetic medium compared to mucin, other genes involved in cell division were found to be upregulated. Three genes, namely cell division inhibitor (Amuc_1176), FtsH (Amuc_0348) and the cell division trigger factor (Amuc_1052) were significantly upregulated under high and low GlcNAc conditions. FtsH encodes a metalloprotease which plays a role in the quality control of integral membrane proteins in *E. coli*. In *A. muciniphila* this gene may be upregulated due to the elongated membranes that were observed, increasing the quality control of these membrane proteins. Furthermore, the overproduction of the trigger factor was found to cause defective cell division in *E. coli* (Guthrie and Wickner 1990). Therefore, the upregulation of this gene Amuc_1052 may also be involved in the observed cell elongation of *A. muciniphila*. The upregulation of cell division genes in the mucin condition supports the differences observed in cell size between mucin and glucose/GlcNAc conditions. Only one cell division gene was significantly differentially expressed when comparing condition A to conditions B and C, which was Amuc_1176. Next to this difference, no significant differences were observed in the transcriptome data of genes involved in cell division of conditions A-C. Overall, the upregulation of these genes in mucin and GlcNAc conditions support the differences in cell size observed in the microscopy pictures.

The protein Amuc_1100 is gaining increasing interest in several studies for its positive effect on host health (Ottman et al. 2017, Wang et al. 2021). The gene cluster associated with pili production, including Amuc_1100, were significantly upregulated in the condition supplemented with mucin compared to the GlcNAc conditions. The proteome data supports this observation, but the protein abundance ratio observed was less than 10. However, as the proteome data sets relate to relative amounts of proteins, absolute amounts of proteins could be higher in the GlcNAc conditions as the OD_{600} value was approximately 8-fold higher in the high-GlcNAc condition than the mucus condition. Therefore, considering the large difference between optical densities, the upregulation of this gene cluster in mucin may not have a negative effect on the use of *A. muciniphila* cells or Amuc_1100 from food-grade medium supplemented with glucose and GlcNAc.

The upregulation of multiple stress-related genes and gene clusters were identified in fermentations on GlcNAc compared to mucin. First, a cluster including a phosphate

ABC transporter system was upregulated (Amuc_1294 until Amuc_1308). The upregulation of this gene cluster may indicate a phosphate limitation in these cultures (Hudek et al. 2016). To overcome this limitation, additional phosphate sources could be added to food-grade medium supplemented with glucose and GlcNAc. Furthermore, several genes previously found to be involved in the oxygen stress-response of *A. muciniphila* were found to be upregulated in the conditions without mucin as well (Ouwerkerk et al. 2016). However, these fermentations were run anaerobically simultaneously as was the mucin condition. Therefore, it is likely that this stress-response was not specific for oxygen, but rather a form of cross-protection against other stresses (den Besten et al. 2010). Another stress-response that was activated in conditions containing glucose and GlcNAc was the production of EPS (Amuc_2077-2096). Interestingly, the expression of the genes involved in EPS production decreased along with the decreasing concentration of GlcNAc. The production of EPS in bacteria is often a mechanism to cope with harsh environmental conditions, as extensively studied for lactic acid bacteria (Nguyen et al. 2020). For *A. muciniphila*, this condition with a high concentration of glucose and GlcNAc in the medium, with limiting medium components may be sub-optimal. However it is not limiting growth rate and biomass production as observed in these fermentations. We showed that pea peptone-based food-grade medium supplemented with glucose and GlcNAc instead of mucin results in high biomass formation of *A. muciniphila*, that may be used for its production for therapeutic purposes.

Other comparisons of the growth of *A. muciniphila* on mucin versus specific carbon sources have been made (van der Ark et al. 2018, Ottman et al. 2017). A transcriptome comparison was made comparing cultivations supplemented with mucin and cultivations supplemented with glucose as available carbon source (Ottman et al. 2017). Despite the cultivation differences, the cultures with glucose as carbon source also showed upregulation of stress-related genes in comparison to mucin, as was also identified in our study (Ottman et al. 2017). It is important to note that even though a lot of genes overlapped, there were also differences between this study and ours, in terms of differentially expressed stress-related genes. Furthermore, differences were also documented for genes and proteins involved in mucin degradation in both studies. In this study, especially the proteome study revealed that on protein level it was clearly visible that the mucin culture had an upregulation of proteins involved in mucin degradation, since these proteins were located in the top protein abundance ratios. Similar findings were documented previously (Ottman et al. 2017). In contrast, similar differences in the expression of genes involved in cell division were not found in this previous study. This may be due to the low growth rates and final biomass that was observed in the cultures with mucin only, while in our studies high growth rates and biomass were observed.

In conclusion, we showed that pea peptone-based food-grade medium supplemented with glucose and GlcNAc instead of mucin results in high biomass formation of *A. muciniphila*, that may be used for its production for therapeutic purposes. The differences between growth on mucin and growth on glucose and GlcNAc were shown on transcriptome and proteome levels. However, the KEGG metabolism pathways showed high similarity between conditions, where no significant differences could be identified. Furthermore, if minimal EPS production is required, the transcriptome data indicates that this may be achieved by decreasing the GlcNAc concentration. Lastly, the use of synthetic medium affects the cell morphology of *A. muciniphila*, resulting in elongated cells. Overall, our data suggests that the food-grade medium composition described here could be used to produce *A. muciniphila* in high yields for therapeutic purposes.

Acknowledgements

We are grateful to Dr Bart Smit (NIZO) for a gift of industrial peptones.

Material and methods

Bacterial strain and culture conditions

The type-strain *Akkermansia muciniphila* Muc^T (ATCC BAA-835) was used for all cultivation experiments.

Basal medium was used in the fermentations for the initial experiments including soy medium and mucin medium and pre-cultures for the pea peptone fermentors with the following composition: KH2PO4 (0.4 g/L), Na2HPO4 (0.53 g/L), NH4Cl (0.3 g/L), NaCl (0.3 g/L), MgCl2*6H2O (0.1 g/L), 1 mL trace elements in acid (50 mM HCl, 1mM H_3BO_3, 0.5 mM $MnCl_2$*$4H_2O$, 7.5 mM $FeCl_2$*$4H_2O$, 0.5 mM $CoCl_2$, 0.1 mM $NiCl_2$, and 0.5 mM $ZnCl_2$, 0.1 mM $CuCl_2$*$2H_2O$), 1 mL trace elements in alkaline (10 mM NaOH, 0.1 mM Na_2SeO_3, 0.1 mM Na_2WO_4, and 0.1 mM Na_2MoO_4), and 1 mL resazurin solution (500 mg/L) (Plugge 2005, Derrien et al. 2004). After autoclaving the following components were added to the medium: 1% (v/v) of the vitamin solution (per liter: 11 g $CaCl_2$, 20 mg biotin, 200 mg nicotinamide, 100 mg p-aminobenzoic acid, 200 mg thiamin (vitamin B1), 100 mg pantothenic acid, 500 mg pyridoxamine, 100 mg cyanocobalamin (vitamin B12), and 100 mg riboflavin) and 5% (v/v) of reducing solution (per liter: 80 g NaHCO3, 20 mL Na2S*9H2O solution (240 g/L) and 10 g cysteine-HCl).

For the initial experiments, soy medium and mucin medium were prepared. To prepare soy medium, 16 g/L soy peptone (AM41, Organotechnie SAS) was added to basal medium. In addition, GlcNAc and glucose were added in equimolar amounts to a total of 25 mM (Sigma-Aldrich). Mucin medium was prepared by adding 0.5% hog gastric mucin (Sigma-Aldrich) to basal medium.

Pre-cultures grown for the anaerobic fermentations supplemented with pea peptone were cultivated in basal medium supplemented with tryptone (20 g/L) and L-threonine (4 g/L) with the following carbon source composition: 12.5 mM N-acetylglucosamine (GlcNAc) and 12.5 mM glucose. The cultures were grown in anaerobic conditions and incubated at 37°C for 48 hours (non-shaking).

Food-grade medium was used for the main experiments with the following composition: KH2PO4 (0.4 g/L), Na2HPO4 (0.669 g/L), NH4Cl (0.3 g/L), NaCl (0.3 g/L), MgCl2 6H2O (0.1 g/L), pea peptone A482 (OrganoTechnie SAS, 32 g/L), L-threonine (4 g/L). After autoclaving 2 mL of reducing solution containing NaHCO3 (40 g/L) and L-cysteine*HCl (5 g/L) and 1% (v/v) of vitamin solution (see above) were added to the medium. The medium was inoculated with 1% (v/v) of the pre-culture. Anaerobic fermentations using this medium were performed as described in the next section.

Anaerobic fermentation

The fermentations were conducted in four parallel bioreactors (DasGip, Eppendorf, Germany) using 700 mL of food-grade medium containing either glucose and GlcNAc in three different ratios (3:1, 10:1 or 20:1 glucose to GlcNAc, named A, B, and C respectively) or mucus (Condition D) with a final total concentration of 150 mM or 0.5% crude mucin. The pH was set at 6.8 and a stirring rate of 100 rpm was applied with N2/CO2 gas flow (80%/20%). The medium of all four fermentors was inoculated with 1% (v/v) of cultures pre-grown on tryptone medium. The fermentation was terminated after 72 hours. Samples were taken for OD measurements, HPLC analysis, microscopic analysis, RNA sequencing (triplicates) and proteomics (duplicates). Samples for HPLC analysis were stored at -20°C until use. Samples (10 ml) for RNA sequencing and proteomics were taken at early, mid and end exponential phase and centrifuged for 30 minutes at 4700 rpm at 4°C after which the supernatant was removed. Then, 1 mL of RNAlater was added to the pellets of the samples for RNA sequencing. Lastly, the samples for both RNA sequencing (in triplicate) and proteomics (in duplicate) were snap-frozen in liquid nitrogen and stored in -80°C.

HPLC

Samples were obtained at different timepoints during the fermentation period for the analysis of fermentation products. Crotonate was used as the internal standard. The

external standards were GlcNAc, glucose, acetate, propionate, succinate, lactate and 1,2-propanediol. The substrates and fermentation products were measured using a Shimadzu LC_2030C equipped with a refractive index detector and a Shodex SH1011 column. Two runs were performed for each sample using an oven temperature of 45°C and 75°C with a pump flow of 1.0 mL/min and 0.9 mL/min, respectively. For both runs 0.01N H_2SO_4 was used as eluent. All samples and standards (10 µl) ran for 15 minutes. The concentrations of the standards were ranging between 2.5 mM and 60 mM. Lastly, the fermentation profiles obtained with HPLC were used to calculate the carbon and energy balances at the endpoint of all fermentations.

RNA isolation and transcriptome analysis

RNA isolation was performed as described previously (Shetty et al. 2022). Further processing of the total RNA was performed by Novogene (Cambridge, United Kingdom) and paired end sequences of 150 bp were obtained using an Illumina platform. Transcriptome analysis has been performed as previously described (Hagi et al. 2020). All further analysis was done using R version 3.6.3 in Rstudio version 1.2.5019.

Sample preparation for nLC-MS/MS and analysis

Total protein was isolated from culture samples. Ice-cold 100 mM Tris buffer (pH 8) was added to the pellets in variable amounts up to approximately 500 µl and 200 µl of the resuspended cells was transferred to low-binding Eppendorf tubes. The tubes were centrifuged repeatedly for 1 min at 10.000 x g until the supernatant was clear. Then, the supernatant was removed and 200 µl of ice-cold 100 mM Tris buffer (pH 8) was added again. The cells were resuspended after which the centrifugation was repeated. After removing the last supernatant, the cells were resuspended in 200 µl 100 mM Tris (pH 8) and aliquoted per 50 µl in low-binding Eppendorf tubes. Subsequently, the samples were sonicated for 15 seconds. The protein concentration was measured using the Pierce™ BCA Protein Assay Kit to dilute all samples to a concentration of 1 µg/µl in a final volume of 60 µl using 100 mM Tris. Then, 6 µl of 150 mM dithiothreitol (Sigma Life Science) was added to the diluted sample followed by incubation at 37°C for 45 minutes. After incubation, the sample was mixed with 198µl 8 M urea (Sigma-Aldrich) and 27 µl 150 mM acrylamide and incubated for 30 minutes at room temperature. Subsequently, 4 µl of 10% trifluoroacetic acid (TFA, Alfa Aesar Chemicals) and 8 µl SpeedBeads™ magnetic carboxylate modified particles (50%, GE Healthcare 45152105050250 and 50% Thermo Scientific 65152105050250, washed twice with MilliQ water) and 750 µl acetonitrile (Biosolve B.V.) were added to the sample solution. Next, the mixtures were incubated for 20 minutes at room temperature and the liquid was removed. Then, the beads were washed twice on a magnetic rack (Cell Signaling Technology) with 1 mL 70% ethanol and with 1 mL 100% acetonitrile, respectively. Afterwards, 100 µl of 5 ng/µl trypsin (Roche Diagnostic GmbH) in 50 mM

ammonium bicarbonate was added to the beads containing the sample and subjected to overnight digestion at room temperature. The digestion was stopped by adding 4 µl 10% TFA to the sample. Then, the samples were placed on the magnetic rack to obtain the first supernatant. The remaining beads were washed with 100 ml/L formic acid. This solution was then combined with the first supernatant.

Micro Columns (µcolumns) were prepared by adding two C18 disks (Affinisep AttractSPE™ Disk Bio C18), 200 µl methanol and 4 µL 50% Lichroprep RP-18 in methanol into a 200 µL pipette tip. The µcolumn was then eluted and washed with 100 µl methanol and equilibrated with 100 µl 1 mL/L formic acid in water before use. The samples with the cell lysates were then transferred to the µcolumn. After elution and washing with 100 µL 1 mL/L formic acid in water, 50 µl of (1:1) formic acid and acetonitrile solution was added onto the µcolumn and eluted into a clean 0.5 mL low-binding Eppendorf tube. Subsequently, the samples were concentrated to a final volume of approximately 10 µl using an Eppendorf Concentrator Plus. Lastly, the volume was adjusted to 50 µl using 1 mL/L formic acid before storage at -20°C until further processing.

Peptide samples were measured (nLC1000 - Orbitrap Exploris 480) and data analysis was performed as previously described (Feng et al. 2022). The database that was used for the analysis of the samples in this study was the Akkermansia_muciniphila_baa-835_UP000001031 uniprot database.

Supplementary information

Table S1: Number of differentially expressed genes (DEGs) between conditions A-D.

Growth fase	Sample comparison	DEGs
Growth curve comparison	A_T27 vs A_T34	703
	A_T34 vs _AT48	992
	A_T27 vs A_T48	1567
	B_T48 vs B_T72	162
	C_T55 vs C_T72	113
Mid exponential fase comparisons	A_T27 vs B_T48	135
	A_T27 vs C_T55	252
	A_T27 vs D_T10	1524
	B_T48 vs C_T55	2
	B_T48 vs D_T10	1474
	C_T55 vs D_T10	1584
Late exponential fase comparisons	A_T48 vs B_T72	1045
	A_T48 vs C_T72	1279
	A_T48 vs D_T10	1764
	B_T72 vs C_T72	93
	B_T72 VS D_T10	1605
	C_T72 vs D_T10	1576

Table S2: Transcriptome comparison of genes associated with mucus degradation in condition A mid (high GlcNAc) versus condition D (mucin)

Locus tag	log2FoldChange	padj	Protein name
Amuc_0846	3.029032	1.2E-51	alpha-L-fucosidase
Amuc_1934	2.456818	6.1E-33	hypothetical protein
Amuc_1801	1.887985	5.68E-57	alpha/beta hydrolase
Amuc_0060	1.638833	1.02E-29	alpha-N-acetylglucosaminidase
Amuc_1667	1.556094	1.23E-23	glycoside hydrolase family 2
Amuc_1003	1.486429	2.78E-15	alpha/beta hydrolase
Amuc_0697	1.425169	8.28E-23	glycoside hydrolase family 43 protein
Amuc_0397	1.418074	7.8E-21	family 20 glycosylhydrolase
Amuc_1666	1.379359	5.52E-21	glycoside hydrolase family 2
Amuc_0146	1.340154	1.7E-29	alpha-L-fucosidase
Amuc_1118	1.223986	1.89E-36	alkaline phosphatase family protein
Amuc_1187	1.221864	5.68E-27	alpha-galactosidase
Amuc_0698	1.105217	7.36E-25	glycoside hydrolase family 43 protein
Amuc_1074	1.065008	3.65E-26	sulfatase
Amuc_1480	0.972497	3.21E-15	serine hydrolase
Amuc_1480	0.972497	3.21E-15	serine hydrolase
Amuc_0623	0.773493	3E-06	glycoside hydrolase
Amuc_0176	0.599369	6.54E-09	S1C family serine protease
Amuc_2018	0.596068	3.68E-05	beta-N-acetylhexosaminidase
Amuc_2148	0.516922	5.16E-06	beta-N-acetylhexosaminidase
Amuc_0868	0.479888	0.000511	beta-hexosaminidase
Amuc_0369	0.456739	0.003023	beta-N-acetylhexosaminidase
Amuc_0875	0.414539	0.008304	glycoside hydrolase family 16 protein
Amuc_0565	0.331763	0.004612	arylsulfatase
Amuc_1033	0.307783	0.005211	sulfatase
Amuc_1815	0.303716	0.011557	family 20 glycosylhydrolase
Amuc_0465	0.235546	0.026227	peptidoglycan DD-metalloendopeptidase family protein
Amuc_1032	0.220703	0.026616	beta-N-acetylhexosaminidase
Amuc_1655	0.090327	0.482277	sulfatase
Amuc_1106	0.055918	0.611021	aminopeptidase P N-terminal domain-containing protein
Amuc_0187	0.014549	0.925992	M20/M25/M40 family metallo-hydrolase
Amuc_1686	0.011227	0.911369	beta-galactosidase
Amuc_2040	-0.02955	0.78512	M3 family metallopeptidase
Amuc_2040	-0.02955	0.78512	M3 family metallopeptidase
Amuc_0953	-0.16938	0.05859	sulfatase-like hydrolase/transferase
Amuc_1669	-0.19317	0.177881	beta-N-acetylhexosaminidase
Amuc_0391	-0.21162	0.039018	peptidoglycan DD-metalloendopeptidase family protein
Amuc_0451	-0.34278	0.00079	sulfatase-like hydrolase/transferase
Amuc_0824	-0.35736	0.000128	discoidin domain-containing protein

Table S2: *(Continued)*

Locus tag	log2FoldChange	padj	Protein name
Amuc_1631	-0.35866	0.000523	carboxy terminal-processing peptidase
Amuc_0186	-0.35894	0.000573	glycoside hydrolase N-terminal domain-containing protein
Amuc_0491	-0.36299	0.005238	arylsulfatase
Amuc_1791	-0.49896	1.07E-06	serine protease
Amuc_0121	-0.57793	5.33E-10	arylsulfatase
Amuc_0863	-0.60839	2.87E-07	glycoside hydrolase family 88 protein
Amuc_1755	-0.7505	3.61E-18	sulfatase
Amuc_1008	-0.80833	1.11E-17	DUF5110 domain-containing protein
Amuc_1924	-0.85708	1.6E-22	family 20 glycosylhydrolase
Amuc_0670	-0.85736	1.31E-18	trypsin-like peptidase domain-containing protein
Amuc_0539	-0.87473	4.7E-24	glycoside hydrolase family 2
Amuc_1220	-0.91739	3.8E-15	alpha-N-acetylglucosaminidase
Amuc_0625	-0.96669	2.76E-20	glycoside hydrolase
Amuc_1835	-0.96966	4.97E-28	exo-alpha-sialidase
Amuc_0010	-1.0224	6.23E-30	alpha-L-fucosidase
Amuc_0253	-1.13921	6.49E-25	peptidoglycan DD-metalloendopeptidase family protein
Amuc_2019	-1.18361	3.21E-41	beta-N-acetylhexosaminidase
Amuc_0482	-1.26175	4.55E-35	alpha/beta superfamily hydrolase
Amuc_0290	-1.32324	2.19E-40	DUF4982 domain-containing protein
Amuc_0771	-1.33832	2.46E-51	beta-galactosidase
Amuc_2164	-1.35102	2.26E-60	glycoside hydrolase family protein
Amuc_0392	-1.63941	4.04E-67	alpha-L-fucosidase
Amuc_1438	-1.6473	4.23E-75	NPCBM/NEW2 domain-containing protein
Amuc_1120	-1.96278	7.78E-93	glycoside hydrolase N-terminal domain-containing protein
Amuc_2136	-2.04295	1.7E-105	family 20 glycosylhydrolase
Amuc_2108	-2.6918	2.6E-156	glycoside hydrolase family 16 protein

Table S3: Transcriptome comparison of genes associated with mucus degradation in Condition C mid (low GlcNAc) versus condition D (mucin)

Locus tag	log2FoldChange	padj	Product
Amuc_0846	3.754718	1.72E-71	alpha-L-fucosidase
Amuc_1934	3.191431	7.13E-36	hypothetical protein
Amuc_1667	2.278195	1.42E-42	glycoside hydrolase family 2
Amuc_0060	2.274802	2.89E-33	alpha-N-acetylglucosaminidase
Amuc_1003	2.122856	2.31E-31	alpha/beta hydrolase
Amuc_1666	2.063007	1.82E-27	glycoside hydrolase family 2
Amuc_0397	2.028033	4.75E-29	family 20 glycosylhydrolase
Amuc_0697	1.745188	3.16E-24	glycoside hydrolase family 43 protein
Amuc_0146	1.595206	2.45E-20	alpha-L-fucosidase
Amuc_1187	1.586474	1.2E-29	alpha-galactosidase
Amuc_1801	1.536623	3.52E-39	alpha/beta hydrolase
Amuc_1118	1.307422	9.69E-40	alkaline phosphatase family protein
Amuc_0623	1.290364	6.49E-11	glycoside hydrolase
Amuc_2018	1.276793	2.33E-11	beta-N-acetylhexosaminidase
Amuc_1074	1.155738	4.67E-26	sulfatase
Amuc_0369	1.114282	1.26E-09	beta-N-acetylhexosaminidase
Amuc_0868	1.036281	1.4E-10	beta-hexosaminidase
Amuc_0875	0.991038	2.1E-09	glycoside hydrolase family 16 protein
Amuc_1480	0.988689	9.1E-14	serine hydrolase
Amuc_1480	0.988689	9.1E-14	serine hydrolase
Amuc_1815	0.898541	1.15E-08	family 20 glycosylhydrolase
Amuc_2148	0.837119	2.62E-11	beta-N-acetylhexosaminidase
Amuc_0565	0.819136	8.82E-08	arylsulfatase
Amuc_1655	0.67328	2.06E-05	sulfatase
Amuc_0176	0.644557	2.75E-13	S1C family serine protease
Amuc_0698	0.597355	3.89E-07	glycoside hydrolase family 43 protein
Amuc_1669	0.443797	0.00492	beta-N-acetylhexosaminidase
Amuc_1033	0.429984	0.000291	sulfatase
Amuc_0187	0.403632	0.008943	M20/M25/M40 family metallo-hydrolase
Amuc_0491	0.354112	0.02718	arylsulfatase
Amuc_1686	0.306453	0.001833	beta-galactosidase
Amuc_1032	0.305161	0.005649	beta-N-acetylhexosaminidase
Amuc_2040	0.215492	0.050936	M3 family metallopeptidase
Amuc_2040	0.215492	0.050936	M3 family metallopeptidase
Amuc_0465	0.027547	0.809597	peptidoglycan DD-metalloendopeptidase family protein
Amuc_0451	0.017655	0.89086	sulfatase-like hydrolase/transferase
Amuc_0863	-0.11909	0.441686	glycoside hydrolase family 88 protein
Amuc_0186	-0.12904	0.325208	glycoside hydrolase N-terminal domain-containing protein

Table S3: *(Continued)*

Locus tag	log2FoldChange	padj	Product
Amuc_1106	-0.33774	0.012257	aminopeptidase P N-terminal domain-containing protein
Amuc_0391	-0.35144	0.000195	peptidoglycan DD-metalloendopeptidase family protein
Amuc_1220	-0.40193	0.027665	alpha-N-acetylglucosaminidase
Amuc_0953	-0.44922	2.71E-05	sulfatase-like hydrolase/transferase
Amuc_1791	-0.5708	2.65E-08	serine protease
Amuc_0824	-0.62419	3.75E-06	discoidin domain-containing protein
Amuc_0670	-0.70285	6.47E-10	trypsin-like peptidase domain-containing protein
Amuc_1924	-0.73272	4.84E-11	family 20 glycosylhydrolase
Amuc_1755	-0.73309	5.97E-15	sulfatase
Amuc_1631	-0.82144	4.31E-14	carboxy terminal-processing peptidase
Amuc_0010	-0.83262	8.13E-17	alpha-L-fucosidase
Amuc_1008	-0.89613	4.73E-16	DUF5110 domain-containing protein
Amuc_0121	-0.90925	2.75E-16	arylsulfatase
Amuc_0539	-0.95109	7.99E-23	glycoside hydrolase family 2
Amuc_1835	-1.04385	8.39E-30	exo-alpha-sialidase
Amuc_0253	-1.08749	7.52E-24	peptidoglycan DD-metalloendopeptidase family protein
Amuc_2164	-1.15385	2.18E-42	glycoside hydrolase family protein
Amuc_0625	-1.20551	3.16E-22	glycoside hydrolase
Amuc_2019	-1.21407	5.2E-37	beta-N-acetylhexosaminidase
Amuc_0771	-1.22178	5.02E-39	beta-galactosidase
Amuc_0482	-1.30073	6.64E-27	alpha/beta superfamily hydrolase
Amuc_0290	-1.66194	1.29E-51	DUF4982 domain-containing protein
Amuc_0392	-1.86949	1.73E-85	alpha-L-fucosidase
Amuc_1438	-1.88993	1.37E-80	NPCBM/NEW2 domain-containing protein
Amuc_1120	-1.93016	1.74E-51	glycoside hydrolase N-terminal domain-containing protein
Amuc_2136	-2.38675	8.69E-85	family 20 glycosylhydrolase
Amuc_2108	-2.72574	3.2E-137	glycoside hydrolase family 16 protein

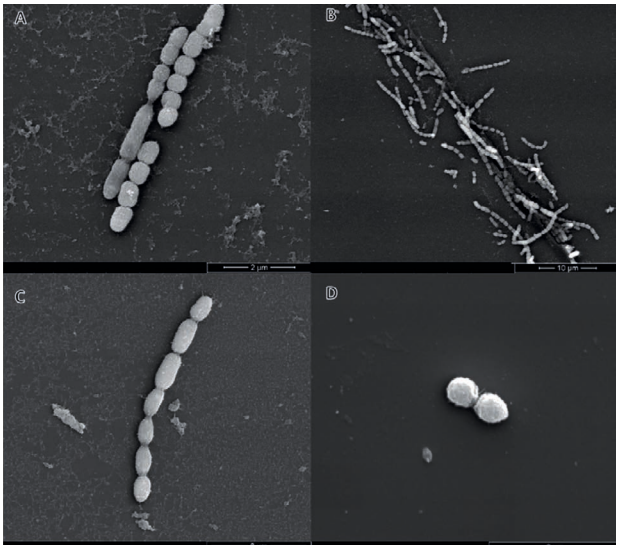

Figure S1. Scanning electron micrographs of *A. muciniphila* cultured on soy medium (A, B and C). The cells are elongated or do not divide properly. Normal shaped cells were observed in mucus medium (D).

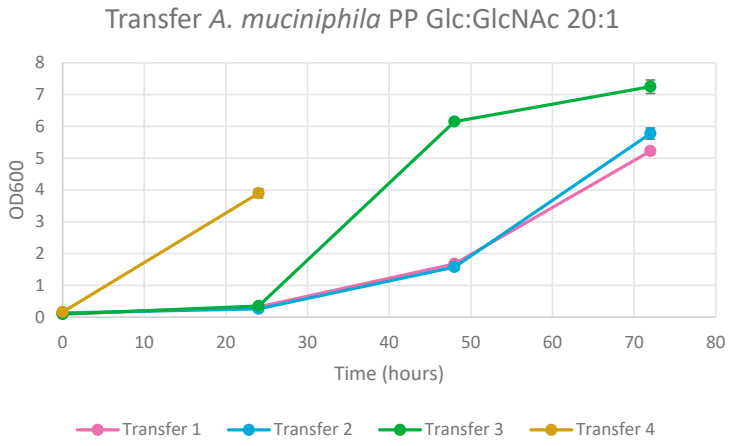

Figure S2: OD measurements of *A. muciniphila* after multiple transfers to a new serum bottle using the medium composition of condition C.

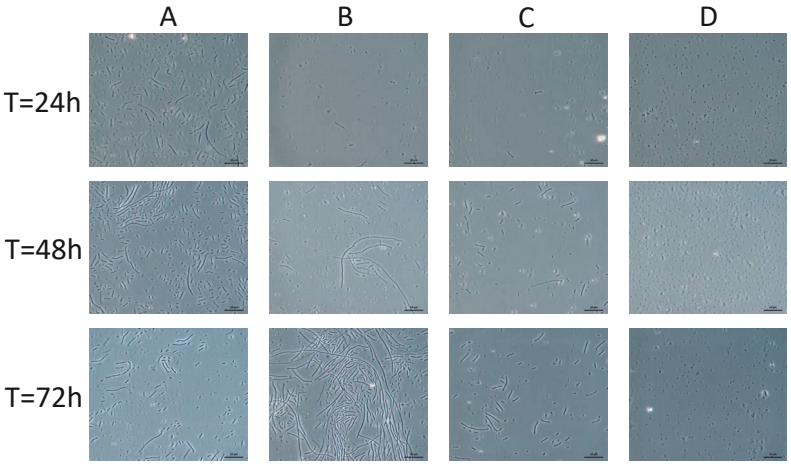

Figure S3: Microscope images of all conditions over time.

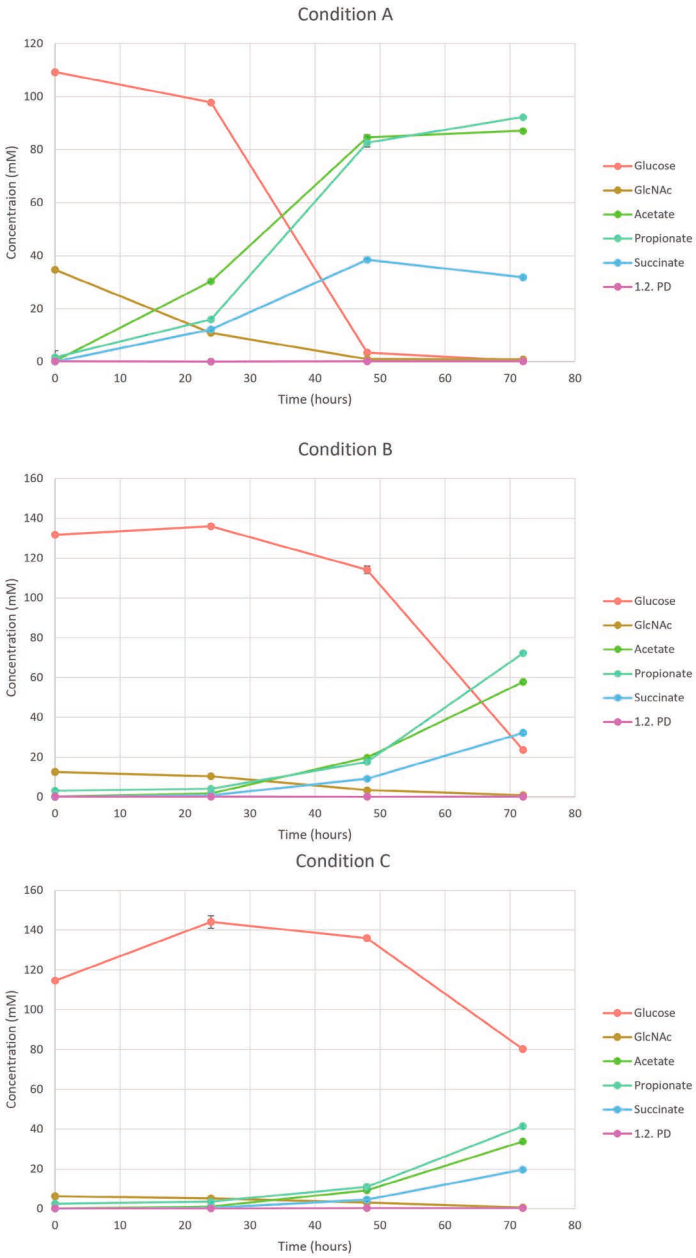

Figure S4: Sugar uptake and metabolite production by *A. muciniphila* on cultivation condition A, B and C.

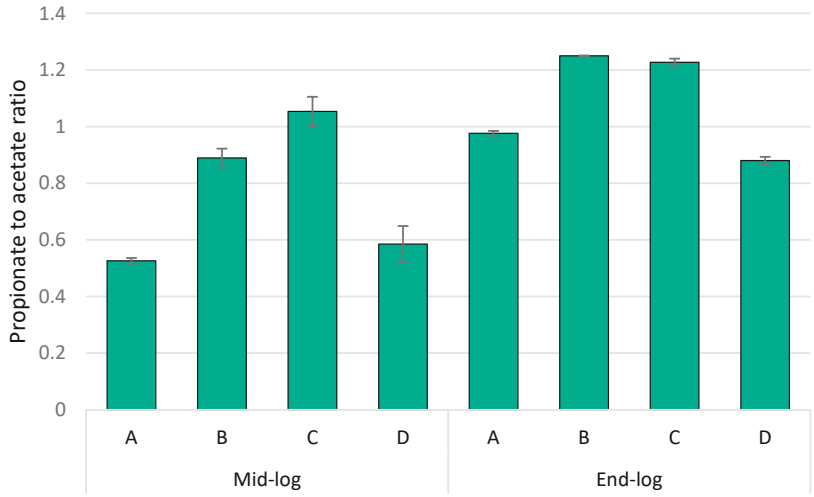

Figure S5: Overview of propionate:acetate ratio's over time.

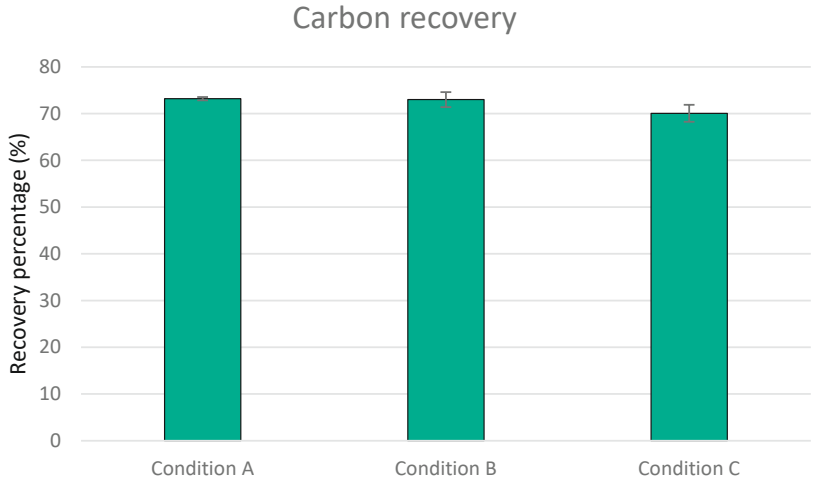

Figure S6: Carbon balances of condition A-C calculated at the end-point of each fermentation.

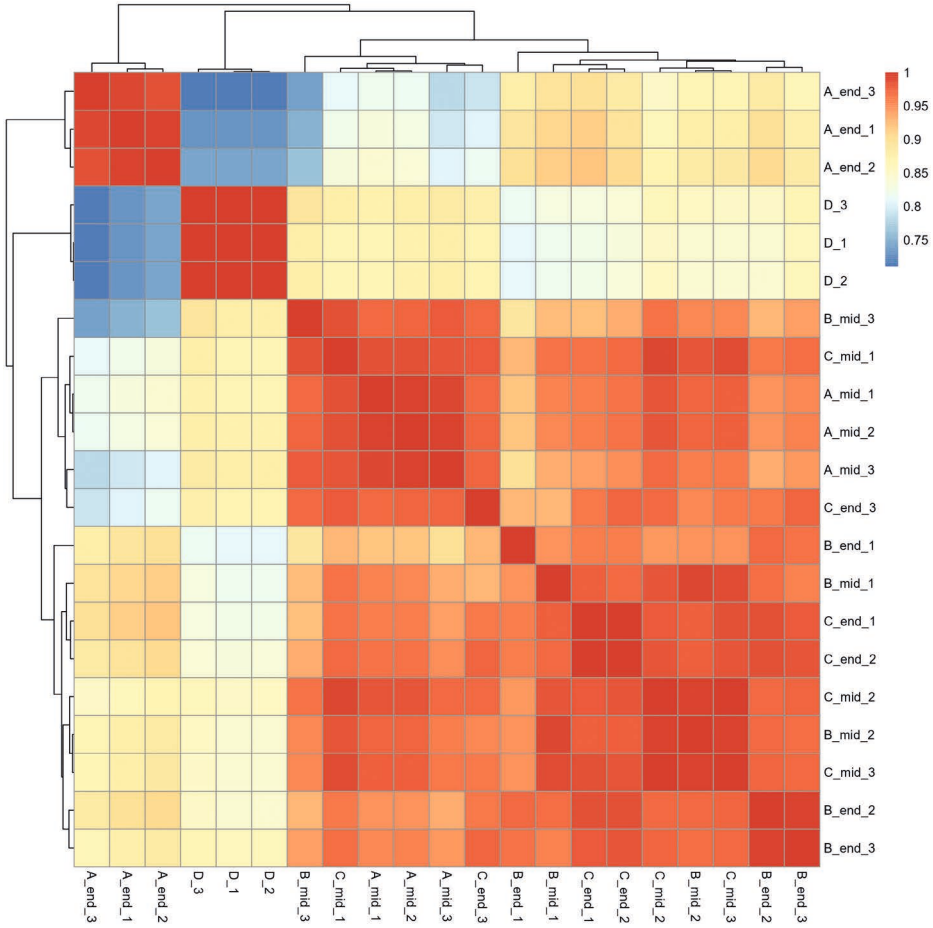

Figure S7: Heatmap based on the transcriptome data of all samples.

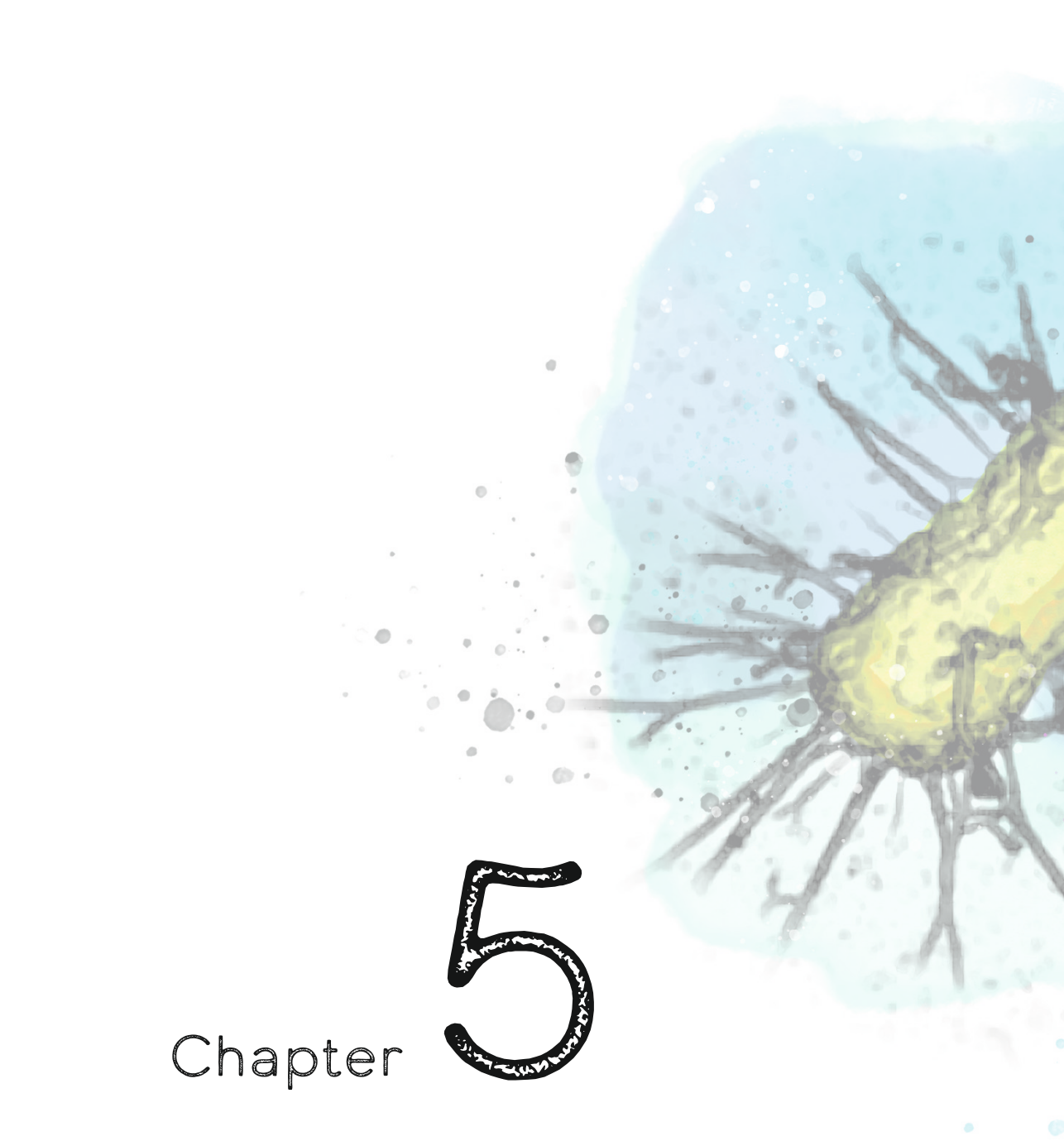

Chapter 5

Akkermansia muciniphila produces fucose-containing exopolysaccharides

Sharon Y. Geerlings, Madelon Logtenberg, Maria-Carolina Rodriguez-Daza, Sjef Boeren, Bart Nijsse, Henk Schols, Martin Pabst, Yuemei Lin, Mark van Loosdrecht, Willem M. de Vos and Clara Belzer

Abstract

Microbial exopolysaccharides (EPS) are produced by a variety of bacteria from different ecosystems. An increasing interest has been observed for EPS produced by beneficial microbes. Their EPS varies widely in composition and structure and may exert diverse health benefits. This project aimed to assess the capability of the next-generation therapeutic microbe *A. muciniphila* to produce EPS, as well as characterized the EPS that was produced. Bioinformatic analysis led to the identification of a complete and partly inducible EPS production pathway in *A. muciniphila* involving a Wzx flippase. Furthermore, in this study we showed evidence for fucose-containing EPS production by *A. muciniphila* cultivated on different carbon source ratios in food-grade medium. The main monosaccharides present in *A. muciniphila* EPS are fucose, galactose, glucose and N-Acetylglucosamine (GlcNAc). Furthermore, our results indicate that a higher GlcNAc concentration in the medium results in an increased production of EPS that is positively correlated with the expression of genes involved in EPS production. Lastly, the production of sialic acids was detected in medium supplemented with glucose and GlcNAc. Altogether, our results indicate that *A. muciniphila* can produce EPS through the Wzx/Wzy-dependent pathway in variable amounts depending on the culturing conditions that are used.

Introduction

Akkermansia muciniphila is a gut microbiome member that is described to exert a beneficial effect on its host. *A. muciniphila* was found to be inversely correlated to several diseases (including diabetes, obesity and inflammation) and associated with a healthier metabolic status (Le Chatelier et al. 2013, Everard et al. 2013, Schneeberger et al. 2015, Dao et al. 2016). More recently, a clinical trial has shown that administration of pasteurized *A. muciniphila* in humans resulted in improved insulin sensitivity, reduced insulinemia and plasma total cholesterol as well as reduction of body weight including reduced fat mass and hip circumference (Depommier et al. 2019). Several underlying mechanisms have been demonstrated in the immunomodulatory and metabolic potential of *A. muciniphila* to counteract obesity and diabetes. For instance, the membrane protein Amuc_1100 is a critical component responsible for driving improved inflammatory and metabolic outcomes in the host (Ottman et al. 2017, Plovier et al. 2017). Still, other mechanisms involving microbial by-products leading to the host-microbe interactions remain to be explored. In this study we aim to identify and characterize EPS production in *A. muciniphila*, which may be another factor in its mechanism to affect host health.

Numerous bacteria can produce polysaccharides that are then exported out of the cell, known as exopolysaccharides (EPS). Microbial EPS consist of sugar units connected by glycosidic linkages and vary from linear to heavily branched (Sutherland 1994, Zeidan et al. 2017). Bacterial polysaccharides can either be categorized as capsular polysaccharides bound to the cell or EPS which are either loosely bound or fully secreted. The polymers can either be homopolymers containing only one type of monosaccharide or heteropolysaccharides containing different monosaccharides. The monomer composition of EPS varies between species and strains (Korcz and Varga 2021). Four mechanisms have been described for EPS production in bacteria: Wzx/Wzy-dependent pathway, the ATP-binding cassette (ABC) transporter-dependent pathway, the synthase-dependent pathway and extracellular synthesis by use of a single sucrase protein (Schmid et al. 2015).

In general, microbial EPS serve as natural adhesives and cell protection against environmental stresses such as extreme pH, temperatures, desiccation, and toxic compounds (Schmid 2018, Zeidan et al. 2017). It has been shown that EPS of non-pathogenic bacteria can have beneficial effects on the host and the gut microbiota (Salazar et al. 2008, Salazar et al. 2019, Riaz Rajoka et al. 2018). The health potential of EPS extends to antimicrobial, immunomodulatory (acting as effector molecules), anti-inflammatory and antioxidant activities among others (Jones et al. 2014, Zhou et al. 2017, Verma et al. 2018). Particularly, many studies focused on EPS production

of commercialized probiotics including lactic acid bacteria (LAB) and bifidobacteria (Angelin and Kavitha 2020). These EPS were investigated for their prebiotic effect, enhancing beneficial bacterial populations in the gut (Ryan et al. 2015). For example, it has been shown that EPS produced by gut bacteria was used by other bacteria in the community as a carbon source (Salazar et al. 2008, Rios-Covian et al. 2016). Furthermore, EPS produced by several bacterial species protected the host against the colonization of gut pathogens including *Helicobacter pylori* (Jones et al. 2014, Marcial et al. 2017, Fanning et al. 2012). Lastly, fucose containing-EPS (fuc-EPS) have obtained increased interest in both food and pharmaceutical industries as a promising source of fucose due to their antioxidant, prebiotic, anticancer, anti-inflammatory and anti-viral activities (Xiao et al. 2022). Since specific EPS structures may be linked to health benefits, it is important to gain knowledge about these bacterial EPS associated with health (Rossi et al. 2015).

EPS production by *A. muciniphila* has not been confirmed to date. However, it has been previously suggested that *A. muciniphila* may produce EPS as a protection mechanism against the presence of oxygen and dietary polyphenols, based on transcriptome and qPCR data, respectively (Ouwerkerk et al. 2016, Rodriguez-Daza 2020). In these studies, *A. muciniphila* was grown on mucin-containing media that are not suitable to study EPS because of many contaminants in slaughterhouse-derived mucus. Hence, we use food-grade medium to assess EPS biosynthesis by *A. muciniphila* and further characterize the produced EPS. Gaining more insights into the structure of the EPS produced by *A. muciniphila* may lead to uncovering mechanisms involved in the beneficial microbe-microbe and host-microbe interactions of this bacterium as well as its therapeutic and food applications.

Results

Increased viscosity observed in the high-GlcNAc condition

One of the characteristics of EPS production is the increased viscosity of the culture medium. Therefore, we measured the viscosity of the culture's supernatant to obtain an indication on which condition *A. muciniphila* produces and releases the highest concentration of EPS (**Figure 1**). The anaerobic fermentations include three conditions: High-GlcNAc (glucose:GlcNAc ratio 3:1), low-GlcNAc (glucose:GlcNAc ratio 20:1) and mucus (0.5%). The highest viscosity was detected in the end-log phase of high-GlcNAc. The viscosity in the end-log phases decreases along with the decreasing starting concentration of GlcNAc in these cultures. The decreasing viscosity observed with an increase of shear rate indicates all supernatant samples, except for the medium

control, are non-Newtonian fluids meaning that the viscosity is a function of the shear rate. Lastly, the viscosity of the medium control was equal to the viscosity of water.

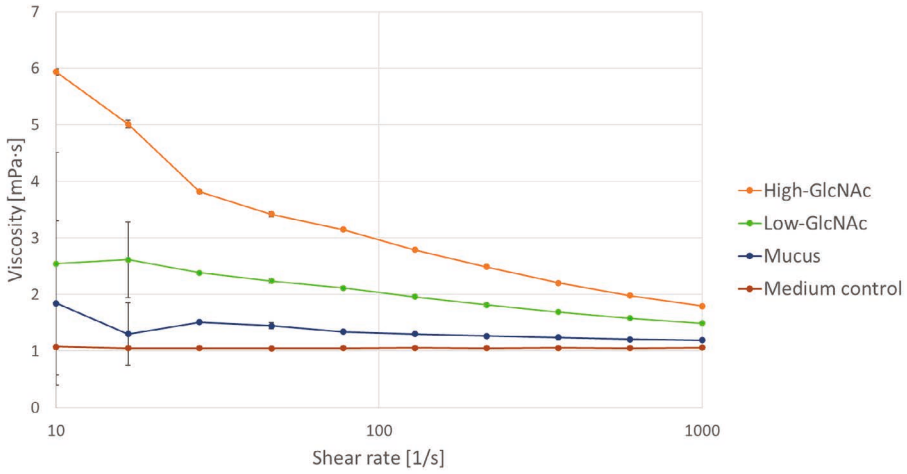

Figure 1: Viscosity measurements of end-log conditions high-GlcNAc, low-GlcNAc and mucus including the food-grade medium control supplemented with the same concentration of glucose and GlcNAc.

A. muciniphila produces heteropolysaccharides containing fucose

To assess which monosaccharides were produced by *A. muciniphila* as part of its EPS, *A. muciniphila* was cultivated in batch cultures on minimal medium from which EPS was isolated. A negative control with medium only was also included to measure the background. However, the concentration of monosaccharides measured in the control was negligible. Therefore, we can conclude that the monosaccharides measured in the EPS isolate were produced by *A. muciniphila*. The monosaccharide analysis showed that *A. muciniphila* produces heteropolysaccharides (**Table 1**). EPS isolated from *A. muciniphila* grown in minimal medium mainly consisted of fucose, galactose, glucose and GlcNAc in ratio fucose:galactose:glucose:GlcNAc 1:1:2:1. Furthermore, fucose production was also detected in food-grade medium containing glucose and GlcNAc (**Table S1**). The presence of pea-peptone in this medium interfered with the monosaccharide analysis. However since minimum amounts of fucose were present in the medium control, fucose production by *A. muciniphila* as part of its EPS could also be confirmed in this medium. The observation of fucose production by *A. muciniphila* as part of its EPS structure is novel and has not been reported previously.

Table 1: Monosaccharide analysis of isolated EPS from minimal medium, including a negative control. Abbreviations: galacturonic acid (GalA), glucuronic acid (GlcA) and N-acetylglucosamine (GlcNAc).

	Monosaccharide analysis w/w(%)										
Isolated *A. muciniphila* EPS	**Fucose**	**Arabinose**	**Rhamnose**	**Galactose**	**Glucose**	**Xylose**	**Mannose**	**GalA**	**GlcA**	**GlcNAc**	**Total**
	4.6	0	0	4.1	9.0	0	0	0	0	4.6	22.3

Sialic acids detected as part of *A. muciniphila* EPS in glucose/GlcNAc rich medium

Additional characteristics of EPS and confirmation of the production of extracellular polysaccharides by *A. muciniphila* were determined using FTIR. Unwashed and freeze-dried pellets of the anaerobic fermentations were used for the FTIR measurements. In the spectrum of the high-and low-GlcNAc conditions, the shoulder peak at 1730 cm^{-1} is assigned to the presence of sialic acids (**Figure 2**). In contrast, there is no shoulder peak at 1730 cm^{-1} in the cell pellet derived from the mucus condition. This indicates sialic acids are being produced as part of *A. muciniphila* EPS when the medium is supplemented with glucose and GlcNAc.

The relative higher ratio of peak intensity at 1550 cm^{-1} and at 1629 cm^{-1} indicates that, there are proteins with longer side chain produced extracellularly with glucose and GlcNAc as the carbon source. These peaks are not as sharp as in the high-and low-GlcNAc conditions, implying that proteins with a longer side chain are not dominant under mucus conditions. In addition, the strong peak at 1020 cm^{-1} clearly shows that there are also other carbohydrates produced in medium supplemented with glucose and GlcNAc. If the ratio of the intensity of peak 1020 cm^{-1} and the intensity of peak 1550 cm^{-1} are considered, it indicates that the higher the glucose to GlcNAc ratio results in higher amount of carbohydrates. Considering the typical band of carbohydrates at 950-1200 cm^{-1}, in the mucus condition there are peaks at 1043 cm^{-1} and 1078 cm^{-1}, indicating the presence of carbohydrates and phosphate, while in the high-and low-GlcNAc conditions on food grade medium, the peak at 1020 cm^{-1} appeared as dominant, indicating there are carbohydrates produced extracellularly.

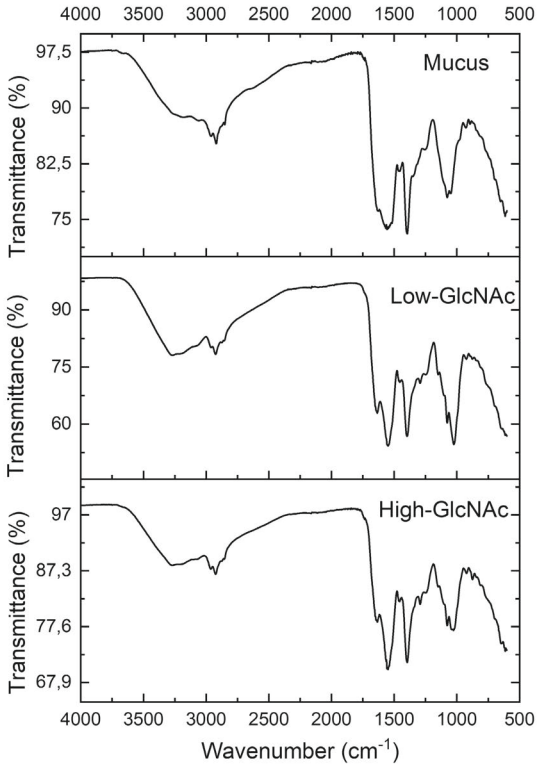

Figure 2: **FTIR spectra of cell pellets derived from high-GlcNAc, low-GlcNAc and mucus fermentations.** The shoulder peak at 1730 cm^{-1} is assigned to the presence of sialic acids, the peak at 1020 cm^{-1} indicates carbohydrates are produced extracellularly and the ratio between the intensity of the peaks at 1550 cm^{-1} and 1629 cm^{-1} indicates extracellular production of proteins with longer side chains.

Proposed EPS production system

The viscosity measurements, monosaccharide analysis and FTIR analysis indicate the capability of *A. muciniphila* to produce extracellular heteropolysaccharides. However, these techniques don't identify the EPS production system *A. muciniphila* employs. Bioinformatics analysis on the genome of *A. muciniphila* using a combination of Rapid Annotations using Subsystems Technology (RAST) and the annotation in the National Center for Biotechnology Information (NCBI) was performed to identify the system *A. muciniphila* might use to produce EPS. This analysis predicted that *A. muciniphila* has the Wzx/Wzy-dependent pathway for EPS production (**Figure 3**). One gene in this system, O-antigen polymerase (Wzy), could not be identified in the genome of *A. muciniphila* using the abovementioned bioinformatics analysis.

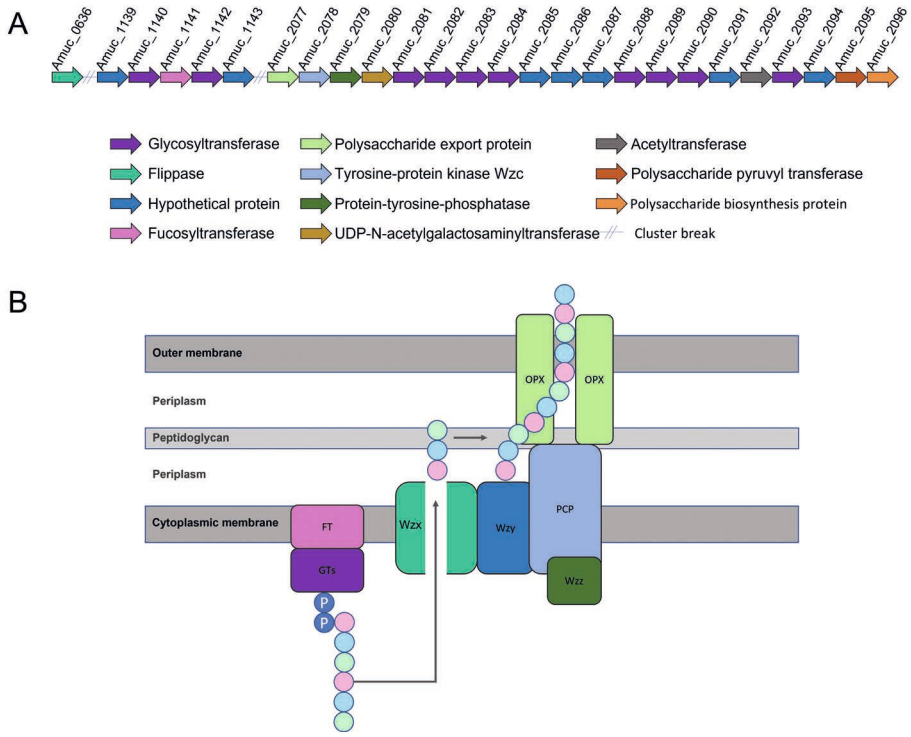

Figure 3: A) Proposed system for EPS production by *A. muciniphila* based on the Wzx/Wzy-dependent pathway and a cluster of glycosyltransferases and fucosyltransferases. B) Schematic overview of the proposed system for EPS production by *A. muciniphila*. The colors of the proteins in this schematic overview correspond with the colors of the gene cluster above. Putative genes of the EPS production system: Amuc_0636 (Wzx flippase), Amuc_2086 (Wzy polymerase), Amuc_2078 (PCP), Amuc_2079 (Wzz) and Amuc_2077 (OPX).

A protein BLAST against *A. muciniphila* using Wzy identified in *Escherichia coli* did not result in any hits with possibly uncharacterized proteins in *A. muciniphila*. Therefore, a homolog could not be identified for the O-antigen polymerase Wzy. However, the O-antigen polymerase derived from *E. coli* contains a conserved protein domain family named Wzy_C, that was also identified in 3 proteins in the proteome of *A. muciniphila* Muc^T: B2ULE4 (encoded by Amuc_0088), B2ULW8 (encoded by Amuc_0168) and B2UPL7 (encoded by Amuc_2086) using InterPro (Hunter et al. 2009). All three proteins are uncharacterized proteins and possible Wzy polymerase candidates for EPS production by *A. muciniphila*.

Fucose production by *A. muciniphila* has not been observed previously. Interestingly, *A. muciniphila's* genome does contain a GDP-fucose synthetase (Amuc_1248). The

Kyoto Encyclopedia of Genes and Genomes (KEGG) showed that Amuc_1248 is a part of the biosynthesis of nucleotide sugars pathway, where glucose is converted to GDP-fucose in multiple reactions (**Figure 4**). In KEGG, the conversion of Man-6P to Man-1P could not be linked to a gene in the genome of *A. muciniphila*. However, the genome of *A. muciniphila* does contain a gene encoding for phosphomannomutase, namely Amuc_0155. With this gene, *A. muciniphila* has the full genomic capacity to produce GDP-fucose for the implementation in its EPS. Interestingly, all genes of the pathway to produce GDP-fucose are expressed in the transcriptome data across all conditions included in this study. Therefore, it is likely that *A. muciniphila* produces GDP-fucose through this pathway for its implementation in EPS.

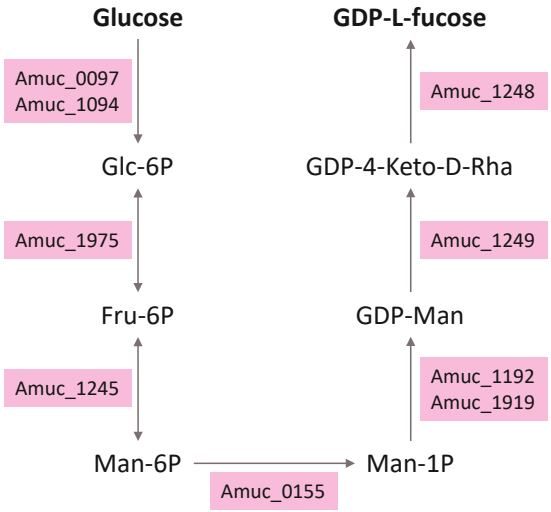

Figure 4: Production pathway of GDP-L-fucose.

A. muciniphila exhibited higher gene expression of EPS clusters in high-GlcNAc medium

Both transcriptomics and proteomics were used to assess the expression of annotated genes and proteins involved in EPS production by *A. muciniphila*, including the EPS production cluster containing genes belonging to the Wzx/Wzy-dependent pathway (Amuc_2077 until Amuc_2096) as well as the glycosyl transferase cluster (Amuc_1139 until Amuc_1143). Cells grown to mid-log phases have been used to compare the expression of genes involved in EPS production between high-GlcNAc, low-GlcNAc and mucus (**Figure 5**).

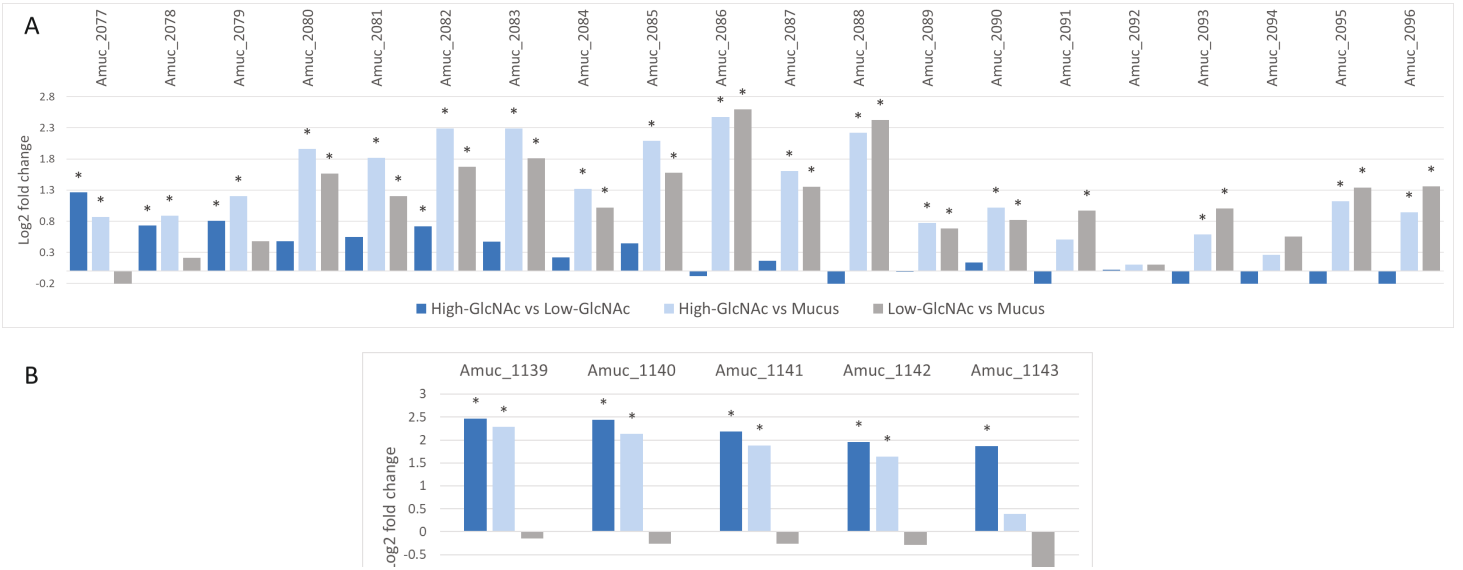

Figure 5: Comparison of Log2 fold changes of genes involved in EPS production between high-GlcNAc, low-GlcNAc and mucus (n=3). A) EPS gene cluster Amuc_2077 until Amuc_2096. B) Glycosyl transferase cluster Amuc_1139 until Amuc_1143. Significant differences between conditions are indicated with an asterisk (fold change > 1.5 and *p*-value < 0.05).

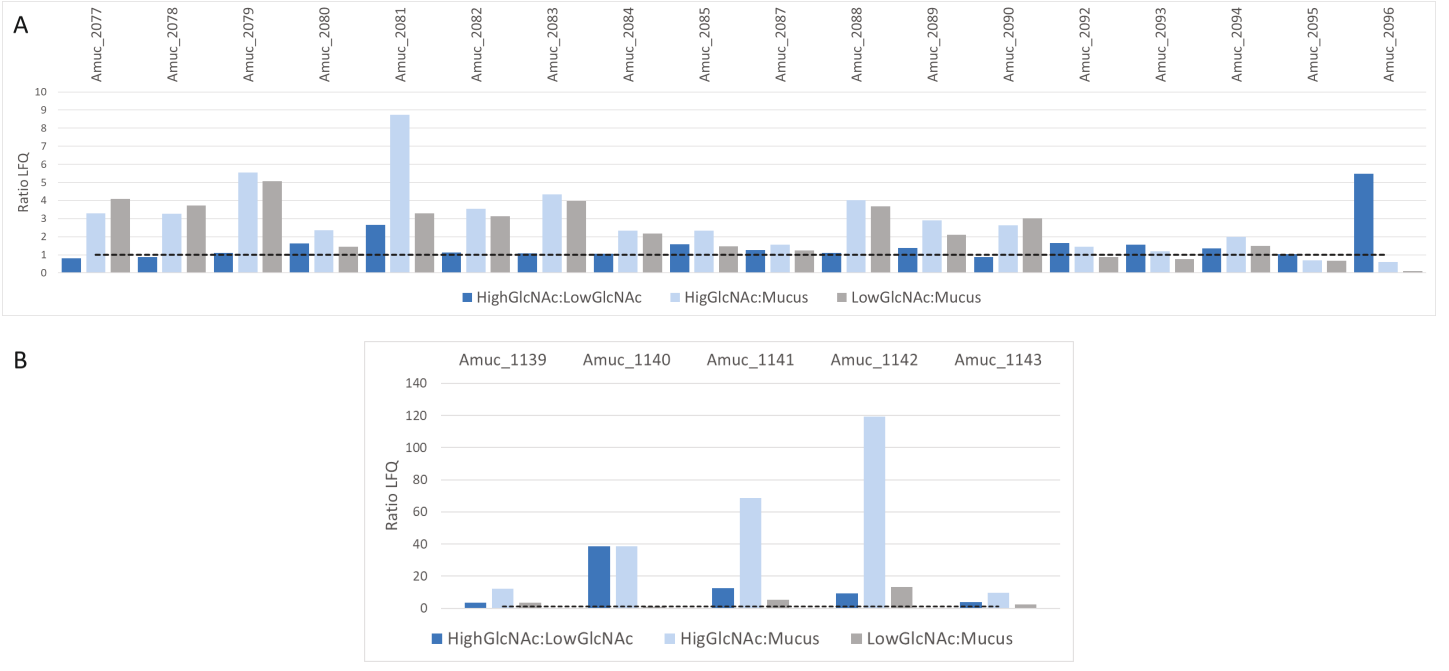

Figure 6: Comparison of ratio LFQs of proteins involved in EPS production between high-GlcNAc, low-GlcNAc and mucus (n=2). A) EPS gene cluster Amuc_2077 until Amuc_2096. B) Glycosyl transferase cluster Amuc_1139 until Amuc_1143. The baseline in the graph was set at value 1.

The expression of the genes Amuc_2077 until Amuc_2079 were significantly higher in high-GlcNAc, as compared to low-GlcNAc and mucus. Similar results were found for the glycosyl transferase gene cluster Amuc_1139 until Amuc_1142, where the expression of genes was significantly higher in high-GlcNAc, than low-GlcNAc and mucus. When comparing low-GlcNAc to mucus, the first genes of the EPS cluster (Amuc_2077-Amuc_2079) were not significantly differentially expressed. However, the remaining of this cluster, excluding Amuc_2092 and Amuc_2094, were all significantly higher in low-GlcNAc as compared to mucus.

Overall, the differences observed between high-GlcNAc and low-GlcNAc indicate a higher expression of EPS proteins in high-GlcNAc conditions, as also observed in the gene expression data (**Figure 6**). However, the ratios do not show differences as large as shown in the gene expression data. The protein expression of the GH cluster showed consistently higher protein expression in high-GlcNAc compared to low-GlcNAc. Which corresponds with the gene expression of this cluster in the mid-logarithmic phase. The abundance of the proteins belonging to the glycosyl transferase was overall the lowest in the mucus condition. In addition, the abundance of three out of five proteins of the glycosyl transferase cluster was not measured in the mucus condition.

Discussion

In this study, we showed evidence for EPS production by *A. muciniphila* cultivated in both food-grade and minimal medium supplemented with glucose and GlcNAc. The bioinformatics analysis showed that *A. muciniphila* may produce EPS through the Wzx/Wzy-dependent pathway. Our results indicate that a higher GlcNAc concentration in the medium results in increased production of EPS. Furthermore, we have identified the main monosaccharides in *A. muciniphila* EPS, which are fucose, galactose, glucose and GlcNAc in ratio 1:1:2:1, respectively.

A. muciniphila possibly uses the Wzx/Wzy-dependent pathway to produce EPS. In this pathway various glycosyltransferases synthesize a repeating unit intracellularly. This repeating unit is then translocated to the periplasm by flippase Wzx, after which polymerization occurs through polymerase Wzy and a polysaccharide co-polymerase protein (PCP). The PCP realizes the transport of EPS together with the outer membrane polysaccharide export protein. Most proteins involved in the Wzx/Wzy-dependent pathway have been identified in the genome of *A. muciniphila*. The Wzy protein may be encoded by Amuc_2086, which is part of the EPS gene cluster identified in this study. This protein was identified based on the presence of Wzy_C, a conserved domain in Wzy of *E. coli*. Furthermore, with RAST annotation we identified two other

genes involved in EPS production: tyrosine protein kinase Wzc (Amuc_2078) and protein tyrosine phosphatase (Amuc_2079). The protein Wzc is involved in high-level polymerization of capsular polysaccharides in *E. coli* and is part of the translocation capsule, as well as Wzb (protein tyrosine phosphatase) which dephosphorylates Wzc (Whitfield 2006). In *Bacillus subtilis* it was shown that the tyrosine kinase was responsible for self-regulation of exopolysaccharide production in this organism (Elsholz et al. 2014).

Dietary polyphenols were found to induce capsular polysaccharide production by *A. muciniphila*, specifically activating the capsular exopolysaccharide biosynthesis protein (Amuc_1413) and the polysaccharide sorting system PEP-CTERM/EpsH identified by qPCR analysis, but not polysaccharide export protein Amuc_2077 (Rodriguez-Daza 2020). However, in our study, we could not correlate the expression of the gene encoding for EpsH and the protein itself with the increasing EPS production in different fermentation conditions. Dietary polyphenols exert anti-inflammatory and antimicrobial activities and have been shown to modulate the colonic microbiota composition (Mosele et al. 2015, Xie et al. 2015). In the presence of polyphenols, *A. muciniphila* displayed an antibiotic-related molecular adaptation (Rodriguez-Daza 2020). These systems were not found to be upregulated between conditions with varying glucose:GlcNAc ratios in our study. It is important to note that unlike our study, the response to polyphenols using a selection of genes was measured with qPCR, did not address the complete transcriptome. Another stress condition where *A. muciniphila* might use EPS production as a protection mechanism is oxygen stress (Ouwerkerk et al. 2016). In this study, Amuc_2081, part of the proposed EPS production system, was significantly upregulated in the aerated growth condition, compared to the anaerobic growth condition. Most genes in this system were upregulated in the oxygen condition, but not significantly. Previously, a different study has compared the growth of *A. muciniphila* in medium supplemented with mucus and glucose (Ottman et al. 2017). Under glucose conditions, the entire gene cluster of Amuc_2079 to Amuc_2098 was significantly upregulated in comparison to mucus. In the present study, all genes of the gene cluster from Amuc_2077 until Amuc_2096 were significantly upregulated in the high-GlcNAc condition as compared to mucus, except for three genes (Amuc_2091, Amuc_2092, and Amuc_2094). Similar results were observed for the glycosyl transferase cluster (Amuc_1139 until Amuc_1143), where 4 out of 5 genes were significantly upregulated under the high-GlcNAc condition compared to mucus. Altogether, these different stress conditions or varying carbon sources may induce different responses of *A. muciniphila* in terms of EPS production, possibly activating polysaccharide sorting system PEP-CTERM/EpsH or the Wzy/Wzx-dependent pathway.

The main monosaccharides in EPS produced by *A. muciniphila* are fucose, galactose, glucose and GlcNAc in ratio 1:1:2:1, respectively. Fucose is abundant in mucus, human milk and bacterial glycans. In the gut, fucose was found to play an essential role in the establishment of the gut microbiota, as well as later in the established gut microbiota (Garber et al. 2021). Fucose was present in the mucus growth condition, but not in the medium conditions with different ratios of glucose to GlcNAc and the minimal medium used in the experiments of this study. However, *A. muciniphila* was able to incorporate fucose in its EPS. The ability of *A. muciniphila* to metabolize fucose has been shown previously (Ottman et al. 2017, Kostopoulos et al. 2020). In contrast, the production of fucose by *A. muciniphila* has not been observed previously. Fuc-EPS obtained increased attention due to the easily controlled processing procedures, fast and reproducible production and its applications in both food and medicine fields (Xiao et al. 2022). Therefore, *A. muciniphila* EPS may potentially be applied for therapeutic purposes, However, further research on the effect of *Akkermansia* EPS on host health has yet to be completed.

Furthermore, the structural stability of EPS produced by *A. muciniphila* should be studied for its application. For example, four EPS-producing LAB were found to have high thermostability with melting points above 224°C (Abid et al. 2018). This suggests the possibility that pasteurized *A. muciniphila*, as previously applied (Depommier et al. 2019), still contains EPS (Abid et al. 2018). The presence of EPS may then also have immune-modulating effects, interacting with the intestinal environment as observed for other beneficial bacteria (Castro-Bravo et al. 2018).

For the characterization of *A. muciniphila* EPS, we mainly focused on the EPS found in the supernatant of the cultures. However, a recent study including four bifidobacterial strains showed distinct structural differences in entirely excreted EPS compared to membrane-associated EPS (Ferrari et al. 2022). In our study, FTIR analysis indicated that extracellular carbohydrates are present in the pellet of *A. muciniphila,* including the production of sialic acids in conditions containing GlcNAc and glucose. However, the sialic acids were not detected in EPS isolates obtained from the supernatant. Therefore, *A. muciniphila* may also produce membrane-associated EPS, which may be structurally different from EPS found in the supernatant.

In conclusion, we identified Fuc-EPS produced by *A. muciniphila*, its components, the genetic machinery *A. muciniphila* may be using and differences in EPS production between conditions. This information can be used for future research to study the role of EPS produced by *A. muciniphila* in host health and in the gut microbiota. Lastly, the differences in EPS production throughout the different cultivation conditions may help to optimize the cultivation of this beneficial microbe for therapeutic applications.

Material and methods

Cultivation conditions

The type strain *Akkermansia muciniphila* Muc^T (ATCC BAA-835) was used for all cultivation experiments. Pre-cultures grown for the anaerobic fermentations supplemented with pea peptone were cultivated in tryptone medium with the following composition: KH_2PO_4 (0.4 g/L), Na_2HPO_4 (0.53 g/L), NH_4Cl (0.3 g/L), NaCl (0.3 g/L), $MgCl_2$*$6H_2O$ (0.1 g/L), 1 mL trace elements in acid (50 mM HCl, 1mM H_3BO_3, 0.5 mM $MnCl_2$*$4H_2O$, 7.5 mM $FeCl_2$*$4H_2O$, 0.5 mM $CoCl_2$, 0.1 mM $NiCl_2$, and 0.5 mM $ZnCl_2$, 0.1 mM $CuCl_2$*$2H_2O$), 1 mL trace elements in alkaline (10 mM NaOH, 0.1 mM Na_2SeO_3, 0.1 mM Na_2WO_4, and 0.1 mM Na_2MoO_4), tryptone (20 g/L), L-threonine (4 g/L) and 1 mL resazurin solution (500 mg/L). After autoclaving the following components were added to the medium: 1% (v/v) of the vitamin solution (per liter: 11 g $CaCl_2$, 20 mg biotin, 200 mg nicotinamide, 100 mg p-aminobenzoic acid, 200 mg thiamin (vitamin B1), 100 mg pantothenic acid, 500 mg pyridoxamine, 100 mg cyanocobalamin (vitamin B12), and 100 mg riboflavin) and 5% (v/v) of reducing solution (per liter: 80 g $NaHCO_3$, 20 mL Na_2S*$9H_2O$ solution (240 g/L) and 10 g cysteine-HCl), 12.5 mM N-acetylglucosamine (GlcNAc) and 12.5 mM glucose (Sigma-Aldrich, Saint Louis, United States). The pre-cultures were grown in anaerobic conditions and incubated at 37°C for 48 hours (non-shaking).

Food-grade medium was used for the main experiments with the following composition: KH_2PO_4 (0.4 g/L), Na_2HPO_4 (0.669 g/L), NH_4Cl (0.3 g/L), NaCl (0.3 g/L), $MgCl_2$ $6H_2O$ (0.1 g/L), pea peptone A482 (OrganoTechnie, La Courneuve, France 32 g/L), L-threonine (4 g/L). After autoclaving 2 mL of reducing solution containing $NaHCO_3$ (40 g/L) and L-cysteine*HCl (5 g/L) and 1% (v/v) of vitamin solution were added to the medium. The medium was inoculated with 1% (v/v) of the pre-culture. Anaerobic fermentations using this medium were performed as described in the next section.

Minimal medium was used for further characterization of *A. muciniphila* EPS. This medium is a modified version of tryptone medium where only tryptone was omitted to reduce background in EPS analysis. These cultures were grown in anaerobic serum bottles and were incubated for 48 hours at 37°C (non-shaking).

Anaerobic fermentation

The anaerobic fermentations were performed using food-grade medium as described in the previous section. Four conditions were tested: High-GlcNAc (glucose:GlcNAc ratio 3:1), low-GlcNAc (glucose:GlcNAc ratio 20:1) and mucus (0.5% mucus). The different proportions of glucose and GlcNAc were chosen to assess the effect of carbon source ratios on EPS production by *A. muciniphila*. The last condition containing 0.5% mucus

from porcine stomach (Type III, Sigma-Aldrich, Saint Louis, United States) served as a control closer to the conditions in the mucus layer of the gut and the availability of carbon sources therein.

The fermentations were conducted in three parallel bioreactors (DasGip, Eppendorf, Hamburg, Germany) using 700 mL of food-grade medium containing either glucose and GlcNAc in two different ratios or hog-gastric mucin with a final concentration of 150 mM or 0.5% crude mucin. The pH was set at 6.8 and a stirring rate of 100 rpm was applied with N2/CO2 gas flow (80%/20%). The medium of all four fermentors was inoculated with 1% (v/v) of cultures pre-grown on tryptone medium. The fermentation was terminated after 72 hours. Samples were taken for OD measurements, HPLC analysis, microscopic analysis, RNA sequencing and proteomics. Samples for HPLC analysis were stored at -20°C until use. Samples for RNA sequencing and proteomics were taken at early, mid and end exponential phase and centrifuged for 30 minutes at 4700 rpm at 4°C, after which the supernatant was removed. Then, 1 mL of RNAlater was added to the pellets of the samples for RNA sequencing. Lastly, the samples for both RNA sequencing and proteomics were snap-frozen in liquid nitrogen and stored at -80°C.

Exopolysaccharides extraction

Samples taken from the anaerobic cultivations on food-grade medium and minimal medium were centrifuged twice at 10,000 x g for 20 minutes at 4°C. The ethanol precipitation method was used to isolate EPS as described by Nikolic et al. 2012 with modifications (Nikolic et al. 2012). Chilled ethanol was added to the supernatant in a ratio of 2:1 and stored for 48 hours at 4°C. The precipitate was collected by centrifugation at 12,000 x g for 20 minutes at 4°C. The pellet was dissolved in purified water while keeping the volume to a minimum. Then, the precipitate was dialyzed against purified water using 3.5k snake-skin dialysis membranes (Thermo Scientific, Waltham, United states) at 4°C for 48 hours. During these 48 hours, the purified water was changed three times. The dialyzed retentate was stored at -80°C for 2 hours, prior to lyophilization until completely dry. Crude EPS was stored at -80°C.

The purification of crude EPS was performed as described previously with few modifications (Nikolic et al. 2012). The sample was added to a buffer containing 50 mM Tris-HCl and 10 mM MgSO4*7H2O at a final concentration of 5 mg/mL. DNase type I (Sigma-Aldrich, Saint Louis, United States) was added at a final concentration of 2.5 µg/mL. Subsequently, the solution was incubated for 6 hours at 37°C. Next, pronase E (Sigma-Aldrich, Saint Louis, United States) was added at a final concentration of 50 µg/mL after which the solution was incubated for 18 hours at 37°C. After the incubation, trichloroacetic acid (TCA) was added to a final concentration of 12% and stirred at

room temperature for 30 minutes. Then, the solution was centrifuged at 12.000 xg for 20 minutes at 4°C, after which the supernatant was collected. The pH was adjusted to a pH ranging between 4.0 and 5.0. Lastly, the solution was dialyzed against purified water for three days while changing the water daily before lyophilization.

FTIR

Culture samples were centrifuged at 4700xg for 30 min at 4°C. After centrifugation, the supernatant of all samples was discarded and only the pellet was stored at -80°C for two days. Samples were then lyophilized for a day after which Fourier transform infrared (FTIR) analysis was performed. The FTIR spectrum of each sample was recorded on a FTIR Spectrometer (Perkin Elmer, Shelton, USA) at room temperature, with a wavenumber range from 500 cm-1 to 4000 cm-1. In total, eight scans were performed per measurement of each condition.

Viscosity measurements

The rheological behavior of polysaccharide-rich supernatants was measured at a 25.00 ± 0.01° C temperature using a physica MCR 501 rheometer (P-PTD200+H-PTD200) (Anton Paar, Graz, Austria), equipped with a parallel plate geometry (CP50-1 SN16804). 600 µL of the sample was used to fill the gap between the plates. A total of 10 measuring points were recorded with a point duration of 10 s. Logarithmic flow curves were plotted based on the shear stress (viscosity) (mPa.s) as a function of the shear rate from 10 to 1000 1/s. The data obtained was analyzed by Anton Paar RheoCompass™ V1.25.422 software. As a control, supernatants from the non-inoculated culture medium were used.

Monosaccharide analysis

The monosaccharide composition was determined using high-performance anion exchange chromatography (HPAEC) with pulsed amperometric detection (PAD). Prior to HPAEC-PAD analysis, samples were hydrolyzed using 2M trifluoroacetic acid (1h at 121 °C). Ten µL of the sample was injected into an ICS-5000 HPLC system (Dionex, Sunnyvale, CA, USA) equipped with a CarboPac PA1 guard column (2 mm ID ×50 mm), a CarboPac PA-1 column (2 mm ID ×250 mm; both from Dionex Corporation, Sunnyvale, United States) and an ED40 EC-detector in the PAD mode (Dionex, Sunnyvale, United States). The column temperature was set at 20 °C and mobile phases were kept under helium flushing. The flow rate was set at 0.4 mL/min. Mobile phase A (0.1M sodium hydroxide), B (1M sodium acetate in 0.1M sodium hydroxide) and C (milli-Q water) were used with the following elution profile: 0– 37.0 min, 100% C; 37.1 min, 100% A ; 37.2– 48.0 min, 10.0-17.3% B; 48.1-53.0 min, 100% B; 53.1–61.0 min, 100% A; 61.1–76.0 min, 100% C. A post-column alkali addition (0.5 M NaOH; 0.1 mL/min) was used from 0.0 to 27.0 min and from 51.1 to 66.0 min. All samples were analyzed in duplicate.

Standards of fucose, arabinose, rhamnose, galactose, glucose, xylose, mannose, GlcNAc, galacturonic acid and glucuronic acid were used for quantification. The collected data was analyzed using Chromeleon 7.2 software (Dionex Corporation, Sunnyvale, United States).

Identification of the EPS gene cluster

Bioinformatics analysis was applied to identify the system *A. muciniphila* uses to produce EPS. First, the annotation of *A. muciniphila* Muc^T was obtained from the National Center for Biotechnology Information (NCBI). Furthermore, Rapid Annotations using Subsystems Technology (RAST) was used to annotate the genome (Aziz et al. 2008). By combining the results from both analyses, a hypothesis was formulated on the pathway that *A. muciniphila* may be using to produce EPS. To confirm the expression of genes and proteins involved in EPS production, transcriptomic and proteomic analyses were performed.

RNA isolation and transcriptome analysis

RNA isolation was performed as described previously (Shetty et al. 2022). Further processing of the total RNA was performed by Novogene (Cambridge, United Kingdom) using the platform Illumina PE150. Transcriptome analysis has been performed as previously described (Hagi et al. 2020). All further analysis was done using R version 3.6.3 in Rstudio version 1.2.5019. Genes were considered significantly different with adjusted p values <0.05 in combination with fold-changes >1.5 (log-fold change >0.58).

Sample preparation for nLC-MS/MS and analysis

Total protein was isolated from culture samples. Ice-cold 100 mM Tris buffer (pH 8) was added to the pellets in variable amounts up to approximately 500 µl and 200 µl of the resuspended cells was transferred to low-binding Eppendorf tubes. The tubes were centrifuged repeatedly for 1 min at 10.000 x g until the supernatant was clear. Then, the supernatant was removed and 200 µl of ice-cold 100 mM Tris buffer (pH 8) was added again. The cells were resuspended after which the centrifugation was repeated. After removing the last supernatant, the cells were resuspended in 200 µl 100 mM Tris (pH 8) and aliquoted per 50 µl in low-binding Eppendorf tubes. Subsequently, the samples were sonicated for 15 seconds using the Soniprep 150 (MSE, London, UK). The protein concentration was measured using the Pierce™ BCA Protein Assay Kit (Thermo Scientific, Waltham, United states) to dilute all samples to a concentration of 1 µg/µl in a final volume of 60 µl using 100 mM Tris. Then, 6 µl of 150 mM dithiothreitol (Sigma Life Science, Saint Louis, United States) was added to the diluted sample followed by incubation at 37°C for 45 minutes. After incubation, the sample was mixed with 198µl 8 M urea (Sigma-Aldrich, Saint Louis, United States) and 27 µl 150 mM acrylamide and incubated for 30 minutes at room temperature. Subsequently,

4 µl of 10% trifluoroacetic acid (TFA, Alfa Aesar Chemicals, Haverhill, United states) and 8 µl SpeedBeads™ magnetic carboxylate modified particles (50%, GE Healthcare 45152105050250 and 50% Thermo Scientific 65152105050250, washed twice with MilliQ water) and 750 µl acetonitrile (Biosolve B.V.) were added to the sample solution. Next, the mixtures were incubated for 20 minutes at room temperature and the liquid was removed. Then, the beads were washed twice on a magnetic rack (Cell Signaling Technology, Danvers, United States) with 1 mL 70% ethanol and with 1 mL 100% acetonitrile, respectively. Afterwards, 100 µl of 5 ng/µl trypsin (Roche Diagnostic GmbH, Mannheim, Germany) in 50 mM ammonium bicarbonate was added to the beads containing the sample and subjected to overnight digestion at room temperature. The digestion was stopped by adding 4 µl 10% TFA to the sample. Then, the samples were placed on the magnetic rack to obtain the first supernatant. The remaining beads were washed with 100 ml/L formic acid. This solution was then combined with the first supernatant.

Micro Columns (µcolumns) were prepared by adding two C18 disks (Affinisep AttractSPE™ Disk Bio C18, Le Houlme, France), 200 µl methanol and 4 µL 50% Lichroprep RP-18 (Sigma-Aldrich, Saint Louis, United States) in methanol into a 200 µL pipette tip. The µcolumn was then eluted and washed with 100 µl methanol and equilibrated with 100 µl 1 mL/L formic acid in water before use. The samples with the cell lysates were then transferred to the µcolumn. After elution and washing with 100 µL 1 mL/L formic acid in water, 50 µl of (1:1) formic acid and acetonitrile solution was added onto the µcolumn and eluted into a clean 0.5 mL low-binding Eppendorf tube. Subsequently, the samples were concentrated to a final volume of approximately 10 µl using an Eppendorf Concentrator Plus. Lastly, the volume was adjusted to 50 µl using 1 mL/L formic acid before storage at -20°C until further processing.

Peptide samples were measured (nLC1000 - Orbitrap Exploris 480) and data analysis was performed as previously described (Feng et al. 2022). The database that was used for the analysis of the samples in this study was the Akkermansia_muciniphila_baa-835_UP000001031 uniprot database.

Supplementary information

Table S1: Monosaccharide analysis of *A. muciniphila* EPS extracted from food-grade medium.

EPS extracts	Monosaccharide analysis w/w(%)										
	Fucose	Arabinose	Rhamnose	Galactose	Glucose	Xylose	Mannose	GalA	GlcA	GlcNAc	Total
high-GlcNAc	3.5	2.6	0.5	5.2	2.9	0.5	0	4.4	0.5	N/A	20.1
Low-GlcNAc	1.9	3.7	0.7	6	2.2	0.7	0	4.8	0.5	N/A	20.6
Food-grade medium (-)	0.1	3.5	0.8	5	0.7	0.8	0	3.4	0.7	N/A	15

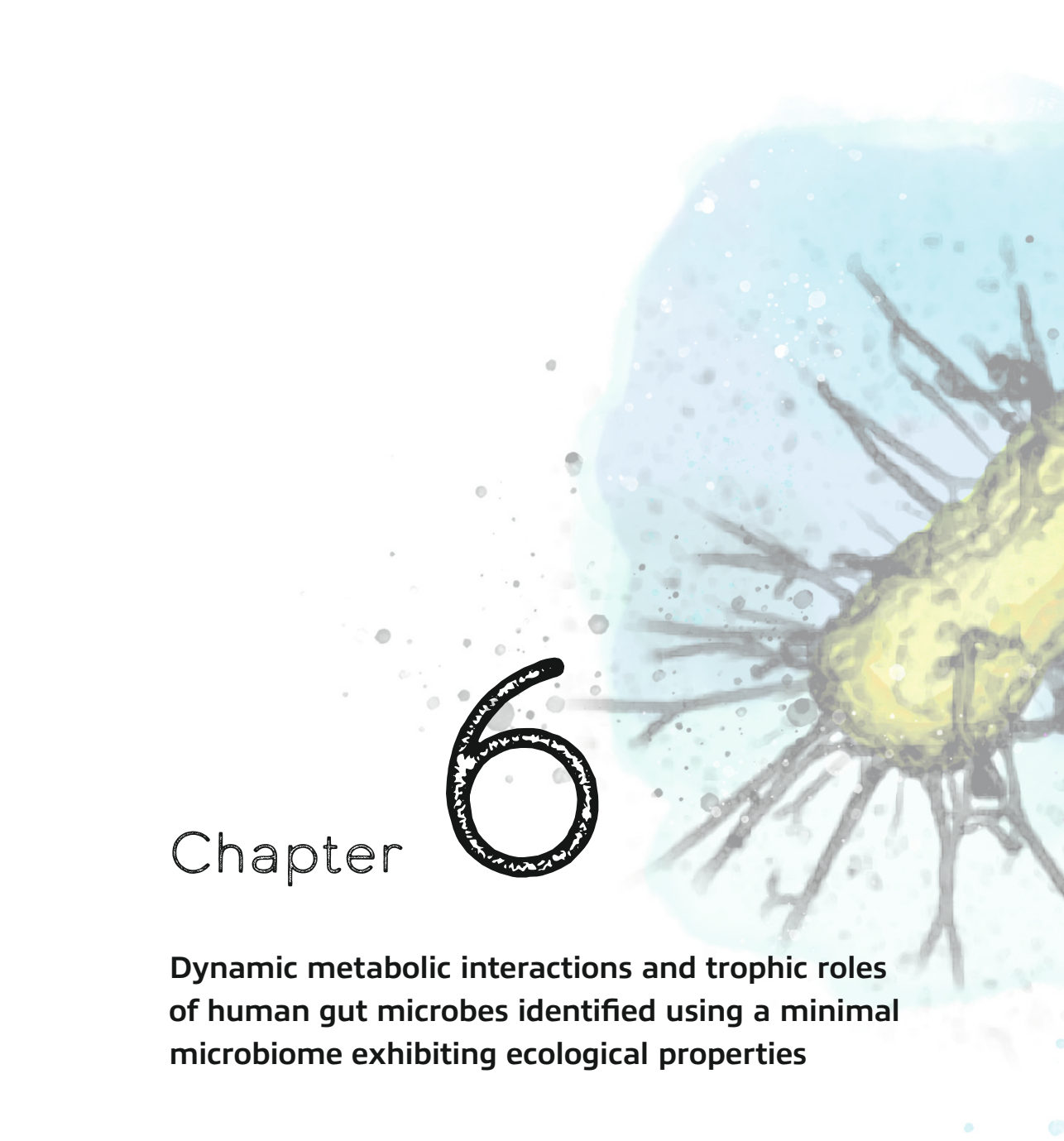

Chapter 6

Dynamic metabolic interactions and trophic roles of human gut microbes identified using a minimal microbiome exhibiting ecological properties

Sudarshan A. Shetty*, Ioannis Kostopoulos*, Sharon Y. Geerlings*, Hauke Smidt, Willem M. de Vos**, Clara Belzer****

*These authors contributed equally
**Equal contribution; co-correspondence

The ISME Journal doi: 10.1038/s41396-022-01255-2

Abstract

Microbe-microbe interactions in the human gut are influenced by host derived glycans and diet. The high complexity of the gut microbiome poses a major challenge for unravelling the metabolic interactions and trophic roles of key microbes. Synthetic minimal microbiomes provide a pragmatic approach to investigate their ecology including metabolic interactions. Here, we rationally designed a synthetic microbiome termed Mucin and Diet based Minimal Microbiome (MDb-MM) by taking into account known physiological features of 16 key bacteria. We combined 16S rRNA gene-based composition analysis, metabolite measurements and metatranscriptomics to investigate community dynamics, stability, inter-species metabolic interactions and their trophic roles. The 16 species co-existed in the *in vitro* gut ecosystems containing a mixture of complex substrates representing dietary fibers and mucin. The triplicate MDb-MM's followed the Taylor's power law and exhibited strikingly similar ecological and metabolic patterns. The MDb-MM exhibited resistance and resilience to temporal perturbations as evidenced by the abundance and metabolic end-products. Microbe-specific temporal dynamics in transcriptional niche overlap and trophic interaction network explained the observed co-existence in a competitive minimal microbiome. Overall, the present study provides crucial insights into the co-existence, metabolic niches and trophic roles of key intestinal microbes in a highly dynamic and competitive *in vitro* ecosystem.

Introduction

The complexity of interactions within the human gut microbiome contributes to providing health benefits to its host. However, the same complexity presents a major challenge for deciphering metabolic and ecological interactions between the intestinal microbes. Understanding these complex interactions, at both community and individual taxa level, is crucial for the development of effective microbiome modulation strategies (Shetty et al. 2017, Costello et al. 2012, Gilbert and Lynch 2019). The human intestinal tract includes several hundred species mainly belonging to the phyla Actinobacteria, Bacteroidetes, Firmicutes, Verrucomicrobia, Proteobacteria and others (Li et al. 2014). Recently, synthetic microbial communities assembled from host-derived strains have received considerable attention for understanding ecological and metabolic features of the microbiome (De Roy et al. 2014, Grosskopf and Soyer 2014, Shetty et al. 2019). Synthetic microbial communities of the human gut can be studied under controlled conditions *in vitro* (D'Hoe et al. 2018, Venturelli et al. 2018, Elzinga et al. 2019, Bui et al. 2019, Belzer et al. 2017, Soto-Martin et al. 2020). *In vitro* intestinal models allow for stable and controllable conditions as well as frequent sampling of the microbial community that may not be possible with animal models for technical and ethical reasons (Macfarlane and Macfarlane 2007, Venema and van den Abbeele 2013). Combining *in vitro* intestinal models with defined microbial communities holds potential for understanding community assembly and structure, compositional and functional dynamics in time and plasticity of microbial interactions.

Studies employing *in vitro* intestinal models till date have applied either batch, continuous single or semi-continuous or multi-stage fermentation models (El Hage et al. 2019, Silverman et al. 2018, Tanner et al. 2014, Van den Abbeele et al. 2010, Shetty et al. 2022). An important aspect of the host-associated microbiome is the dietary intake of the host that often follows circadian rhythms and can give rise to stages of excess carbon and energy source and periodic carbon starvation. Both of these aspects may have a profound influence on the compositional and functional dynamics of the microbial community. In fact, previous *in vitro* studies have revealed that nutrient periodicities can affect microbial community dynamics and physiological functionality (Carrero-Colón et al. 2006, Carrero-Colón et al. 2006). Nutrient periodicity is an important factor that may lead to selection of well adapted taxa, affect microbe-microbe interactions and microbe-environment interactions as well as provide an opportunity for invading species to successfully establish in a community (Carrero-Colón et al. 2006, Carrero-Colón et al. 2006, Mallon et al. 2015, Symons and Arnott 2014). In the human intestinal tract, two major sources of carbon and energy are dietary and host-derived polysaccharides (mainly secreted mucin) that all have a strong deterministic effect on the microbiome (Desai et al. 2016, Cotillard et al. 2013,

David et al. 2014). The diet can be highly variable on sub-daily time scales posing a major selective pressure on the gut microbiome (Johnson et al. 2019). Dietary sources, especially complex fiber-derived polysaccharides that reach the colon in a virtually unmodified way, lead to the creation of diverse niches that can support a higher diversity of microbes (Pereira and Berry 2017). In addition, the periodicity and variability in supply of dietary fibers can give rise to dynamic regimes of niche availability consequently affecting interactions between the diet responsive microbes. On the contrary, mucin is a stable source of carbon and energy within a host and is shown to promote stability of the gut microbiome (Duncan et al. 2019). Therefore, both diet and mucin play a major role in supporting diverse microbial communities and give rise to complex microbe-microbe interactions.

To understand microbe-microbe interactions within a complex community, it is important to create a community that exhibits ecophysiological properties similar to natural ecosystems (Shetty et al. 2022). Community level ecological properties such as resistance and resilience to perturbations, presence of competitors for nutrients as well as mutualists that support metabolic co-operation can be designed in a synthetic minimal microbiome (Shetty et al. 2019). Here, we sought to investigate microbe-microbe interactions in a synthetic minimal gut microbiome over a period of 20 days under controlled conditions. To explore temporal ecophysiological interactions, the community was assembled in triplicate bioreactors with constant supply of mucin and pulse of the main dietary **D**iet **o**rigin **S**ubstrates (DoS) *viz*. pectin, resistant starch, inulin and xylan. The experiment was designed with various perturbations to test for aspects such as vacant niche occupation by introducing a non-core strain, *Blautia hydrogenotrophica*, increased dietary intake by doubling the concentration of DoS, loss of a key metabolite that is required for growth of specific bacteria by removal of exogenous acetate (coinciding with replenishing of feed medium), diet starvation by subjecting the community to periods of elongated fasting i.e., no addition of DoS for >24 h and increase in substrate feeding rate (**Fig. 1**). Over a 20-day operation of the artificial gut system, we sampled the three bioreactors at 61 time points each (~3 samples/day) and tested the impact of aforementioned events on the dynamics of MDb-MM composition, structure and function. The integrative analysis of temporal measurements of metabolites, 16S rRNA gene amplicons and metatranscriptomes allowed us to unravel community dynamics and metabolic interactions using a synthetic minimal microbiome.

Results

Design of the synthetic Mucin and Diet based Minimal Microbiome (MDb-MM)

We sought to assemble a minimal microbiome that consists of bacterial strains relevant to the human colonic microbiome and mimics key ecological and metabolic properties (**Fig. 1**). Therefore, the selection of strains was rationally guided by ecophysiological aspects, such as high prevalence (>50%) and minimum abundances threshold of 0.001% in human colonic microbiota, ability to degrade mucin or common multiple dietary polysaccharides that reach the colon in a virtually unmodified form (pectin, xylan, starch and inulin) and their breakdown products. We screened 1155 human gut metagenomes from the curated Metagenomic database and obtained a list of 64 core species (Supplementary table S1). Majority of these species belonged to Firmicutes (35 species) and Bacteroidetes (25 species). Actinobacteria, Proteobacteria and Verrucomicrobia were represented by five, three and one species respectively. We chose representative strains from Firmicutes, Bacteroidetes, Actinobacteria and Verrucomicrobia. *Bilophila* and *Escherichia* were the two most prevalent genera within Proteobacteria, and we excluded these in this study, because of their low contribution to the overall composition in the human gut metagenomes analysed in this study. Among the core microbiota phyla, Proteobacteria comprised the lowest fraction (1.04%) of the total counts, compared to Firmicutes (46.6%), Bacteroidetes (43.9%), Actinobacteria (6.8%) and Verrucomicrobia (1.4%).

During selection of the candidate strains, we considered competition for growth substrates, known metabolic cross feeding on lactate and 1,2-propanediol (1,2-PD) and the ability to produce lactate or common short chain fatty acids (SCFAs) such as formate, acetate, propionate and butyrate. The details of the representative strains, their known growth substrates and fermentation end products relevant to the current study are given in **Table 1**.

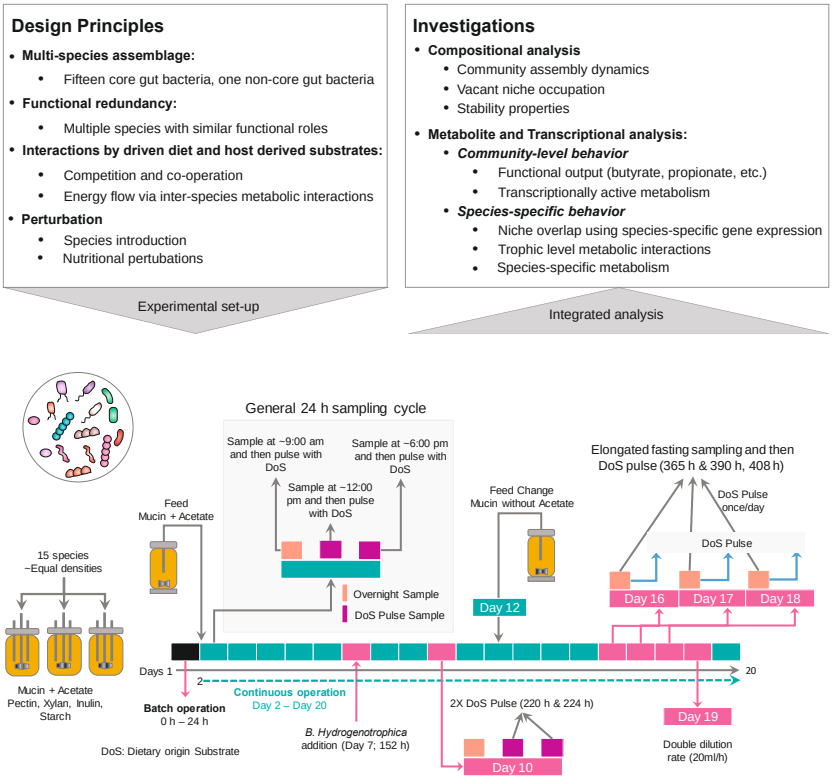

Figure 1: MDb-MM design principles, experiment setup and investigations. Key aspects that were considered when designing the MDb-MM included building a multi-species minimal microbiome with functional redundancy and trophic interactions and potential vacant niches to test niche occupation. The experimental set-up included pulse feeding the bioreactors with **D**iet **o**rigin **S**ubstrates (DoS) and introducing perturbations like the addition of new species, increase dietary intake (2X DoS pulse), removal of key metabolite and nutrient starvation. Details about the sampling time points for composition, metabolites and metatranscriptome are depicted in supplementary figure S2.

Table 1: General metabolic features of species for which depicted strains were used for MDb-MM. Abbreviations: Acetate (A), Butyrate (B), Propionate (P), Lactate (L), Formate (F), Ethanol (E), 1,2-Propanediol (1,2-PD), Succinate (S)

Species	Strain used/source	Known substrates	Metabolite production*	References
Akkermansia muciniphila	MucT/ATCC BAA-835	mucin, N-acetylglucosamine, N- acetylgalactosamine, fucose	A, P, L, 1,2-PD	(Belzer et al. 2017, Derrien et al. 2004)
Bacteroides ovatus	HMP strain 3_8_47FAA	starch, xylan, inulin	A, P, L, 1,2-PD	(Degnan et al. 1997, Hemsworth et al. 2016, Macfarlane et al. 1990, Sonnenburg et al. 2010)
Bacteroides xylanisolvens	HMP strain 2_1_22	pectin, starch, xylan	A, P, L	(Despres et al. 2016)
Anaerobutyricum soehngenii	L2-7/DSM 17630	sugars, DL-lactate, 1,2-PD	B, P, F, CO_2, H_2	(Engels et al. 2016, Shetty et al. 2018, Duncan et al. 2004)
Coprococcus catus	ATCC 27761	fructose, mannitol, glucose, mannose, lactate	B, P, A, S, H_2	(Holdeman and Moore 1974, Reichardt et al. 2014)
Flavonifractor plautii	HMP strain 7_1_58FAA	glucose, maltose, xylose, lysine	L, B, P	(Vital et al. 2017)
Eubacterium sireaum	DSM 15702	starch, glucose, maltose	A, E, L, B, S	(Duncan et al. 2016, MOORE et al. 1976)
Agathobacter rectalis	DSM 17629	starch, glucose, lactose, xylose, cellobiose, l-arabinose, trehalose, sorbitol, N-acetylglucosamine	B, A, H_2, L	(Cockburn et al. 2015, Riviere et al. 2015, Duncan and Flint 2008)
Roseburia intestinalis	DSM 14610	starch, glucose, xylose, xylan, arabinose	B, F, L	(Duncan et al. 2002, Leth et al. 2018)
Faecalibacterium prausnitzii	A2-165	pectin, inulin, fructose, glucose	B, A, H_2, L	(Duncan et al. 2002, Lopez-Siles et al. 2012)
Subdoligranulum variabile	DSM 15176	N-acetyl-glucosamine, N-acetyl-mannosamine, cellobiose, dextrin, fructose, fucose, galactose, galacturonic acid, α-glucose, α-lactose, maltose, maltotriose, Mannose, melibiose, rhamnose, salicin, sucrose	B, L, A, S	(Holmstrom et al. 2004)

Table 1: *(Continued)*

Species	Strain used/source	Known substrates	Metabolite production*	References
Ruminococcus bromii	ATCC 27255	starch, glucose, fructose, galactose	A, F, P, L, E	(Crost et al. 2018, Ze et al. 2012)
Blautia obeum	DSM 25238	arabinose, cellobiose, lactose, mannose, maltose, raffinose, xylose, L-fucose	A, 1,2-PD, P	(Bui et al. 2019, Liu et al. 2008)
Collinsella aerofaciens	DSM 3979	starch, maltose, glucose, sucrose	E, H_2, A, L; F	(Kageyama et al. 1999)
Bifidoabcterium adolescentis	L2-32	inulin, starch, lactose, glucose, xylose, sorbitol, cellobiose, maltose	F, A, L	(Riviere et al. 2015, Falony et al. 2009, Ramirez-Farias et al. 2009)
Blautia hydrogenotrophica	DSM 10507	cellobiose, lactose, mannose, raffinose, glucose, H_2/CO_2, H_2/formate	A, L	(Liu et al. 2008, Bernalier et al. 1996)
**SCFA production varies depending on growth substrates*				

Assembly, co-existence and ecological properties of MDb-MM

We assembled a MDb-MM consisting of 15 strains representing the core microbiota under batch conditions with both mucin and DoS (Supplementary table S1 & Supplementary Fig. S2). At 24 h, continuous feed was introduced with mucin and acetate (since some of the strains require it for growth), while DoS were introduced as pulsed feeding thrice daily for the majority of the time points. The species abundance in the MDb-MM was tracked by sequencing of 16S rRNA gene amplicons, and total copies of 16S rRNA genes of the community were quantified using qPCR at 61 time points (Supplementary Fig. S2). The initial 15 species were detected in the three bioreactors for the entire 20-day operation (**Fig. 2A**).

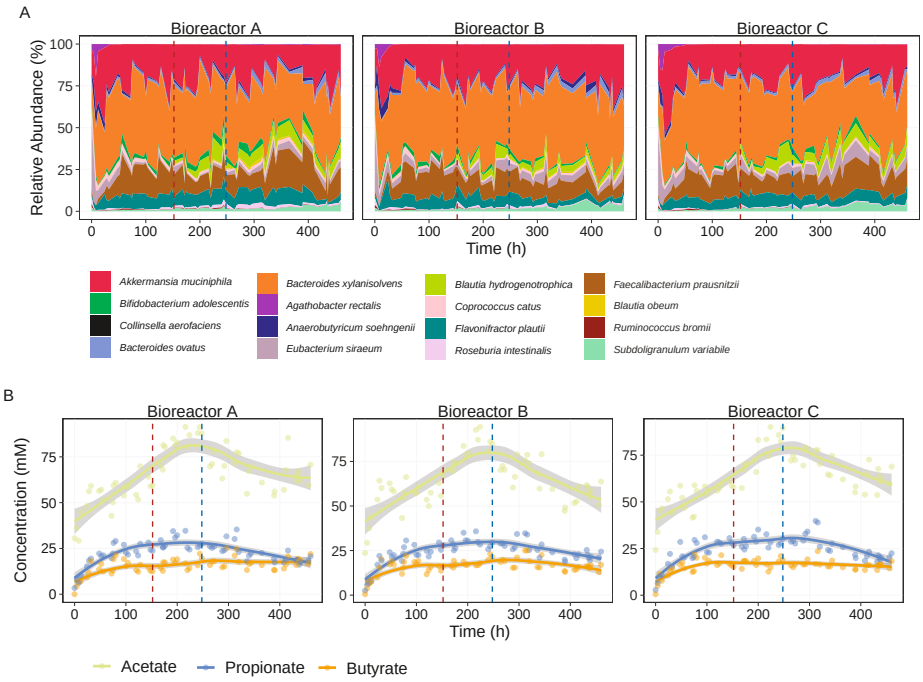

Figure 2: Global response of the MDb-MM. A) Temporal compositional dynamics of the MDb-MM. B) Concentration of major SCFAs, acetate, butyrate, propionate produced by MDb-MM in the three bioreactors. The vertical dotted lines, red indicates introduction of *B. hydrogenotrophica* (152 h) and blue indicates removal of acetate/feed change (248h). The curved line represents the locally weighted smoothing (LOESS) for each of the bioreactors and the grey shaded region around these lines shows 95% confidence intervals for the fit. This was calculated and visualized with the default geom_smooth function in ggplot2 R package.

To test vacant niche occupation, the 16th species, *B. hydrogenotrophica* was added at 152 h. At 264 h, the abundance of *B. hydrogenotrophica* was below the amplicon sequencing detection limit. The DoS pulse events resulted in a significant increase in total biomass (optical density; $O.D_{600}$) but this was not captured with total 16S rRNA gene qPCR (Supplementary Fig. S3). No differences in community evenness and number of species contributing to 90% of the total community abundances were detected after DoS pulse events (Supplementary Fig. S4). A steady increase in butyrate, acetate and propionate concentration was observed until the point of removal of acetate from fresh growth media (**Fig. 2**B). Lactate, succinate, and formate were detected in relatively low concentrations (Supplementary Fig. S5). Formate concentration declined after the removal of exogenous acetate from feed. After 300 h, lactate was not detected in the three bioreactors.

In the first 148 h, before the introduction of disturbances, only propionate was produced in significantly higher concentrations in overnight samples (Wilcoxon test, $p<0.001$, Supplementary Fig. S6A). The propionate concentration was also significantly higher after addition of *B. hydrogenotrophica* (Wilcoxon test, $p<0.001$, Supplementary Fig. S6B). However, after the influx of exogenous acetate was stopped, the concentrations of acetate and butyrate were significantly lower in overnight samples (Wilcoxon test, $p<0.0001$) compared to DoS samples, while propionate production was not significantly affected (Supplementary Fig. S6B). These results demonstrate that the successful assembly of the MDb-MM was achieved in the three bioreactors with presence of the 16 species. The major fermentation end products of MDb-MM were acetate, propionate and butyrate for a period of 460 hours. Overall, based on optical densities and metabolite profiles, the MDb-MM was observed to be responsive to DoS pulse feeding as noticed by increase in total biomass (optical density; $O.D_{600}$), and *B. hydrogenotrophica* was able to stably colonize the MDb-MM when introduced into the community after 152 hours.

Temporal dynamics of MDb-MM community

The MDb-MM showed changes in community structure over time with similar compositions between triplicate bioreactors (**Fig. 3**A). Recent studies on longitudinal human microbiome data have revealed a linear relationship between log(variance) and log(mean), i.e., species with higher mean abundances tend to also exhibit higher variance in population densities (Marti et al. 2017, Vandeputte et al. 2021, Ji et al. 2020). This property is known as the Taylor's power law (Taylor and Woiwod 1980). We evaluated whether the MDb-MM assembled in the three bioreactors showed similar time-dependent behavior observed in human gut microbiome (Taylor and Woiwod 1980, Taylor 1961). The MDb-MM in the three bioreactors exhibited a linear relationship between log variance and log mean abundance with a slope of 1.45, 1.37 and 1.36

for bioreactor A, B and C, respectively (**Fig. 3**B, C and D). In all three bioreactors, the two most abundant species *Bacteroides xylanisolvens* and *Akkermansia muciniphila* exhibited highest variance while *C. aerofaciens* had lowest variance and was least abundant.

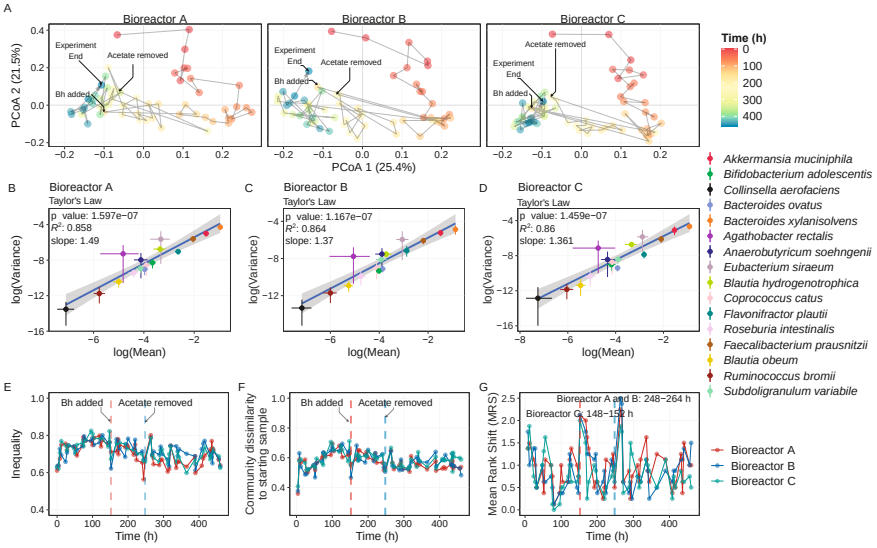

Figure 3: Community level patterns in MDb-MM. A) Principal coordinates analysis plot depicting succession of the MDb-MM community over time, community similarity was calculated using Canberra distance. The numbers at each point indicate the time in days of the fermentation experiment. B, C and D) Power law relationship between variance and mean abundances. The linear regression line is blue and the shaded region represents the confidence interval (geom_smooth function, method=lm). The bars around points represent the lower and upper confidence interval for mean and variance for each of the taxa. E) Temporal changes in inequality (Gini coefficient) in the community in the three bioreactors. F) Community divergence based on Canberra distances. G) Mean rank shift of the MDb-MM in the three bioreactors calculated using the codyn R package.

Evenness of species abundances can influence functional stability of microbial communities (Wittebolle et al. 2009). We used the Gini coefficient as a measure of evenness, which has values between 0 to 1. Here, 1 indicates a highly uneven community composition (Handcock and Morris 2006). The mean Gini coefficient for the starting MDb-MM at 0 h was 0.62 (±0.01). At the end of the experiment at 460 h, the Gini coefficient for MDb-MM was 0.6, 0.63, 0.62 for bioreactor A, B and C respectively. The

overall mean (± standard deviation) for inequality in MDb-MM was 0.70 ± 0.05, 0.71 ± 0.04 and 0.71 ± 0.05 for bioreactor A, B and C respectively during the entire experiment.

The long-term divergence of the MDb-MM in all the three bioreactors followed similar trends over time (**Fig. 3**F). The MDb-MM showed higher deviation from the starting composition during the first phase of the experiment before feed change followed by relatively stable dissimilarities after feed change. Convergence of the three MDb-MM showed similar patterns (Supplementary Fig. S7A). The correlation between community distances and lagged time intervals further supported directional change which was similar in the three bioreactors (Supplementary Fig. S7B). Next, we carried out mean rank shift analysis to identify events when drastic changes occurred in the species ranks (order of relative abundance) within the community. During the initial phase (up to ~100 h) there was a progressive decline in mean rank shift (MRS), but introduction of *B. hydrogenotrophica* caused large fluctuations as did the change of feed with removal of acetate in all three bioreactors (**Fig. 3**G). The compositional dynamics was highly similar between the three bioreactors (Pearson's correlation; A and B, r= 0.93; A and C, r= 0.92; and B and C, r=0.95). These data support highly coherent community level features of the MDb-MM between the three bioreactors.

Temporal stability properties of MDb-MM

The observations thus far indicated that the MDb-MM was responsive to the pulse feeding events and perturbation events i.e., addition of *B. hydrogenotrophica* and removal acetate. However, it was unclear if the MDb-MM possesses ecological stability i.e., does the MDb-MM exhibit resistance and resilience to perturbations. To investigate this, we tested the following stability properties of MDb-MM in the three bioreactors (Liu et al. 2018): a) resistance (RS) as the ability of MDb-MM to resist change after perturbations; b) displacement speed (DS) as the pace at which MDb-MM is displaced upon perturbations; c) resilience (RL) as the ability of MDb-MM to return to the reference state after a perturbation event, d) elasticity (E) as the pace at which MDb-MM recovers after displacement due to a perturbation event. The MDb-MM in all three bioreactors exhibited resistance to the change of feed that no longer contained acetate, as for the majority of the time it was observed within the reference state boundary (**Fig. 4**A and B). In instances where it crossed the reference state boundary, the MDb-MM in all three bioreactors returned to the reference state community (**Fig. 4**A).

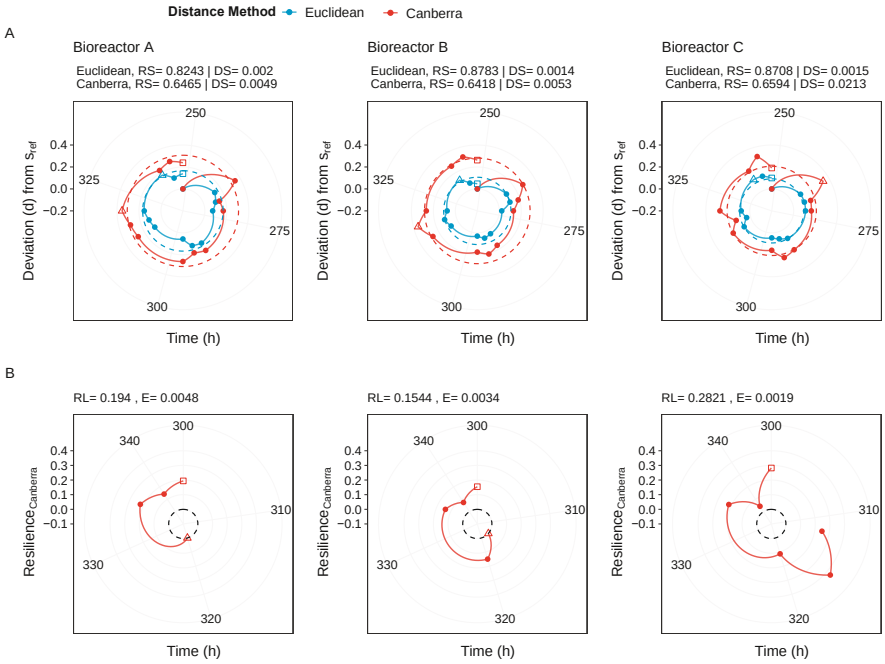

Figure 4: Stability properties of MDb-MM. A) Community changes from reference phase calculated using Canberra and Euclidean distance. The boundary of reference phase was calculated using the method described by Liu et al., 2018 (Liu et al. 2018) . The shaded region and brown dashed line depict reference phase boundary based on Canberra distance, while the blue dashed line depicts reference boundary based on Euclidean distance. The hollow triangles represent time points when maximal deviation from reference state was observed. B) Resilience of the MDb-MM after removal of Acetate. The black dashed line depicts reference boundary based on Canberra distance. The stability was calculated with 152 h (introduction of *B. hydrogenotrophica*) as the starting time, removal of acetate/feed change (248h) as the disturbance event and experiment end point was before elongated fasting was initiated in the three systems (344 h). Abbreviations: RS, resistance; DS, displacement speed; RL, resilience and DS, displacement speed.

Among the three bioreactors, MDb-MM in C had highest displacement (DS=0.021) compared to A (DS=0.004) and B (DS=0.005), that is deviation from the reference boundary. MDb-MM in bioreactor C also showed highest resilience (RL=0.282) compared to A (RL=0.194) and B (RL=0.154). The larger displacement and resilience values for MDb-MM in bioreactor C suggests the high resilience of MDb-MM and its ability to return to its reference state even after showing the highest deviation in composition (Liu et al. 2018). Similar patterns were observed when subsequent perturbation events of elongated fasting and increasing substrate feeding rate from

10 ml/h to 20 ml/h were included in the stability analysis (Supplementary Fig. S8 A and B). However, the recovery to the reference community state after doubling the substrate feeding rate was on/near the boundary (dashed line, Supplementary Fig. S8 A and B) of the reference community state at the end of the experiment.

Community level transcriptional activity

For a subset of the time points, we performed metatranscriptome sequencing. We analyzed the transcriptional response at two levels, KEGG orthologs (KOs) as well as gut metabolic modules (GMMs), the latter of which take into account the combination of KOs that are part of specific metabolic modules relevant to the human gut microbiome (Vieira-Silva et al. 2016). The community level functional divergence using relative abundances of taxa, GMMs and KOs showed similar divergence over time and was linked to changes in the community structure over time (**Fig. 5**A, Supplementary Fig. S9). Temporal variation in MDb-MM community composition correlated significantly with transcriptional response at both GMM ($Mantel_{Amplicon\ vs\ GMM}$ $r = 0.40$, $p = 0.001$) and KO level ($Mantel_{Amplicon\ vs\ KEGG}$ $r = 0.35$, $p = 0.001$) (**Fig. 5**A, B and C). The KEGG and GMM profiles showed good agreement in capturing the temporal variation in MDb-MM gene expression ($Mantel_{KEGG\ vs\ GMM}$ $r = 0.87$, $p = 0.001$). Next, to identify community-level transcriptional response to nutrient periodicity, we compared GMM expression at specific time points (**Fig. 5**D-F). GMMs linked to carbohydrate degradation were upregulated in the DoS, while mucin and amino acid degradation were upregulated in overnight samples (**Fig. 5** D, E and F). The butyrate production related module "Acetyl-CoA pathway" was significantly upregulated in the DoS samples (52 h and 248 h) in absence of *B. hydrogenotrophica* when exogenous acetate was provided, and after removal of acetate (248 h and 264 h) (**Fig. 5**D, E and F). In accordance with HPLC data, we observed significantly higher amounts of transcripts encoding enzymes involved in propionate production in overnight samples (48 h) before addition of *B. hydrogenotrophica* (**Fig. 5**A). After removal of exogenous acetate, there was a significant upregulation of the GMM for formate conversion and homoacetogenesis (264 h), which coincided with an increase in formate concentration observed in metabolite analysis (**Fig. 5**F and Supplementary Fig. S5).

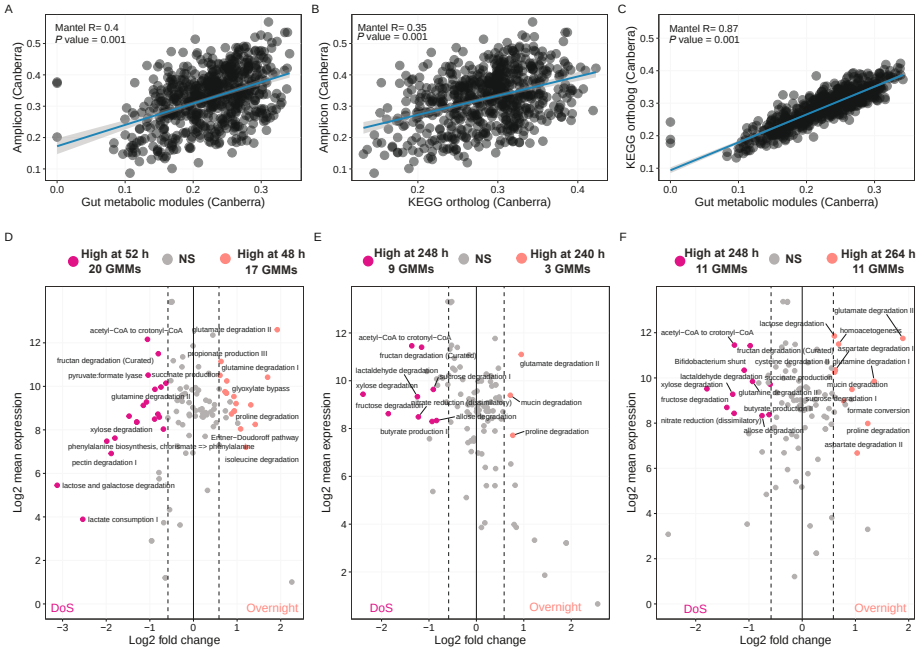

Figure 5: Correlation between compositional and functional succession and transcriptomics response of MDb-MM. Mantel test for correlation between compositional functional community similarity based on Canberra distance. A) Comparison of community similarity based on 16S rRNA gene relative abundance versus gut metabolic module relative abundances. B) Comparison of community similarity based on 16S rRNA gene relative abundance versus KEGG ortholog relative abundances. Each circle in these scatter plots represent pair-wise Canberra distances between samples. C) Comparison of gut metabolic module relative abundance versus KEGG ortholog relative abundances. D-E-F) Differential expression of GMMs in DoS and overnight samples. Before the addition of *B. hydrogenotrophica* with exogenous acetate (48 h vs 52 h). With *B. hydrogenotrophica* and exogenous acetate (240 h vs 248 h). With *B. hydrogenotrophica* and without exogenous acetate (248 h vs 264 h). Modules with adjusted *p* value >= 0.01 and with fold change of absolute value >= 1.5 are labelled.

Dynamic niche overlap among MDb-MM species

In order to better understand the co-existence of 16 species in the three bioreactors we investigated species specific metabolic traits. By design, the MDb-MM had multiple species capable of carrying out similar functions - for example, *B. ovatus*, *R. bromii*, *E. siraeum* and *A. rectalis* can degrade starch (**Table 1**). Moreover, none of the MDb-MM species were competitively excluded from the system suggesting potential niche partitioning because multiple substrates were available in our system. Therefore, we quantified niche overlap between species in MDb-MM and investigated if there is temporal changes in pair-wise species behaviors. We started by calculating the

pairwise niche overlap between each of the species at each of the time points for which we had obtained metatranscriptomes. Metabolic module expression was used as quantitative traits for calculating the niche overlap indices. We used only those GMM traits which are involved in either degradation or consumption of substrates and end-product metabolites (Supplementary **Table S2**). In this case, a lower niche overlap between species would suggest higher niche segregation and *vice versa*.

All species demonstrated temporal variation in niche overlap with other species in MDb-MM, highlighting the dynamic nature of inter-species interactions in the MDb-MM (**Fig. 6**). Comparison of pairwise distributions of niche overlap values revealed that the complex substrate degraders, *B. xylanisolvens*, *A. muciniphila*, *A. rectalis*, *B. adolescentis*, *S. variabile*, *F. prausnitzii* and *R. bromii* showed comparatively higher niche overlap (>0.75) with each other (Supplementary Fig. S10). *C. catus*, *A. soehngenii* and *E. siraeum* often had the lowest niche overlap with the other strains in the community. For some of the time points, *A. rectalis* had low number of transcripts for several of the GMM traits and we were unable to measure pair-wise niche overlaps. We then compared the overall expression of GMM traits for all species at different time points and observed niche segregation based on transcriptional responses of metabolic pathways consistently in the three bioreactors (**Fig. 7**A). The two *Bacteroides* species exhibited low niche segregation and *C. aerofaciens* and the two *Blautia* species were closely located on the two-dimensional ordination plot. *C. catus*, *A. soehngenii* and *F. plautii* had distinct transcriptional patterns. These data suggest that the observed co-existence likely resulted from each species occupying a specific metabolic niche and that inter-species cross-feeding supported non-complex substrate degraders forming a trophic interaction network.

Trophic guilds and niches of MDb-MM species

The metabolic flow and biomass distribution within the gut is largely driven by bacteria with specialized molecular machineries capable of degrading complex carbon sources (Wang et al. 2019). The action of polysaccharide degraders (primary consumers) results in niche construction that may be dependent on the source substrate as well as their metabolic pathways. Consequently, this leads to formation of a hierarchal organization within the community into trophic levels (Wang et al. 2019). Here, based on metatranscriptomic species-level assignment of transcriptional expression of GMMs, we broadly classified them into four trophic guilds similar to those reported previously from computational simulations (Wang et al. 2019) (see **Fig. 7**B and methods). Transcriptional contribution of species to each of the trophic guilds revealed the inter-species connectedness of resource utilization.

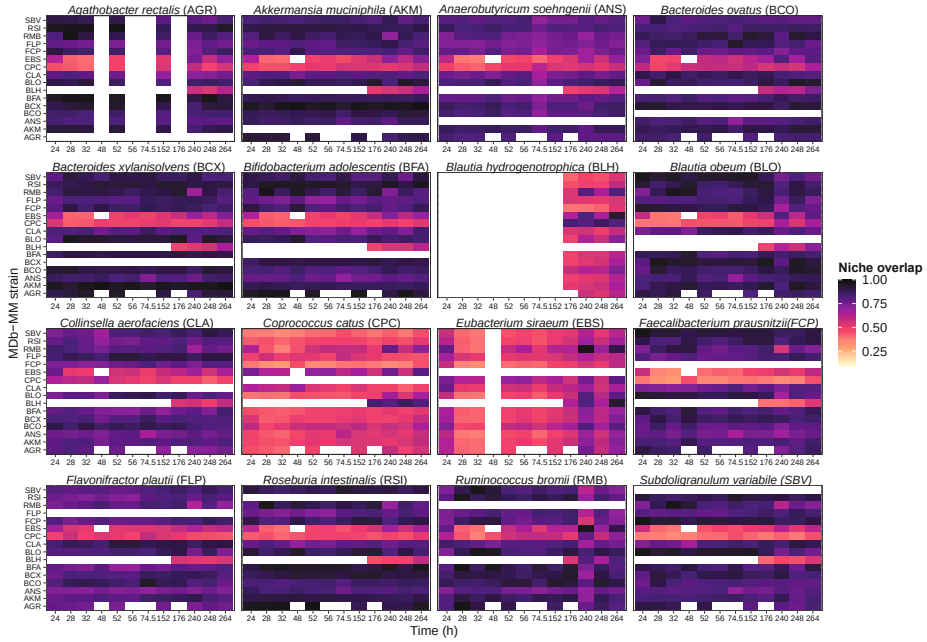

Figure 6: Temporal niche overlap of individual species in MDb-MM. The pair-wise niche overlap for each species is plotted as a heatmap with darker color intensity indicate high niche overlap. The abbreviations for species name used on the y-axis are given in brackets of panel headings. The missing values are represented by white color. These are time points when one of the species from the pair had less than 50 counts for GMM traits and hence niche overlap could not be calculated. These are prominent for *A. rectalis and B. hydrogenotrophica. A. rectalis* had one of the lowest 16S rRNA abundances at the initial time points of continuous operation of the bioreactors. *B. hydrogenotrophica* was added at 152 h but RNAseq sample was taken before its addition to the system.

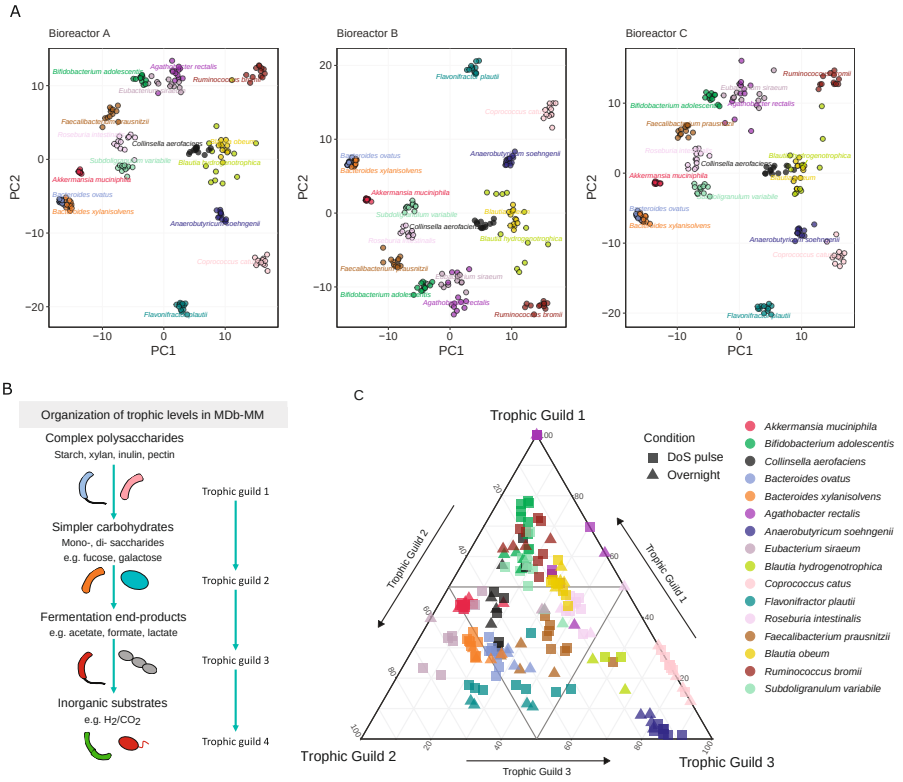

Figure 7: Transcriptional niche segregation and trophic guilds within the MDb-MM. A) A Principal Component Analysis (PCA) based on GMM trait expression used in trophic guild analysis. The abundances were Hellinger transformed before calculating the Canberra distances. Multiple circles for each species are different time points. The species labels are positioned around the centroids for that particular species. B) Schematic for organization of metabolic roles into trophic guilds. Trophic guild 1 is for polysaccharide and mucin degradation, trophic guild 2 consists of mono-di-saccharides trophic guild 3 consists of consumption of fermentation ends/by-products and trophic guild 4 consists of those consuming inorganic substrates for growth. C) Ternary plot indicates the trophic status of the minimal microbiome strains at different time points. For every strain at a given time point, we summed its expression and calculated the relative expression for each trophic guild. The proximity of the symbols to the apex of the triangle is proportional to the averaged potential contribution of each strain to trophic guilds. The trophic guild 4 is not shown in this figure. The ranking of species within each trophic guild is provided in Supplementary Fig. S11.

Ranking of MDb-MM strains based on the relative proportions of their GMM expression within each trophic guild revealed temporally changing trophic roles (Supplementary **Fig. 11**). This suggested that trophic roles are dynamic in MDb-MM. In addition, these observations also suggested that transcriptional expression of individual species for each of the trophic level can be variable. Furthermore, to investigate whether the trophic role is associated with abundance of species in the community we compared the relative abundance of species and its ranking within a trophic guild. We observed that bacteria that are dominant in trophic guild 1 had higher abundances while those dominating trophic guilds 3 or 4 had lower relative abundances in the MDb-MM (Supplementary **Fig. 12**). This suggests that the species dominating trophic guild 1 are usually present in higher abundances in microbiomes.

The two most abundant species in MDb-MM (**Fig. 1**D, 5A), *A. muciniphila* and *B. xylanisolvens,* contributed to two trophic guilds: degradation of complex substrates i.e., trophic guild 1 and degradation of simpler carbohydrates i.e., trophic guild 2 (**Fig. 7**). Known starch degraders, *R. bromii*, *B. ovatus*, *C. aerofaciens*, *E. siraeum* and *A. rectalis* showed transcriptional segregation across the trophic guild 1 and 2 axis. *S. variabile*, *B. adolescentis* and *R. bromii* dominated trophic guild 1 and showed metabolic activity for arabinoxylan, fructan and starch degradation, respectively (Supplementary Fig. S13).

The action of species occupying trophic guild 1 can give rise to extracellular mono- and di-saccharides that can be utilized by species that lack specialized molecular machineries for polysaccharide degradation. In our system, breakdown of mucin, pectin, inulin, starch and xylan could result in simple mono- and di-saccharides such as fucose, galactose, galacturonate, fructose, maltose or xylose as major simple carbohydrates. Within trophic guild 2, fucose transport and degradation genes were identified to be transcribed in *A. muciniphila* and *B. obeum* (Supplementary Fig. S14). In addition, transcription of galactose metabolism genes was predominantly detected in *A. muciniphila*, *B. ovatus* and *B. xylanisolvens*. Galacturonate is the main component in pectin, and *F. prausnitzii* and to some extent *B. ovatus* and *B. xylanisolvens* were found to express genes involved in its degradation (Supplementary Fig. S14).

We classified consumption of fermentation end products such as acetate, lactate, 1,2-PD and formate as trophic guild 3. These are mostly major end products of carbohydrate fermentation, while utilization of H_2 and CO_2, inorganic by-products of acidogenesis, are classified here as trophic guild 4. Specialist trophic guilds could be assigned to *A. soehngenii*, *B. hydrogenotrophica* and *C. catus* as their transcriptional activity was largely contributing to trophic guild 3 (**Fig. 7** and Supplementary Fig. S15). *F. plautii* showed variation across trophic guild 2 and 3. In our experimental setup, acetate was

exogenously supplied until 248 h to the MDb-MM and then removed from the feed. Expression of modules for acetate to acetyl Co-A via I and II (acetate kinase pTKA) was observed in *A. soehngenii*, *F. prausnitzii*, *B. obeum*, *B. hydrogenotrophica* and *F. plautii* (Supplementary Fig. S15). *A. soehngenii* and *F. prausnitzii* are known to have improved growth in the presence of acetate, which would explain the activity for consuming acetate (Duncan et al. 2002, Duncan et al. 2004). Cross-feeding of lactate resulting from the metabolism of polysaccharide degraders such as *Bifidobacterium* and *Lactobacillus* by butyrate producers in the human gut is well known (Duncan et al. 2004, Louis and Flint 2017). Here, we detected very low amounts of lactate in the metabolite analysis which resembles the situation in fecal samples where lactate is hardly detected (Duncan et al. 2004). This can be explained by the significant transcriptional activity for lactate consumption primarily *via* the *lctABCDE* pathway (Supplementary Fig. S14). *A. soehngenii* showed high transcriptional activity for utilization of lactate plus acetate, which further confirms our previous observation of this being a specialized niche for this organism (Shetty et al. 2022, Shetty et al. 2020). *C. catus* demonstrated activity for lactate consumption but is known only to consume the L-form of lactate, while *A. soehngenii* can use both the D- and L-forms of lactate (Sheridan et al. 2021). Fucose fermentation results in production of 1,2-PD, which is another well-known cross-feeding metabolite (Engels et al. 2016, Louis and Flint 2017). While we did not detect any 1,2-PD, there was higher transcriptional activity for utilization of 1,2-PD in *A. soehngenii* compared to *B. obeum,* which also produces propionate (Supplementary Fig. S10) (El Hage et al. 2019, Reichardt et al. 2014). Transcriptional activity for autotrophic growth on H_2 and CO_2 using formate dehydrogenase and formate-tetrahydrofolate ligase was observed in *B. hydrogenotrophica*. Other than CO_2 and H_2, we observed active processes for dissimilatory nitrate and sulphate metabolism within guild 4. Among the two *Bacteroides* species, *B. xylanisolvens* was the dominant species in the MDb-MM and had higher contribution to trophic guild 4, which was observed to be linked to higher expression of the nitrate reduction module. Dissimilatory nitrate reduction to ammonium may be an advantageous strategy for higher growth rate in competitive ecosystems. In summary, the 16 species in the MDb-MM co-existed by occupying and interacting at different trophic levels to form a complex web of inter-species interactions.

Discussion

Due to technological and practical limitations, deciphering the community dynamics and microbe-microbe interactions is challenging using fecal or other intestinal samples derived from human. Here, we investigated microbe-microbe and microbe-environment interactions at species and community level within a highly controlled

setting, using a defined microbiome that we subjected to detailed compositional, transcriptional and metabolic analysis. The three most important aspects of this study are (i) assembly of a human minimal microbiome that exhibits ecologically relevant interactions, (ii) the experimental set-up which included nutrient periodicity and (iii) a set of specific biotic and abiotic perturbations that allowed to address the resilience of the system. All of these aspects are crucial for better understanding the interactions dynamics within human intestinal microbial communities (De Roy et al. 2014, Shetty et al. 2019). Our rational selection was largely driven by understanding of the anaerobic physiology of key human gut microbes. Knowledge of microbial physiology was complemented by considering ecological aspects at the community level such as assembly, co-existence, competition for resources and cross-feeding. This enabled us to first demonstrate the applicability of ecological concepts, e.g., Taylor's law, community turnover, divergence, resistance and resilience, and then to investigate the species level metabolic interactions using metatranscriptomics (Costello et al. 2012, Venturelli et al. 2018, Billick and Case 1994, Chung et al. 2018, Kilpatrick and Ives 2003, Plichta et al. 2016, Relman 2012). The MDb-MM exhibited significant correlation with respect to dynamics of composition, metabolic output and transcriptional response in replicate bioreactors. This supported previous observations in synthetic microbiomes that a common pool of species shows similar/reproducible assembly and community level dynamics under similar growth condition and exposure to similar perturbation events (Krause et al. 2020, Oliphant et al. 2019, Weiss et al. 2021). This is equivalent to the classical enrichment experiments where the emergent community assembly can be driven by selecting for specific bacteria or consortia with specific substrates and/or environmental factors such as high salt, pH or temperature (Overmann 2006). Future research is warranted to test whether a different combination of species than the one used here, would result in similar community level behaviors under identical perturbations (Symons and Arnott 2014, Oliphant et al. 2019). Additionally, modelling of synthetic microbiota based on complementary wet lab experiments can further increase our understanding of interactions and dependencies in the gut (Krause et al. 2020, Schape et al. 2019, Bauer et al. 2017). Nonetheless, we demonstrated how ecophysiology guided design of synthetic minimal microbiomes combined with metatranscriptomics is a promising avenue to investigate core concepts in ecology and unravel potential metabolic interactions.

At individual taxa level, we observed highly variable compositional and functional responses. This could be attributed to potential technical variation in measurements and/or deterministic chaos (Silverman et al. 2018, Karkaria 2021). At community level the behavior can be rather deterministic as observed with similar divergence, mean rank shift and inequality in triplicate MDb-MMs when subjected to similar external perturbations (Oliphant et al. 2019, de Cárcer 2019, Vellend 2010). It is,

however, important to note that our system was highly controlled with only one event of immigration (addition of *B. hydrogenotrophica*) and stochastic processes such as dispersal limitation not being enforced in our experimental setup (Zhou and Ning 2017). Nevertheless, our observation of deterministic assembly of MDb-MM has some implications for designing microbiome modulation strategies, where achieving community level stability in both composition and function may be crucial. Examples are resistance to invasion or enhanced butyrate production, which can be achieved by targeting ecosystem level properties using appropriate prebiotics (Shetty et al. 2017, Chung et al. 2016, Gibson 1999). These prebiotics may not necessarily target a specific species but a group of species whose fundamental niche allows for "insurance" to absorb the impact of daily stochastic and destabilizing forces (Relman 2012, Yachi and Loreau 1999).

The investigation of species-specific transcriptional responses revealed that the core gut microbes used in this study have highly evolved metabolic strategies which could explain their co-existence with other seemingly competitive core species. The co-existence is likely due to the ability of these core gut microbes to dynamically regulate the transcriptional response for utilizing specific carbon and energy sources that are vacant (Pereira and Berry 2017, Plichta et al. 2016). This allows individual species to occupy the niches that become available over time either, due to external (inflow of diet) or changing metabolic behavior of competitor species. For instance, we observed, at transcriptional level, changing patterns of polysaccharide utilization among the species that are part of the first trophic guild where no single species dominated transcriptional contributions for the entire duration of the experiment. These observations provide support for the role of "functional insurance" as result of the presence of competitive species in maintaining community composition, structure and functional stability.

Another aspect of host-associated microbial communities is the immigration of new species which can have an impact on the overall community (Schmidt et al. 2019, Milani et al. 2019). By introducing *B. hydrogenotrophica* in the established minimal microbiome, we demonstrated a widely appreciated role of vacant niches in supporting survival of immigrating species (Pereira and Berry 2017, Kearney et al. 2018). Despite its fundamental niche being diverse including the ability to utilize several simple carbohydrates that were available, *B. hydrogenotrophica* likely utilized H_2/CO_2 and/or formate as observed with active expression of the formate conversion module (Liu et al. 2008). When we removed exogenous acetate, butyrate production declined, and this can be attributed to the fact that acetate is one of the key metabolites for its production. Importantly, after removal of exogenous acetate, *B. hydrogenotrophica* showed high expression of modules linked to homoacetogenesis thus highlighting

its contribution to acetate production. This could have aided in stabilizing the community because butyrogenic species such as *A. soehngenii*, *F. prausnitzii* and *R. intestinalis* require acetate for improved growth. This highlights the potential for cyclic interactions where end-products of lower trophic guilds can help species occupying higher trophic guilds. Overall, these data provide support for a specialized niche of *B. hydrogenotrophica* that includes inorganic substrates and/or formate (D'Hoe et al. 2018, Bui et al. 2019, Plichta et al. 2016). *B. hydrogenotrophica* can be considered a key species, which can potentially support production of butyrate. For instance, enhancing butyrate production *via* prebiotics can lead to significant amounts of gases and therefore recycling these into acetate by autotrophic acetogens such as *B. hydrogenotrophica* can further support butyrate production in a trophic network with butyrate producers (Duncan et al. 2004).

The flow of energy in biological ecosystems is widely described via trophic structures where energy flows from one level to another (Wang et al. 2019, Rigler 1975). The so-called keystone species are usually defined for taxa at higher trophic levels (Ze et al. 2012, Trosvik and Muinck 2015). Our analysis highlights the difficulties in assigning strict hierarchy based on single and specific trophic roles for individual taxa, especially because the breakdown of complex substrates results in simpler substrates, which the primary degrader can also utilize. Furthermore, the temporal differences we observed in dominance of each bacterium within the trophic guilds indicates that functional roles of bacteria can vary over time within a community. We observed certain taxa with a prominent role within specific trophic guilds. For instance, *A. soehngenii* and *C. catus* were predominantly part of the trophic guild level 3 which involves consuming fermentation end-products, lactate and 1,2-PD. This observation further supports our previous findings that *A. soehngenii* occupies an energetically challenging niche, i.e. the consumption of lactate and acetate (Shetty et al. 2022). In contrast, *B. hydrogenotrophica* occupied the lowest trophic guild consuming inorganic substrates. Thus, MDb-MM allowed us to unravel functional roles of each of the key gut species in presence of other core microbiota. In addition, we were able to identify potential metabolic interactions and cross-feeding occurring within the MDb-MM by investigating trophic guilds associations based on species specific transcriptional profiles for GMMs related to degradation of complex substrates, production and consumption of fermentation products like formate and lactate.

Our experimental system did not take the host-aspect into account, which will influence the community composition and dynamics (Foster et al. 2017). Hence, improvements can be envisaged by incorporating the MDb-MM in an *in vitro* model such as HUMix and organoid cell cultures (Venema and van den Abbeele 2013, Shah et al. 2016, Lukovac et al. 2014), that comprise host features such as aspects of the

immune system. The ability to track abundances of closely related species across time points in synthetic communities is crucial. Here, we used short amplicons of the V5-V6 (~280 bp) region of the 16S rRNA gene and noticed non-specific amplification of *B. hydrogenotrophica* at few time points prior to its addition. In such scenarios, using whole shotgun metagenomics might provide better resolution. One of the major challenges we faced during this study was the difficulty in predicting the metabolic functions based simply on automated annotation and analysis. For instance, the identification of an amylase gene (K01176, alpha-amylase [EC:3.2.1.1]) with high expression in *A. muciniphila* suggested its contribution to starch degradation. This gene is likely coding for a glycoside hydrolase involved in breaking glycosidic linkages present in mucin and is not involved in starch degradation. These observations highlight the need for careful curation and interpretation of -omics based functional analysis of fecal samples where the majority of the species remain uncharacterized. With some manual curation of the published GMMs, we were able to capture >87% of the variation between samples that were identified at KO level annotation. This suggests that it is also valuable to investigate other key functions such as those involved in signaling and processing, virulence, vitamin and co-factor biosynthesis and their role in the species dynamics we observed in this study. We did not include bile salts in our media, and several key vitamins and co-factors such as vitamin B_{12} were provided exogenously. Therefore, impact of these key compounds on the community remains unknown. In addition, a bioreactor with similar setup but with constant supply of DoS could help in identifying if the pulse feeding played a role in co-existence of all species till the end of the experiment.

In this study, we created a minimal microbiome that exhibits ecological stability properties and intricate metabolic interactions that are observed in more diverse and complex natural ecosystems. We provide experimental evidence for temporally variable niche occupation as one of the important mechanisms by which species competing for similar resources can co-exist in a dynamic ecosystem. In addition, we demonstrate how metatranscriptomics can be used to assign quantitative traits for identifying niche overlap at transcriptional level. We foresee the use of data generated in this study to serve as a useful resource for ecologists, systems biologists and microbiome experts for developing predictive ecological and metabolic models and improving our understanding of the human gut microbiome.

Acknowledgements

We thank Prof. dr. AJ Stams and Dr. Nam Bui for useful discussions. We thank Steven Aalvink and Ineke Heikamp de Jong for technical support. We also thank Prokopis

Konstanti for his assistance and support on library preparation prior to 16S rRNA gene sequencing.

Materials and Methods

Species selection for the composition of the synthetic MDb-MM

Taxonomic composition data from metagenomic studies was obtained from the curatedMetagenomicData data package (v1.18.2) (Pasolli et al. 2017). To identify the taxa that are part of the core microbiota we analyzed species level data from 1155 "Western healthy" human gut metagenomes covering general populations from North America and Europe. A total of 64 metagenomic species, which were present in at least 50% of all samples were analyzed with a minimum relative abundance of 0.00001 (Wilke 2018).

Bacterial strains used in this study

The following strains were obtained from the German Collection of Microorganisms and Cell Cultures (DSMZ, Braunschweig, Germany) or the American Type Culture Collection (ATCC, Manassas, USA): *Agathobacter rectalis (DSM 17629), Eubacterium siraeum* (DSM 15702), *Roseburia intestinalis* (DSM 14610), *Subdoligranulum variabile* (DSM 15176), *Blautia obeum* (DSM 25238),*Blautia hydrogenotrophica* (DSM 10507), *Coprococcus catus* (ATCC 27761), *Ruminococcus bromii* (ATCC 27255) and *Collinsella aerofaciens* (DSM 3979/ATCC 25986). *Anaerobutyricum soehngenii* (DSM 17630, L2-7) was kindly provided by Prof. Harry J. Flint's group (University of Aberdeen, UK). The strains from the human microbiome project (HMP) catalogue were *Bacteroides* sp. 3_8_47FAA (*Bacteroides ovatus*), *Bacteroides* sp. 2_1_22 (*Bacteroides xylanisolvens*) and *Flavonifractor plautii* 7_1_58FAA. Furthermore, *Akkermansia muciniphila* (ATCC BAA-835), *Bifidobacterium adolescentis* (L2-32) and *Faecalibacterium prausnitzii* (A2-165) were taken from the culture collection of the Laboratory of Microbiology, Wageningen University & Research, The Netherlands.

Medium composition for MDb-MM strains

All strains were grown in a medium with the following composition: KH_2PO_4 *(0.408 g/L),* $Na_2HPO_4.2H_2O$ (0.534 g\L), NH_4Cl (0.3 g/L), NaCl (0.3 g/L), $MgCl_2*6H_2O$ (0.1 g/L), $NaHCO_3$ *(4 g/L), yeast extract (2 g/L), beef extract (2 g/L),* CH_3COONa (2.46 g/L), casitone (2 g/L), peptone (2 g/L), cysteine-HCl (0.5 g/L), carbohydrates (1.1 g/L), resazurin (0.5 mg/L), 1 mL trace elements in acid (50 mM HCl, 1mM H_3BO_3, 0.5 mM $MnCl_2*4H_2O$, 7.5 mM $FeCl_2*4H_2O$, 0.5 mM $CoCl_2$, 0.1 mM $NiCl_2$ and 0.5 mM $ZnCl_2$, 0.1 mM $CuCl_2*2H_2O$), 1 mL trace elements in alkaline (10 mM NaOH, 0.1 mM Na_2SeO_3, 0.1 mM Na_2WO_4 and 0.1 mM Na_2MoO_4), 1 mL hemin solution (50 mg hemin, 1 mL 1N NaOH, 99 mL dH_2O), 0.2

mL vitamin K1 solution (0.1 mL vitamin K1, 20 mL 95% EtOH). After autoclaving and before inoculation, 1% of vitamin solution was added (11 g/L $CaCl_2$, 20 mg biotin, 200 mg nicotinamide, 100 mg p-aminobenzoic acid, 200 mg thiamin (vitamin B_1), 100 mg panthothenic acid, 500 mg pyridoxamine, 100 mg cyanocobalamin (vitamin B_{12}) and 100 mg riboflavin). This basal medium composition was used for both pre-cultures and the bioreactors and the feed with differences in carbon source supplementation.

For pre-cultures, the bacteria were grown in serum bottles in anoxic conditions with 80/20 CO_2/N_2 as mixed gas using different combinations of carbon sources (Supplementary table S3). The pre-cultures were incubated non-shaking at 37°C for 24 h.

Anaerobic bioreactor operation

Fermentations were conducted in three parallel bioreactors (DasGip, Eppendorf, Germany) filled with 300 ml of the abovementioned growth medium at 37°C, at a stirring rate of 100 rpm. For the first 24 h, the bioreactors were operated in batch mode where the 300 mL growth medium was supplemented with 5 g/L mucin from porcine stomach type III (Sigma Aldrich) as well as Diet origin Substrates (DoS) which comprised of 1.11 g/L of each of xylan (beechwood, Apollo scientific, U.K.), soluble starch (from potato) (Sigma-Aldrich, USA), inulin (from chicory) (Sigma-Aldrich, USA) and pectin (from apple) (Sigma-Aldrich, USA) at the beginning of the fermentation. The carbon sources, except for mucin, were prepared as 60 g/L stock solutions. These stock solutions were prepared anoxically in serum bottles and autoclaved prior to adding the carbon sources to the bioreactors. The pH was controlled at 6.8.

The bioreactors were inoculated with a normalized O.D. of 1.0 of each one of the abovementioned species in order to have the same cells abundance at the beginning of the fermentation. A single inoculum mix was prepared from the same pre-cultures. The three bioreactors thus represent technical replicates for a single experiment. This was done to avoid potential technical errors in preparation of starting inoculum which may influence the behavior of species within the community resulting in inter-bioreactor differences. After allowing the species to grow for 24 h, continuous operation of the bioreactors was initiated. The flow rate of the feed was set to 10 mL/h with a medium retention time of 30 h. In our experiment we used a retention time of 30 h, which is within the range of gut transit times (Asnicar et al. 2021, Tottey et al. 2017, Roager et al. 2016).

In the first phase of continuous feed supply i.e., from 24 h up to 248 h, basal medium in the feed consisted of 5 g/L mucin and 30 mM of sodium acetate. During the continuous operation, the bioreactors were spiked three times a day with a 4 h gap with DoS

(xylan, soluble starch, inulin and pectin) with a final concentration of 1 g/L in each bioreactor. After the first 24 h, we initiated pulsed feeding of DoS and sampled for metabolite and 16S rRNA gene analysis as follows: The 24 h sample taken at ~ 9:00 h represented overnight sample and after sampling the bioreactors were pulsed with DoS and the community allowed to grow undisturbed until ~13:00 h. At this time, we collected samples for analysis and immediately following this a second DoS pulse was introduced. We then allowed the MDb-MM to grow until ~17:00 h at which point we sampled again. This represented the second DoS pulse sample of the day. This was followed by a third DoS pulse, the MDb-MM grew overnight, and the next day at 9:00 h we sampled to repeat the cycle of sample-pulse-grow-sample-pulse. At 248 h of bioreactor operation, we replenished the feed with freshly prepared anoxic growth medium but this time we removed sodium acetate and only 0.5% mucin was added.

During the fermentation period (two weeks) different perturbations were introduced in the system. These disturbances included the addition of *Blautia hydrogenotrophica*, the increase of the concentration of carbohydrates addition to 2.22 g/L, elongation of the fasting period from 16 to 21 h, increase of the substrate feeding rate to 20 ml/h. These events are depicted in Supplementary **Fig. 2**. Samples were taken during both the fasting and feeding period and at every perturbation point (Schematic overview **Fig. 1** and Supplementary **Fig. 2**). Samples for DNA and HPLC were stored at -20 °C. Samples for RNA were centrifuged at 4816 x g for 30 min at 4 °C. Then, 1 mL of RNAlater was added to the pellet, the pellets were snap-frozen in liquid nitrogen and stored at -80 °C.

High performance liquid chromatography (HPLC)

For fermentation product analysis, samples were obtained at different time points of the incubation period. Crotonate was used as the internal standard, and the external standards were lactate, formate, acetate, propionate, butyrate, isobutyrate, 1,2-PD, sialic acid and glucose. Standards were prepared in the following concentrations: 2.5 mM, 5 mM, 10 mM and 20 mM. Substrate conversion and product formation were measured with Shimadzu LC_2030C equipped with a refractive index detector and a Shodex SH1011 column. The oven temperature was set at 45 ˚C with a pump flow of 1.00 mL/min using 0.01N H_2SO_4 *as eluent. All samples and standards (10 µl injection volume) ran for 20 min.*

DNA isolation and library preparation

Genomic DNA was extracted using the FAST DNA Spin kit (MP Biomedicals, Fisher Scientific, The Netherlands) following the manufacturer's instructions. We included positive controls, a mock community DNA with known composition (Ramiro-Garcia et al. 2016) and reagent controls for DNA extraction and PCR. The concentration

of genomic DNA was measured fluorometrically using Qubit dsDNA BR assay (Invitrogen). The hypervariable region V5-V6 (~280 bp) of the 16S rRNA gene was amplified with Phusion Hot Start II DNA polymerase (2 U/µL) for 25 cycles using 0.05 µM of each primer (784F - 1064R) that both contained sample-specific barcodes at their 5'-end. The amplification program for PCR included an initial step of 98 °C for 30 s, then 25 cycles of at 98 °C for 10 s, followed by an annealing step at 42 °C for 10 s and elongation step at 72 °C for 10 s and a final extension at 72 °C for 7 min. PCR products were purified using MagBio beads according to the manufacturer's protocol. Purified products were quantified using Qubit dsDNA BR assay kit (Life Technologies, USA) and were pooled in equimolar amounts into one single library. After pooling, the mixed libraries were concentrated using MagBio beads to a concentration needed by the sequencing company. The samples were sequenced on a NovaSeq platform (Illumina) in 2x150 base paired-end mode at Novogene (U.K).

qPCR

The total abundance of all species in the synthetic community was determined by qPCR. The DNA concentrations were measured fluorometrically (Qubit dsDNA BR assay, Invitrogen) and adjusted to 1 ng/µL by diluting them in DNase/RNase free water and prior to use as the template in qPCR. Universal primers targeting the 16S rRNA gene of all the species (1369F 5'-CGG TGA ATA CGT TCY CGG-3' and 1492R 5'-GGWTACCTTGTTACGACTT-3'; 123 bp) were used for quantification. A standard curve targeting the 16S rRNA gene of *B. thetaiotaomicron was prepared with nine standard concentrations from* 10^0 *to* 10^8 *gene copies/µL. The qPCR was performed in triplicate with iQ SYBR green supermix (Bio-Rad, USA) in a total volume of 13 µL prepared with primers at 500 nM in 384-wells plates with the wells sealed with optical sealing tape. Amplification was performed with an iCycler (Bio-Rad): one cycle of 95* °C for 5 min; 40 cycles of 95 °C for 15 s, 60° *C for 20 s and 72* °C for 30 s each; one cycle of 95 °C for 1 min; and a stepwise increase of temperature from 60 °C to 95 °C (at 0.5 °C per 5 s) to obtain melt curve data. Data were analysed using CFX Manager 3.0 (Bio-Rad).

RNA isolation

The cells (10 mL) were centrifuged at 4816 x g for 15 min at 4 °C and the supernatant was discarded. Total RNA was isolated by combining enzymatic lysis, the Trizol reagent and the RNeasy mini kit (QIAGEN, Germany). A mixture of lysozyme (15 mg/mL), mutanolysin (10U/mL) and Proteinase K (100 µg/mL) in 1X TE buffer was added to the pellet normalizing to an OD600 of 2.0 per 100 µL of this mixture. The samples were mixed by vortexing and incubated at room temperature for 10 min. After 5 min of incubation, the samples were vortexed again. Four microliters of p-mercaptoethanol mixed with 400 µL RLT buffer was added to the sample.

Subsequently 1 mL of Trizol reagent was added to 100 µl of the sample. This mixture was transferred to a sterile tube containing 0.8 g of glass beads (diameter of 0.1 mm). The tubes were homogenized by bead beating three times for 1 min at 5.5 m/s, while cooling the samples on ice in between steps (bead beater, Brand). Then, 200 µL of ice-cold chloroform was added. The tubes were mixed gently and centrifuged at 12,000 x *g for 15 min at 4 °C. The RNA isolation was continued following the manufacturer's instructions of the RNeasy mini kit, including an on-column DNase step using DNase I recombinant, RNase-free, (Roche Diagnostics, Germany) incubating at 37* °C for 30 min. RNA concentration was measured using Qubit and the quality was determined by the Qsep100 bioanalyzer (BiOptic inc, Taiwan). The RNA samples were stored at -80 °C until further processing. Further processing such as removal of rRNA, library preparation and sequencing was performed by Novogene using platform NovaSeq PE150 (Illumina).

Bioinformatics

Amplicon data analysis

The 16S rRNA gene amplicon sequencing data was analyzed using the DADA2 R package (Callahan et al. 2016). Raw data (total 4,27,03,796 reads) was filtered to remove low quality reads and reads with more than 2 errors and those matching the PhiX (filterAndTrim function) resulting a total of 4,18,65,602 reads which were then subjected to removal of chimeric sequences (removeBimeraDenovo, consensus method), an average of 225083 ± 102107 reads per samples were obtained (Supplementary **Table S4**). We used a custom database consisting of 16S rRNA gene sequences fetched from the genomes of the 16 bacterial strains used in this study using barnap (available at https://github.com/mibwurrepo/Shetty_et_al_MDbMM16) (Seemann 2018). On average 97 ± 1.9% of the reads were assigned to the MDb-MM strains (Supplementary **Table S4**). Taxonomic assignment was done using the RDP classifier (Wang et al. 2007). The unique amplicon sequence variants (ASVs) were merged at species level using the *tax_glom()* function in phyloseq (v1.32) (McMurdie and Holmes 2013). The species counts were normalized for the differences in 16S rRNA gene copy number (Supplementary **Table S3**) and absolute counts were calculated as described previously (Jian et al. 2020). Further analysis of the community composition and structure was done using the microbiome R package (v.1.10.0) (Lahti and Shetty 2018). Data visualization packages, ggplot2 and ggpubr R packages were used for plotting figures (Kassambara 2018, Wickham 2011).

Metatranscriptomics analysis

A total of 816752875 raw paired-end reads totaling to 244.9 giga base pairs were obtained from thirty-six samples (Supplementary **Table S5**). We followed the

approach described in the SAMSA2 pipeline (Westreich et al. 2018). The forward and reverse adaptors were filtered using Trimmomatic (v0.36) (settings: PE -phred33, SLIDINGWINDOW:4:15, MINLEN:70) and then merged using pear (v0.9.10) (Bolger et al. 2014, Zhang et al. 2013). Merged reads matching the ribosomal rRNA were removed with SortMeRNA (v2.1) (Kopylova et al. 2012). A custom database was created from genome sequences of all the bacterial strains used in this study. All the genome sequences in FASTA format were downloaded from the NCBI genome database. For consistency all the genomes were re-annotated using Prokka (v1.12) and the 16S rRNA gene copy numbers for individual strains were identified using the barrnap (v0.9) tool (Seemann 2018, Seemann 2014). The amino acid sequences from each strain were then combined to create a database compatible with DIAMOND (v 0.9.22.123) using the *makedb* function (Buchfink et al. 2014). The ribosomal sequences depleted reads were annotated with DIAMOND using blastx. The DIAMOND output files were further analyzed in R. The corresponding codes are available at (https://github.com/mibwurrepo/Shetty_et_al_MDbMM16). The amino-acid sequences obtained from genomes were also annotated using the KEGG databases using the GhostKola tool for KEGG ortholog (KO) annotations (Kanehisa et al. 2016).

Gut metabolic modules (GMMs)

We did additional curation for the metabolic modules from our previous study to incorporate further refinements for the strains used in this study (Shetty et al. 2022). The curated GMMs are available at the GitHub repository of this study (https://github.com/mibwurrepo/Shetty_et_al_MDbMM16). We used counts per million normalized KO abundances (*cpm* function in edgeR R package v3.24.3) for profiling the metabolic modules using the omixer-rpmR R package (v0.3.1) (Robinson et al. 2010, Darzi et al. 2016). The parameters for the *rpm* function in omixer-rpmR, were as follows, score.estimator= "median", contribute = 0.5, KO=2, distribute=NULL.

Niche overlap and trophic organisation

A lower niche overlap (NO) would suggest higher transcriptional niche segregation and vice-versa between species. We used the NO index using the kernel density estimates approached described by Mouillot et al. 2005. The function to calculate niche overlap was adapted from here https://github.com/umr-marbec/nicheoverlap/blob/master/nicheoverlap.R This niche overlap index is non-parametric and assumes no normality in trait values. We used the GMM framework in which we used metabolic module expression as quantitative traits for calculation of niche overlap index. A schematic figure depicting the calculation approach is shown in Supplementary Fig. S16. We calculated pairwise niche overlap using the species GMM trait abundances for each of the time points separately as the area of overlap between the density distributions of traits. For every pair of species, we removed traits that did not sum up

to 50 counts. We also excluded GMM traits for central metabolism such as glycolysis and the pentose phosphate pathway among others and used only those associated with degradation, consumption or production. A list of GMMs and classification of trophic levels in provided in the Supplementary table S2.

Supplementary information

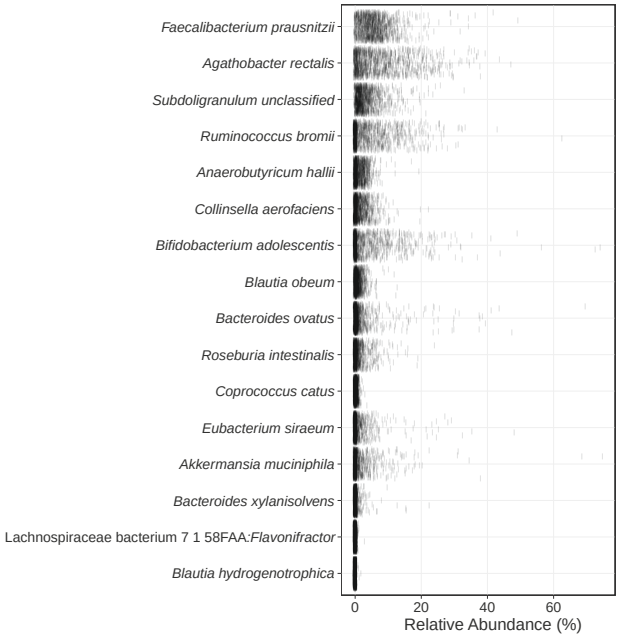

Supplementary figure S1: Relative abundance of MDb-MM species in 1155 human gut metagenomes. Each line represents one sample. Except for *B.hydrogenotrophica*, all other strains are part of the core microbiota at a relative abundance cut-off of 0.001% and prevalence of >50%.

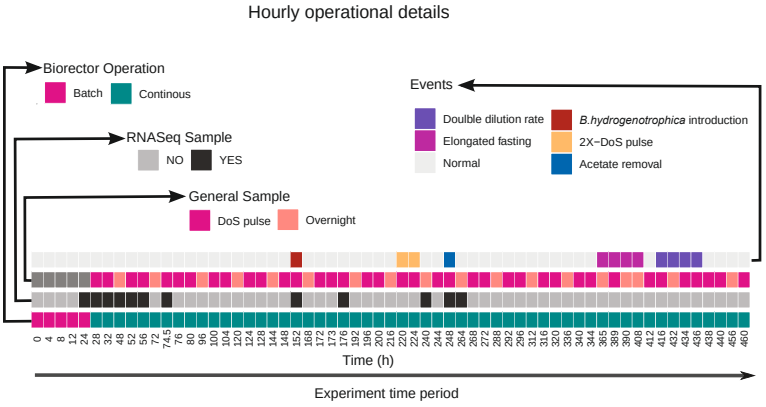

Supplementary figure S2: Detailed sampling timepoints. For all the time points shown here samples were collected for metabolites and 16S rRNA gene analysis. For RNASeq, 12 time points were chosen for analysis.

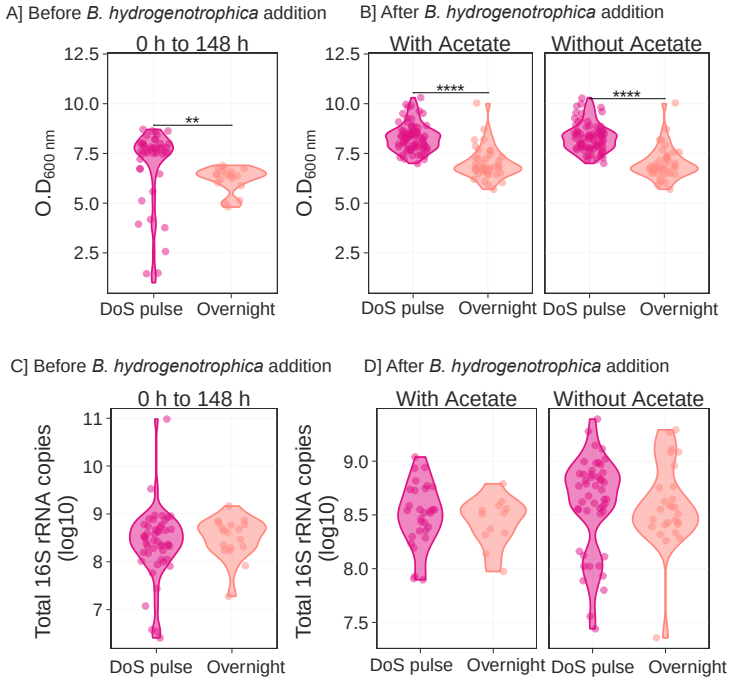

Supplementary figure S3: Comparison of optical density and total 16S rRNA gene copies. A) Comparison of optical density (O.D600) after DoS pulse (n= 48) and in overnight (n= 18) samples before addition of *B. hydrogenotrophica* B) Comparison of optical density (O.D600) after DoS pulse and in overnight samples after addition of *B. hydrogenotrophica* with (DoS, n= 30, Overnight, n= 12) and without exogenous acetate (DoS, n= 48, Overnight, n= 27). C) Comparison of total 16S rRNA gene copies after DoS pulse (n= 48) and in overnight samples (n= 18) before addition of *B. hydrogenotrophica* D) Comparison of total 16S rRNA gene copies after DoS pulse and in overnight samples after addition of *B. hydrogenotrophica* with acetate (DoS, n= 30, Overnight, n= 12) and without exogenous acetate (DoS, n= 48, Overnight, n= 27). The counts were transformed to log10. We used Wilcoxon test for pair-wise comparison corrected for multiple testing using the Benjamini–Hochberg FDR method. * = $p < 0.05$, ** = $p < 0.001$ and *** = $p < 0.0001$.

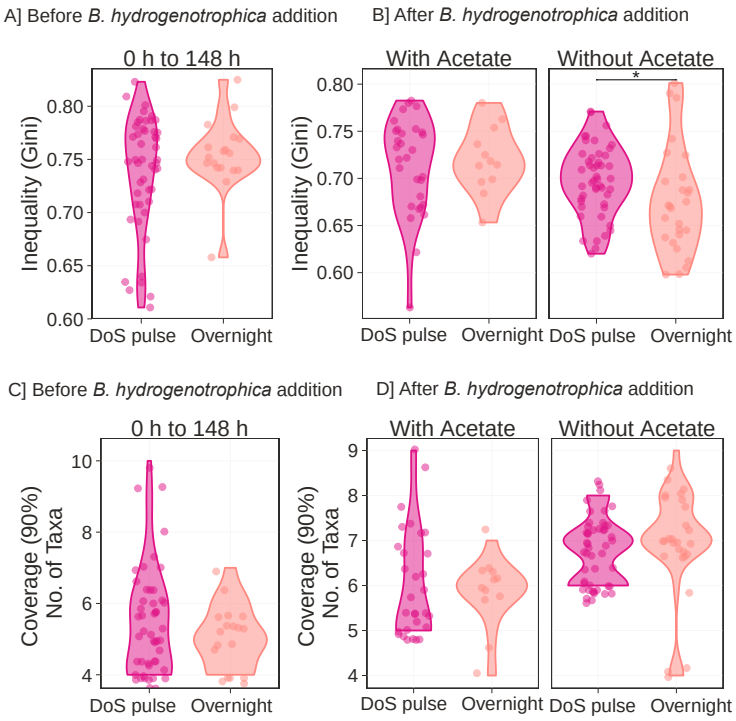

Supplementary figure S4: Comparison of inequality and coverage. A) Comparison of community evenness after DoS pulse (n= 48) and in overnight samples (n= 18) before addition of *B. hydrogenotrophica.* B) Comparison of community evenness after DoS pulse and in overnight samples after addition of *B. hydrogenotrophica* with acetate (DoS, n= 30, Overnight, n= 12) and without (DoS, n= 48, Overnight, n= 27) exogenous acetate. C) Comparison of total number of species contributing to 90% of the total abundance after DoS pulse and in overnight samples before addition of *B. hydrogenotrophica* D) Comparison of total number of species contributing to 90% of the total abundance after DoS pulse (n= 48) and in overnight samples (n= 18) after addition of *B. hydrogenotrophica* with acetate (DoS, n= 30, Overnight, n= 12) and without (DoS, n= 48, Overnight, n= 27) exogenous acetate. We used Wilcoxon test for pair-wise comparison corrected for multiple testing using the Benjamini–Hochberg FDR method. * = $p < 0.05$, ** = $p < 0.001$ and *** = $p < 0.0001$.

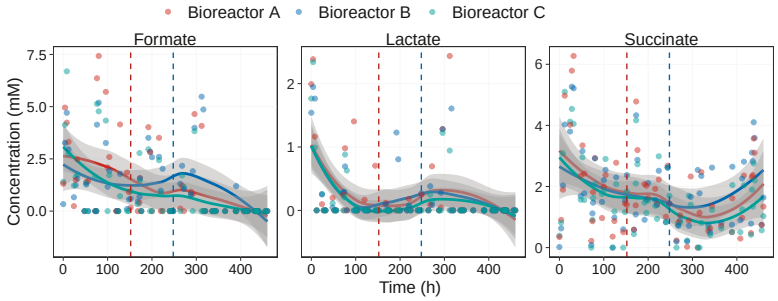

Supplementary figure S5: Concentration of SCFAs detected in minor concentration in the three bioreactors. The vertical dashed red lines indicates introduction of *B. hydrogenotrophica* (152 h) and blue line indicates removal of acetate/feed change (248h). The curved line represent the locally weighted smoothing (LOESS) for each of the bioreactors and the grey shaded region around these lines shows 95% confidence intervals for the fit. This was calculated and visualized with the default geom_smooth function in ggplot2 R package.

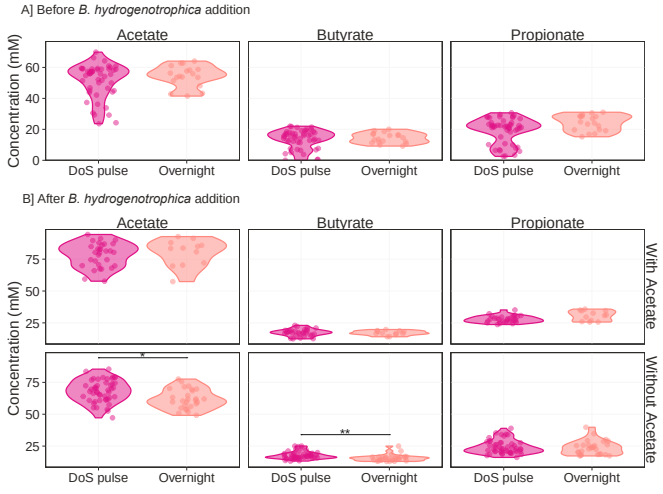

Supplementary figure S6: Comparison of SCFA production. A) The first 148 h before introduction of any disturbance event in the system (DoS pulse, n= 48 and Overnight, n= 18). B) After introduction of *B. hydrogenotrophica* as well as removal of acetate. With acetate number of samples for DoS pulse, n= 30 and for overnight, n= 12. Without acetate number of samples for DoS pulse, n= 48 and for overnight, n= 27. We used Wilcoxon test for pair-wise comparison corrected for multiple testing using the Benjamini–Hochberg FDR method. * = $p < 0.05$, ** = $p < 0.001$ and *** = $p < 0.0001$.

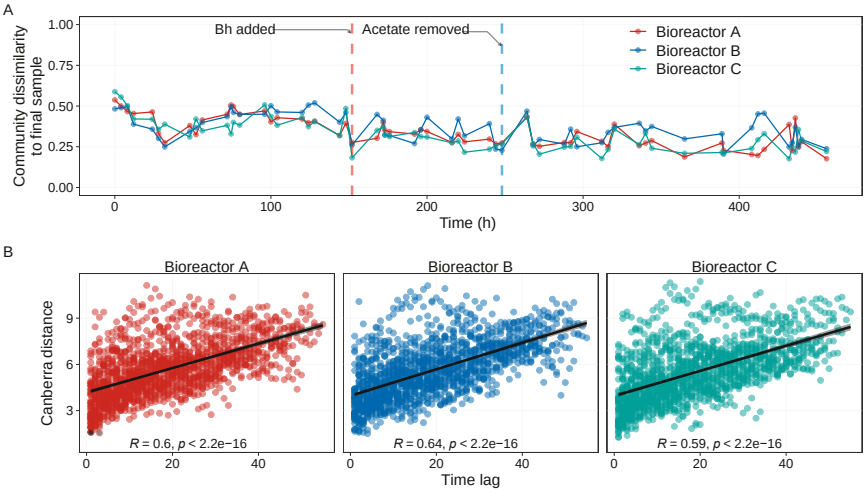

Supplementary figure S7: Temporal patterns in community succession. A) Temporal convergence patterns of MDb-MM in the three bioreactors (Canberra distance). B) Community change over time based on Canberra distances, with modified codes from the codyn R package which uses Euclidean distances.

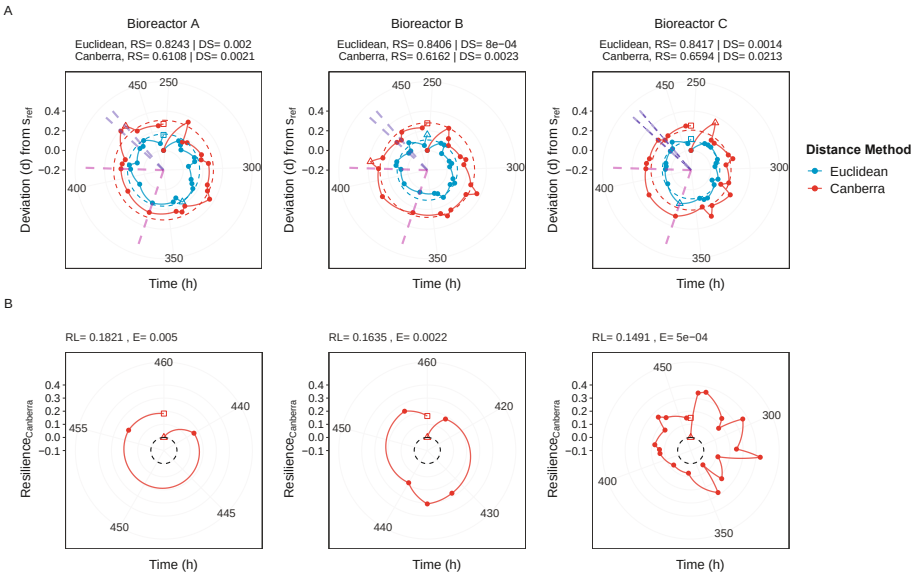

Supplementary figure S8: Stability properties of MDb-MM in presence of multiple perturbations. A) Community changes from the reference state calculated using Canberra and Euclidean distance. The reference boundary was calculated using the method described by Liu et al., 2018. The shaded region and brown dashed line depict reference boundary based on Canberra distance, while the blue dashed line depicts reference state boundary based on Euclidean distance. The hollow triangles represent timepoints when maximal deviation from reference state was observed. The lavender-colored dashed line indicates elongated fasting samples and blue colored dashed line indicates the doubling of dilution rate from 10ml/h to 20ml/h. B) Resilience of the MDb-MM in presence of multiple perturbations. The black dashed line depicts the reference boundary for deviation from disturbance event based on Canberra distance. The stability was calculated with 152 h (introduction of *B. hydrogenotrophica*) as the starting time, removal of acetate/feed change (248h) as the specific disturbance event and experiment end point was 460 h, when the experiment was ended. Abbreviations: RS, resistance; DS, displacement speed; RL, resilience and DS, displacement speed.

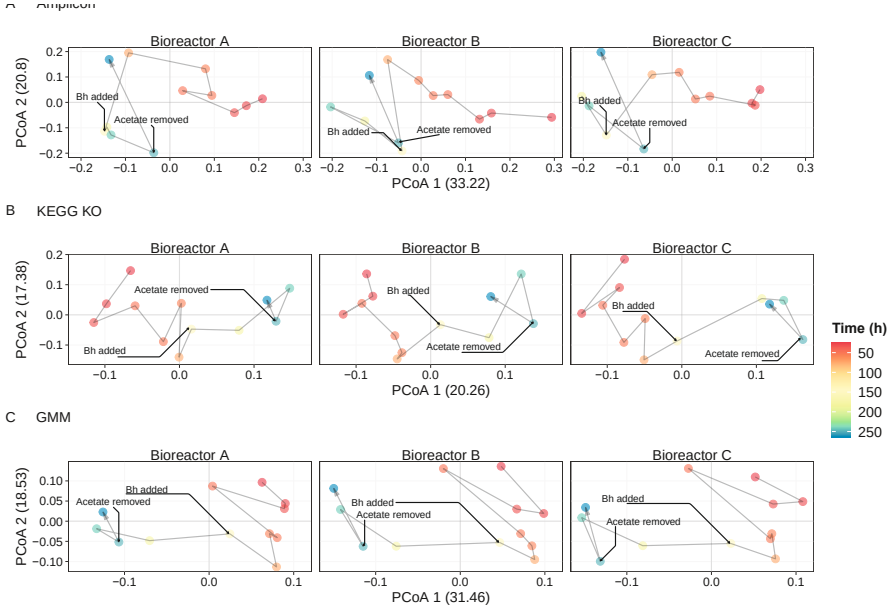

Supplementary figure S9: Temporal compositional and transcriptional succession of MDb-MM. Comparison of compositional and transcriptional community divergence. A) Community divergence based on Canberra distances using relative abundances of 16S rRNA gene. Only timepoints with metatranscriptomics data were analyzed. B) Community convergence based on Canberra distances using relative expression of Kyoto Encyclopedia for Genes and Genomes (KEGG) ortholog. C) Community convergence based on Canberra distances using relative expression of Gut metabolic modules (GMMs). Each circle is labelled with corresponding timepoints for clarity.

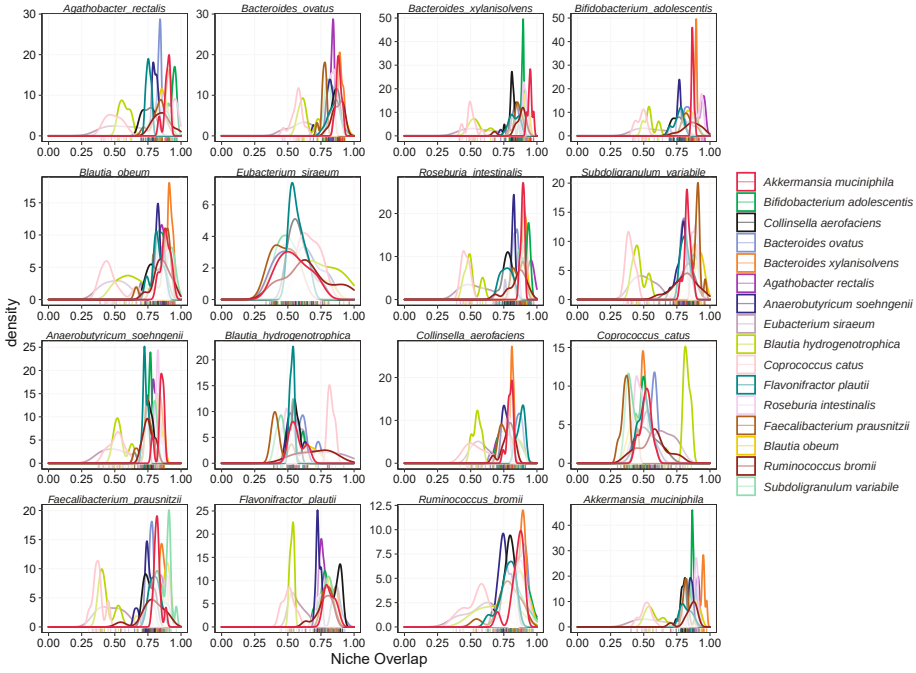

Supplementary figure S10: Comparison of pair-wise niche overlap between species. The niche overlap of each of the species was compared with other species in the community across timepoints. For details about niche overlap calculation are described in the methods section.

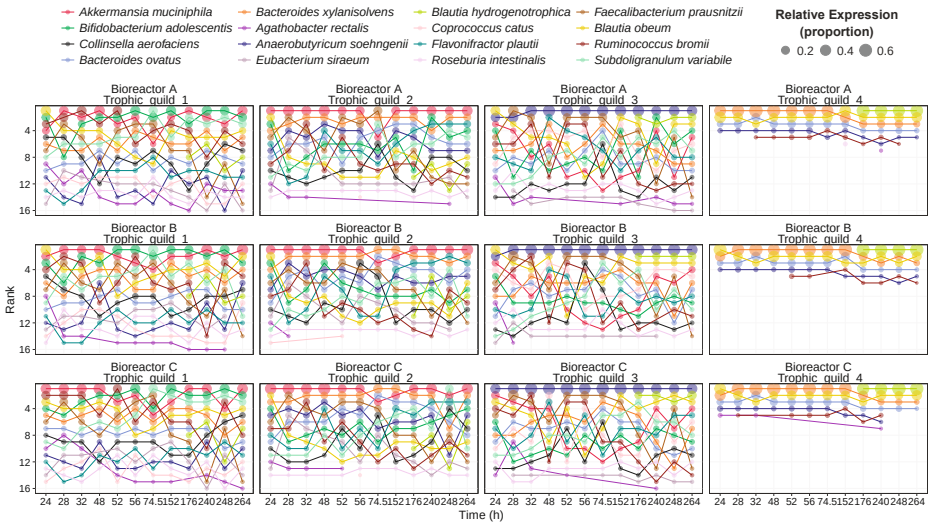

Supplementary figure S11: Dynamic trophic roles of MDb-MM species. For each trophic guild, each species was ranked based on their relative expression at each time point. The y-axis is ordered in reverse such that the high-ranking species is at the top and low-ranking species at the bottom. The size of the circle represents the relative expression of a species within a trophic guild.

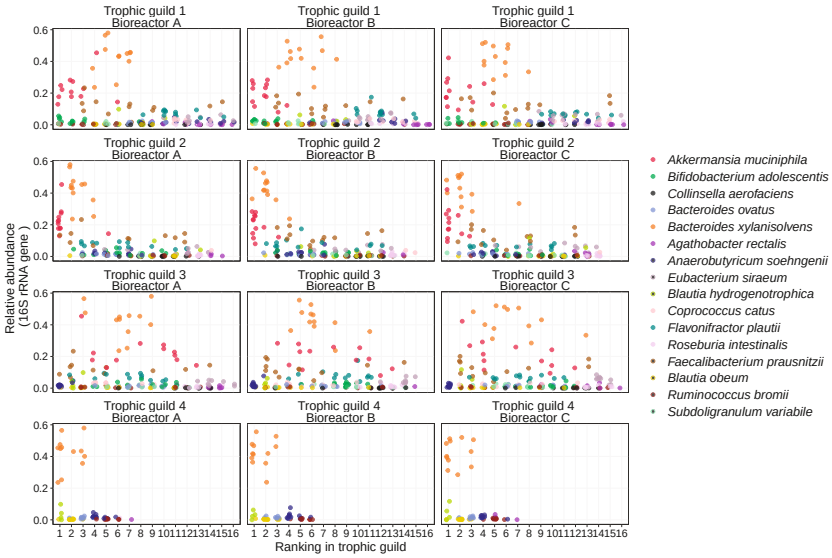

Supplementary figure S12: Relationship between species relative abundance and its rank within a trophic guild. Each circle represents 16S rRNA gene based relative abundance of the species at different time points and its rank within a trophic guild. For each trophic guild, each species was ranked based on their relative expression at each time point.

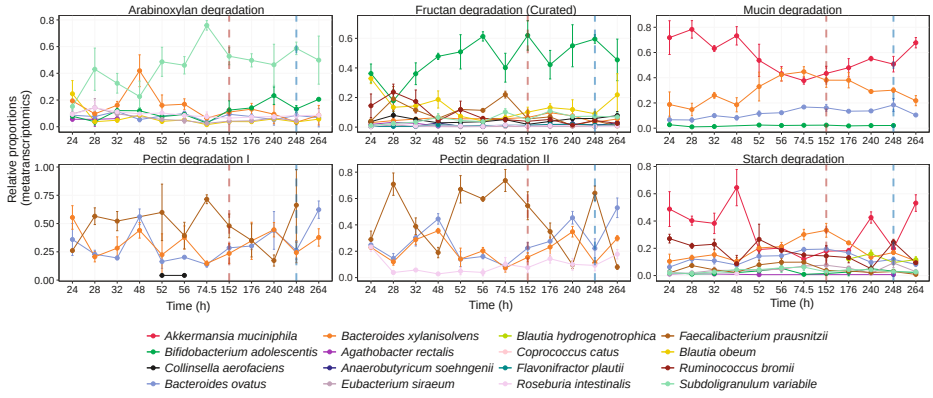

Supplementary figure S13: Species specific contributions to complex substrate degradation (trophic guild 1). The relative proportions of species specific GMM expression are shown here. The vertical dashed red lines indicate introduction of *B. hydrogenotrophica* (152 h) and blue line indicates removal of acetate/feed change (248h).

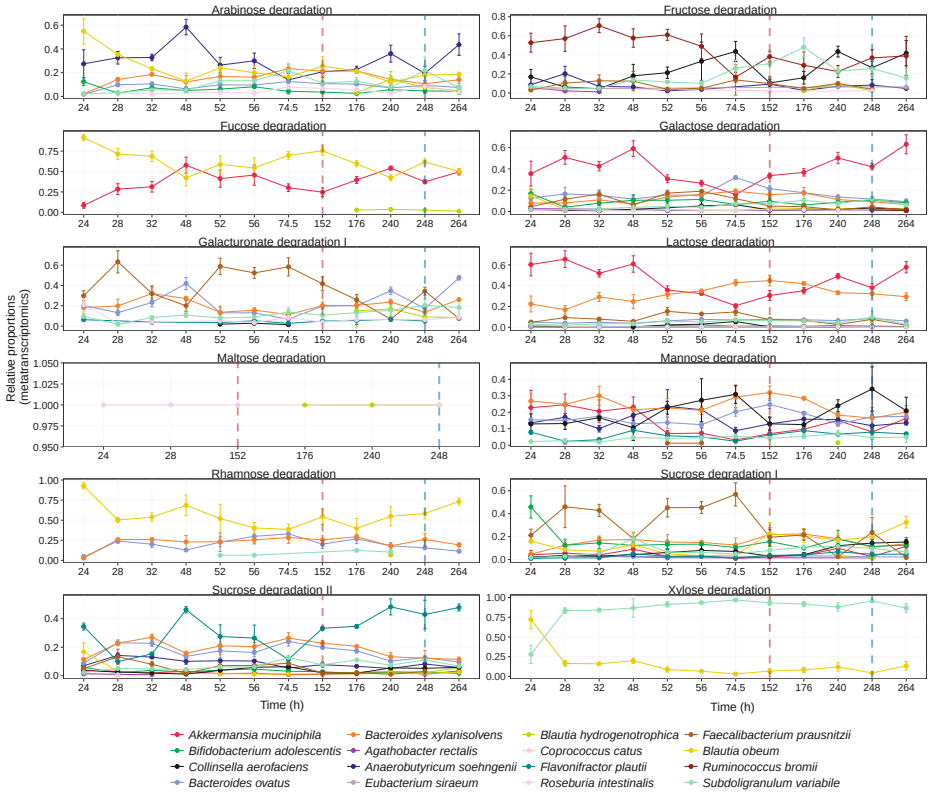

Supplementary Figure S14: Species specific contributions to public goods (trophic guild 2). The relative proportions of species specific GMM expression are shown here. The vertical dashed red lines indicate introduction of *B. hydrogenotrophica* (152 h) and blue line indicates removal of acetate/feed change (248h).

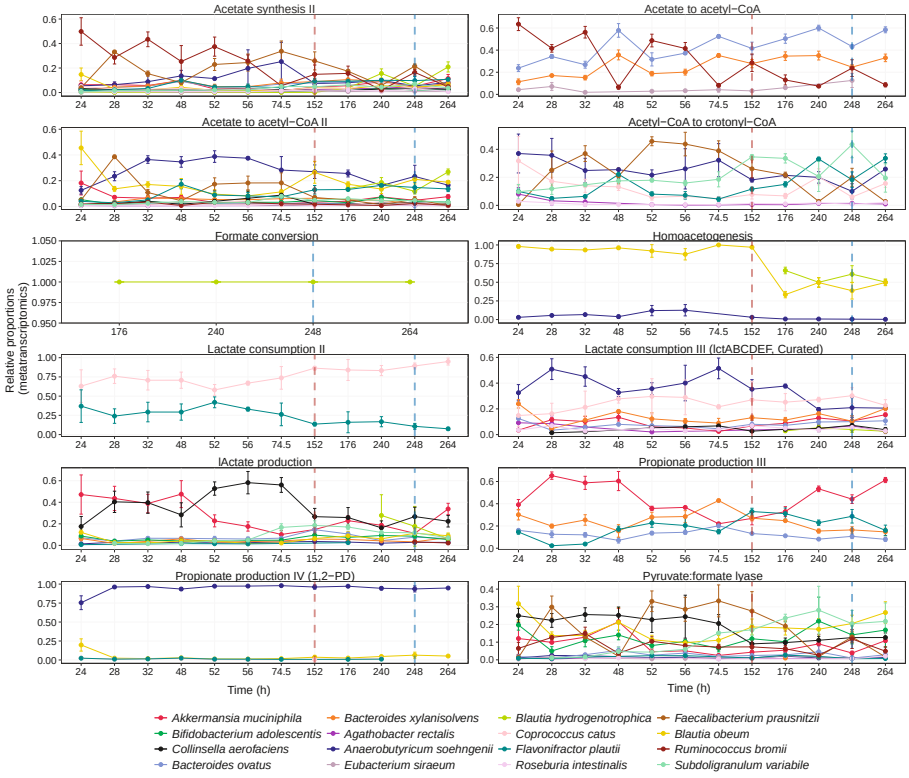

Supplementary Figure S15: Species specific contributions to SCFA metabolism. The relative proportions of species specific GMM expression are shown here. The vertical dashed red lines indicate introduction of *B. hydrogenotrophica* (152 h) and blue line indicates removal of acetate/feed change (248h).

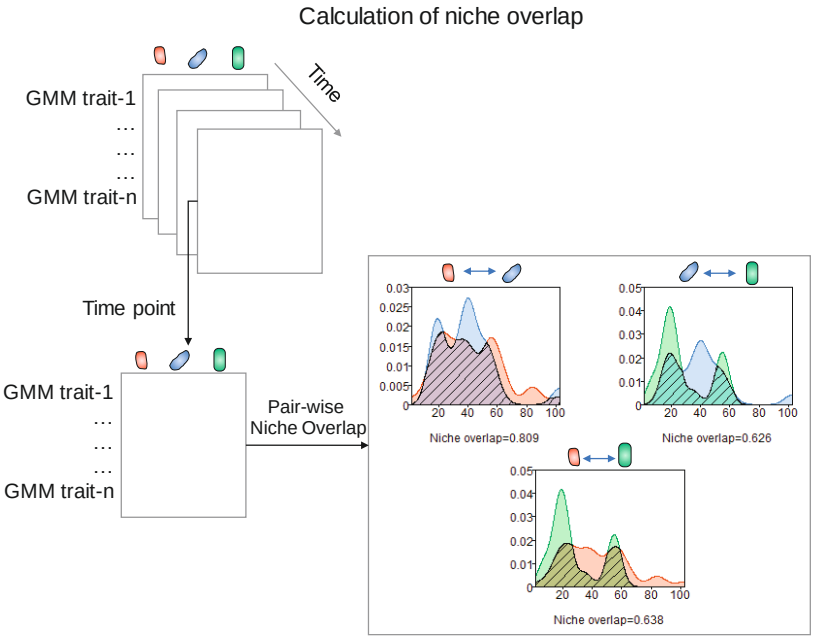

Supplementary Figure S16: Schematic representation of pair-wise niche overlap calculation. We used GMM trait expression values for calculating niche overlap. Only those GMM traits used for calculating trophic guild are used. A density distribution of traits is calculated for each species and overlap between the density distributions corresponding to the shaded are is estimated. This is done for all species pairs at each time point for every bioreactor separately.

Supplementary Table S1: Prevalence of core species identified in 1155 gut metagenomes with a prevalence of >50% and minimum abundance threshold of 0.001%. The 15 core species part of MDb-MM are highlighted in bold. The 16th non-core species is *Blautia hydrogenotrophica.*

Taxa	Prevalence (%)
Subdoligranulum unclassified	**99.83**
Ruminococcus torques	99.74
Faecalibacterium prausnitzii	**99.22**
Ruminococcus obeum	**98.27**
Eubacterium rectale	**97.14**
Oscillibacter unclassified	95.58
Bacteroides uniformis	94.20
Dorea formicigenerans	92.55
Eubacterium hallii	**91.77**
Dorea longicatena	91.69
Bacteroides ovatus	**90.82**
Bacteroides vulgatus	90.82
Coprococcus comes	90.22
Roseburia inulinivorans	89.61
Roseburia hominis	89.35
Lachnospiraceae bacterium 7 1 58FAA	**88.40**
Lachnospiraceae bacterium 5 1 63FAA	87.19
Collinsella aerofaciens	**85.89**
Bifidobacterium longum	85.89
Alistipes putredinis	83.72
Clostridium leptum	83.46
Coprococcus catus	**83.12**
Anaerostipes hadrus	83.03
Alistipes shahii	82.42
Eubacterium eligens	82.25
Alistipes onderdonkii	82.25
Streptococcus salivarius	82.16
Bilophila unclassified	82.08
Ruminococcus bromii	**82.08**
Eubacterium ramulus	81.90
Bacteroides dorei	80.17
Lachnospiraceae bacterium 3 1 46FAA	79.91
Bacteroides thetaiotaomicron	78.53
Bifidobacterium adolescentis	**78.01**
Alistipes finegoldii	77.58
Barnesiella intestinihominis	77.58
Ruminococcus sp 5 1 39BFAA	77.14

Supplementary Table S1: *(Continued)*

Taxa	Prevalence (%)
Bacteroidales bacterium ph8	76.28
Eubacterium ventriosum	75.67
Roseburia intestinalis	**75.24**
Bacteroides xylanisolvens	**74.63**
Bacteroides caccae	73.42
Streptococcus parasanguinis	73.42
Parabacteroides merdae	72.03
Parabacteroides distasonis	71.34
Adlercreutzia equolifaciens	70.48
Eubacterium siraeum	**69.18**
Veillonella unclassified	64.24
Akkermansia muciniphila	**63.98**
Odoribacter splanchnicus	63.29
Escherichia coli	63.12
Anaerotruncus unclassified	61.73
Alistipes senegalensis	61.21
Bilophila wadsworthia	60.52
Clostridium bartlettii	59.91
Holdemania filiformis	57.84
Alistipes indistinctus	57.32
Streptococcus thermophilus	57.32
Peptostreptococcaceae noname unclassified	57.06
Ruminococcus lactaris	54.29
Bacteroides cellulosilyticus	52.21
Ruminococcus gnavus	51.00
Bacteroides stercoris	50.65
Eggerthella unclassified	50.56

Supplementary Table S2: Gut metabolic modules that were characterized as part of trophic guilds. Note that the module id were modified form original publication to incorporate the curation done for this research.

module_id	module_name	category_1	trophic_included	trophic_level	trophic_guild
MF0097	homoacetogenesis	gas metabolism	yes	4	trophic_guild_4
MF0098	hydrogen metabolism	gas metabolism	yes	4	trophic_guild_4
MF0099	methanogenesis - methyl-coM	gas metabolism	yes	4	trophic_guild_4
MF0100	methanogenesis from carbon dioxide	gas metabolism	yes	4	trophic_guild_4
MF0101	nitrate reduction (dissimilatory)	inorganic nutrient metabolism	yes	4	trophic_guild_4
MF0102	sulfate reduction (dissimilatory)	gas metabolism	yes	4	trophic_guild_4
MF0059	anaerobic fatty acid beta-oxidation	lipid degradation	yes	3	trophic_guild_3
MF0075	acetate to acetyl-CoA	organic acid metabolism	yes	3	trophic_guild_3
MF0077	formate conversion	organic acid metabolism	yes	3	trophic_guild_3
MF0079	lactate consumption I	organic acid metabolism	yes	3	trophic_guild_3
MF0080	lactate consumption II	organic acid metabolism	yes	3	trophic_guild_3
MF0083	succinate consumption	organic acid metabolism	yes	3	trophic_guild_3
MF0104	lactate consumption III (lctABCDEF, Curated)	organic acid metabolism	yes	3	trophic_guild_3
MF0108	propionate production IV (1,2-PD)	organic acid metabolism	yes	3	trophic_guild_3
MF00075	acetate to acetyl-CoA II	organic acid metabolism	yes	3	trophic_guild_3
MF0006	lactose degradation	carbohydrate degradation	yes	2	trophic_guild_2
MF0007	lactose and galactose degradation	carbohydrate degradation	yes	2	trophic_guild_2
MF0008	maltose degradation	carbohydrate degradation	yes	2	trophic_guild_2
MF0009	melibiose degradation	carbohydrate degradation	yes	2	trophic_guild_2
MF0010	sucrose degradation I	carbohydrate degradation	yes	2	trophic_guild_2
MF0011	sucrose degradation II	carbohydrate degradation	yes	2	trophic_guild_2
MF0012	trehalose degradation	carbohydrate degradation	yes	2	trophic_guild_2
MF0013	allose degradation	carbohydrate degradation	yes	2	trophic_guild_2

Supplementary Table S2: *(Continued)*

module_id	module_name	category_1	trophic_included	trophic_level	trophic_guild
MF0014	arabinose degradation	carbohydrate degradation	yes	2	trophic_guild_2
MF0015	fructose degradation	carbohydrate degradation	yes	2	trophic_guild_2
MF0016	fucose degradation	carbohydrate degradation	yes	2	trophic_guild_2
MF0017	galactose degradation	carbohydrate degradation	yes	2	trophic_guild_2
MF0018	mannose degradation	carbohydrate degradation	yes	2	trophic_guild_2
MF0019	rhamnose degradation	carbohydrate degradation	yes	2	trophic_guild_2
MF0020	ribose degradation	carbohydrate degradation	yes	2	trophic_guild_2
MF0021	xylose degradation	carbohydrate degradation	yes	2	trophic_guild_2
MF0022	galacturonate degradation I	carbohydrate degradation	yes	2	trophic_guild_2
MF0023	galacturonate degradation II	carbohydrate degradation	yes	2	trophic_guild_2
MF0060	glycerol degradation I	lipid degradation	yes	2	trophic_guild_2
MF0061	glycerol degradation II	lipid degradation	yes	2	trophic_guild_2
MF0062	glycerol degradation III	lipid degradation	yes	2	trophic_guild_2
MF0078	lactaldehyde degradation	carbohydrate degradation	yes	2	trophic_guild_2
MF0081	methanol conversion	gas metabolism	yes	2	trophic_guild_2
MF0105	cellobiose degradation I (curated)	carbohydrate degradation	yes	2	trophic_guild_2
MF0001	arabinoxylan degradation	carbohydrate degradation	yes	1	trophic_guild_1
MF0002	fructan degradation (Curated)	carbohydrate degradation	yes	1	trophic_guild_1
MF0003	pectin degradation I	carbohydrate degradation	yes	1	trophic_guild_1
MF0004	pectin degradation II	carbohydrate degradation	yes	1	trophic_guild_1
MF0005	starch degradation	carbohydrate degradation	yes	1	trophic_guild_1
MF0064	triacylglycerol degradation	lipid degradation	yes	1	trophic_guild_1
MF0103	mucin degradation	glycoprotein degradation	yes	1	trophic_guild_1

Supplementary Table S2: *(Continued)*

module_id	module_name	category_1	trophic_included	trophic_level	trophic_guild
MF0024	phenylalanine degradation	amino acid degradation	no	not_assigned	not_assigned
MF0025	tryptophan degradation	amino acid degradation	no	not_assigned	not_assigned
MF0026	tyrosine degradation I	amino acid degradation	no	not_assigned	not_assigned
MF0027	tyrosine degradation II	amino acid degradation	no	not_assigned	not_assigned
MF0028	aspartate degradation I	amino acid degradation	no	not_assigned	not_assigned
MF0029	aspartate degradation II	amino acid degradation	no	not_assigned	not_assigned
MF0030	glutamate degradation I	amino acid degradation	no	not_assigned	not_assigned
MF0031	glutamate degradation II	amino acid degradation	no	not_assigned	not_assigned
MF0032	glutamate degradation III	amino acid degradation	no	not_assigned	not_assigned
MF0033	alanine degradation I	amino acid degradation	no	not_assigned	not_assigned
MF0034	alanine degradation II	amino acid degradation	no	not_assigned	not_assigned
MF0035	glycine degradation	amino acid degradation	no	not_assigned	not_assigned
MF0036	isoleucine degradation	amino acid degradation	no	not_assigned	not_assigned
MF0037	leucine degradation	amino acid degradation	no	not_assigned	not_assigned
MF0038	methionine degradation I	amino acid degradation	no	not_assigned	not_assigned
MF0039	methionine degradation II	amino acid degradation	no	not_assigned	not_assigned
MF0040	proline degradation	amino acid degradation	no	not_assigned	not_assigned
MF0041	valine degradation I	amino acid degradation	no	not_assigned	not_assigned
MF0042	asparagine degradation	amino acid degradation	no	not_assigned	not_assigned
MF0043	cysteine biosynthesis/homocysteine degradation	amino acid degradation	no	not_assigned	not_assigned
MF0044	cysteine degradation I	amino acid degradation	no	not_assigned	not_assigned
MF0045	cysteine degradation II	amino acid degradation	no	not_assigned	not_assigned

Supplementary Table S2: *(Continued)*

module_id	module_name	category_1	trophic_included	trophic_level	trophic_guild
MF0046	glutamine degradation I	amino acid degradation	no	not_assigned	not_assigned
MF0047	glutamine degradation II	amino acid degradation	no	not_assigned	not_assigned
MF0048	serine degradation	amino acid degradation	no	not_assigned	not_assigned
MF0049	threonine degradation I	amino acid degradation	no	not_assigned	not_assigned
MF0050	threonine degradation II	amino acid degradation	no	not_assigned	not_assigned
MF0051	arginine degradation I	amino acid degradation	no	not_assigned	not_assigned
MF0052	arginine degradation II	amino acid degradation	no	not_assigned	not_assigned
MF0053	arginine degradation III	amino acid degradation	no	not_assigned	not_assigned
MF0054	arginine degradation IV	amino acid degradation	no	not_assigned	not_assigned
MF0055	arginine degradation V	amino acid degradation	no	not_assigned	not_assigned
MF0056	histidine degradation	amino acid degradation	no	not_assigned	not_assigned
MF0057	lysine degradation I	amino acid degradation	no	not_assigned	not_assigned
MF0058	lysine degradation II	amino acid degradation	no	not_assigned	not_assigned
MF0063	glyoxylate bypass	lipid degradation	no	not_assigned	not_assigned
MF0065	Bifidobacterium shunt	central metabolism	no	not_assigned	not_assigned
MF0066	Entner-Doudoroff pathway	central metabolism	no	not_assigned	not_assigned
MF0067	glycolysis (preparatory phase)	central metabolism	no	not_assigned	not_assigned
MF0068	glycolysis (pay-off phase)	central metabolism	no	not_assigned	not_assigned
MF0069	NADH:ferredoxin oxidoreductase	gas metabolism	no	not_assigned	not_assigned
MF0070	pentose phosphate pathway (oxidative phase)	central metabolism	no	not_assigned	not_assigned
MF0071	pentose phosphate pathway (non-oxidative branch)	central metabolism	no	not_assigned	not_assigned
MF0072	pyruvate dehydrogenase complex	central metabolism	no	not_assigned	not_assigned

Supplementary Table S2: *(Continued)*

module_id	module_name	category_1	trophic_included	trophic_level	trophic_guild
MF0073	pyruvate:ferredoxin oxidoreductase	central metabolism	no	not_assigned	not_assigned
MF0074	pyruvate:formate lyase	central metabolism	no	not_assigned	not_assigned
MF0076	4-aminobutyrate degradation	amino acid degradation	no	not_assigned	not_assigned
MF0082	putrescine degradation	amines and polyamines degradation	no	not_assigned	not_assigned
MF0084	succinate conversion to propionate	organic acid metabolism	yes	not_assigned	not_assigned
MF0085	urea degradation	amines and polyamines degradation	yes	not_assigned	not_assigned
MF0086	acetyl-CoA to acetate	organic acid metabolism	no	not_assigned	not_assigned
MF0087	acetyl-CoA to crotonyl-CoA	organic acid metabolism	no	not_assigned	not_assigned
MF0088	butyrate production I	organic acid metabolism	yes	not_assigned	not_assigned
MF0089	butyrate production II	organic acid metabolism	yes	not_assigned	not_assigned
MF0090	ethanol production I	alcohol metabolism	yes	not_assigned	not_assigned
MF0091	ethanol production II	alcohol metabolism	yes	not_assigned	not_assigned
MF0092	lactate production	organic acid metabolism	yes	not_assigned	not_assigned
MF0093	propionate production I	organic acid metabolism	yes	not_assigned	not_assigned
MF0094	propionate production II	organic acid metabolism	yes	not_assigned	not_assigned
MF0095	propionate production III	organic acid metabolism	yes	not_assigned	not_assigned
MF0096	succinate production	organic acid metabolism	yes	not_assigned	not_assigned
MF0106	1,2 propanediol production I (lactaldehyde, curated)	diol metabolism	no	not_assigned	not_assigned
MF0107	1,2 propanediol production II (Hydroxyacetone, curated)	diol metabolism	no	not_assigned	not_assigned
MF00020	serine biosynthesis, glycerate-3P => serine	amino acid biosynthesis	no	not_assigned	not_assigned

Supplementary Table S2: *(Continued)*

module_id	module_name	category_1	trophic_included	trophic_level	trophic_guild
MF00018	threonine biosynthesis, aspartate => homoserine => threonine	amino acid biosynthesis	no	not_assigned	not_assigned
MF00033	ectoine biosynthesis, aspartate => ectoine	amino acid degradation	no	not_assigned	not_assigned
MF00021	cysteine biosynthesis, serine => cysteine	amino acid biosynthesis	no	not_assigned	not_assigned
MF00338	cysteine biosynthesis, homocysteine + serine => cysteine	amino acid biosynthesis	no	not_assigned	not_assigned
MF00609	cysteine biosynthesis, methionine => cysteine	amino acid biosynthesis	no	not_assigned	not_assigned
MF00017	methionine biosynthesis, apartate => homoserine => methionine	amino acid biosynthesis	no	not_assigned	not_assigned
MF00019	valine/isoleucine biosynthesis, pyruvate => valine / 2-oxobutanoate => isoleucine	amino acid biosynthesis	no	not_assigned	not_assigned
MF00535	isoleucine biosynthesis, pyruvate => 2-oxobutanoate	amino acid biosynthesis	no	not_assigned	not_assigned
MF00570	isoleucine biosynthesis, threonine => 2-oxobutanoate => isoleucine	amino acid biosynthesis	no	not_assigned	not_assigned
MF00432	leucine biosynthesis, 2-oxoisovalerate => 2-oxoisocaproate	amino acid biosynthesis	no	not_assigned	not_assigned
MF00016	lysine biosynthesis, succinyl-DAP pathway, aspartate => lysine	amino acid biosynthesis	no	not_assigned	not_assigned
MF00525	lysine biosynthesis, acetyl-DAP pathway, aspartate => lysine	amino acid biosynthesis	no	not_assigned	not_assigned
MF00526	lysine biosynthesis, DAP dehydrogenase pathway, aspartate => lysine	amino acid biosynthesis	no	not_assigned	not_assigned
MF00527	lysine biosynthesis, DAP aminotransferase pathway, aspartate => lysine	amino acid biosynthesis	no	not_assigned	not_assigned

Supplementary Table S2: *(Continued)*

module_id	module_name	category_1	trophic_included	trophic_level	trophic_guild
MF00030	lysine biosynthesis, AAA pathway, 2-oxoglutarate => 2-aminoadipate => lysine	amino acid biosynthesis	no	not_assigned	not_assigned
MF00433	lysine biosynthesis, 2-oxoglutarate => 2-oxoadipate	amino acid biosynthesis	no	not_assigned	not_assigned
MF00031	lysine biosynthesis, mediated by LysW, 2-aminoadipate => lysine	amino acid biosynthesis	no	not_assigned	not_assigned
MF00028	ornithine biosynthesis, glutamate => ornithine	amino acid biosynthesis	no	not_assigned	not_assigned
MF00763	ornithine biosynthesis, mediated by LysW, glutamate => ornithine	amino acid biosynthesis	no	not_assigned	not_assigned
MF00844	arginine biosynthesis, ornithine => arginine	amino acid biosynthesis	no	not_assigned	not_assigned
MF00845	arginine biosynthesis, glutamate => acetylcitrulline => arginine	amino acid biosynthesis	no	not_assigned	not_assigned
MF00029	urea cycle	amines and polyamines degradation	no	not_assigned	not_assigned
MF00015	proline biosynthesis, glutamate => proline	amino acid biosynthesis	no	not_assigned	not_assigned
MF00026	histidine biosynthesis, PRPP => histidine	amino acid biosynthesis	no	not_assigned	not_assigned
MF00022	shikimate pathway, phosphoenolpyruvate + erythrose-4P => chorismate	amino acid biosynthesis	no	not_assigned	not_assigned
MF00023	tryptophan biosynthesis, chorismate => tryptophan	amino acid biosynthesis	no	not_assigned	not_assigned
MF00024	phenylalanine biosynthesis, chorismate => phenylalanine	amino acid biosynthesis	no	not_assigned	not_assigned
MF00025	tyrosine biosynthesis, chorismate => tyrosine	amino acid biosynthesis	no	not_assigned	not_assigned
MF00040	tyrosine biosynthesis, prephanate => pretyrosine => tyrosine	amino acid biosynthesis	no	not_assigned	not_assigned

Supplementary Table S2: *(Continued)*

module_id	module_name	category_1	trophic_included	trophic_level	trophic_guild
MGB006	glutamate biosynthesis I	amino acid biosynthesis	no	not_assigned	not_assigned
MGB007	glutamate biosynthesis II	amino acid biosynthesis	no	not_assigned	not_assigned
MGB044	acetate synthesis II	organic acid metabolism	no	not_assigned	not_assigned
MGB045	acetate synthesis III	organic acid metabolism	no	not_assigned	not_assigned
MGB046	acetate synthesis IV	organic acid metabolism	no	not_assigned	not_assigned

Supplementary Table S3: Candidate strains used in this study. All strains, except *C. catus* were grown for 24 h. *C. catus* was grown for 48 h due to its flow growth and to achieve sufficient biomass for the experiment.

Species	Strain	Inoculation (%)	16S rRNA gene copies/genome	Substrate pre-culture
A. muciniphila	ATCC BAA-835	1	3	Crude mucin
B. ovatus	HMP strain 3_8_47FAA	1	2	20 mM galactose, 20 mM xylose and 0.2% starch
B. xylanisolvens	HMP strain 2_1_22	1	1	20 mM galactose, 20 mM xylose and 0.2% starch
A. soehngenii	DSM 17630 (L2-7)	2	8	60 mM glucose
C. catus	ATCC 27761	1	1	60 mM glucose
Flavonifractor plautii	HMP strain 7_1_58FAA	2	1	20 mM glucose, 20 mM galactose and 20 mM xylose
E. sireaum	DSM 15702	2	1	30 mM glucose, 20 mM maltose and 0.1% starch
A. rectalis	DSM 17629	1	5	20 mM glucose, 20 mM lactose and 20 mM xylose
R. intestinalis	DSM 14610	2	3	30 mM glucose, 20 mM maltose and 0.1% starch
F. prausnitzii	A2-165	1	2	30 mM glucose and 30 mM fructose
S. variabile	DSM 15176	1	4	60 mM glucose
R. bromii	ATCC 27255	2	2	30 mM glucose and 30 mM fructose
B. obeum	DSM 25238	2	5	30 mM glucose and 30 mM fructose
C. aerofaciens	DSM 3979	1	6	30 mM glucose, 20 mM maltose and 0.1% starch
B. adolescentis	L2-32	1	4	20 mM glucose, 20 mM lactose and 20 mM xylose
B. hydrogenotrophica	DSM 10507	2	1	60 mM glucose

Supplementary Table S4: Amplicon sequencing raw data information and total 16S rRNA gene copies in each sample. The last two columns contain percent of reads assigned to MDb-MM reads and not classified as MDb-MM strains.

Timepoint	SampleID	Raw reads	Filtered reads	Percent surviving	qPCR total 16S rRNA copies	MDb-MM (%)	Non-MDb-MM (%)
0	F5T0	210840	206942	98.2	3811346.4	88.66	11.34
	F6T0	210157	206286	98.2	3486041.6	90.33	9.67
	F8T0	267888	262586	98.0	2576053.0	91.27	8.73
4	F5T4	289071	282481	97.7	27489889.8	95.17	4.83
	F6T4	256351	252155	98.4	11919416.9	93.75	6.25
	F8T4	337504	331433	98.2	87488576.8	95.93	4.07
8	F5T8	422420	414086	98.0	268629666.3	98.47	1.53
	F6T8	384591	377621	98.2	212352319.4	98.36	1.64
	F8T8	329572	323392	98.1	239534469.8	98.40	1.60
12	F5T12	181667	178044	98.0	936122605.8	97.75	2.25
	F6T12	270986	266133	98.2	443360166.2	97.70	2.30
	F8T12	263445	257749	97.8	922600757.1	98.33	1.67
24	F5T24	288674	281794	97.6	222347670.3	97.85	2.15
	F6T24	257533	252976	98.2	292764928.7	96.79	3.21
	F8T24	292276	286756	98.1	604937439.2	98.14	1.86
28	F5T28	179955	176292	98.0	171579937.3	97.36	2.64
	F6T28	283110	278143	98.2	81282242.7	97.15	2.85
	F8T28	293628	287326	97.9	216556050.2	97.78	2.22
32	F5T32	431612	423642	98.2	300904450.0	98.02	1.98
	F6T32	432546	424692	98.2	379349453.1	97.70	2.30
	F8T32	329900	323795	98.1	278021559.3	97.81	2.19

Supplementary Table S4: *(Continued)*

Timepoint	SampleID	Raw reads	Filtered reads	Percent surviving	qPCR total 16S rRNA copies	MDb-MM (%)	Non-MDb-MM (%)
48	F5T48	286647	281747	98.3	415567781.5	98.06	1.94
	F6T48	286379	280766	98.0	176832265.7	98.23	1.77
	F8T48	301374	297383	98.7	206863233.5	98.40	1.60
52	F5T52	233339	222394	95.3	900844321.6	98.15	1.85
	F6T52	310861	306146	98.5	553743176.3	97.28	2.72
	F8T52	272200	266928	98.1	758584484.5	97.22	2.78
56	F5T56	162171	159720	98.5	224283973.6	97.02	2.98
	F6T56	322208	315806	98.0	112548896.5	97.55	2.45
	F8T56	298463	293128	98.2	57974429.2	98.32	1.68
72	F5T72	193876	190819	98.4	709672233.7	98.00	2.00
	F6T72	420939	412116	97.9	640409852.9	97.46	2.54
	F8T72	345906	339524	98.2	728797534.0	97.83	2.17
74	F5T74	89989	88724	98.6	3340302331.0	98.48	1.52
	F6T74	212558	209228	98.4	347025789.6	99.15	0.85
	F8T74	245601	241253	98.2	331978131.1	99.31	0.69
76	F5T76	230526	227019	98.5	111713348.3	97.66	2.34
	F6T76	257017	252626	98.3	102902522.9	98.00	2.00
	F8T76	327394	320770	98.0	98969912.5	97.92	2.08
80	F5T80	248711	243642	98.0	539898202.1	97.75	2.25
	F6T80	382296	375316	98.2	999117561.6	97.87	2.13
	F8T80	276439	269318	97.4	178381303.3	97.91	2.09

Supplementary Table S4: *(Continued)*

Timepoint	SampleID	Raw reads	Filtered reads	Percent surviving	qPCR total 16S rRNA copies	MDb-MM (%)	Non-MDb-MM (%)
80	F5T80	347580	341800	98.3	156912853.6	97.90	2.10
	F6T80	112418	110163	98.0	212274142.0	98.30	1.70
	F8T80	294291	290517	98.7	422869144.3	98.01	1.99
96	F5T96	365868	359464	98.2	19040516.2	98.13	1.87
	F6T96	388956	382045	98.2	168486235.1	98.39	1.61
	F8T96	471210	462344	98.1	82544366.4	98.25	1.75
100	F5T100	408868	401376	98.2	191429422.6	97.20	2.80
	F6T100	294048	288605	98.1	476904931.3	98.09	1.91
	F8T100	338425	332501	98.2	233403880.2	98.48	1.52
104	F5T104	137152	134527	98.1	390467572.3	97.62	2.38
	F6T104	39021	37355	95.7	451218769.7	97.87	2.13
	F8T104	131841	128709	97.6	601134955.6	97.47	2.53
120	F5T120	338660	332616	98.2	196024068.3	97.97	2.03
	F6T120	228880	224573	98.1	586485314.9	97.45	2.55
	F8T120	163372	159914	97.9	477031944.8	97.75	2.25
124	F5T124	153385	149463	97.4	95866766509.0	97.16	2.84
	F6T124	183696	180358	98.2	475763320.9	97.60	2.40
	F8T124	219202	214663	97.9	745523354.7	97.57	2.43
128	F5T128	168687	165799	98.3	847714466.9	97.72	2.28
	F6T128	154708	151469	97.9	595189834.3	97.91	2.09
	F8T128	183450	179262	97.7	531853926.2	98.16	1.84

Supplementary Table S4: *(Continued)*

Timepoint	SampleID	Raw reads	Filtered reads	Percent surviving	qPCR total 16S rRNA copies	MDb-MM (%)	Non-MDb-MM (%)
144	F5T144	32695	31880	97.5	444916153.3	98.09	1.91
	F6T144	111683	109416	98.0	503724206.9	98.15	1.85
	F8T144	67768	66700	98.4	1463121363.0	97.81	2.19
148	F5T148	377995	371462	98.3	151166193.0	98.05	1.95
	F6T148	388611	381639	98.2	788775873.3	98.28	1.72
	F8T148	488616	479462	98.1	212514528.5	98.24	1.76
152	F5T152	79979	77608	97.0	243868402.6	97.83	2.17
	F6T152	237216	231590	97.6	347478949.8	98.79	1.21
	F8T152	214765	210479	98.0	355885846.5	98.92	1.08
168	F5T168	112196	109419	97.5	420659464.2	99.36	0.64
	F6T168	89610	87863	98.1	330497181.9	97.85	2.15
	F8T168	136085	133557	98.1	615758408.8	97.87	2.13
172	F5T172	75737	74460	98.3	266837025.0	97.41	2.59
	F6T172	177439	174079	98.1	556893816.9	97.96	2.04
	F8T172	162036	159218	98.3	272839232.3	97.49	2.51
173	F5T173	161812	153651	95.0	156027000.5	97.75	2.25
	F6T173	176820	173056	97.9	330339381.5	97.42	2.58
	F8T173	213648	208980	97.8	225832216.3	97.62	2.38
176	F5T176	210490	206388	98.1	80951607.6	97.82	2.18
	F6T176	167480	164131	98.0	85175651.0	97.89	2.11
	F8T176	169790	166588	98.1	78936721.3	97.66	2.34

Supplementary Table S4: *(Continued)*

Timepoint	SampleID	Raw reads	Filtered reads	Percent surviving	qPCR total 16S rRNA copies	MDb-MM (%)	Non-MDb-MM (%)
192	F5T192	242578	237194	97.8	137786044.5	98.12	1.88
	F6T192	75931	74582	98.2	207343758.1	97.18	2.82
	F8T192	85133	83860	98.5	94219228.2	97.56	2.44
196	F5T196	421088	413078	98.1	545519592.3	98.06	1.94
	F6T196	271859	266700	98.1	873706311.7	98.15	1.85
	F8T196	312282	306701	98.2	860563021.5	97.59	2.41
200	F5T200	179903	176895	98.3	342314548.2	97.76	2.24
	F6T200	173702	170053	97.9	224106034.3	97.84	2.16
	F8T200	166959	163260	97.8	330102734.6	97.98	2.02
216	F5T216	202287	198344	98.1	360630081.9	97.81	2.19
	F6T216	149467	146145	97.8	348669878.0	98.19	1.81
	F8T216	198885	196021	98.6	322967882.2	98.05	1.95
220	F5T220	340948	334363	98.1	171261464.5	97.95	2.05
	F6T220	429747	422259	98.3	291049825.1	97.89	2.11
	F8T220	303549	296468	97.7	198438613.7	98.45	1.55
224	F5T224	290979	285129	98.0	352413111.5	97.92	2.08
	F6T224	287974	282895	98.2	193675021.2	97.52	2.48
	F8T224	238586	232434	97.4	355810051.0	98.38	1.62
240	F5T240	233721	223697	95.7	215544316.7	98.49	1.51
	F6T240	285825	281579	98.5	384018604.1	98.08	1.92
	F8T240	346143	339661	98.1	233370625.0	98.36	1.64

Supplementary Table S4: *(Continued)*

Timepoint	SampleID	Raw reads	Filtered reads	Percent surviving	qPCR total 16S rRNA copies	MDb-MM (%)	Non-MDb-MM (%)
244	F5T244	106372	104144	97.9	1092769931.0	97.41	2.59
	F6T244	163055	160289	98.3	655598078.0	96.64	3.36
	F8T244	219925	216450	98.4	590764214.5	97.40	2.60
248	F5T248	213043	209475	98.3	534199847.6	97.47	2.53
	F6T248	78381	75327	96.1	577591995.7	97.32	2.68
	F8T248	167425	164199	98.1	385333536.9	97.29	2.71
264	F5T264	234603	229664	97.9	287490600.2	97.48	2.52
	F6T264	266624	261264	98.0	258908643.3	97.55	2.45
	F8T264	141639	137293	96.9	181813421.3	97.86	2.14
268	F5T268	165188	162453	98.3	144846641.8	97.56	2.44
	F6T268	73166	70252	96.0	324617721.8	97.20	2.80
	F8T268	187429	183740	98.0	364339799.0	97.77	2.23
272	F5T272	130408	127139	97.5	2462501607.0	97.74	2.26
	F6T272	369512	361808	97.9	764086186.9	97.71	2.29
	F8T272	348184	341568	98.1	1889205265.0	97.66	2.34
288	F5T288	350815	343853	98.0	389926217.4	97.87	2.13
	F6T288	426277	418957	98.3	192033918.3	97.35	2.65
	F8T288	365267	356972	97.7	443261372.0	97.76	2.24
292	F6T292	244145	239296	98.0	63050321.2	97.87	2.13
	F8T292	224190	219609	98.0	77310402.0	94.25	5.75
	F5T292	222344	218095	98.1	27582857.1	97.82	2.18

Supplementary Table S4: *(Continued)*

Timepoint	SampleID	Raw reads	Filtered reads	Percent surviving	qPCR total 16S rRNA copies	MDb-MM (%)	Non-MDb-MM (%)
296	F5T296	74723	73541	98.4	441374757.3	97.47	2.53
	F6T296	150069	147349	98.2	353585909.5	97.71	2.29
	F8T296	164958	162174	98.3	341824423.5	97.21	2.79
312	F5T312	274438	268590	97.9	1210623309.0	97.92	2.08
	F6T312	443578	435392	98.2	245447356.5	99.06	0.94
	F8T312	403761	396856	98.3	375050587.9	98.00	2.00
316	F5T316	191052	187028	97.9	818296324.6	98.45	1.55
	F6T316	70165	68929	98.2	669411208.0	97.92	2.08
	F8T316	98923	97413	98.5	542521525.7	97.35	2.65
320	F5T320	337777	331944	98.3	783894145.6	97.81	2.19
	F6T320	208340	204445	98.1	440390676.9	97.10	2.90
	F8T320	136861	133960	97.9	715022138.2	97.74	2.26
336	F5T336	263710	258282	97.9	216505506.3	97.15	2.85
	F6T336	268277	262252	97.8	583499608.2	96.79	3.21
	F8T336	261637	257292	98.3	354471362.9	96.88	3.12
340	F5T340	51517	50393	97.8	750163444.0	97.54	2.46
	F6T340	161744	158917	98.3	754064898.6	98.22	1.78
	F8T340	93422	92077	98.6	588347287.7	97.39	2.61
344	F5T344	214682	211447	98.5	36032437.0	97.60	2.40
	F6T344	213417	209475	98.2	591433996.6	97.46	2.54
	F8T344	303193	296988	98.0	85602362.6	97.27	2.73

Supplementary Table S4: *(Continued)*

Timepoint	SampleID	Raw reads	Filtered reads	Percent surviving	qPCR total 16S rRNA copies	MDb-MM (%)	Non-MDb-MM (%)
365	F5T365	249317	245911	98.6	1219663043.0	96.54	3.46
	F6T365	200982	197523	98.3	422532660.8	94.63	5.37
	F8T365	249676	245215	98.2	910852430.0	95.80	4.20
389	F5T389	142083	138950	97.8	132931719.7	95.04	4.96
	F6T389	197856	193697	97.9	105111792.2	96.47	3.53
	F8T389	157593	153641	97.5	104901279.4	92.76	7.24
390	F5T390	77908	76143	97.7	283078844.4	95.41	4.59
	F6T390	281946	276140	97.9	22730688.7	97.09	2.91
	F8T390	339244	332975	98.2	1295842650.0	93.46	6.54
408	F5T408	174450	170261	97.6	268315303.8	92.88	7.12
	F6T408	190247	185582	97.5	270678668.8	96.19	3.81
	F8T408	163435	160150	98.0	207804613.0	92.10	7.90
412	F5T412	103855	101676	97.9	929399946.5	92.83	7.17
	F6T412	176445	173402	98.3	676731413.4	97.89	2.11
	F8T412	198037	195009	98.5	708764184.1	93.90	6.10
416	F5T416	278198	272688	98.0	988667622.9	94.35	5.65
	F6T416	288975	282533	97.8	1402823509.0	95.77	4.23
	F8T416	244715	240297	98.2	407296698.6	95.61	4.39
432	F5T432	55443	54430	98.2	372236302.0	96.74	3.26
	F6T432	113149	110776	97.9	323119950.3	97.40	2.60
	F8T432	113635	111354	98.0	256142659.2	92.87	7.13

Supplementary Table S4: *(Continued)*

Timepoint	SampleID	Raw reads	Filtered reads	Percent surviving	qPCR total 16S rRNA copies	MDb-MM (%)	Non-MDb-MM (%)
434	F5T434	178198	173784	97.5	474662304.4	94.06	5.94
	F6T434	235014	230232	98.0	401200912.7	97.18	2.82
	F8T434	244691	239931	98.1	1050501826.0	93.91	6.09
436	F5T436	227510	222919	98.0	959072907.8	97.54	2.46
	F6T436	164048	160612	97.9	660149532.3	94.33	5.67
	F8T436	95561	93271	97.6	346499010.0	94.34	5.66
438	F5T438	113857	110825	97.3	379745452.1	95.02	4.98
	F6T438	41071	40268	98.0	634776777.4	96.75	3.25
	F8T438	53752	52849	98.3	417160091.3	94.76	5.24
440	F5T440	214101	210367	98.3	129244967.9	94.70	5.30
	F6T440	236084	231795	98.2	359900591.5	96.73	3.27
	F8T440	148357	144614	97.5	106115248.7	95.04	4.96
456	F5T456	262064	256565	97.9	563782664.3	91.45	8.55
	F6T456	392966	385848	98.2	1954787393.0	98.15	1.85
	F8T456	554165	544757	98.3	1854261984.0	91.59	8.41
460	F5T460	67963	66529	97.9	1302747839.0	91.17	8.83
	F6T460	162087	159239	98.2	969977502.4	96.99	3.01
	F8T460	98527	97089	98.5	615081513.3	87.51	12.49

Supplementary Table S5: Reads statistics for metatranscriptome sequencing.

Timepoint	Sample ID	Raw Reads	Clean Reads	Error Rate (%)	Q20(%)	Q30(%)	GC Content (%)
24 h	F5T24	22510218	22345873	0.03	97.78	93.59	48.05
	F6T24	22505088	22301265	0.03	97.78	93.62	48.65
	F8T24	23938428	23653126	0.03	97.96	94.03	48.69
28 h	F5T28	23445687	23169642	0.03	97.77	93.53	48.47
	F6T28	20915651	20587416	0.03	97.66	93.36	48.02
	F8T28	31023722	30772505	0.03	97.66	93.34	47.64
32 h	F5T32	23196573	23016159	0.03	97.55	93.03	47.66
	F6T32	21059415	20866971	0.03	97.6	93.16	47.19
	F8T32	23431154	23235304	0.03	97.59	93.15	47.6
48 h	F5T48	24581426	24364344	0.03	97.09	92.07	50.8
	F6T48	27669986	27431356	0.03	97.75	93.59	49.73
	F8T48	19975946	19614457	0.03	97.88	93.89	49.71
52 h	F5T52	24154417	23852997	0.03	97.31	92.42	49.96
	F6T52	24977274	24693836	0.03	97.7	93.43	48.82
	F8T52	21691291	21492803	0.03	97.78	93.56	47.06
56 h	F5T56	24368167	24092192	0.03	97.78	93.59	48.86
	F6T56	21551870	21264878	0.03	97.93	93.98	49.3
	F8T56	20884681	20654025	0.03	97.71	93.45	47.25
74.5h	F5T74T5	24991237	24633215	0.03	97.37	92.79	53.47
	F6T74T5	24787587	24424072	0.03	97.8	93.8	49.12
	F8T74T5	21061858	20831029	0.03	97.83	93.72	47.99

Supplementary Table S5: *(Continued)*

Timepoint	Sample ID	Raw Reads	Clean Reads	Error Rate (%)	Q20(%)	Q30(%)	GC Content (%)
152 h	F5T152	20126710	19789707	0.03	97	91.88	49.77
	F6T152	19982195	19754286	0.03	97.06	92	49.7
	F8T152	23065403	22876366	0.03	96.97	91.8	49.36
176 h	F5T176	25409034	25132415	0.03	97.39	92.63	49.14
	F6T176	23946432	23727878	0.03	96.97	91.73	49.08
	F8T176	20407642	20315381	0.03	97.12	92.12	49.61
240 h	F5T240	23439378	23121953	0.03	97.32	92.55	51.87
	F6T240	21489739	21337826	0.03	97.02	91.9	49.25
	F8T240	21267837	21029334	0.03	97.1	92.06	49.72
248 h	F5T248	21525048	21248891	0.03	96.94	91.72	49.27
	F6T248	24239734	23942665	0.03	97.16	92.14	47.8
	F8T248	24161528	23732221	0.03	97.3	92.52	49.27
264 h	F5T264	23474287	23110742	0.03	97.19	92.23	49.89
	F6T264	20955892	20733904	0.03	96.97	91.84	49.35
	F8T264	19904164	19601841	0.03	96.98	91.76	48.87

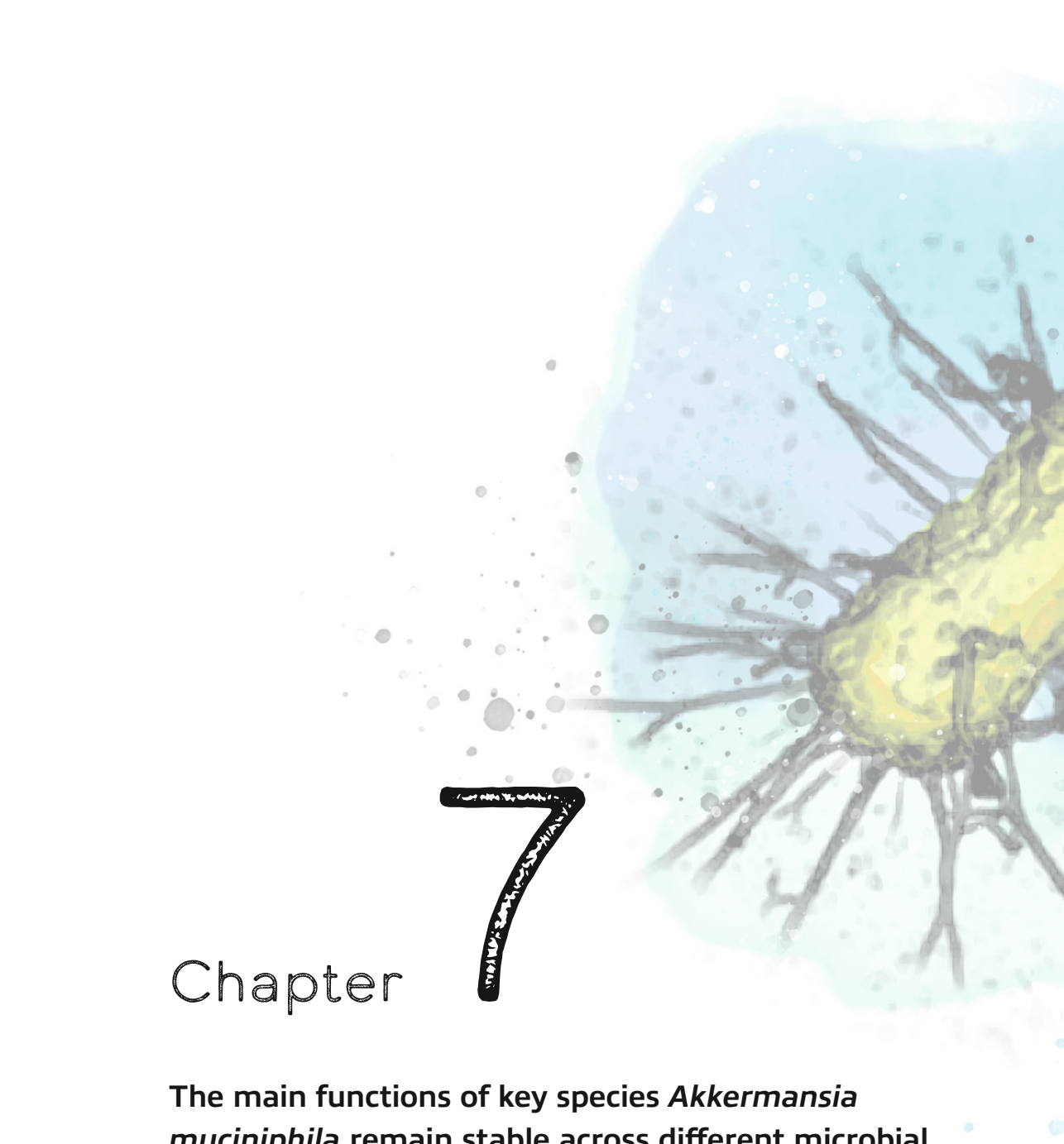

Chapter 7

The main functions of key species *Akkermansia muciniphila* remain stable across different microbial ecosystems

Sharon Y. Geerlings*, Ioannis Kostopoulos*, Sudarshan A. Shetty, Bart Nijsse, Willem M. de Vos, Jan Knol & Clara Belzer

*These authors contributed equally

Abstract

Akkermansia muciniphila resides in the mucosal layer in the gut. In this niche, *A. muciniphila* was found to be a key species of the gut microbiota. This bacterium has an extraordinary capacity to degrade the mucus glycans in order to thrive in a competitive environment as the gut. We compared existing transcriptional databases to assess the response of *A. muciniphila* in different ecological networks ranging from mono-, to co-cultures to more complex ecosystems of synthetic communities *in vitro* and *in vivo*. Our results indicate that *A. muciniphila*'s overall transcriptional response is altered under different environmental conditions. However, the expression of key functions such as mucin glycans degrading ability, pili and EPS production is stable throughout different ecosystems and independent of environmental conditions.

Introduction

The human gut harbors a complex and diverse microbial community, commonly referred to as the gut microbiota. The gut microbiota is considered to play an important role in host health. Within the gut ecosystem, mucus layer lining the intestinal epithelium is a prominent niche available for bacteria that possess specialized enzymatic machinery for mucin foraging. *Akkermansia muciniphila* is a prominent species residing in the mucus layer with the ability to degrade mucin (Derrien et al. 2004). *A. muciniphila* is currently the only representative of the Verrucomicrobia phylum in the human gut and present in high numbers with an abundance ranging from 0.5-5% (Cani and de Vos 2017). The abundance of *A. muciniphila* is mostly linked to a healthy status in humans, although a few exceptions have been reported likely due to confounding factors (Cani and de Vos 2017). A few examples are the decreased abundance of *A. muciniphila* in humans with diseases, such as type 2 diabetes, obesity and inflammatory bowel disease (IBD) (Png et al. 2010, Zhang et al. 2013, Dao et al. 2016, Yassour et al. 2016)

A. muciniphila utilizes mucin as the sole carbon, nitrogen and energy source (Derrien et al. 2004). Mucus is continuously produced in the colon by the host epithelial cells. The major component of the human colonic mucus layer is the protein MUC2. These MUC2 proteins are rich in proline (P), threonine (T) and serine (S) PTS domains that are densely O-glycosylated (Johansson et al. 2008, Johansson et al. 2011). The genome of *A. muciniphila* is composed of one circular chromosome of 2.7 Mbp coding for 2,176 protein-coding genes, of which 65% was assigned a putative function. Despite its relatively small genome size, this bacterium is, in terms of function, mainly dedicated to mucus degradation (van Passel et al. 2011). A recent study predicted that the genome of *A. muciniphila* contains genes encoding for 61 proteins involved in mucus degradation (Ottman et al. 2017). The enzymes involved in this process mainly include proteases, sulfatases, glycosyl hydrolases, and sialidases. Furthermore, it has been shown that N-acetylglucosamine (GlcNAc) and l-threonine are essential for *A. muciniphila*'s growth in minimal medium (van der Ark et al. 2018). Auxotrophy for l-threonine was predicted using the genome scale model for *A. muciniphila* (Ottman et al. 2017). Reduced genome sizes with auxotrophies are considered as a hallmark for life in a host associated symbiotic lifestyle for bacteria. Both GlcNAc and l-threonine are present in mucus. Therefore, the necessity for these components further indicates the adaptation to its mucosal niche.

Considering the important role of *A. muciniphila* in host health, its metabolic properties have been extensively investigated at different levels of complexity, mostly ranging from monoculture to defined consortia (van der Ark et al. 2018, Ouwerkerk

et al. 2016, Chia et al. 2018, Van Herreweghen et al. 2017, Kovatcheva-Datchary et al. 2019). These studies have utilized *in vitro* and rodent model systems combined with metabolite and transcriptomic approaches. The availability of transcriptomic data from numerous studies provides an opportunity to unravel the transcriptional landscape of *A. muciniphila* under different environmental conditions. In the present study, we leverage RNAseq data ranging from monoculture to multi-species metatranscriptomes generated recently to investigate the transcriptional landscape of *A. muciniphila* under varying growth conditions. The datasets used in this study consisted of following growth conditions: (i) monoculture of *A. muciniphila* and co-culture of *A. muciniphila* and *Bacteroides thetaiotaomicron in vitro* in bioreactors under a continuous flow of mucin glycans, (ii) mono-colonization of germ-free mice with *A. muciniphila* and co-colonization with *A. muciniphila* and *B. thetaiotaomicron,* and (iii) *A. muciniphila* grown in a 15 species synthetic community under a continuous flow of mucin glycans and periodically addition of carbohydrates (pectin, xylan, starch, inulin). Analysis of the abovementioned transcriptomics and metatranscriptomics networks revealed that *A. muciniphila* has a continuous expression of genes related to mucus degradation, EPS production and pili synthesis, independent of the changing environments. However, genes involved in stress response are regulated in response to the changing environment.

Results

Datasets and RNA sequencing quality control

In this study, we used existing transcriptional databases of *A. muciniphila* in different ecological networks ranging from mono-, to co- cultures to more complex ecosystems of synthetic communities *in vivo* and *in vitro.* The present study includes three transcriptional datasets that were generated from two different experiments: the SynCom study (Shetty et al. 2022) and the comparison of the *in vitro* mono- and co-culture with the *in vivo* experiment (Kostopoulos et al. 2021).

The percentage of reads mapped to the genome of *A. muciniphila* varied within conditions as well as between conditions (**Table 1**). Notably, the percentage of mapped reads varied according to the experimental set-up. Highest mapping of reads was observed in the mono-cultures experiments. In vitro, a higher number of species in the experiment results in a lower number of reads mapped to the genome of *A. muciniphila*. The *in vivo* dataset contains the highest total number of reads. However, three samples of the *in vivo* study were covered by <1% of *A. muciniphila*'s genome.

The variation in the transcriptional response of *A. muciniphila* between different conditions was minimized using relative abundances of the gene counts. In that way, the abundance of each gene was normalized across all samples of the different studies, allowing us to compare the different ecosystem studies.

Table 1: RNA sequencing coverage and total amount of quality filtered reads of all conditions.

Sample Name	Coverage (%)	Total number of reads
Cecum_mono_1	3.50%	58877899
Cecum_mono_2	16.30%	63665811
Cecum_mono_3	8.80%	59789081
Cecum_mono_4	4.70%	62125268
Distal_mono_1	1.10%	64185933
Distal_mono_2	1.80%	68772752
Distal_mono_3	2.00%	59668290
Cecum_co_1	0.80%	69830646
Cecum_co_2	2.10%	58284293
Cecum_co_3	3.00%	80785928
Cecum_co_4	2.60%	66105956
Distal_co_1	0.50%	69718577
Distal_co_2	0.50%	33520653
Distal_co_3	1.20%	63510452
Monoculture_1	41.10%	8042495
Monoculture_2	52.70%	8290259
Monoculture_3	52.40%	7889334
Co.culture_1	16.10%	9053550
Co.culture_2	17.00%	9277837
Co.culture_3	12.90%	10470948
SynCom_muc_1	9.30%	24051669
SynCom_carb_1	4.40%	24097707
SynCom_muc_2	8.00%	27309425
SynCom_carb_2	3.10%	21306330
SynCom_carb_3	3.60%	20656932
SynCom_muc_3	10.40%	19737563

Transcriptional landscape of *A. muciniphila* under different environmental conditions

We conducted ordination analysis of the overall transcriptional response of *A. muciniphila* to monitor the most variable differences in gene expression under different environmental conditions. Redundancy analysis (RDA) indicated that both

the experiment and the location affected gene expression, explaining 29.64% and 19.14% of the variation (**Figure 1**a & Supplementary **Figure 1**a). RDA showed that each experimental condition clustered together with distinct separation between the *in vivo* and *in vitro* studies. There was no clear separation between the samples within the *in vivo* experiments. On the other hand, in the *in vitro* experiments, the SynCom study separated from mono- and co-culture. This indicates an altered gene expression when *A. muciniphila* is in the presence of fifteen other species in the community as well as the different media composition between experiments.

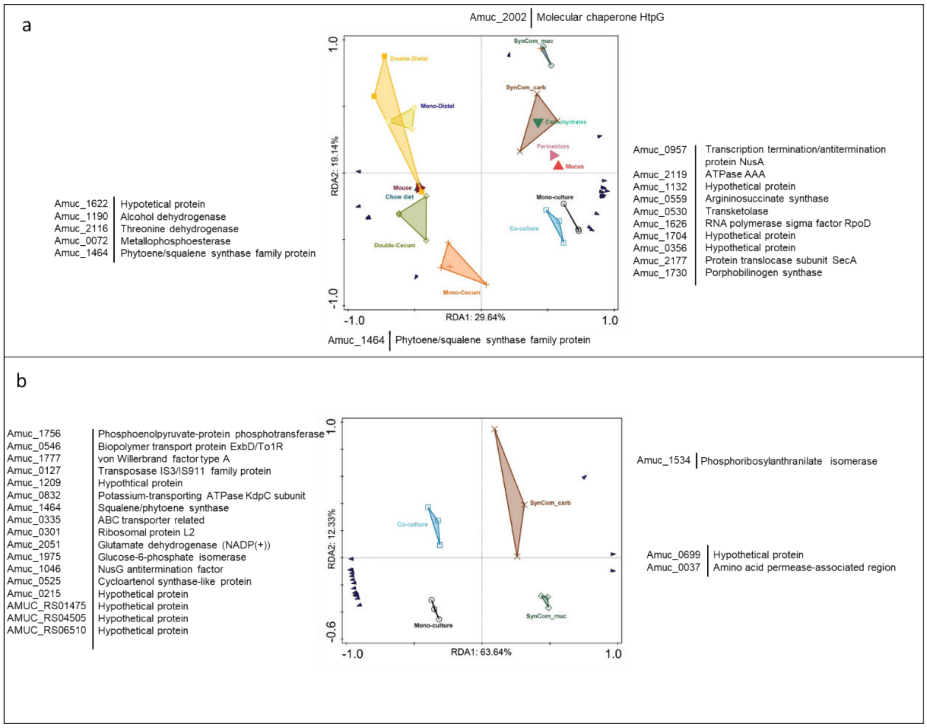

Figure 1: Ordination analysis of the ecosystem studies and the most variable expressed genes. a) RDA analysis showing the 20 most variable genes. b) RDA analysis showing the 20 most variable genes of the *in vitro* studies. The plots were generated by Canoco.

The altered gene expression between *in vitro* experiments was confirmed by a subsequent RDA of the *in vitro* studies. This analysis showed that the gene expression was affected by the microbial population in the culture and/or the different media composition between the two studies, explaining 63.64% and 12.33% of the total variation (**Figure 1**b & Supplementary **Figure 2**b). RDA illustrated distinct clustering of mono-cultures, co-cultures and SynCom_muc. Furthermore, there was a difference

observed in *A. muciniphila*'s transcriptional response when carbohydrates were present in the synthetic community.

The analysis of the expression of KEGG pathways in different conditions revealed two pathways (carbohydrate and amino acid metabolism) that were highly abundant across all the environmental conditions in all the datasets (**Figure 2**). Transcripts belonging to the carbohydrate metabolism pathway exhibited above 4% and up to 6% of relative abundance and those associated with amino acid pathway had above 2% and up to 4% of relative abundance for all the samples included in this study. Moreover, transcripts involved in glycan biosynthesis and metabolism process were highly abundant (>2%). In contrast, transcripts related to genes involved in drug resistance, biosynthesis of other secondary metabolites and metabolism of the terpenoids and polyketides were relatively low abundant.

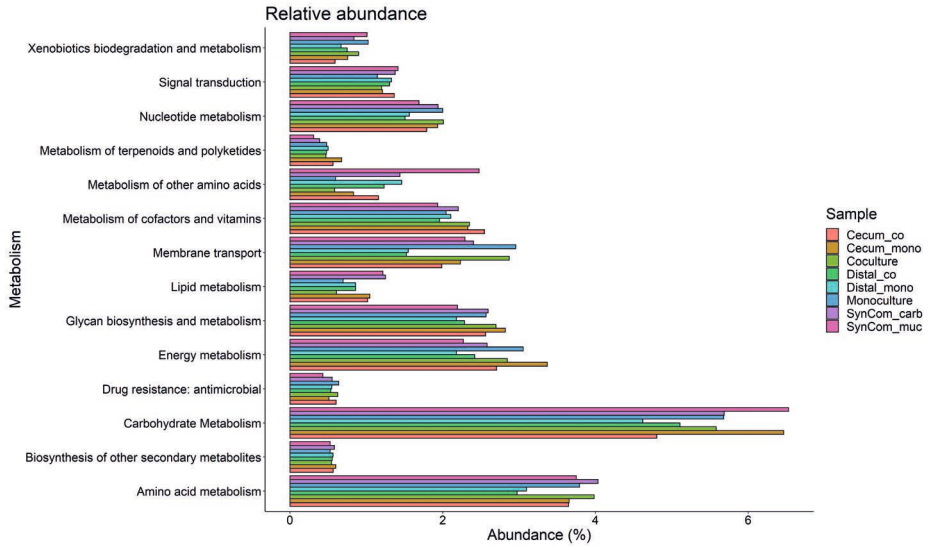

Figure 2: Relative abundances of KEGG pathways expressed by *A. muciniphila* in different environmental conditions.

Top variable genes in response to environmental changes

The comparison of the different studies revealed variability in the gene expression profile of *A. muciniphila* (**Figure 3**). We assessed the most variable genes detected in the relative abundance RNAseq dataset between *in vivo* and *in vitro* conditions. A high variability across samples was observed of a gene encoding anaerobic ribonucleoside triphosphate reductase activity protein (Amuc_0860). The relative abundance of this

gene in *A. muciniphila's* transcriptome was higher in *in vivo* conditions compared to *in vitro* conditions. In addition, three 23S rRNA genes (AMUC_RS06530, AMUC_RS01455, and AMUC_RS04525) were on average higher in *in vivo* samples compared to in vitro samples. Next to these rRNA genes, the relative abundance of three hypothetical proteins (Amuc_1569, Amuc_0016 and Amuc_0460) and an ATP-dependent chaperone ClpB (Amuc_0836) were on average specifically higher in samples taken from the distal colon of mice mono-colonized with *A. muciniphila*. In contrast, the relative abundance of Amuc_1098 (Ottman et al. 2017) encoding a type II and II secretion system protein (PiliQ) was highest in the *in vitro* monoculture and co-culture. Furthermore, a subset of genes in *A. muciniphila's* transcriptome showed higher relative abundances of several genes in the synthetic community with mucus as the main carbon source. These genes encode glutamate decarboxylase (Amuc_0372), autotransporter domain-containing protein (Amuc_0687), thioredoxin (Amuc_0691), molecular chaperone DnaK (Amuc_1406), rubrerythrin (Amuc_2055) and catalase HPII (Amuc_2070).

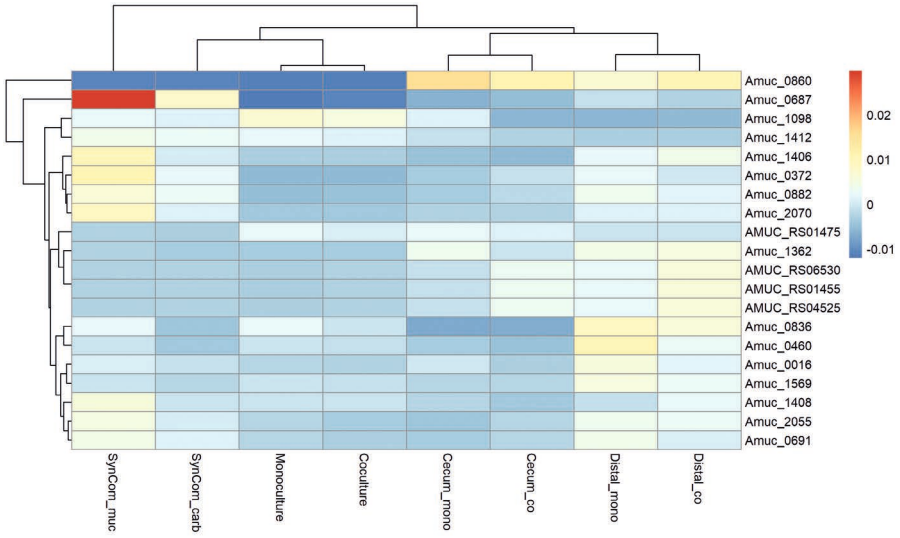

Figure 3: Heatmap of the 20 most variable *A. muciniphila* genes between the different studies

Key functions of *A. muciniphila* across different ecosystems

To assess the key functions of *A. muciniphila* across different ecosystems, we focused on mucus degradation, EPS production and pili production (**Figure 4**). The data suggests that all three functions are exerted by *A. muciniphila* in all of the conditions tested and only non-significant differences were found (Supplementary **Figure 1**).

A. muciniphila is known for being a mucin degrading bacterium, and thereby provides the host with several health benefits. Even though the overall mucus degradation pattern was found to be similar, the data revealed minor differences between *in vitro* and *in vivo* experiments (**Figure 4**a). The gene with the overall highest relative abundance among mucus degradation genes was Amuc_0824 encoding a glycosyl hydrolase GH family 2 (GH2). However, in synthetic communities three other genes were shown to have higher relative abundances than Amuc_0824. These genes were Amuc_0290 (GH family 2 sugar binding), Amuc_1120 (glycoside hydrolase N-terminal domain-containing protein) and Amuc_2136 (GH20). Even though the order in which the genes are expressed showed differences, all four genes were present in the top 10 genes with the highest relative abundances throughout all the conditions. This indicates that these four genes form the basis of mucus degradation, independent of the environmental condition. When focusing on the genes in the top 10, *in vivo*, *A. muciniphila* seems to adapt to the environment by using an exo-alpha-sialidase (Amuc_0625) and glycoside hydrolase family 18 (Amuc_2164), while *in vitro* this was an arylsulfatase (Amuc_0121).

The mechanism of exopolysaccharides (EPS) produced by *A. muciniphila* has not yet been revealed. Therefore, putative EPS-associated genes in the genome of *A. muciniphila* were used to analyze EPS production between different ecosystems (**Figure 4**b). Four genes were found to have a stable high abundance across EPS-associated genes among all conditions. These genes include a hypothetical protein that is part of a glycosyl hydrolase cluster (Amuc_1143), two polysaccharide biosynthesis tyrosine autokinases (Amuc_1413 and (Amuc_2078) and a polysaccharide export protein (Amuc_1414).

Another key function of *A. muciniphila* is pili production. In this function the main gene expression pattern was similar. Within all conditions, the key outer membrane protein involved in the production of type 4 pili (Amuc_1098) (Ligthart et al. 2020) was found to have the highest relative abundance among pili associated genes. The second and third most abundant pili-associated genes within all conditions were a type II secretion system protein (Amuc_0394) and pilus assembly protein PilM (Amuc_1101), respectively. Both Amuc_1098 and Amuc_1101 are part of the Amuc_1100 pili cluster. However, transcription of the Amuc_1100 gene was not detected in any of the conditions included in this study. Furthermore, the overall relative abundances of another cluster Amuc_1583 – 1586 (prepilin-type N-terminal cleavage/methylation domain-containing protein, type II secretion system F family protein, type II/IV secretion system protein and Flp pilus assembly complex ATPase component TadA) were found to be lower than that of the Amuc_1100 cluster in all conditions. Overall, transcripts of pili production genes were present and similar in terms of the expression of different pili production systems in all conditions.

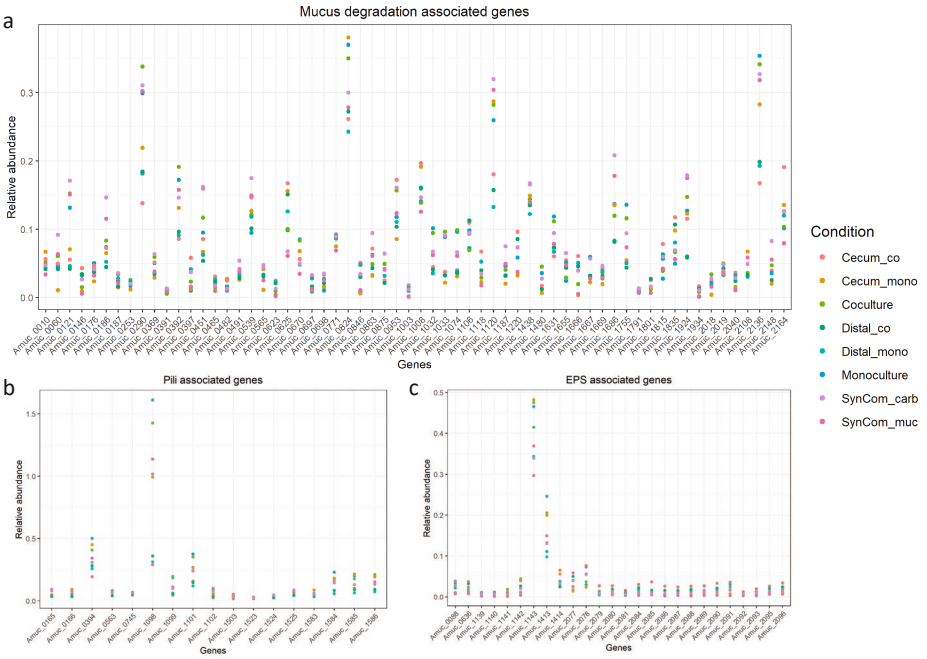

Figure 4: Relative abundance comparison of *A. muciniphila*'s key functions across the different ecosystems. a) mucus degradation associated genes, b) pili associated genes and c) EPS associated genes.

Discussion

This study made use of current transcriptomic databases and mined them for the expression profiles of *A. muciniphila*. This gave new insight into the transcriptional response of *A. muciniphila* in different ecosystems with increasing ecological complexity. Our results indicate that *A. muciniphila*'s overall transcriptional response is altered under different environmental conditions. However, the transcription of genes involved in mucus and glycan degradation, pili production and EPS production by *A. muciniphila* showed no significant differences throughout different ecosystems and are independent of environmental changes.

This study showed that the ecosystem complexity as well as the location and diet supplementation were substantial factors that led to the establishment of four different ecological *A. muciniphila* niches. We demonstrated that carbohydrate metabolism and glycan biosynthesis and metabolism pathways were among the most abundantly expressed pathways across all the samples used in this study irrespective

to location (*in vitro* and/or *in vivo*), diet intervention, and complexity of the culture (mono- or co-culture). A possible explanation for this might be that *A. muciniphila*'s ability to access the mucin glycans in any ecosystem will not change its fitness in the community. On the contrary, *A. muciniphila* in a competitive environment would increase its hydrolytic capacity by upregulating Glycoside Hydrolases (GHs) and mucin degrading genes. It is been described before that when *A. muciniphila* shared nutrients with the butyrate producer, *Anaerostipes caccae*, upregulation of mucin-degrading genes was observed (Chia et al. 2018). Additionally, it has also been described that in the presence of *B. thetaiotaomicron* in a solely mucin glycans environment, *A. muciniphila* upregulated GHs that target core glycosidic linkages found in mucin structure (Kostopoulos et al. 2021). Furthermore, in a mice study with synthetic microbiota, *A. muciniphila* and *Bacteroides caccae* showed increased expression of their *O*-glycan responsive genes in a fiber-free diet compared to a fiber-rich diet (Desai et al. 2016). Therefore, *A. muciniphila*'s glycans degrading activity was not significantly altered under different conditions where mucin glycans can be used as nutrient source. This is also depicted in the comparison of the relative abundance of *A. muciniphila* mucin-degrading genes.

The comparison of the different studies revealed, primary, separation in the transcriptional response of *A. muciniphila* between *in vivo* and *in vitro* studies. Even though the different experimental designs in this study grouped together in the ordination analysis, no distinct variation was observed between the complexity of the culture. However, the comparison only of the *in vitro* fermentations illustrated variation of *A. muciniphila* transcriptional response between the studies with increasing the microbial population in the bioreactors. A possible explanation for this could be that in the presence of other glycan degrading members in the community, *A. muciniphila* will change its gene response in order to be able to survive in a highly competitive environment. In the co-culture experiment, *A. muciniphila* shared the nutritional environment (mucin glycans) with the glycan generalist *B. thetaiotaomicron*. Bacteroidetes species that are abundant in the human gut (Martens et al. 2008, Salyers et al. 1977) have the ability to release antimicrobial proteins, the so-called membrane attack perforin proteins (MACPF) that are used to reduce the antagonism within microbial communities (Chatzidaki-Livanis et al. 2014, Roelofs et al. 2016). *B. thetaiotaomicron* significantly upregulated a gene encoding the MACPF protein targeting to reduce *A. muciniphila*'s fitness in the system (Kostopoulos et al. 2021). The structure and the activity of this protein has been characterized before (Xu et al. 2010). In the same study, it is suggested that *A. muciniphila* was able to counteract *B. thetaiotaomicron*'s attack by upregulating ABC transporters, two-component system encoding genes as well as LPS core biosynthesis genes. It has been described before

that LPS core biosynthesis genes and ABC transporters are required for antimicrobial peptide resistance (Wang et al. 2016, Ahmad et al. 2020, Sharp et al. 2019).

In the SynCom study, *A. muciniphila* has a stable abundance throughout the whole period of the experiment. The presence of other glycan-degrading bacteria in the community such as *Bacteroides xylanisolvens*, *Bacteroides ovatus* and *Bifidobacterium adolescentis* did not affect *A. muciniphila*'s function in the community. Another *in vivo* synthetic microbiota study, showed that *A. muciniphila*'s abundance was not affected by the presence of other glycan-degrading bacteria in the community, but its abundance was increased 2-fold only during the transition from fiber-rich to fiber-free diet (Desai et al. 2016). In the present study, the ordination analysis showed that *A. muciniphila*'s transcriptional response differentiated during the periodically addition of carbohydrates. Therefore, a fiber-rich diet could be considered as an influential factor for *A. muciniphila*'s response in a community.

Next, we monitored the most variable genes among the different studies. The analysis revealed the variable expression of multiple genes related to stress responses, including glutamate decarboxylase (Amuc_0372), autotransporter domain-containing protein (Amuc_0687), thioredoxin (Amuc_0691), molecular chaperone DnaK (Amuc_1406), rubrerythrin (Amuc_2055) and catalase HPII (Amuc_2070). These genes were found to be related to acid and oxidative stress responses in bacteria (Storz et al. 1990). Glutamate decarboxylase (GAD) is implicated in acid tolerance in several genera (Feehily and Karatzas 2013). Using this system, the decarboxylation of glutamate results in the uptake of one intracellular proton (H+) and thereby promotes acid tolerance. In *Escherichia coli* the GAD system was found to be the most important acid resistance mechanism (Capitani et al. 2003, Foster 2004). However, exposure of E. coli O157:H7 to H2O2 indicated the GAD system also promotes resistance against oxidative stress. Furthermore, molecular chaperone DnaK, involved in protein folding, was found to be induced in stresses other than heat shock, including acid and oxidative stresses (Susin et al. 2006). Thioredoxin, rubrerythrin and catalase HPII all play a role in oxidative stress resistance. *Akkermansia* ruberythrin was also detected in another study using mice samples, where it reflected the exposure of *A. muciniphila* to reactive oxygen or nitrogen species during inflammation (Berry et al. 2012). The relative abundances of these stress-related genes were highest in SynCom supplemented with mucus as the main carbon source. The oxygen reduction capacity of *A. muciniphila* through aerobic respiration has previously been shown (Ouwerkerk et al. 2016). In this study it was shown that *A. muciniphila* likely uses the Cytochrome bd complex in combination with other genes involved in the oxidative stress response such as superoxide dismutase, rubrerythrin, catalase HPII and alkyl hydroperoxide reductase. Interestingly, the relative abundance of the cytochrome bd

complex was not higher in SynCom_muc compared to the other conditions included in this study. Therefore, it is unlikely that the stress response revealed in SynCom_muc is due to the direct presence of oxygen, but more likely due to the presence of reactive oxygen species. We hypothesize that a lack of additional carbohydrates next to mucus, causes competition between bacterial species takes place leading to the production of antimicrobial products. This hypothesis is also supported by the SynCom OD_{600} measurements. The overnight fasting period, where the community was only supplemented with mucus without other complex carbohydrates, resulted in a drop in OD and qPCR analysis (Shetty et al. 2022).

For both EPS production and pili production, the expression pattern of genes was stable in complexity and conditions. In mucus degradation, the genes with the highest and lowest relative abundance within this subset were similar between conditions. However, variation between genes in each condition was observed. This might be due to changes in medium or mucus batches, as well as changes in complexity. For example, the main difference observed between conditions was found in SynCom. In this condition the gene with the highest relative abundance in mucus degradation was Amuc_2136, a beta-N-acetylhexosaminidase belonging to GH20. In contrast, Amuc_0824, a beta-galactosidase belonging to GH2, was shown to have the highest relative abundance among mucus degradation genes in all other conditions. This indicates that in a more complex community, *A. muciniphila* prioritizes to cleave GlcNAc or GalNAc from mucin glycans over beta-D-galactose residues in low complexity experiments. Even though Amuc_0824 is part of the top four mucus degradation genes in SynCom, this shows a consistent difference between conditions. The reason for this difference may be the complexity of the community in SynCom as compared to the other conditions.

Despite small variations in relative abundances of genes involved in the key functions of *A. muciniphila*, this data shows that overall *A. muciniphila* similarly exerts the key functions in all conditions included in this study. This data indicates that the key functions of *A. muciniphila* remain stable throughout different ecosystems and independent of environmental changes as long as mucus is available. This specialistic and competitive niche occupation is indicative for its relative high abundance and occurrence within the mucosal layer.

Acknowledgements

Frederik Bäckhed, Petia Kovatcheva-Datchary and Steven Aalvink are acknowledged for their important contribution on the studies involved in this research.

Material and methods

Studies and samples

We included RNA sequencing data from several studies with environmental and dietary differences (**Table 2**). Each of the conditions included in the study consists of multiple replicates (**Figure 5**). In the first condition, *A. muciniphila* was cultivated in mono-cultivations and co-cultivations (with *B. thetaiotaomicron*) in continuous fermentors. The second condition is an in vivo mouse study where *A.* mice were colonized with *A. muciniphila* mono-colonization and co-colonization (with *B. thetaiotaomicron*). In the last condition, *A. muciniphila* was cultivated as part of a synthetic community with 14 other species in in continuous fermentors. From this experiment, two different conditions were included: fasting with mucus as the main carbon source and feeding with additional carbohydrates and mucus.

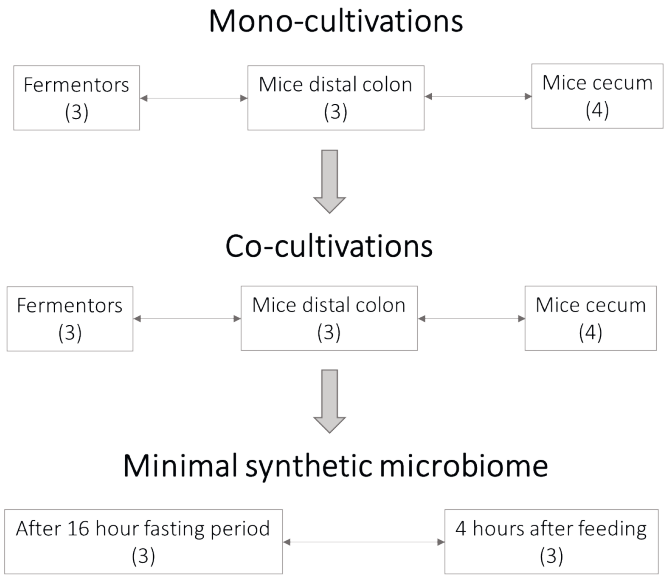

Figure 5: Conditions included in this study.

In vitro fermentation of *A. muciniphila* in mono- and co-culture

In vitro fermentations were conducted in three parallel bioreactors (DasGip, Eppendorf, Germany) filled with 250 ml of basal medium as it has been described before (ref for basal media) at 37°C, at a controlled pH of 6.5 and at a stirring rate of 150 rpm. The bioreactors and the feed bottle were supplemented with 0.5% of crude mucin, 1% of vitamin solution and at the beginning of the fermentation. Anaerobic conditions

were succeeded by sparging the media with N_2/CO_2 continuously (6 sL/h). Experiments were performed with 1% (v/v) supplementation of $CaCl_2$ and vitamin mixture as described previously. The media in both feed and bioreactors were reduced with 0.05% l-Cysteine-HCl in order to achieve anaerobic conditions. The bioreactors were inoculated with a normalized O.D. of 1.0 of both species to achieve same starting cells density in the beginning of the fermentation. The flow rate of the feed was set at 20 ml/h and the recovery rate of media was 12.5 hours. The growth was measured by spectrophotometer as optical density at 600 nm. Both cultures were normalized to O.D. = 1.0 prior to bioreactors addition. The experiment was done in three biological replicates.

In vivo fermentation of *A. muciniphila* in mono- and co-culture

All the mouse experiments were performed using protocols approved by the University of Gothenburg Animal Studies Committee. Female Swiss Webster germ free mice have been housed in experimental isolators during the colonization period. Mice were fasted 4h prior gavage (intragastrical) with 0.2 ml of active culture (for both mono- and co-colonizations). For *B. thetaiotaomicron* mono- (n=5 mice) and bi-colonization (n=7 mice) have used 10^8 CFU/ml. For *A. muciniphila* (n=8 mice) mono-colonization 10^9 CFU/ml have used. For all three colonization, mice were inoculated with a single gavage of the respective culture. During the experiment, the mice had free to autoclaved water and food. The mice received during the whole period of the colonization chow diet (5021 rodent diet, LabDiet; fat 9% wt/wt) (Supplementary Table X). Intestinal segments (ileum, cecum and distal colon) and feces were harvested after14-days of colonization and immediately stored in RNA Later (Sigma) at -20°C until further processed.

Synthetic community

The synthetic communities were cultivated in the following medium: KH_2PO_4 (0.408 g/L), $Na_2HPO_4.2H_2O$ (0.534 g\L), NH_4Cl (0.3 g/L), NaCl (0.3 g/L), $MgCl_2*6H_2O$ (0.1 g/L), $NaHCO_3$ (4 g/L), yeast extract (2 g/L), beef extract (2 g/L), CH_3COONa (2.46 g/L), casitone (2 g/L), peptone (2 g/L), cysteine-HCl (0.5 g/L), carbohydrates (1.1 g/L), resazurin (0.5 mg/L), 1 mL trace elements in acid (50 mM HCl, 1mM H_3BO_3, 0.5 mM $MnCl_2*4H_2O$, 7.5 mM $FeCl_2*4H_2O$, 0.5 mM $CoCl_2$, 0.1 mM $NiCl_2$, and 0.5 mM $ZnCl_2$, 0.1 mM $CuCl_2*2H_2O$), 1 mL trace elements in alkaline (10 mM NaOH, 0.1 mM Na_2SeO_3, 0.1 mM Na_2WO_4, and 0.1 mM Na_2MoO_4), 1 mL haemin solution (50 mg haemin, 1 mL 1N NaOH, 99 mL dH_2O), 0.2 mL vitamin K1 solution (0.1 mL vitamin K1, 20 mL 95% EtOH). After autoclaving and before inoculation, 1% of vitamin solution was added (11 g/L $CaCl_2$, 20 mg biotin, 200 mg nicotinamide, 100 mg p-aminobenzoic acid, 200 mg thiamin (vitamin B1), 100 mg panthothenic acid, 500 mg pyridoxamine, 100 mg cyanocobalamin (vitamin B12), and 100 mg riboflavin). Initially the medium contained 0.5% crude mucin and 1.11 g/L of each xylan, soluble starch, inulin and pectin. The fermentors were spiked

three times a day with a 4-hour gap using four carbohydrates (xylan, soluble starch, inulin and pectin) with an end concentration of 0.1% each. The feed consisted of this medium supplemented with 0.5% crude mucin. Each fermentor, three in total, was inoculated with 15 gut species: *Akkermansia muciniphila* (ATCC BAA-835), *Bacteroides ovatus* (HMP strain 3_8_47FAA), *Bacteroides xylanisolvens* (HMP strain 2_1_22), *Anaerobutyricum soehngenii* (DSM 1736), *Coprococcus catus* (ATCC 27761), *Flavonifactor plautii* (HMP strain 7_1_58FAA), *Eubacterium sireaum* (DSM 15702), *Agathobacter rectalis* (DSM 17629), *Roseburia intestinalis* (DSM 14610), *Faecalibacterium prausnitzii* (A2-165), *Subdoligranulum variabile* (DSM 15176), *Ruminococcus bromii* (ATCC 27255), *Blautia obeum* (DSM 25238), *Collinsella aerofaciens* (DSM 3979/ATCC 25986) and *Bifidobacterium adolescentis* (L2-32).

RNAseq analysis

Illumina reads have been trimmed for low quality and adapters with fastp (v0.20.0) (21) using default settings. rRNA sequences have been removed with bbduk (v38.79) (https://sourceforge.net/projects/bbmap/) using the following parameters k=31 and ref=riboKmers.fa.gz. Transcripts from the reference strain of *A. muciniphila* (GCF_000020225.1) have been quantified with RSEM (v1.3.1)(Li and Dewey 2011) in combination with bowtie2 (v2.3.5.1)(Langmead and Salzberg 2012). Mapping and read quality were inspecting using MultiQC. Raw counts were obtained using Tximport (v1.12.3)(Soneson et al. 2016) and used to calculate the relative abundance of each gene within each sample. Canoco 5 (version 2.8.12) was used for RDA and PCA analysis based on the relative abundance data. All further analysis was done using R version 3.6.3 in Rstudio version 1.2.5019.

Table 2: Overview of the samples with additional ecosystem information.

Sample	Diet	Location	Condition
Monoculture_1	Mucus	Fermentors	Monoculture
Monoculture_2	Mucus	Fermentors	Monoculture
Monoculture_3	Mucus	Fermentors	Monoculture
Coculture_1	Mucus	Fermentors	Coculture
Coculture_2	Mucus	Fermentors	Coculture
Coculture_3	Mucus	Fermentors	Coculture
Cecum_mono_1	Chow diet	Mice	Cecum_mono
Cecum_mono_2	Chow diet	Mice	Cecum_mono
Cecum_mono_3	Chow diet	Mice	Cecum_mono
Cecum_mono_4	Chow diet	Mice	Cecum_mono
Cecum_co_1	Chow diet	Mice	Cecum_co
Cecum_co_2	Chow diet	Mice	Cecum_co
Cecum_co_3	Chow diet	Mice	Cecum_co
Cecum_co_4	Chow diet	Mice	Cecum_co
Distal_mono_1	Chow diet	Mice	Distal_mono
Distal_mono_2	Chow diet	Mice	Distal_mono
Distal_mono_3	Chow diet	Mice	Distal_mono
Distal_co_1	Chow diet	Mice	Distal_co
Distal_co_2	Chow diet	Mice	Distal_co
Distal_co_3	Chow diet	Mice	Distal_co
SynCom_muc_1	Mucus	Fermentors	SynCom_mucus
SynCom_muc_2	Mucus	Fermentors	SynCom_mucus
SynCom_muc_3	Mucus	Fermentors	SynCom_mucus
SynCom_carb_1	Carbohydrates and mucus	Fermentors	SynCom_carb
SynCom_carb_2	Carbohydrates and mucus	Fermentors	SynCom_carb
SynCom_carb_3	Carbohydrates and mucus	Fermentors	SynCom_carb

Supplementary information

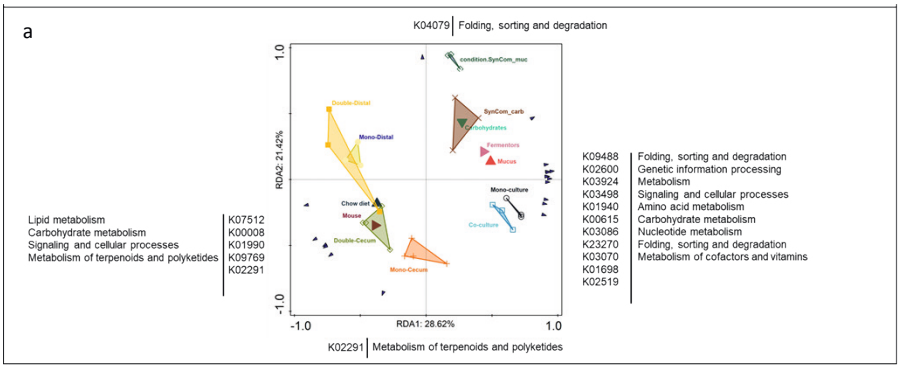

Supplementary Figure 1: Ordination analysis of the ecosystem studies and the most variable expressed KEGG Orthologies (KOs). a) RDA analysis showing the 20 most variable KOs within all studies involved in this study, b) RDA analysis showing the 20 most variable Kos within the *in vitro* studies. The plots were generated by Canoco.

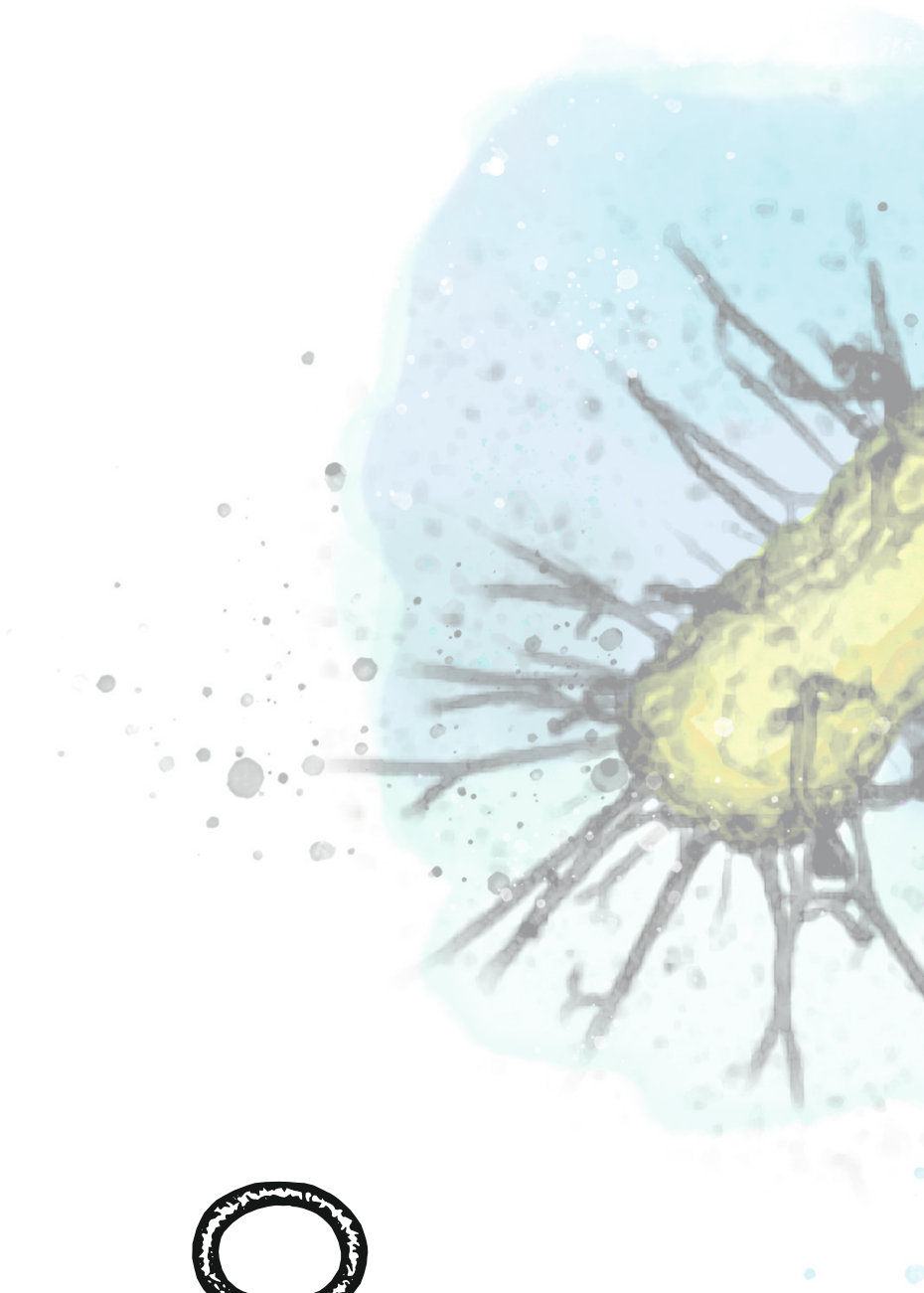

Chapter 8

General discussion

Since the isolation of *A. muciniphila* in 2004, numerous studies have addressed the ecology, physiology and genomics of this intestinal symbiont. Due to its function in host health, this bacterium has received considerable attention over the last two decades and is considered a promising candidate as next-generation probiotic and therapeutic agent. In this thesis, we assessed the functions of *A. muciniphila* in the human body and other mammalian hosts, as well as in *in vitro* and *in vivo* models including a multi-species synthetic community. Furthermore, we gained insight into one of the physiological characteristics of *A. muciniphila* during growth in industrial media, which contributed to identifying the genes and pathway of exopolysaccharide (EPS) production. The observations and findings described in the research chapters of this thesis will be discussed below, followed by concluding remarks and perspectives on future research of *A. muciniphila*.

Akkermansia-like species in the human body

The human body contains a high variety of coexisting microorganisms, which form various microbial communities in human body parts such as the skin, oral cavity, gut and vagina (Gilbert et al. 2018). In **chapter 2** we reviewed the presence of *Akkermansia*-like spp. in the human gastrointestinal tract based on their 16S rRNA sequence and metagenomics signatures to understand its colonization pattern in time and space. This analysis revealed the presence of *A. muciniphila*-like bacteria next to the colon in the oral cavity, pancreas, biliary system, small intestine, the appendix and human milk.

The presence of *Akkermansia*-like bacteria in human milk suggests a role in colonization of breast-fed infants. *A. muciniphila* signatures have been detected in colonic samples from infants a few weeks after birth. After the publication of the review in **chapter 2**, multiple studies have been published focusing on the utilization of human milk oligosaccharides (HMOs) by *A. muciniphila* (Kostopoulos et al. 2020, Luna et al. 2022, Ottman 2015). The hypothesis of the capability to utilize HMOs was risen by the structural resemblance between mucus glycans and HMOs and supported by the earlier observed growth in mother's milk (Ottman 2015)(**Figure 1**). Proteome data confirmed the functionality of key-glycan degrading enzymes (α-*L-fucosidases,* β-*galactosidases, exo*-α-*sialidases and* β-*acetylhexosaminidases) of A. muciniphila* Muc^T in the degradation of several HMO structures including 2'-fucosyllactose, lacto-*N*-tetraose, lactose, 3'-siallylactose and lacto-*N*-triose II (Kostopoulos et al. 2020). More recently, the utilization efficiency of HMOs was determined for a broad range of human-associated *Akkermansia* strains (Luna et al. 2022). Phylogenetic analysis identified four phylogroups (AmI-AmIV) using their isolates and those of a previous study (Luna et al. 2022, Guo et al. 2017). Phylogenomics revealed differences in the

genomic capacity of these strains to utilize HMOs. However, representative strains of each phylogroup were able to grow using HMOs. The utilization of HMOs enables the survival of *A. muciniphila* in the gut in early life, where it may influence the microbial ecology during the development of the gut microbiota. These findings are in line with our hypothesis in **chapter 2**, suggesting a role of *A. muciniphila* in the colonization of breast-fed infants.

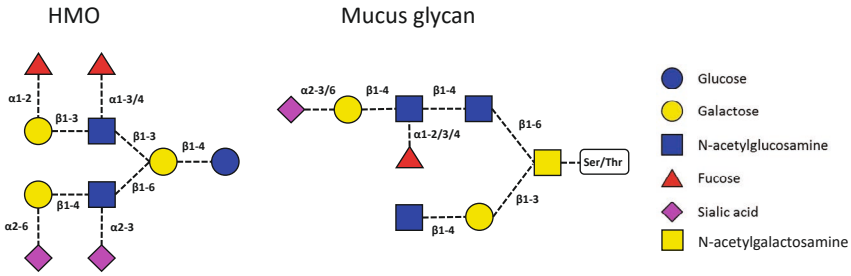

Figure 1: Schematic overview of HMO and mucus glycans, adapted from Akkerman et al. 2018 and Tailford et al. 2015, respectively (Akkerman et al. 2018, Tailford et al. 2015).

Phylogenetic analysis of these 16S rRNA sequences, performed in **chapter 2**, revealed separate clustering of a selection of *Akkermansia*-like spp. derived from the ileum samples in one out of three clades in total. The ileum-derived *Akkermansia*-like spp. clustering separately as well as the ones clustering together with colon samples may have an important role in the ileum. Previously, *A. muciniphila* Muc^{T} was found to colonize the ileum, within 50 μm from the epithelium, of germ-free mice reaching 1.87 (±2.37) × 10^{8} cells/g of ileal content (Derrien et al. 2011). Multiple mouse studies showed effects of *A. muciniphila* on the ileum, including reinforcement of the intestinal barrier, changes in the ileal metabolome related to improvement of gut barrier function as well as anti-aging and anticancer effects (Plovier et al. 2017, Wu et al. 2017, Grajeda-Iglesias et al. 2021). Another study supplementing accelerated aging *Ercc1*$^{-/\Delta 7}$ mice with *A. muciniphila* Muc^{T} observed a decreased expression of genes and pathways associated to inflammation, immune function, and antimicrobial peptide production in the ileum (van der Lugt et al. 2019). Furthermore, *A. muciniphila* supplementation significantly lowered frequencies of activated B cell subtypes and increased frequencies of more immature B cell subtypes in Peyer's patches. Altogether this suggests *A. muciniphila* may contribute to prevent the age-related state of epithelial distress in ileum. Considering most of these studies were performed only with the type-strain Muc^{T}, it would also be of interest to elaborate this study further using *Akkermansia*-like spp. derived from the ileum, for example by isolating and using

the *Akkermansia*-like spp. clustering separately in the phylogenetic tree displayed in **chapter 2** to assess whether their effects on the ileum differ from that of the type-strain Muc^T.

New *Akkermansia* spp. discovery

The presence of *Akkermansia*-like spp. is also widely spread among the animal kingdom, despite differences in GI tract anatomy, diet, host physiology and body temperature. Only one other *Akkermansia* spp., next to *A. muciniphila*, has been described to date. This species was isolated from python feces and named *Akkermansia glycaniphila* Pyt^T (Ouwerkerk et al. 2016). The average nucleotide identity (ANI) of this species was 79.9% as compared to *Akkermansia muciniphila* Muc^T, which is below the recommended cut-off point for species delineation (Ouwerkerk et al. 2016, Goris et al. 2007). Furthermore, phenotypic, phylogenetic and genetic characteristics supported the affiliation of *A. glycaniphila* Pyt^T to the genus *Akkermansia*.

To continue the characterization of *Akkermansia*-like bacteria throughout the animal kingdom, we aimed to isolate *Akkermansia*-like bacteria from different mammalian hosts (**chapter 3**). Here we isolated 10 new *A. muciniphila* strains from the feces of chimpanzee, siamang, mouse, pig, reindeer, horse and elephant. All new strains were found to have low genomic divergence compared to the type-strain, as well as a conserved mucus degradation capability. Here, our mucin-based isolation efforts using mammalian fecal samples did not result in the isolation of novel *Akkermansia* spp. but rather showed high similarities between *Akkermansia* species found in in mammalian and human fecal samples.

Recently, new *A. muciniphila* strains have been isolated from the human gut showing that healthy individuals can carry more than one *A. muciniphila* but very similar strains (Ouwerkerk et al. 2022). Also here, mucus degradation pathways were found to be conserved amongst all isolates. In contrast to these findings and our findings in **chapter 3**, an increasing number of studies are declaring they may have identified candidate species belonging to the *Akkermansia* genus in the human gut (Kumar et al. 2022, Guo et al. 2017, Karcher et al. 2021). Two of these studies are solely based on genome comparisons indicating there may be other *Akkermansia* species present in the human gut (Guo et al. 2017, Karcher et al. 2021). Recently, a novel species has been proposed named *Akkermansia* sp. DSM 33459, isolated from the human gut. The described ANI was 87.58% in comparison to the *A. muciniphila* Muc^T but the 16S rRNA identity was >99 %, questioning the support for describing this as a new species. A few physiological characteristics were also described in this study. However,

this was limited to carbon source tests, cell wall fatty acid analysis and temperature and antibiotic resistance assessments. It is also important to note that the medium conditions used in this study for the characterization of this strain and comparison with the type-strain were not optimal for cultivation of *A. muciniphila* resulting in low biomass with OD600 values below 0.3. The cultivation conditions used in this study did not take the necessity for N-acetylglucosamine and L-threonine into account, as described previously (Ottman et al. 2017, van der Ark et al. 2018). Furthermore, N-acetylglucosamine has not been included in the carbon source assessment and the phenotypic analysis is lacking (Kumar et al. 2022). Therefore, this isolate DSM 33459 may be just a new *A. muciniphila* strain and more experimental data are needed to support the designation of a new species within the *Akkermansia* genus. In general, it would be useful to establish minimal standards to assign new species to the *Akkermansia* genus, as was done for other genera including *Campylobacter*, *Arcobacter*, *Helicobacter* and *Wolinella* (On et al. 2017). With this approach, errors in assigning new species may be minimized.

Bacterial EPS production and the case of *A. muciniphila*

EPS production pathways in bacteria

Four main mechanisms exist for the production of EPS in bacteria: Wzx/Wzy-dependent pathway, the ATP-binding cassette (ABC) transporter-dependent pathway, the synthase-dependent pathway and the dextrase/sucrase-dependent pathway (Schmid 2018). The Wzx/Wzy pathway is mostly used by bacteria to produce branched heteropolysaccharides. Repeating units are assembled by highly specific glycosyltransferases (GTs) and linked to an undecaprenol diphosphate (Und-P) anchor located in the inner membrane. Then, a flippase encoded by the Wzx gene translocates the repeating unit into the periplasm. There, the polymerase, encoded by the Wzy gene, recognizes the repeating units and polymerizes these by backbone assembly. In some cases, polymerization is performed in combination with a co-polymerase, which can be involved in chain length determination. Lastly, the polymer is exported out of the cell by an outer membrane polysaccharide export (OPX) protein. Well known examples of EPS produced through this pathway are xanthan, succinoglycan and different sphingans (Freitas et al. 2017, Schmid et al. 2014, Schmid et al. 2015). In **chapter 5**, we identified that *A. muciniphila* may be using this pathway to produce EPS.

Factors affecting EPS production by bacteria

The yield, size and composition of EPS varies in different strains. Environmental conditions and substrate compositions such as carbon source, nitrogen source, pH,

oxygen and temperature mainly effect the production of EPS by bacteria (Shukla et al. 2019). For example, EPS production by *Bacillus sphaericus*, now reclassified as *Lysinibacillus sphaericus*, was affected by the use of different carbon sources (Yilmaz et al. 2012). In this study, supplementing the culture with fructose resulted in the highest EPS yield. However, a difference in composition was also detected. Both LB medium with and without fructose mainly resulted in EPS consisting of galactose and a low amount of glucuronic acid, whereas medium supplemented with molasses resulted in EPS composed of mannose, galactose and glucuronic acid. In **chapter 5** we found that the EPS yield of *A. muciniphila* is affected by the available carbon source as well, where more EPS is produced in the highest GlcNAc concentration. Furthermore, pH, temperature and carbon source were found to affect the EPS production yield by *Streptococcus thermophilus* (Zisu and Shah 2003). This bacterium is known for its presence in yogurt, where its EPS was found to enhance the texture, viscosity and modify mouthfeel (Broadbent et al. 2003). Lastly, temperature affected EPS production by *Lactobacillus paracasei* strains isolated from kefir (Bengoa et al. 2018). Lower cultivation temperatures resulted in the appearance of a high molecular weight fraction as well as an increase in the total amount of EPS. Altogether, this indicates that optimization of cultivation conditions for different strains is necessary to reach high EPS yields or a specific EPS composition for further biotechnological use. The effect of temperature and pH on EPS production has not yet been tested for *A. muciniphila*. In general, environmental stresses and alterations in growth conditions may be used to optimize EPS production for industrial applications (Nguyen et al. 2020).

Application of bacterial EPS

The biotechnological production of microbial EPS is a faster alternative than for example chemical and plant-derived production (Barcelos et al. 2020). In addition, the market for the use of microbial EPS is expanding due to the possibility of using renewable sources. At present, microbial EPS are used in many industries including the food industry, pharmaceutical industry, cosmetics industry, agriculture and bioremediation and bioleaching among others (Shukla et al. 2019). The most well-known and used EPS used in the food industry is gellan gum, which functions in controlling flavor release in a wide range of pH (Barcelos et al. 2020). This EPS also has a role in texture improvement and physical stability of the food products. Next to gellan gum, EPS produced by lactic acid bacteria are widely used in food industry, where they improve rheological properties of fermented dairy products, such as yogurt. In pharmaceutical industries, EPS are used for several applications including tissue regeneration, controlled release of drugs, tissue engineering and coating of medical devices (Barcelos et al. 2020, Shukla et al. 2019). Especially pullulan is used for a wide variety of applications within pharmaceutical and medical industries

due to its unique linkage pattern resulting in distinctive physical properties. These properties include adhesive ability, the capacity to form fibers and thin transparent biodegradable films impermeable to oxygen (Cheng et al. 2011). As shown in **chapter 5**, *A. muciniphila* produces fucose-containing EPS (fuc-EPS). Fuc-EPS has also been detected in *Bifidobacterium* spp. including *Bifidobacterium pseudocatenulatum* and *Bifidobacterium longum* (Salazar et al. 2009). In this study, the production of Fuc-EPS was found to be strain specific. Similar findings were described for lactic acid bacteria, where two strains belonging to *Lactobacillus gasseri* and *Lactiplantibacillus plantarum* and one *Streptococcus thermophilus* strain were found to produce Fuc-EPS (Juraskova et al. 2022, Korcz and Varga 2021). Fuc-EPS has obtained increased interest in both food and pharmaceutical industries as a promising source for fucose, due to their antioxidant, prebiotic, anti-cancer, anti-inflammatory and anti-viral activities (Xiao et al. 2022). In conclusion, different types of EPS with different properties, may serve a role in many applications, increasing the interest of optimizing the biotechnological production of EPS.

A. muciniphila alone or in a community

In this thesis, we studied *A. muciniphila* in both mono-cultivations and communities throughout the different chapters. The availability of transcriptional data from these chapters and others (Kostopoulos et al. 2021) allowed for a comparison of *A. muciniphila* in different ecosystems in **chapter 7**. Here we demonstrated that *A. muciniphila* exerts its key functions stably throughout different ecosystems in the presence of mucin glycans, including mono-and co-cultivations in fermentors and mice, and in a synthetic community in fermentors. These key functions include mucus degradation, pili production and EPS production.

Even though the expression of genes associated with EPS production did not show significant differences between conditions, EPS produced by *A. muciniphila* may still be altered in a co-cultivation or community. As discussed previously, carbon source availability could also affect the EPS composition and yield (Yilmaz et al. 2012, Zisu and Shah 2003). In the mono-cultivation the medium was supplemented with mucin (Kostopoulos et al. 2021), whereas the synthetic community (**chapter 6** – see below) was supplemented with mucin as well as dietary complex carbohydrates. This may result in the release of different carbon sources into the medium as opposed to the mono-cultivation, possibly affecting EPS composition and yield by *A. muciniphila*. However, to confirm this hypothesis, more experiments should be performed analyzing *A. muciniphila* EPS in co-cultivations, communities or mono-cultivations supplemented with different carbon sources.

In ecological niches, bacteria may rely on each other forming symbiotic relationships, or compete against each other for nutrients or to remain in the current ecological niche (Bauer et al. 2018). So far, the evidence suggests that *A. muciniphila* may not change to a competitive lifestyle as long as mucin is present. For example, it has previously been shown that in a co-culture with *Bacteroides thetaiotaomicron*, the expression profile of *A. muciniphila* was less affected than that of *B. thetaiotaomicron,* which upregulated its glycoside hydrolases (GHs) and mucin degradation activity in the co-cultivation as compared to mono-cultivations (Kostopoulos et al. 2021). In contrast, in *A. muciniphila* the expression of mucin degradation genes was increased in a co-cultivation together with *Anaerostipes caccae* compared to when grown as a monoculture (Chia et al. 2018). These species were not competing for mucin glycans, but *A. caccae* can utilize mucin-derived sugars (Belzer et al. 2017). Therefore, *A. muciniphila* may have increased the expression of mucus degradation genes to increase substrate availability for *A. caccae* in this co-culture (Chia et al. 2018). However, an increase in relative abundance of mucus-degradation genes was not observed in the synthetic community compared to mono-cultivations (**chapter 7**). The expression profiles of mucus-associated genes of *A. muciniphila* based on relative abundances remained stable in the synthetic community as well as mono-and co-cultivations and did not show significant differences between conditions (**chapter 7**). It is also important to note that the synthetic community, described in **chapter 6**, was lacking an additional mucus degrader next to *A. muciniphila*. Therefore, it would be of interest to study whether *A. muciniphila* exhibits competitive behavior in a synthetic community where other mucus degraders are also included. This could include well-known mucus degraders present in the human gut microbiota, such as *Ruminococcus gnavus*, *Ruminococcus torques*, several *Bifidobacterium* and *Bacteroides* species.

Studying the human gut microbiota using synthetic microbial communities

The ecosystem in the human gut is a niche with extremely complex and dynamic interactions (Sung et al. 2017). Many different interactions take place between the microorganisms inhabiting the human gut, leading to both competitive and symbiotic relationships. As explained previously, both dietary fibers and host glycans play an important role in the metabolic activity and interspecies metabolic interactions of the human gut microbiota (Salonen and de Vos 2014, Berkhout et al. 2022). Due to the high complexity of the human gut microbiota, the use of synthetic microbial communities with reduced complexity to study microbe-microbe interactions, as well as host-microbe interactions has obtained considerable attention (Desai et al. 2016, Kovatcheva-Datchary et al. 2019, Oliphant et al. 2019, D'Hoe et al. 2018, Venturelli et

al. 2018). In **chapter 6** we assembled a 16-species synthetic microbial community to study dynamic metabolic interactions and trophic roles under controlled conditions. In this minimal microbiome, both the presence of dietary fibers and host glycans were taken into account.

The increasing use of synthetic microbial communities to study the gut microbiota has also led to discussions about the representability of synthetic communities as compared to the actual community in the gut (Berkhout et al. 2022, Mabwi et al. 2021). In synthetic communities, bacterial species can be chosen based on their function in the human gut. For example, in **chapter 6,** we assembled a synthetic community by choosing species relevant to the human microbiome based on gut metagenome screening, that mimic key ecological and metabolic properties. However, *in vitro* models cannot fully mimic the human gut, but rather approximate this environment. Therefore, there are some disadvantages to the use of synthetic microbial communities as well. To date, not all members of the human gut microbiota have been cultured, which limits the use of bacterial species within the synthetic community (Berkhout et al. 2022). Moreover, due to the limitations in mimicking the natural intestinal environment, microbes that are part of the synthetic community may take on different roles as compared to their role *in vivo*. Lastly, tracing substrates and metabolites in *in vitro* synthetic communities is difficult. Therefore, it is often not possible to distinguish substrate utilization and metabolite production between species. However, this technique also harbors several advantages over using for example whole fecal communities (Mabwi et al. 2021). The use of a known synthetic community allows for controllable and reproducible experiments. Furthermore, a more stable consortium can be created than with the use of fecal samples, without the presence of viruses and pathogens. In addition, key features of the natural ecosystem can be conserved in synthetic communities, while also being susceptible to modelling (Grosskopf and Soyer 2014). For example, synthetic communities may also be used to achieve a certain functional output, beyond solely studying community functions and interactions mimicking the gut microbiota (Clark et al. 2021). Taking both advantages and disadvantages into account, we may not be able to fully mimic the human intestinal environment *in vitro*, but it can give us a lot of information on the activity of species within the ecosystem as well as microbe-microbe interactions and even optimize functional output of the communities.

The use of *A. muciniphila* for therapeutic applications

The growing insights into the role of the human gut microbiota in host health led to an increased interest into the discovery and use of novel microbes to improve

health outcomes, including *A. muciniphila* (Brodmann et al. 2017). Due to the beneficial effects of *A. muciniphila* shown in mouse models, human individuals, and cell lines (explained in detail in **chapter 1**), this bacterium has emerged as one of the most promising next-generation microbes for therapeutic applications. However, several parameters need to be considered, to be able to successfully apply *A. muciniphila* to improve human health including cultivation methods and applying pasteurized or live bacteria. Furthermore, if live cells are needed, several stressors need to be considered such as oxygen, bile acids and antibiotics for the preservation of viable *A. muciniphila* cells.

Cultivation

Recently, a defined minimal medium for the cultivation of *A. muciniphila* was formulated based on the genome scale metabolic model of *A. muciniphila* and the composition of mucin, which *A. muciniphila* uses as sole carbon, nitrogen and energy source (Ottman et al. 2017, van der Ark et al. 2018). This resulted in the identification of the necessity for GlcNAc and L-threonine. Fastest growth was observed in the defined minimal medium supplemented with L-threonine and both glucose and GlcNAc (van der Ark et al. 2018). Therefore, in **chapter 4** we attempted to design a non-allergenic and animal component free, food-grade medium supplemented with L-threonine using both glucose and GlcNAc as carbon sources, allowing for efficient growth to high densities as to provide cost-effective production platforms. We discovered that the use of pea peptone and a high total concentration of the carbon source (150mM) in ratio 3:1 (glucose to GlcNAc) under controlled fermentor conditions, resulted in high biomass yields, reaching an optical density (OD) value of 16 as opposed to an OD value of approximately 2 on mucus medium and minimal medium supplemented with glucose/GlcNAc (Ottman et al. 2017, van der Ark et al. 2018). However, due to the elongated cells observed in our food-grade medium, the previously described relation where an OD_{600} of 1 correlates to 4.0×10^8 CFU per mL is not accurate when assessing growth on this medium (Ouwerkerk et al. 2016). The reason for this is that larger cells scatter more light, which increases the OD_{600} (Volkmer and Heinemann 2011). Therefore, to compare the cell numbers in media with different cell morphologies, quantitative qPCR, CFU counts or flow cytometry could be used. Even though the comparison growth rate and yield between mucus medium and food grade medium is complicated due to cell morphology changes, the large difference in OD_{600} observed in our data indicates food-grade medium may be used to produce *A. muciniphila* in high yields for therapeutic purposes.

Pasteurized vs. live *A. muciniphila*

The differences between the effect of pasteurized and live *A. muciniphila* cells, and *A. muciniphila* derived products have been investigated in several studies in mice

(Plovier et al. 2017, Ashrafian et al. 2021, Raftar et al. 2021, Ashrafian et al. 2019) and Caco-2 cell lines (Shi et al. 2022, Ashrafian et al. 2021). The first study reporting a difference in the use of pasteurized and live *A. muciniphila* found an enhanced effect of pasteurized cells in its capacity to reduce fat mass development, insulin resistance and dyslipidemia in high-fed diet (HFD)-fed mice. Since then, a stronger effect of pasteurized *A. muciniphila* cells than live cells on several parameters was also described for other mouse or cell-line studies (Ashrafian et al. 2021, Ashrafian et al. 2021). These parameters included greater effects in metabolic parameters, preventing the onset of obesity, strengthening gut barrier function, and maintaining immune homeostasis in mice, as well as upregulation of tight-junction proteins and regulation of immune response-related genes in Caco-2 cell lines. In contrast, greater effects of live *A. muciniphila* have also been reported (Ashrafian et al. 2021, Raftar et al. 2021, Shi et al. 2022). In mice, live cells were shown to have greater effects on the modulation of gene expression related to fatty acid synthesis, energy homeostasis and immune response in the liver (Ashrafian et al. 2021). Furthermore, this model also showed a greater effect of live cells on body weight, in contrast to findings in other studies (Raftar et al. 2021). In addition, as compared to pasteurized cells, live *A. muciniphila* was found to have a greater effect on improvement of the gut microbiota composition in mice, reducing the relative abundance of pathobionts while increasing the relative abundance of symbionts (Raftar et al. 2021, Ashrafian et al. 2021). Lastly, in Caco-2 cells, a difference was found in the expression of tight-junction protein claudin1, which was increased greater in the presence of live cells as opposed to pasteurized *A. muciniphila* cells (Shi et al. 2022). Even though some differences have been observed between the use of pasteurized and live *A. muciniphila* cells, all studies confirm the beneficial effects of both treatment methods in mice and Caco-2 cells (Plovier et al. 2017, Ashrafian et al. 2021, Ashrafian et al. 2021, Raftar et al. 2021, Shi et al. 2022). However, the only reported study in humans confirmed the capacity of pasteurized *A. muciniphila* Muc^T cells to be at least as effective as live cells (Depommier et al. 2019).

The mechanisms behind the observed differences between pasteurized and live *A. muciniphila* cells have not been elucidated yet. The initial discovery of the surprising effect of pasteurized *A. muciniphila* cells described the thermostability of the Amuc_1100, a TLR2-agonist that improves the gut barrier and partly exerts the beneficial effects of the bacterium (Plovier et al. 2017). Hence, it has been hypothesized that pasteurization may increase accessibility of certain proteins to the host (Plovier et al. 2017). This may be the case through weakening of the cell wall as a result of pasteurization, leading to increased accessibility of cell wall-associated proteins and the release of cellular proteins. Therefore, using the same number of cells, certain proteins exerting health effects on the host (for example Amuc_1100), may be more accessible, resulting in a greater effect of pasteurized cells on certain health

parameters. In contrast, live *A. muciniphila* cells may have a greater effect in other aspects due to their activity in the gut. For example, by increasing the number of *A. muciniphila* cells, exerting its function as mucin degrader by releasing sugars and through SCFA production, increasing cross-feeding activity with other members of the community. However, to reveal how the different effects on the host of pasteurized and live *A. muciniphila* cells arise, more experiments need to be performed, focusing on the underlying mechanism of certain health effects *A. muciniphila* exhibits on its host in both forms and the differences in content and function of pasteurized and live *A. muciniphila* cells. Lastly, before live *A. muciniphila* can be considered for therapeutic purposes, safety assessments should be performed to apply this form of *A. muciniphila*, which has already been established for the application of pasteurized *A. muciniphila* cells (Druart et al. 2021, Turck et al. 2021). When the differences between live and pasteurized cells on the human host and safety assessments are fully elucidated, decisions may be made on which form of *A. muciniphila* should be applied depending on the desired effect on the host.

Environmental stressors affecting viable delivery of *A. muciniphila*

To ensure viable delivery of *A. muciniphila* into the human gut, several environmental parameters should be considered. First, the antibiotic resistance profile of the bacterium should be determined. In this way it is known which antibiotics would affect the viability of *A. muciniphila*, but it is also important to ensure the absence of transmissible antibiotic resistance to avoid development of new antibiotic-resistant pathogens. Several tests have been performed to determine the antibiotic susceptibility of *A. muciniphila* Muc^T (Dubourg et al. 2013, Cozzolino et al. 2020, Maier et al. 2021, Ouwerkerk 2016). A broad test to determine the antibiotic susceptibility of *A. muciniphila* Muc^T (including 144 antibiotics) showed resistance to nearly all quinolone antibiotics. However, to date no evidence has been found for horizontal acquisition or antibiotic resistance genes that are linked to known genetically transferrable elements in the type-strain (Cani and de Vos 2017, Machado et al. 2022). Another parameter that should be considered is the bile acid tolerance of *A. muciniphila*. For the viable delivery of *A. muciniphila* in the human gut, it needs to survive transit through the small intestine, where the secretion of digestive enzymes and bile cause a harsh environment for microbial growth, unless the bacterial cells are encapsulated. As discussed in **chapter 2,** *Akkermansia*-like sequences were detected in bile and gallstone samples, as well as in the small intestine. Additional experiments also revealed bile resistance when exposed to up to 1% porcine bile and increased growth in culture conditions with bile salt sodium deoxycholate, although most bile salts in this study did inhibit the growth of *A. muciniphila* (van der Ark 2018, Hagi et al. 2020). Therefore, more experiments are needed to determine whether live *A. muciniphila* cells can reach the human large intestine or if other methods are

required, such as encapsulation to protect the cells during gastric passage. This may also protect the live *A. muciniphila* cells against oxygen in the gastric conditions. Even though *A. muciniphila* was found to thrive in the presence of nanomolar concentrations of oxygen, high oxygen concentrations may still affect its viable delivery (Ouwerkerk et al. 2016). A workflow has been described for the preparation and preservation of viable *A. muciniphila* cells (Ouwerkerk et al. 2017). With this workflow, viable cells were retrieved from cecal and colon content of high-fat treated mice. More recently, encapsulation of *A. muciniphila* has obtained increased interest, including double emulsions, double-network hydrogel microstructures, microencapsulation in xanthan and gellan gum, and the latter embedded in dark chocolate (van der Ark et al. 2017, Lu et al. 2021, Marcial-Coba et al. 2018, Marcial-Coba et al. 2019). Altogether, the presence of environmental stressors may be overcome by protection of live cells through encapsulation, resulting in the viable delivery of *A. muciniphila*.

Concluding remarks and future perspectives on *A. muciniphila research*

In this thesis we assessed the presence and functions of *A. muciniphila* throughout the human body and different mammalian hosts, not only showing the stable role of this mucin-degrading bacterium in different mammalian hosts, independent of host physiology, but also suggesting that *A. muciniphila* may play a role in other parts of the human gastrointestinal tract besides the colon. Furthermore, we have identified a novel physiological characteristic, namely the production of fuc-EPS by *A. muciniphila*. Next, the set-up of a 16-species synthetic community in fermentors revealed the ability of *A. muciniphila* to survive in a complex in vitro ecosystem, relying on mucin-utilization pathways, where it was found to be one of the two most abundant species in the community. Lastly, a comparison between the different models used to study *A. muciniphila* showed the main function of this bacterium remain stable in different ecosystems.

Akkermansia muciniphila is a fascinating intestinal symbiont, which has received considerable attention over the last two decades due to its mechanisms of action to improve host health. The safety profile of pasteurized *A. muciniphila* was tested with a long-term evaluation conducted on rats, where no adverse effects were observed (Druart et al. 2021). In addition, administration of pasteurized *A. muciniphila* did not translate into subchronic toxicity and in vitro genotoxicity tests showed negative results. Following this evaluation, pasteurized *A. muciniphila* has been considered safe as food ingredient by the European Food Safety Authority (EFSA) panel at specified conditions of use and intake levels (Turck et al. 2021). Therefore, this bacterium

may now be applied in pasteurized form. Further research should be focused on elucidating the different effects on host health between the use of pasteurized and live *A. muciniphila* cells. Then, when *A. muciniphila* may be used as therapeutic agent, individual-specific decisions can be made on whether the use of pasteurized or live cells would be more suitable. Altogether, this is an important step towards the use of *A. muciniphila* as therapeutic agent with the aim to improve human health.

There are many tools to genetically engineer bacteria, such as CRISPR-Cas, random DNA insertion and recombineering (Riley and Guss 2021). To date, a system for the genetic modification of *A. muciniphila* is lacking. Genetic modification of *A. muciniphila* has previously been attempted using random transposon insertions and enriching bacteriophages targeting *A. muciniphila* for their use to modify genetic content (van der Ark 2018). Unfortunately, these efforts did not lead to the genetic modification of *A. muciniphila*. Recently, a patent application has been published describing the genetic engineering of *A. muciniphila*, but this method has not been confirmed in peer-reviewed *A. muciniphila* studies (Valdivia 2019). The ability to genetically modify *A. muciniphila* can help elucidate the mechanism behind important functions (e.g. mucus degradation, EPS production, pili production and adaptation to stress factors in the human gut) via deletions or overexpression of genes involved in these processes. Altogether, this may be useful for therapeutic purposes (Bravo and Landete 2017, Steidler et al. 2003, Alvarez-Sieiro et al. 2014).

Furthermore, the discovery of *A. muciniphila* fuc-EPS may be another factor in its mechanism to improve host health (Xiao et al. 2022) (**Figure 2**). Therefore, the effect of *A. muciniphila* fc-EPS on host health should be studied. This can be done by isolating and purifying EPS as already described in **chapter 5**. Then this EPS could be used to study host health in for example, mouse models or the use of Caco-2 cell lines as a model of the intestinal epithelial barrier. In these models, the effect of *A. muciniphila* fuc-EPS on the intestinal epithelial barrier and interactions with the mucosal immune system can be studied.

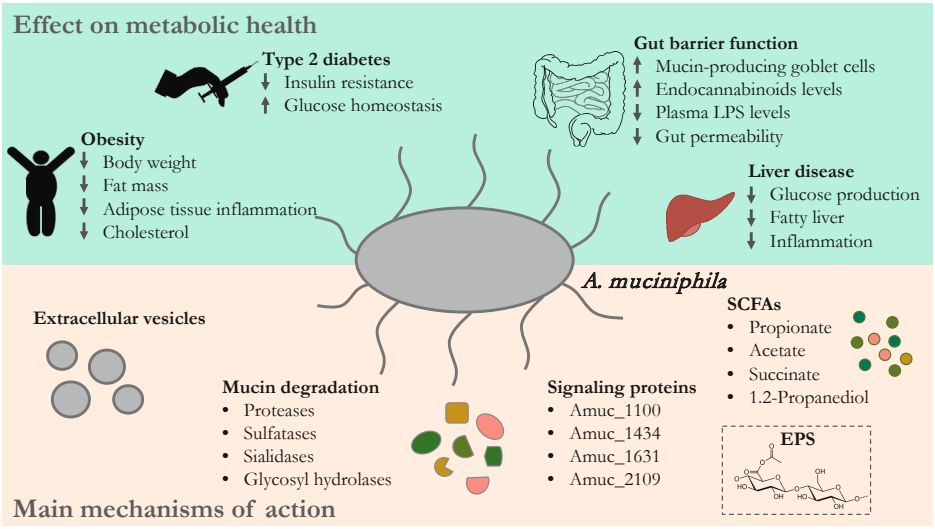

Figure 2: Overview of the effect of *A. muciniphila* on metabolic health and its main mechanisms of action, with the addition of the possible effect of *A. muciniphila* EPS on host health.

Lastly, an adapted set-up of the synthetic minimal microbiome described in **chapter 6** to focus on the mucosal community, could help to elucidate the interactions between *A. muciniphila* and other species associated with the mucosal layer. It has previously been shown that the mucosal layer contains a distinct community compared to the community found in the lumen. By focusing on the interaction of *A. muciniphila* with mucosa-associated bacteria in a synthetic community, interactions such as cross-feeding and competition as well as colonization strategies can be studied. Insights on the colonization strategy of *A. muciniphila* in the mucosal layer with an already existing community may contribute to successful colonization by *A. muciniphila* when supplemented as therapeutic agent in the future. Since the mucosal community resides closely to the host epithelial cells interacting with the host immune system, it may also be of interest to study the mucosa-associated community in a mouse model where bacteria-host interactions can be studied. This information could give more insight into the interactions and colonization of *A. muciniphila* in its ecological niche further contributing to the existing knowledge on the role of *A. muciniphila* in the human gut.

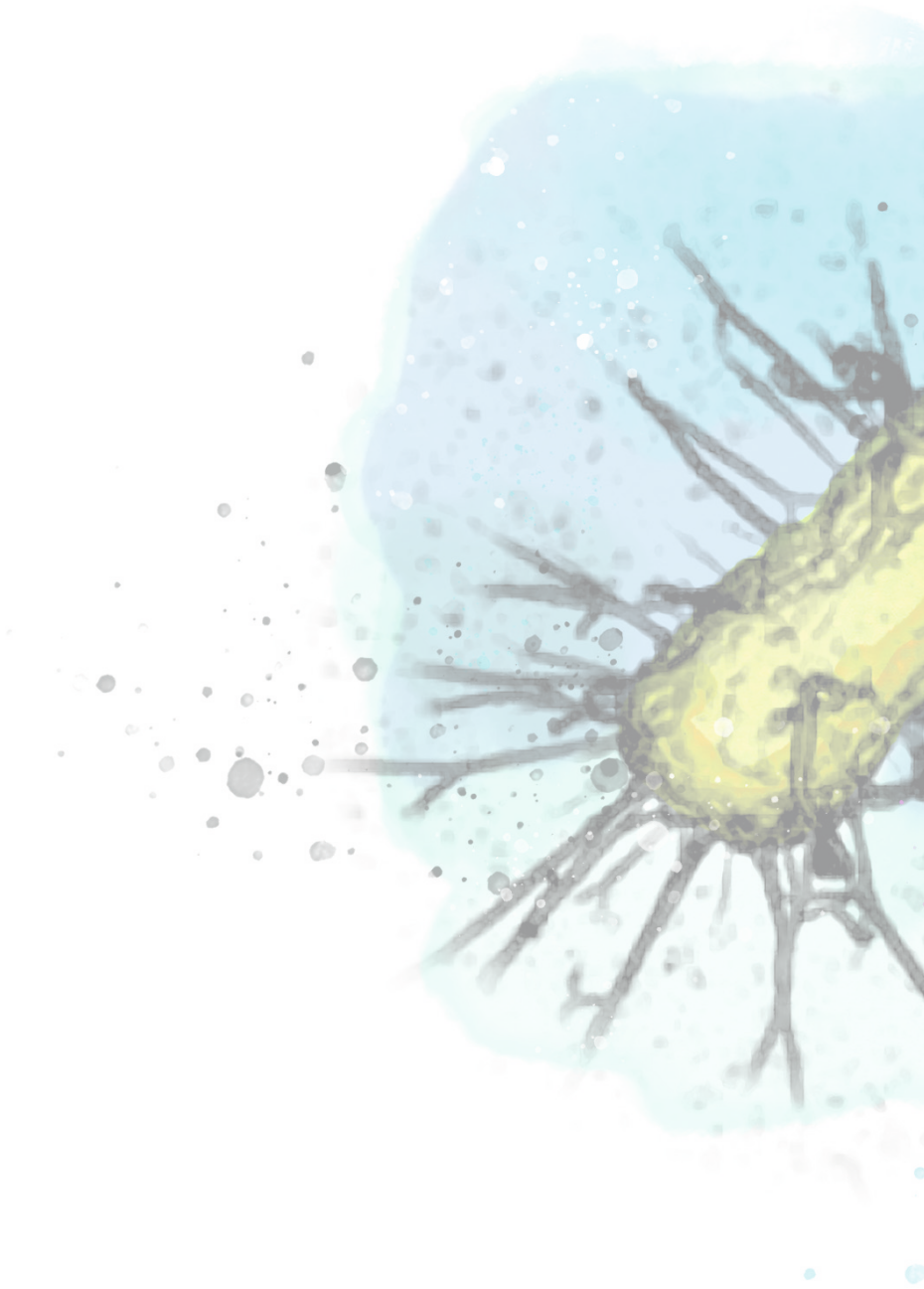

References

References

Aakko, J., H. Kumar, S. Rautava, A. Wise, C. Autran, L. Bode, E. Isolauri and S. Salminen (2017). "Human milk oligosaccharide categories define the microbiota composition in human colostrum." Benef Microbes **8**(4): 563-567.

Aas, J. A., B. J. Paster, L. N. Stokes, I. Olsen and F. E. Dewhirst (2005). "Defining the normal bacterial flora of the oral cavity." J Clin Microbiol **43**(11): 5721-5732.

Abid, Y., A. Casillo, H. Gharsallah, I. Joulak, R. Lanzetta, M. M. Corsaro, H. Attia and S. Azabou (2018). "Production and structural characterization of exopolysaccharides from newly isolated probiotic lactic acid bacteria." Int J Biol Macromol **108**: 719-728.

Adesulu-Dahunsi, A. T., K. Jeyaram, A. I. Sanni and K. Banwo (2018). "Production of exopolysaccharide by strains of Lactobacillus plantarum YO175 and OF101 isolated from traditional fermented cereal beverage." PeerJ **6**: e5326.

Aframian, D. J., T. Davidowitz and R. Benoliel (2006). "The distribution of oral mucosal pH values in healthy saliva secretors." Oral Dis **12**(4): 420-423.

Ahmad, A., S. Majaz and F. Nouroz (2020). "Two-component systems regulate ABC transporters in antimicrobial peptide production, immunity and resistance." Microbiology (Reading) **166**(1): 4-20.

Akkerman, R., M. M. Faas and P. de Vos (2018). "Non-digestible carbohydrates in infant formula as substitution for human milk oligosaccharide functions: Effects on microbiota and gut maturation." Crit Rev Food Sci Nutr **59**(9): 1486-1497.

Allin, K. H., V. Tremaroli, R. Caesar, B. A. H. Jensen, M. T. F. Damgaard, M. I. Bahl, T. R. Licht, T. H. Hansen, T. Nielsen, T. M. Dantoft, A. Linneberg, T. Jorgensen, H. Vestergaard, K. Kristiansen, P. W. Franks, I.-D. consortium, T. Hansen, F. Backhed and O. Pedersen (2018). "Aberrant intestinal microbiota in individuals with prediabetes." Diabetologia **61**(4): 810-820.

Alvarez-Sieiro, P., M. C. Martin, B. Redruello, B. Del Rio, V. Ladero, B. A. Palanski, C. Khosla, M. Fernandez and M. A. Alvarez (2014). "Generation of food-grade recombinant Lactobacillus casei delivering Myxococcus xanthus prolyl endopeptidase." Appl Microbiol Biotechnol **98**(15): 6689-6700.

Ambort, D., M. E. Johansson, J. K. Gustafsson, H. E. Nilsson, A. Ermund, B. R. Johansson, P. J. Koeck, H. Hebert and G. C. Hansson (2012). "Calcium and pH-dependent packing and release of the gel-forming MUC2 mucin." Proc Natl Acad Sci U S A **109**(15): 5645-5650.

Angelakis, E., F. Armougom, F. Carriere, D. Bachar, R. Laugier, J. C. Lagier, C. Robert, C. Michelle, B. Henrissat and D. Raoult (2015). "A Metagenomic Investigation of the Duodenal Microbiota Reveals Links with Obesity." PLoS One **10**(9): e0137784.

Angelin, J. and M. Kavitha (2020). "Exopolysaccharides from probiotic bacteria and their health potential." Int J Biol Macromol **162**: 853-865.

Arumugam, M., J. Raes, E. Pelletier, D. Le Paslier, T. Yamada, D. R. Mende, G. R. Fernandes, J. Tap, T. Bruls, J. M. Batto, M. Bertalan, N. Borruel, F. Casellas, L. Fernandez, L. Gautier, T. Hansen, M. Hattori, T. Hayashi, M. Kleerebezem, K. Kurokawa, M. Leclerc, F. Levenez, C. Manichanh, H. B. Nielsen, T. Nielsen, N. Pons, J. Poulain, J. Qin, T. Sicheritz-Ponten, S. Tims, D. Torrents, E. Ugarte, E. G. Zoetendal, J. Wang, F. Guarner, O. Pedersen, W. M. de Vos, S. Brunak, J. Dore, H. I. T. C. Meta, M. Antolin, F. Artiguenave, H. M. Blottiere, M. Almeida, C. Brechot, C. Cara, C. Chervaux, A. Cultrone, C. Delorme, G. Denariaz, R. Dervyn, K. U. Foerstner, C. Friss, M. van de Guchte, E. Guedon, F. Haimet, W. Huber, J. van Hylckama-Vlieg, A. Jamet, C. Juste, G. Kaci, J. Knol, O. Lakhdari, S. Layec, K. Le Roux, E. Maguin, A. Merieux, R. Melo Minardi, C. M'Rini, J. Muller, R. Oozeer, J. Parkhill, P. Renault, M. Rescigno, N. Sanchez, S. Sunagawa, A. Torrejon, K. Turner, G. Vandemeulebrouck, E. Varela, Y. Winogradsky, G. Zeller, J. Weissenbach, S. D. Ehrlich and P. Bork (2011). "Enterotypes of the human gut microbiome." Nature **473**(7346): 174-180.

Ashrafian, F., S. Keshavarz Azizi Raftar, A. Lari, A. Shahryari, S. Abdollahiyan, H. R. Moradi, M. Masoumi, M. Davari, S. Khatami, M. D. Omrani, F. Vaziri, A. Masotti and S. D. Siadat (2021). "Extracellular vesicles and pasteurized cells derived from Akkermansia muciniphila protect against high-fat induced obesity in mice." Microb Cell Fact **20**(1): 219.

Ashrafian, F., S. Keshavarz Azizi Raftar, A. Shahryari, A. Behrouzi, R. Yaghoubfar, A. Lari, H. R. Moradi, S. Khatami, M. D. Omrani, F. Vaziri, A. Masotti and S. D. Siadat (2021). "Comparative effects of alive and pasteurized Akkermansia muciniphila on normal diet-fed mice." Scientific Reports **11**(1).

Ashrafian, F., A. Shahriary, A. Behrouzi, H. R. Moradi, S. Keshavarz Azizi Raftar, A. Lari, S. Hadifar, R. Yaghoubfar, S. Ahmadi Badi, S. Khatami, F. Vaziri and S. D. Siadat (2019). "Akkermansia muciniphila-Derived Extracellular Vesicles as a Mucosal Delivery Vector for Amelioration of Obesity in Mice." Front Microbiol **10**: 2155.

Asnicar, F., E. R. Leeming, E. Dimidi, M. Mazidi, P. W. Franks, H. Al Khatib, A. M. Valdes, R. Davies, E. Bakker, L. Francis, A. Chan, R. Gibson, G. Hadjigeorgiou, J. Wolf, T. D. Spector, N. Segata and S. E. Berry (2021). "Blue poo: impact of gut transit time on the gut microbiome using a novel marker." Gut **70**(9): 1665-1674.

Assa, A., J. Butcher, J. Li, A. Elkadri, P. M. Sherman, A. M. Muise, A. Stintzi and D. Mack (2016). "Mucosa-Associated Ileal Microbiota in New-Onset Pediatric Crohn's Disease." Inflamm Bowel Dis **22**(7): 1533-1539.

Atuma, C., V. Strugala, A. Allen and L. Holm (2001). "The adherent gastrointestinal mucus gel layer: thickness and physical state in vivo." Am J Physiol Gastrointest Liver Physiol **280**(5): G922-929.

Ayyash, M., B. Abu-Jdayil, P. Itsaranuwat, E. Galiwango, C. Tamiello-Rosa, H. Abdullah, G. Esposito, Y. Hunashal, R. S. Obaid and F. Hamed (2020). "Characterization, bioactivities, and rheological properties of exopolysaccharide produced by novel probiotic Lactobacillus plantarum C70 isolated from camel milk." Int J Biol Macromol **144**: 938-946.

Aziz, R. K., D. Bartels, A. A. Best, M. DeJongh, T. Disz, R. A. Edwards, K. Formsma, S. Gerdes, E. M. Glass, M. Kubal, F. Meyer, G. J. Olsen, R. Olson, A. L. Osterman, R. A. Overbeek, L. K. McNeil, D. Paarmann, T. Paczian, B. Parrello, G. D. Pusch, C. Reich, R. Stevens, O. Vassieva, V. Vonstein, A. Wilke and O. Zagnitko (2008). "The RAST Server: Rapid Annotations using Subsystems Technology." BMC Genomics **9**: 75-75.

Barcelos, M. C. S., K. A. C. Vespermann, F. M. Pelissari and G. Molina (2020). "Current status of biotechnological production and applications of microbial exopolysaccharides." Crit Rev Food Sci Nutr **60**(9): 1475-1495.

Barton, W., N. C. Penney, O. Cronin, I. Garcia-Perez, M. G. Molloy, E. Holmes, F. Shanahan, P. D. Cotter and O. O'Sullivan (2018). "The microbiome of professional athletes differs from that of more sedentary subjects in composition and particularly at the functional metabolic level." Gut **67**(4): 625-633.

Bauer, E., J. Zimmermann, F. Baldini, I. Thiele and C. Kaleta (2017). "BacArena: Individual-based metabolic modeling of heterogeneous microbes in complex communities." PLoS Comput Biol **13**(5): e1005544.

Bauer, M. A., K. Kainz, D. Carmona-Gutierrez and F. Madeo (2018). "Microbial wars: Competition in ecological niches and within the microbiome." Microb Cell **5**(5): 215-219.

Becken, B., L. Davey, D. R. Middleton, K. D. Mueller, A. Sharma, Z. C. Holmes, E. Dallow, B. Remick, G. M. Barton, L. A. David, J. R. McCann, S. C. Armstrong, P. Malkus and R. H. Valdivia (2021). "Genotypic and phenotypic diversity among human isolates of akkermansia muciniphila." mBio **12**(3).

Belzer, C., L. W. Chia, S. Aalvink, B. Chamlagain, V. Piironen, J. Knol and W. M. de Vos (2017). "Microbial Metabolic Networks at the Mucus Layer Lead to Diet-Independent Butyrate and Vitamin B12 Production by Intestinal Symbionts." MBio **8**(5).

Belzer, C. and W. M. de Vos (2012). "Microbes inside–from diversity to function: the case of Akkermansia." ISME J **6**(8): 1449-1458.

Belzer, C., J. G. Kusters, E. J. Kuipers and A. H. van Vliet (2006). "Urease induced calcium precipitation by Helicobacter species may initiate gallstone formation." Gut **55**(11): 1678-1679.

Bengoa, A. A., M. G. Llamas, C. Iraporda, M. T. Duenas, A. G. Abraham and G. L. Garrote (2018). "Impact of growth temperature on exopolysaccharide production and probiotic properties of Lactobacillus paracasei strains isolated from kefir grains." Food Microbiol **69**: 212-218.

Berkhout, M. D., C. M. Plugge and C. Belzer (2022). "How microbial glycosyl hydrolase activity in the gut mucosa initiates microbial cross-feeding." Glycobiology **32**(3): 182-200.

Bernalier, A., A. Willems, M. Leclerc, V. Rochet and M. D. Collins (1996). "Ruminococcus hydrogenotrophicus sp. nov., a new H2/CO2-utilizing acetogenic bacterium isolated from human feces." Arch Microbiol **166**(3): 176-183.

Berry, D., C. Schwab, G. Milinovich, J. Reichert, K. Ben Mahfoudh, T. Decker, M. Engel, B. Hai, E. Hainzl, S. Heider, L. Kenner, M. Müller, I. Rauch, B. Strobl, M. Wagner, C. Schleper, T. Urich and A. Loy (2012). "Phylotype-level 16S rRNA analysis reveals new bacterial indicators of health state in acute murine colitis." ISME Journal **6**(11): 2091-2106.

Berry, D., B. Stecher, A. Schintlmeister, J. Reichert, S. Brugiroux, B. Wild, W. Wanek, A. Richter, I. Rauch, T. Decker, A. Loy and M. Wagner (2013). "Host-compound foraging by intestinal microbiota revealed by single-cell stable isotope probing." Proceedings of the National Academy of Sciences of the United States of America **110**(12): 4720-4725.

Berry, R. J. (1900). "The True Caecal Apex, or the Vermiform Appendix: Its Minute and Comparative Anatomy." J Anat Physiol **35**(Pt 1): 83-100 109.

Biagi, E., C. Franceschi, S. Rampelli, M. Severgnini, R. Ostan, S. Turroni, C. Consolandi, S. Quercia, M. Scurti, D. Monti, M. Capri, P. Brigidi and M. Candela (2016). "Gut Microbiota and Extreme Longevity." Curr Biol **26**(11): 1480-1485.

Biagi, E., L. Nylund, M. Candela, R. Ostan, L. Bucci, E. Pini, J. Nikkila, D. Monti, R. Satokari, C. Franceschi, P. Brigidi and W. De Vos (2010). "Through ageing, and beyond: gut microbiota and inflammatory status in seniors and centenarians." PLoS One **5**(5): e10667.

Bian, X., W. Wu, L. Yang, L. Lv, Q. Wang, Y. Li, J. Ye, D. Fang, J. Wu, X. Jiang, D. Shi and L. Li (2019). "Administration of Akkermansia muciniphila Ameliorates Dextran Sulfate Sodium-Induced Ulcerative Colitis in Mice." Front Microbiol **10**: 2259.

Bidart, G. N., J. Rodriguez-Diaz, V. Monedero and M. J. Yebra (2014). "A unique gene cluster for the utilization of the mucosal and human milk-associated glycans galacto-N-biose and lacto-N-biose in Lactobacillus casei." Mol Microbiol **93**(3): 521-538.

Bik, E. M., C. D. Long, G. C. Armitage, P. Loomer, J. Emerson, E. F. Mongodin, K. E. Nelson, S. R. Gill, C. M. Fraser-Liggett and D. A. Relman (2010). "Bacterial diversity in the oral cavity of 10 healthy individuals." ISME J **4**(8): 962-974.

Billick, I. and T. J. Case (1994). "Higher order interactions in ecological communities: what are they and how can they be detected?" Ecology **75**(6): 1529-1543.

Bland, C., T. L. Ramsey, F. Sabree, M. Lowe, K. Brown, N. C. Kyrpides and P. Hugenholtz (2007). "CRISPR Recognition Tool (CRT): A tool for automatic detection of clustered regularly interspaced palindromic repeats." BMC Bioinformatics **8**(1): 209-209.

Blaser, M. J. (2014). "The microbiome revolution." J Clin Invest **124**(10): 4162-4165.

Bode, L. (2012). "Human milk oligosaccharides: every baby needs a sugar mama." Glycobiology **22**(9): 1147-1162.

Boisvert, S., F. Raymond, É. Godzaridis, F. Laviolette and J. Corbeil (2012). "Ray Meta: Scalable de novo metagenome assembly and profiling." Genome Biology **13**(12).

Bolger, A. M., M. Lohse and B. Usadel (2014). "Trimmomatic: a flexible trimmer for Illumina sequence data." Bioinformatics **30**(15): 2114-2120.

Boyer, J. L. (1986). Mechanisms of Bile Secretion and Hepatic Transport. Physiology of Membrane Disorders. T. E. Andreoli, J. F. Hoffman, D. D. Fanestil and S. G. Schultz. Boston, MA, Springer US: 609-636.

Boyer, J. L. (2013). "Bile formation and secretion." Compr Physiol **3**(3): 1035-1078.

Bravo, D. and J. M. Landete (2017). "Genetic engineering as a powerful tool to improve probiotic strains." Biotechnol Genet Eng Rev **33**(2): 173-189.

Bridgeman, S. C., W. Northrop, P. E. Melton, G. C. Ellison, P. Newsholme and C. D. S. Mamotte (2020). "Butyrate generated by gut microbiota and its therapeutic role in metabolic syndrome." Pharmacological Research **160**: 105174.

Broadbent, J. R., D. J. McMahon, D. L. Welker, C. J. Oberg and S. Moineau (2003). "Biochemistry, genetics, and applications of exopolysaccharide production in Streptococcus thermophilus: a review." J Dairy Sci **86**(2): 407-423.

Brodmann, T., A. Endo, M. Gueimonde, G. Vinderola, W. Kneifel, W. M. de Vos, S. Salminen and C. Gomez-Gallego (2017). "Safety of Novel Microbes for Human Consumption: Practical Examples of Assessment in the European Union." Front Microbiol **8**: 1725.

Brown, A. J., S. M. Goldsworthy, A. A. Barnes, M. M. Eilert, L. Tcheang, D. Daniels, A. I. Muir, M. J. Wigglesworth, I. Kinghorn, N. J. Fraser, N. B. Pike, J. C. Strum, K. M. Steplewski, P. R. Murdock, J. C. Holder, F. H. Marshall, P. G. Szekeres, S. Wilson, D. M. Ignar, S. M. Foord, A. Wise and S. J. Dowell (2003). "The Orphan G protein-coupled receptors GPR41 and GPR43 are activated by propionate and other short chain carboxylic acids." J Biol Chem **278**(13): 11312-11319.

Buchfink, B., C. Xie and D. H. Huson (2014). "Fast and sensitive protein alignment using DIAMOND." Nat Methods **12**(1): 59.

Bui, T. P. N. and W. M. de Vos (2021). "Next-generation therapeutic bacteria for treatment of obesity, diabetes, and other endocrine diseases." Best Pract Res Clin Endocrinol Metab **35**(3): 101504.

Bui, T. P. N., H. A. Schols, M. Jonathan, A. J. M. Stams, W. M. de Vos and C. M. Plugge (2019). "Mutual metabolic interactions in co-cultures of the intestinal *Anaerostipes rhamnosivorans* with an acetogen, methanogen, or pectin-degrader affecting butyrate production." Front Microbiol **10**: 2449.

Burge, S. W., J. Daub, R. Eberhardt, J. Tate, L. Barquist, E. P. Nawrocki, S. R. Eddy, P. P. Gardner and A. Bateman (2013). "Rfam 11.0: 10 years of RNA families." Nucleic Acids Research **41**(D1).

Callahan, B. J., P. J. McMurdie, M. J. Rosen, A. W. Han, A. J. A. Johnson and S. P. Holmes (2016). "DADA2: high-resolution sample inference from Illumina amplicon data." Nat Methods **13**(7): 581.

Cani, P. D. and W. M. de Vos (2017). "Next-Generation Beneficial Microbes: The Case of Akkermansia muciniphila." Front Microbiol **8**: 1765.

Cani, P. D., C. Depommier, M. Derrien, A. Everard and W. M. de Vos (2022). "Akkermansia muciniphila: paradigm for next-generation beneficial microorganisms." Nat Rev Gastroenterol Hepatol.

Capitani, G., D. De Biase, C. Aurizi, H. Gut, F. Bossa and M. G. Grütter (2003). "Crystal structure and functional analysis of Escherichia coli glutamate decarboxylase." The EMBO journal **22**(16): 4027-4037.

Caputo, A., G. Dubourg, O. Croce, S. Gupta, C. Robert, L. Papazian, J. M. Rolain and D. Raoult (2015). "Whole-genome assembly of Akkermansia muciniphila sequenced directly from human stool." Biol Direct **10**: 5.

Carey, H. V., W. A. Walters and R. Knight (2013). "Seasonal restructuring of the ground squirrel gut microbiota over the annual hibernation cycle." Am J Physiol Regul Integr Comp Physiol **304**(1): R33-42.

Carrero-Colón, M., C. H. Nakatsu and A. Konopka (2006). "Effect of nutrient periodicity on microbial community dynamics." Appl Environ Microbiol **72**(5): 3175-3183.

Carrero-Colón, M., C. H. Nakatsu and A. Konopka (2006). "Microbial community dynamics in nutrient-pulsed chemostats." FEMS Microbiol Ecol **57**(1): 1-8.

Carroll, I. M., T. Ringel-Kulka, J. P. Siddle and Y. Ringel (2012). "Alterations in composition and diversity of the intestinal microbiota in patients with diarrhea-predominant irritable bowel syndrome." Neurogastroenterol Motil **24**(6): 521-530, e248.

Case, R. J., Y. Boucher, I. Dahllöf, C. Holmström, W. F. Doolittle and S. Kjelleberg (2007). "Use of 16S rRNA and rpoB genes as molecular markers for microbial ecology studies." Applied and Environmental Microbiology **73**(1): 278-288.

Castro-Bravo, N., J. M. Wells, A. Margolles and P. Ruas-Madiedo (2018). "Interactions of Surface Exopolysaccharides From Bifidobacterium and Lactobacillus Within the Intestinal Environment." Front Microbiol **9**: 2426.

Chakraborty, S., M. Gogoi and D. Chakravortty (2015). "Lactoylglutathione lyase, a critical enzyme in methylglyoxal detoxification, contributes to survival of Salmonella in the nutrient rich environment." Virulence **6**(1): 50-65.

Chang, Y., Y. Yang, N. Xu, H. Mu, H. Zhang and J. Duan (2020). "Improved viability of Akkermansia muciniphila by encapsulation in spray dried succinate-grafted alginate doped with epigallocatechin-3-gallate." International Journal of Biological Macromolecules **159**: 373-382.

Chatzidaki-Livanis, M., M. J. Coyne and L. E. Comstock (2014). "An antimicrobial protein of the gut symbiont Bacteroides fragilis with a MACPF domain of host immune proteins." Mol Microbiol **94**(6): 1361-1374.

Chelakkot, C., Y. Choi, D. K. Kim, H. T. Park, J. Ghim, Y. Kwon, J. Jeon, M. S. Kim, Y. K. Jee, Y. S. Gho, H. S. Park, Y. K. Kim and S. H. Ryu (2018). "Akkermansia muciniphila-derived extracellular vesicles influence gut permeability through the regulation of tight junctions." Exp Mol Med **50**(2): e450.

Chen, Y., F. Ji, J. Guo, D. Shi, D. Fang and L. Li (2016). "Dysbiosis of small intestinal microbiota in liver cirrhosis and its association with etiology." Sci Rep **6**: 34055.

Cheng, K. C., A. Demirci and J. M. Catchmark (2011). "Pullulan: biosynthesis, production, and applications." Appl Microbiol Biotechnol **92**(1): 29-44.

Chia, L. W., B. V. H. Hornung, S. Aalvink, P. J. Schaap, W. M. de Vos, J. Knol and C. Belzer (2018). "Deciphering the trophic interaction between Akkermansia muciniphila and the butyrogenic gut commensal Anaerostipes caccae using a metatranscriptomic approach." Antonie Van Leeuwenhoek.

Choi, Y., S. Bose, J. Seo, J. H. Shin, D. Lee, Y. Kim, S. G. Kang and H. Kim (2021). "Effects of Live and Pasteurized Forms of Akkermansia from the Human Gut on Obesity and Metabolic Dysregulation." Microorganisms **9**(10).

Chung, W. S. F., A. W. Walker, P. Louis, J. Parkhill, J. Vermeiren, D. Bosscher, S. H. Duncan and H. J. Flint (2016). "Modulation of the human gut microbiota by dietary fibres occurs at the species level." BMC Biol **14**(1): 3.

Chung, W. S. F., A. W. Walker, J. Vermeiren, P. O. Sheridan, D. Bosscher, V. Garcia-Campayo, J. Parkhill, H. J. Flint and S. H. Duncan (2018). "Impact of carbohydrate substrate complexity on the diversity of the human colonic microbiota." FEMS Microbiol Ecol.

Clark, R. L., B. M. Connors, D. M. Stevenson, S. E. Hromada, J. J. Hamilton, D. Amador-Noguez and O. S. Venturelli (2021). "Design of synthetic human gut microbiome assembly and butyrate production." Nat Commun **12**(1): 3254.

Clarke, S. F., E. F. Murphy, O. O'Sullivan, A. J. Lucey, M. Humphreys, A. Hogan, P. Hayes, M. O'Reilly, I. B. Jeffery, R. Wood-Martin, D. M. Kerins, E. Quigley, R. P. Ross, P. W. O'Toole, M. G. Molloy, E. Falvey, F. Shanahan and P. D. Cotter (2014). "Exercise and associated dietary extremes impact on gut microbial diversity." Gut **63**(12): 1913-1920.

Claudel-Renard, C., C. Chevalet, T. Faraut and D. Kahn (2003). "Enzyme-specific profiles for genome annotation: PRIAM." Nucleic Acids Research **31**(22): 6633-6639.

Clausen, M. R. and P. B. Mortensen (1995). "Kinetic studies on colonocyte metabolism of short chain fatty acids and glucose in ulcerative colitis." Gut **37**(5): 684-689.

Cockburn, D. W., N. I. Orlovsky, M. H. Foley, K. J. Kwiatkowski, C. M. Bahr, M. Maynard, B. Demeler and N. M. Koropatkin (2015). "Molecular details of a starch utilization pathway in the human gut symbiont Eubacterium rectale." Mol Microbiol **95**(2): 209-230.

Codling, C., L. O'Mahony, F. Shanahan, E. M. Quigley and J. R. Marchesi (2010). "A molecular analysis of fecal and mucosal bacterial communities in irritable bowel syndrome." Dig Dis Sci **55**(2): 392-397.

Collado, M. C., M. Derrien, E. Isolauri, W. M. de Vos and S. Salminen (2007). "Intestinal integrity and Akkermansia muciniphila, a mucin-degrading member of the intestinal microbiota present in infants, adults, and the elderly." Appl Environ Microbiol **73**(23): 7767-7770.

Collado, M. C., K. Laitinen, S. Salminen and E. Isolauri (2012). "Maternal weight and excessive weight gain during pregnancy modify the immunomodulatory potential of breast milk." Pediatr Res **72**(1): 77-85.

Costa, O. Y. A., J. M. Raaijmakers and E. E. Kuramae (2018). "Microbial Extracellular Polymeric Substances: Ecological Function and Impact on Soil Aggregation." Front Microbiol **9**: 1636.

Costea, P. I., F. Hildebrand, M. Arumugam, F. Backhed, M. J. Blaser, F. D. Bushman, W. M. de Vos, S. D. Ehrlich, C. M. Fraser, M. Hattori, C. Huttenhower, I. B. Jeffery, D. Knights, J. D. Lewis, R. E. Ley, H. Ochman, P. W. O'Toole, C. Quince, D. A. Relman, F. Shanahan, S. Sunagawa, J. Wang, G. M. Weinstock, G. D. Wu, G. Zeller, L. Zhao, J. Raes, R. Knight and P. Bork (2018). "Enterotypes in the landscape of gut microbial community composition." Nat Microbiol **3**(1): 8-16.

Costea, P. I., G. Zeller, S. Sunagawa, E. Pelletier, A. Alberti, F. Levenez, M. Tramontano, M. Driessen, R. Hercog, F. E. Jung, J. R. Kultima, M. R. Hayward, L. P. Coelho, E. Allen-Vercoe, L. Bertrand, M. Blaut, J. R. M. Brown, T. Carton, S. Cools-Portier, M. Daigneault, M. Derrien, A. Druesne, W. M. de Vos, B. B. Finlay, H. J. Flint, F. Guarner, M. Hattori, H. Heilig, R. A. Luna, J. van Hylckama Vlieg, J. Junick, I. Klymiuk, P. Langella, E. Le Chatelier, V. Mai, C. Manichanh, J. C. Martin, C. Mery, H. Morita, P. W. O'Toole, C. Orvain, K. R. Patil, J. Penders, S. Persson, N. Pons, M. Popova, A. Salonen, D. Saulnier, K. P. Scott, B. Singh, K. Slezak, P. Veiga, J. Versalovic, L. Zhao, E. G. Zoetendal, S. D. Ehrlich, J. Dore and P. Bork (2017). "Towards standards for human fecal sample processing in metagenomic studies." Nat Biotechnol **35**(11): 1069-1076.

Costello, E. K., J. I. Gordon, S. M. Secor and R. Knight (2010). "Postprandial remodeling of the gut microbiota in Burmese pythons." ISME J **4**(11): 1375-1385.

Costello, E. K., K. Stagaman, L. Dethlefsen, B. J. Bohannan and D. A. Relman (2012). "The application of ecological theory toward an understanding of the human microbiome." Science **336**(6086): 1255-1262.

Cotillard, A., S. P. Kennedy, L. C. Kong, E. Prifti, N. Pons, E. Le Chatelier, M. Almeida, B. Quinquis, F. Levenez and N. Galleron (2013). "Dietary intervention impact on gut microbial gene richness." Nature **500**(7464): 585-588.

Cozzolino, A., F. Vergalito, P. Tremonte, M. Iorizzo, S. J. Lombardi, E. Sorrentino, D. Luongo, R. Coppola, R. Di Marco and M. Succi (2020). "Preliminary evaluation of the safety and probiotic potential of akkermansia muciniphila DSM 22959 in comparison with lactobacillus rhamnosus GG." Microorganisms **8**(2).

Crost, E. H., G. Le Gall, J. A. Laverde-Gomez, I. Mukhopadhya, H. J. Flint and N. Juge (2018). "Mechanistic Insights Into the Cross-Feeding of Ruminococcus gnavus and Ruminococcus bromii on Host and Dietary Carbohydrates." Front Microbiol **9**: 2558.

Csendes, A., M. Fernandez and P. Uribe (1975). "Bacteriology of the gallbladder bile in normal subjects." Am J Surg **129**(6): 629-631.

Cummings, J. H. and G. T. Macfarlane (1991). "The control and consequences of bacterial fermentation in the human colon." J Appl Bacteriol **70**(6): 443-459.

D'Hoe, K., S. Vet, K. Faust, F. Moens, G. Falony, D. Gonze, V. Llorens-Rico, L. Gelens, J. Danckaert, L. De Vuyst and J. Raes (2018). "Integrated culturing, modeling and transcriptomics uncovers complex interactions and emergent behavior in a three-species synthetic gut community." Elife **7**.

Dao, M. C., A. Everard, J. Aron-Wisnewsky, N. Sokolovska, E. Prifti, E. O. Verger, B. D. Kayser, F. Levenez, J. Chilloux, L. Hoyles, M. I.-O. Consortium, M. E. Dumas, S. W. Rizkalla, J. Dore, P. D. Cani and K. Clement (2016). "Akkermansia muciniphila and improved metabolic health during a dietary intervention in obesity: relationship with gut microbiome richness and ecology." Gut **65**(3): 426-436.

Darwin, C. (1871). The descent of man and selection in relation to sex darwin. London, John Murray.

Darzi, Y., G. Falony, S. Vieira-Silva and J. Raes (2016). "Towards biome-specific analysis of meta-omics data." ISME J **10**(5): 1025.

David, L. A., C. F. Maurice, R. N. Carmody, D. B. Gootenberg, J. E. Button, B. E. Wolfe, A. V. Ling, A. S. Devlin, Y. Varma and M. A. Fischbach (2014). "Diet rapidly and reproducibly alters the human gut microbiome." Nature **505**(7484): 559-563.

de Cárcer, D. A. (2019). "A conceptual framework for the phylogenetically constrained assembly of microbial communities." Microbiome **7**(1): 142.

De Roy, K., M. Marzorati, P. Van den Abbeele, T. Van de Wiele and N. Boon (2014). "Synthetic microbial ecosystems: an exciting tool to understand and apply microbial communities." Environ. Microbiol. **16**(6): 1472-1481.

de Vadder, F. and G. Mithieux (2018). "Gut-brain signaling in energy homeostasis: the unexpected role of microbiota-derived succinate." J Endocrinol **236**(2): R105-R108.

de Vos, W. M. (2017). "Microbe Profile: Akkermansia muciniphila: a conserved intestinal symbiont that acts as the gatekeeper of our mucosa." Microbiology **163**(5): 646-648.

de Vos, W. M., H. Tilg, M. Van Hul and P. D. Cani (2022). "Gut microbiome and health: mechanistic insights." Gut **71**(5): 1020.

de Weerth, C., S. Fuentes, P. Puylaert and W. M. de Vos (2013). "Intestinal microbiota of infants with colic: development and specific signatures." Pediatrics **131**(2): e550-558.

Degnan, B. A., S. Macfarlane, M. E. Quigley and G. T. Macfarlane (1997). "Starch utilization by Bacteroides ovatus isolated from the human large intestine." Curr Microbiol **34**(5): 290-296.

den Besten, G., K. van Eunen, A. K. Groen, K. Venema, D. J. Reijngoud and B. M. Bakker (2013). "The role of short-chain fatty acids in the interplay between diet, gut microbiota, and host energy metabolism." J Lipid Res **54**(9): 2325-2340.

den Besten, H. M. W., A. Arvind, H. M. S. Gaballo, R. Moezelaar, M. H. Zwietering and T. Abee (2010). "Short- and Long-Term Biomarkers for Bacterial Robustness: A Framework for Quantifying Correlations between Cellular Indicators and Adaptive Behavior." PLOS ONE **5**(10): e13746.

Depommier, C., A. Everard, C. Druart, H. Plovier, M. Van Hul, S. Vieira-Silva, G. Falony, J. Raes, D. Maiter, N. M. Delzenne, M. de Barsy, A. Loumaye, M. P. Hermans, J.-P. Thissen, W. M. de Vos and P. D. Cani (2019). "Supplementation with Akkermansia muciniphila in overweight and obese human volunteers: a proof-of-concept exploratory study." Nature Medicine **25**(7): 1096-1103.

Depommier, C., A. Everard, C. Druart, H. Plovier, M. Van Hul, S. Vieira-Silva, G. Falony, J. Raes, D. Maiter, N. M. Delzenne, M. de Barsy, A. Loumaye, M. P. Hermans, J. P. Thissen, W. M. de Vos and P. D. Cani (2019). "Supplementation with Akkermansia muciniphila in overweight and obese human volunteers: a proof-of-concept exploratory study." Nat Med **25**(7): 1096-1103.

Depommier, C., M. Van Hul, A. Everard, N. M. Delzenne, W. M. De Vos and P. D. Cani (2020). "Pasteurized Akkermansia muciniphila increases whole-body energy expenditure and fecal energy excretion in diet-induced obese mice." Gut Microbes **11**(5): 1231-1245.

Derrien, M. (2007). Mucin utilisation and host interactions of the novel intestinal microbe Akkermansia muciniphila.

Derrien, M., M. C. Collado, K. Ben-Amor, S. Salminen and W. M. de Vos (2008). "The Mucin degrader Akkermansia muciniphila is an abundant resident of the human intestinal tract." Appl Environ Microbiol **74**(5): 1646-1648.

Derrien, M., P. Van Baarlen, G. Hooiveld, E. Norin, M. Muller and W. M. de Vos (2011). "Modulation of Mucosal Immune Response, Tolerance, and Proliferation in Mice Colonized by the Mucin-Degrader Akkermansia muciniphila." Front Microbiol **2**: 166.

Derrien, M., M. W. van Passel, J. H. van de Bovenkamp, R. G. Schipper, W. M. de Vos and J. Dekker (2010). "Mucin-bacterial interactions in the human oral cavity and digestive tract." Gut Microbes **1**(4): 254-268.

Derrien, M., E. E. Vaughan, C. M. Plugge and W. M. de Vos (2004). "Akkermansia muciniphila gen. nov., sp. nov., a human intestinal mucin-degrading bacterium." Int J Syst Evol Microbiol **54**(Pt 5): 1469-1476.

Desai, M. S., A. M. Seekatz, N. M. Koropatkin, N. Kamada, C. A. Hickey, M. Wolter, N. A. Pudlo, S. Kitamoto, N. Terrapon, A. Muller, V. B. Young, B. Henrissat, P. Wilmes, T. S. Stappenbeck, G. Nunez and E. C. Martens (2016). "A Dietary Fiber-Deprived Gut Microbiota Degrades the Colonic Mucus Barrier and Enhances Pathogen Susceptibility." Cell **167**(5): 1339-1353 e1321.

Despres, J., E. Forano, P. Lepercq, S. Comtet-Marre, G. Jubelin, C. J. Yeoman, M. E. Miller, C. J. Fields, N. Terrapon, C. Le Bourvellec, C. M. Renard, B. Henrissat, B. A. White and P. Mosoni (2016). "Unraveling the pectinolytic function of Bacteroides xylanisolvens using a RNA-seq approach and mutagenesis." BMC Genomics **17**: 147.

Distrutti, E., L. Monaldi, P. Ricci and S. Fiorucci (2016). "Gut microbiota role in irritable bowel syndrome: New therapeutic strategies." World J Gastroenterol **22**(7): 2219-2241.

Dlugosz, A., B. Winckler, E. Lundin, K. Zakikhany, G. Sandstrom, W. Ye, L. Engstrand and G. Lindberg (2015). "No difference in small bowel microbiota between patients with irritable bowel syndrome and healthy controls." Sci Rep **5**: 8508.

Donaldson, G. P., S. M. Lee and S. K. Mazmanian (2016). "Gut biogeography of the bacterial microbiota." Nat Rev Microbiol **14**(1): 20-32.

Douillard, F. P., A. Ribbera, R. Kant, T. E. Pietilä, H. M. Järvinen, M. Messing, C. L. Randazzo, L. Paulin, P. Laine, J. Ritari, C. Caggia, T. Lähteinen, S. J. J. Brouns, R. Satokari, I. von Ossowski, J. Reunanen, A. Palva and W. M. de Vos (2013). "Comparative Genomic and Functional Analysis of 100 Lactobacillus rhamnosus Strains and Their Comparison with Strain GG." PLoS Genetics **9**(8): e1003683-e1003683.

Druart, C., H. Plovier, M. Van Hul, A. Brient, K. R. Phipps, W. M. de Vos and P. D. Cani (2021). "Toxicological safety evaluation of pasteurized Akkermansia muciniphila." Journal of Applied Toxicology **41**(2): 276-290.

Drula, E., M.-L. Garron, S. Dogan, V. Lombard, B. Henrissat and N. Terrapon (2022). "The carbohydrate-active enzyme database: functions and literature." Nucleic Acids Research **50**(D1): D571-D577.

Dubourg, G., F. Cornu, S. Edouard, A. Battaini, M. Tsimaratos and D. Raoult (2017). "First isolation of Akkermansia muciniphila in a blood-culture sample." Clin Microbiol Infect **23**(9): 682-683.

Dubourg, G., J. C. Lagier, F. Armougom, C. Robert, G. Audoly, L. Papazian and D. Raoult (2013). "High-level colonisation of the human gut by Verrucomicrobia following broad-spectrum antibiotic treatment." Int J Antimicrob Agents **41**(2): 149-155.

Duncan, K., K. Carey-Ewend and S. Vaishnava (2019). "In situ analysis of mucus residing bacterial community reveals an ecological niche key for gut microbiome stability." BioRxiv: 675918.

Duncan, S. H. and H. J. Flint (2008). "Proposal of a neotype strain (A1-86) for Eubacterium rectale. Request for an opinion." Int J Syst Evol Microbiol **58**(Pt 7): 1735-1736.

Duncan, S. H., G. L. Hold, A. Barcenilla, C. S. Stewart and H. J. Flint (2002). "*Roseburia intestinalis* sp. nov., a novel saccharolytic, butyrate-producing bacterium from human faeces." Int J Syst Evol Microbiol **52**(5): 1615-1620.

Duncan, S. H., G. L. Hold, H. J. Harmsen, C. S. Stewart and H. J. Flint (2002). "Growth requirements and fermentation products of *Fusobacterium prausnitzii*, and a proposal to reclassify it as *Faecalibacterium prausnitzii* gen. nov., comb. nov." Int J Syst Evol Microbiol **52**(6): 2141-2146.

Duncan, S. H., P. Louis and H. J. Flint (2004). "Lactate-utilizing bacteria, isolated from human feces, that produce butyrate as a major fermentation product." Appl Environ Microbiol **70**(10): 5810-5817.

Duncan, S. H., W. R. Russell, A. Quartieri, M. Rossi, J. Parkhill, A. W. Walker and H. J. Flint (2016). "Wheat bran promotes enrichment within the human colonic microbiota of butyrate-producing bacteria that release ferulic acid." Environ Microbiol **18**(7): 2214-2225.

Eckburg, P. B., E. M. Bik, C. N. Bernstein, E. Purdom, L. Dethlefsen, M. Sargent, S. R. Gill, K. E. Nelson and D. A. Relman (2005). "Diversity of the human intestinal microbial flora." Science **308**(5728): 1635-1638.

El Hage, R., E. Hernandez-Sanabria, M. Calatayud Arroyo, R. Props and T. Van de Wiele (2019). "Propionate-Producing Consortium Restores Antibiotic-Induced Dysbiosis in a Dynamic in vitro Model of the Human Intestinal Microbial Ecosystem." Front Microbiol **10**: 1206.

Elsholz, A. K., S. A. Wacker and R. Losick (2014). "Self-regulation of exopolysaccharide production in Bacillus subtilis by a tyrosine kinase." Genes Dev **28**(15): 1710-1720.

Elzinga, J., J. van der Oost, M. de Vos Willem and H. Smidt (2019). "The Use of Defined Microbial Communities To Model Host-Microbe Interactions in the Human Gut." Microbiology and Molecular Biology Reviews **83**(2): e00054-00018.

Engels, C., H.-J. Ruscheweyh, N. Beerenwinkel, C. Lacroix and C. Schwab (2016). "The common gut microbe *Eubacterium hallii* also contributes to intestinal propionate formation." Front. Microbiol. **7**: 713.

Espey, M. G. (2013). "Role of oxygen gradients in shaping redox relationships between the human intestine and its microbiota." Free Radic Biol Med **55**: 130-140.

Everard, A., C. Belzer, L. Geurts, J. P. Ouwerkerk, C. Druart, L. B. Bindels, Y. Guiot, M. Derrien, G. G. Muccioli, N. M. Delzenne, W. M. de Vos and P. D. Cani (2013). "Cross-talk between Akkermansia muciniphila and intestinal epithelium controls diet-induced obesity." Proc Natl Acad Sci U S A **110**(22): 9066-9071.

Falony, G., T. Calmeyn, F. Leroy and L. De Vuyst (2009). "Coculture fermentations of Bifidobacterium species and Bacteroides thetaiotaomicron reveal a mechanistic insight into the prebiotic effect of inulin-type fructans." Appl Environ Microbiol **75**(8): 2312-2319.

Falush, D., T. Wirth, B. Linz, J. K. Pritchard, M. Stephens, M. Kidd, M. J. Blaser, D. Y. Graham, S. Vacher, G. I. Perez-Perez, Y. Yamaoka, F. Mégraud, K. Otto, U. Reichard, E. Katzowitsch, X. Wang, M. Achtman and S. Suerbaum (2003). "Traces of human migrations in Helicobacter pylori populations." Science **299**(5612): 1582-1585.

Fan, Y. and O. Pedersen (2021). "Gut microbiota in human metabolic health and disease." Nat Rev Microbiol **19**(1): 55-71.

Fanning, S., J. Hall Lindsay, M. Cronin, A. Zomer, J. MacSharry, D. Goulding, M. O'Connell Motherway, F. Shanahan, K. Nally, G. Dougan and D. van Sinderen (2012). "Bifidobacterial surface-exopolysaccharide facilitates commensal-host interaction through immune modulation and pathogen protection." Proceedings of the National Academy of Sciences **109**(6): 2108-2113.

Fanning, S., L. J. Hall, M. Cronin, A. Zomer, J. MacSharry, D. Goulding, M. O. Motherway, F. Shanahan, K. Nally, G. Dougan and D. van Sinderen (2012). "Bifidobacterial surface-exopolysaccharide facilitates commensal-host interaction through immune modulation and pathogen protection." Proc Natl Acad Sci U S A **109**(6): 2108-2113.

Fedorova, O. S., M. M. Fedotova, T. S. Sokolova, E. A. Golovach, Y. V. Kovshirina, T. S. Ageeva, A. E. Kovshirina, O. S. Kobyakova, L. M. Ogorodova and P. Odermatt (2018). "Opisthorchis felineus infection prevalence in Western Siberia: A review of Russian literature." Acta Trop **178**: 196-204.

Feehily, C. and K. A. G. Karatzas (2013). Role of glutamate metabolism in bacterial responses towards acid and other stresses. Journal of Applied Microbiology, Blackwell Publishing Ltd. **114:** 11-24.

Feng, Y., T. P. N. Bui, A. J. M. Stams, S. Boeren, I. Sanchez-Andrea and W. M. de Vos (2022). "Comparative genomics and proteomics of Eubacterium maltosivorans: functional identification of trimethylamine methyltransferases and bacterial microcompartments in a human intestinal bacterium with a versatile lifestyle." Environ Microbiol.

Ferrari, M., L. Hameleers, M. C. A. Stuart, M. M. P. Oerlemans, P. de Vos, E. Jurak and M. T. C. Walvoort (2022). "Efficient isolation of membrane-associated exopolysaccharides of four commercial bifidobacterial strains." Carbohydr Polym **278**: 118913.

Flint, H. J., K. P. Scott, P. Louis and S. H. Duncan (2012). "The role of the gut microbiota in nutrition and health." Nat Rev Gastroenterol Hepatol **9**(10): 577-589.

Foster, J. W. (2004). Escherichia coli acid resistance: Tales of an amateur acidophile. Nature Reviews Microbiology, Nature Publishing Group. **2:** 898-907.

Foster, K. R., J. Schluter, K. Z. Coyte and S. Rakoff-Nahoum (2017). "The evolution of the host microbiome as an ecosystem on a leash." Nature **548**(7665): 43.

Freitas, F., C. A. V. Torres and M. A. M. Reis (2017). "Engineering aspects of microbial exopolysaccharide production." Bioresour Technol **245**(Pt B): 1674-1683.

Garber, J. M., T. Hennet and C. M. Szymanski (2021). "Significance of fucose in intestinal health and disease." Mol Microbiol **115**(6): 1086-1093.

Garcia-Villalba, R., H. Vissenaekens, J. Pitart, M. Romo-Vaquero, J. C. Espin, C. Grootaert, M. V. Selma, K. Raes, G. Smagghe, S. Possemiers, J. Van Camp and F. A. Tomas-Barberan (2017). "Gastrointestinal Simulation Model TWIN-SHIME Shows Differences between Human Urolithin-Metabotypes in Gut Microbiota Composition, Pomegranate Polyphenol Metabolism, and Transport along the Intestinal Tract." J Agric Food Chem **65**(27): 5480-5493.

Gass, J., H. Vora, A. F. Hofmann, G. M. Gray and C. Khosla (2007). "Enhancement of dietary protein digestion by conjugated bile acids." Gastroenterology **133**(1): 16-23.

Geerlings, S. Y., I. Kostopoulos, W. M. de Vos and C. Belzer (2018). "Akkermansia muciniphila in the Human Gastrointestinal Tract: When, Where, and How?" Microorganisms **6**(3).

Gibson, G. R. (1999). "Dietary modulation of the human gut microflora using the prebiotics oligofructose and inulin." J. Nutr. **129**(7): 1438S-1441S.

Gilbert, J. A., M. J. Blaser, J. G. Caporaso, J. K. Jansson, S. V. Lynch and R. Knight (2018). "Current understanding of the human microbiome." Nat Med **24**(4): 392-400.

Gilbert, J. A. and S. V. Lynch (2019). "Community ecology as a framework for human microbiome research." Nat Med **25**(6): 884-889.

Gilroy, R., A. Ravi, M. A.-O. Getino, I. Pursley, D. L. Horton, N. A.-O. Alikhan, D. Baker, K. Gharbi, N. A.-O. Hall, M. A.-O. Watson, E. A.-O. Adriaenssens, E. A.-O. Foster-Nyarko, S. Jarju, A. Secka, M. Antonio, A. Oren, R. A.-O. Chaudhuri, R. La Ragione, F. Hildebrand and M. A.-O. Pallen (2021). "Extensive microbial diversity within the chicken gut microbiome revealed by metagenomics and culture." PeerJ(9).

Gomez-Gallego, C., M. C. Collado, G. Perez, T. Ilo, U. M. Jaakkola, M. J. Bernal, M. J. Periago, R. Frias, G. Ros and S. Salminen (2014). "Resembling breast milk: influence of polyamine-supplemented formula on neonatal BALB/cOlaHsd mouse microbiota." Br J Nutr **111**(6): 1050-1058.

Goris, J., K. T. Konstantinidis, J. A. Klappenbach, T. Coenye, P. Vandamme and J. M. Tiedje (2007). "DNA-DNA hybridization values and their relationship to whole-genome sequence similarities." Int J Syst Evol Microbiol **57**(Pt 1): 81-91.

Górska, S., W. Jachymek, J. Rybka, M. Strus, P. B. Heczko and A. Gamian (2010). "Structural and immunochemical studies of neutral exopolysaccharide produced by Lactobacillus johnsonii 142." Carbohydrate Research **345**(1): 108-114.

Grajeda-Iglesias, C., S. Durand, R. Daillere, K. Iribarren, F. Lemaitre, L. Derosa, F. Aprahamian, N. Bossut, N. Nirmalathasan, F. Madeo, L. Zitvogel and G. Kroemer (2021). "Oral administration of Akkermansia muciniphila elevates systemic antiaging and anticancer metabolites." Aging (Albany NY) **13**(5): 6375-6405.

Grander, C., T. E. Adolph, V. Wieser, P. Lowe, L. Wrzosek, B. Gyongyosi, D. V. Ward, F. Grabherr, R. R. Gerner, A. Pfister, B. Enrich, D. Ciocan, S. Macheiner, L. Mayr, M. Drach, P. Moser, A. R. Moschen, G. Perlemuter, G. Szabo, A. M. Cassard and H. Tilg (2018). "Recovery of ethanol-induced Akkermansia muciniphila depletion ameliorates alcoholic liver disease." Gut.

Green, T. J., R. Smullen and A. C. Barnes (2013). "Dietary soybean protein concentrate-induced intestinal disorder in marine farmed Atlantic salmon, Salmo salar is associated with alterations in gut microbiota." Vet Microbiol **166**(1-2): 286-292.

Grosskopf, T. and O. S. Soyer (2014). "Synthetic microbial communities." Curr Opin Microbiol **18**: 72-77.

Grzeskowiak, L., M. C. Collado, C. Mangani, K. Maleta, K. Laitinen, P. Ashorn, E. Isolauri and S. Salminen (2012). "Distinct gut microbiota in southeastern African and northern European infants." J Pediatr Gastroenterol Nutr **54**(6): 812-816.

Grzeskowiak, L., M. M. Gronlund, C. Beckmann, S. Salminen, A. von Berg and E. Isolauri (2012). "The impact of perinatal probiotic intervention on gut microbiota: double-blind placebo-controlled trials in Finland and Germany." Anaerobe **18**(1): 7-13.

Guinane, C. M., A. Tadrous, F. Fouhy, C. A. Ryan, E. M. Dempsey, B. Murphy, E. Andrews, P. D. Cotter, C. Stanton and R. P. Ross (2013). "Microbial composition of human appendices from patients following appendectomy." MBio **4**(1).

Gum, J. R., Jr., J. J. Ho, W. S. Pratt, J. W. Hicks, A. S. Hill, L. E. Vinall, A. M. Roberton, D. M. Swallow and Y. S. Kim (1997). "MUC3 human intestinal mucin. Analysis of gene structure, the carboxyl terminus, and a novel upstream repetitive region." J Biol Chem **272**(42): 26678-26686.

Guo, X., S. Li, J. Zhang, F. Wu, X. Li, D. Wu, M. Zhang, Z. Ou, Z. Jie, Q. Yan, P. Li, J. Yi and Y. Peng (2017). "Genome sequencing of 39 Akkermansia muciniphila isolates reveals its population structure, genomic and functional diverisity, and global distribution in mammalian gut microbiotas." BMC Genomics **18**(1): 800.

Guo, X., J. Zhang, F. Wu, M. Zhang, M. Yi and Y. Peng (2016). "Different subtype strains of Akkermansia muciniphila abundantly colonize in southern China." J Appl Microbiol **120**(2): 452-459.

Guthrie, B. and W. Wickner (1990). "Trigger factor depletion or overproduction causes defective cell division but does not block protein export." Journal of bacteriology **172**(10): 5555-5562.

Haberman, Y., T. L. Tickle, P. J. Dexheimer, M. O. Kim, D. Tang, R. Karns, R. N. Baldassano, J. D. Noe, J. Rosh, J. Markowitz, M. B. Heyman, A. M. Griffiths, W. V. Crandall, D. R. Mack, S. S. Baker, C. Huttenhower, D. J. Keljo, J. S. Hyams, S. Kugathasan, T. D. Walters, B. Aronow, R. J. Xavier, D. Gevers and L. A. Denson (2014). "Pediatric Crohn disease patients exhibit specific ileal transcriptome and microbiome signature." J Clin Invest **124**(8): 3617-3633.

Hadfield, J., N. J. Croucher, R. J. Goater, K. Abudahab, D. M. Aanensen and S. R. Harris (2018). "Phandango: an interactive viewer for bacterial population genomics." Bioinformatics **34**(2): 292-293.

Haft, D. H., I. T. Paulsen, N. Ward and J. D. Selengut (2006). "Exopolysaccharide-associated protein sorting in environmental organisms: the PEP-CTERM/EpsH system. Application of a novel phylogenetic profiling heuristic." BMC Biol **4**: 29.

Hagi, T., S. Y. Geerlings, B. Nijsse and C. Belzer (2020). "The effect of bile acids on the growth and global gene expression profiles in Akkermansia muciniphila." Applied Microbiology and Biotechnology **104**(24): 10641-10653.

Handcock, M. S. and M. Morris (2006). Relative distribution methods in the social sciences, Springer Science & Business Media.

Hanssen, N. M. J., W. M. de Vos and M. Nieuwdorp (2021). "Fecal microbiota transplantation in human metabolic diseases: From a murky past to a bright future?" Cell Metab **33**(6): 1098-1110.

Harry, E., L. Monahan and L. Thompson (2006). Bacterial Cell Division: The Mechanism and Its Precison. International Review of Cytology, Academic Press. **253:** 27-94.

Hartman, A. L., D. M. Lough, D. K. Barupal, O. Fiehn, T. Fishbein, M. Zasloff and J. A. Eisen (2009). "Human gut microbiome adopts an alternative state following small bowel transplantation." Proc Natl Acad Sci U S A **106**(40): 17187-17192.

Hemsworth, G. R., A. J. Thompson, J. Stepper, L. F. Sobala, T. Coyle, J. Larsbrink, O. Spadiut, E. D. Goddard-Borger, K. A. Stubbs, H. Brumer and G. J. Davies (2016). "Structural dissection of a complex Bacteroides ovatus gene locus conferring xyloglucan metabolism in the human gut." Open Biol **6**(7).

Hernandez, M. A. G., E. E. Canfora, J. W. E. Jocken and E. E. Blaak (2019). "The Short-Chain Fatty Acid Acetate in Body Weight Control and Insulin Sensitivity." Nutrients **11**(8).

Hofmann, A. F. (1976). "The enterohepatic circulation of bile acids in man." Adv Intern Med **21**: 501-534.

Holdeman, L. V. and W. E. C. Moore (1974). "New Genus, Coprococcus, Twelve New Species, and Emended Descriptions of Four Previously Described Species of Bacteria from Human Feces." International Journal of Systematic and Evolutionary Microbiology **24**(2): 260-277.

Holmstrom, K., M. D. Collins, T. Moller, E. Falsen and P. A. Lawson (2004). "Subdoligranulum variabile gen. nov., sp. nov. from human feces." Anaerobe **10**(3): 197-203.

Hong, P. Y., J. A. Croix, E. Greenberg, H. R. Gaskins and R. I. Mackie (2011). "Pyrosequencing-based analysis of the mucosal microbiota in healthy individuals reveals ubiquitous bacterial groups and micro-heterogeneity." PLoS One **6**(9): e25042.

Hosseini, E., C. Grootaert, W. Verstraete and T. Van de Wiele (2011). "Propionate as a health-promoting microbial metabolite in the human gut." Nutrition Reviews **69**(5): 245-258.

Hu, X., Y. Zhao, Y. Yang, W. Gong, X. Sun, L. Yang, Q. Zhang and M. Jin (2020). "Akkermansia muciniphila Improves Host Defense Against Influenza Virus Infection." Front Microbiol **11**: 586476.

Hudek, L., D. Premachandra, W. A. Webster and L. Brau (2016). "Role of Phosphate Transport System Component PstB1 in Phosphate Internalization by Nostoc punctiforme." Appl Environ Microbiol **82**(21): 6344-6356.

Hung, G. U., C. C. Tsai and W. Y. Lin (2006). "Development of a new method for small bowel transit study." Ann Nucl Med **20**(6): 387-392.

Hunter, S., R. Apweiler, T. K. Attwood, A. Bairoch, A. Bateman, D. Binns, P. Bork, U. Das, L. Daugherty, L. Duquenne, R. D. Finn, J. Gough, D. Haft, N. Hulo, D. Kahn, E. Kelly, A. Laugraud, I. Letunic, D. Lonsdale, R. Lopez, M. Madera, J. Maslen, C. McAnulla, J. McDowall, J. Mistry, A. Mitchell, N. Mulder, D. Natale, C. Orengo, A. F. Quinn, J. D. Selengut, C. J. Sigrist, M. Thimma, P. D. Thomas, F. Valentin, D. Wilson, C. H. Wu and C. Yeats (2009). "InterPro: the integrative protein signature database." Nucleic Acids Res **37**(Database issue): D211-215.

Hunter, S., P. Jones, A. Mitchell, R. Apweiler, T. K. Attwood, A. Bateman, T. Bernard, D. Binns, P. Bork, S. Burge, E. De Castro, P. Coggill, M. Corbett, U. Das, L. Daugherty, L. Duquenne, R. D. Finn, M. Fraser, J. Gough, D. Haft, N. Hulo, D. Kahn, E. Kelly, I. Letunic, D. Lonsdale, R. Lopez, M. Madera, J. Maslen, C. McAnulla, J. McDowall, C. McMenamin, H. Mi, P. Mutowo-Muellenet, N. Mulder, D. Natale, C. Orengo, S. Pesseat, M. Punta, A. F. Quinn, C. Rivoire, A. Sangrador-Vegas, J. D. Selengut, C. J. A. Sigrist, M. Scheremetjew, J. Tate, M. Thimmajanarthanan, P. D. Thomas, C. H. Wu, C. Yeats and S. Y. Yong (2012). "InterPro in 2011: New developments in the family and domain prediction database." Nucleic Acids Research **40**(D1): D306-D306.

Hyatt, D., G. L. Chen, P. F. LoCascio, M. L. Land, F. W. Larimer and L. J. Hauser (2010). "Prodigal: Prokaryotic gene recognition and translation initiation site identification." BMC Bioinformatics **11**(1): 119-119.

Inagaki, T., A. Moschetta, Y. K. Lee, L. Peng, G. Zhao, M. Downes, R. T. Yu, J. M. Shelton, J. A. Richardson, J. J. Repa, D. J. Mangelsdorf and S. A. Kliewer (2006). "Regulation of antibacterial defense in the small intestine by the nuclear bile acid receptor." Proc Natl Acad Sci U S A **103**(10): 3920-3925.

Isanapong, J., W. Sealy Hambright, A. G. Willis, A. Boonmee, S. J. Callister, K. E. Burnum, L. Pasa-Tolic, C. D. Nicora, J. T. Wertz, T. M. Schmidt and J. L. Rodrigues (2013). "Development of an ecophysiological model for Diplosphaera colotermitum TAV2, a termite hindgut Verrucomicrobium." ISME J **7**(9): 1803-1813.

Islam, K. B., S. Fukiya, M. Hagio, N. Fujii, S. Ishizuka, T. Ooka, Y. Ogura, T. Hayashi and A. Yokota (2011). "Bile acid is a host factor that regulates the composition of the cecal microbiota in rats." Gastroenterology **141**(5): 1773-1781.

Jackson, H. T., E. F. Mongodin, K. P. Davenport, C. M. Fraser, A. D. Sandler and S. L. Zeichner (2014). "Culture-independent evaluation of the appendix and rectum microbiomes in children with and without appendicitis." PLoS One **9**(4): e95414.

Ji, B. W., R. U. Sheth, P. D. Dixit, K. Tchourine and D. Vitkup (2020). "Macroecological dynamics of gut microbiota." Nat Microbiol **5**(5): 768-775.

Jian, C., P. Luukkonen, H. Yki-Järvinen, A. Salonen and K. Korpela (2020). "Quantitative PCR provides a simple and accessible method for quantitative microbiota profiling." PloS one **15**(1): e0227285.

Jiang, W., N. Wu, X. Wang, Y. Chi, Y. Zhang, X. Qiu, Y. Hu, J. Li and Y. Liu (2015). "Dysbiosis gut microbiota associated with inflammation and impaired mucosal immune function in intestine of humans with non-alcoholic fatty liver disease." Sci Rep **5**: 8096.

Johansson, M. E., D. Ambort, T. Pelaseyed, A. Schutte, J. K. Gustafsson, A. Ermund, D. B. Subramani, J. M. Holmen-Larsson, K. A. Thomsson, J. H. Bergstrom, S. van der Post, A. M. Rodriguez-Pineiro, H. Sjovall, M. Backstrom and G. C. Hansson (2011). "Composition and functional role of the mucus layers in the intestine." Cell Mol Life Sci **68**(22): 3635-3641.

Johansson, M. E. and G. C. Hansson (2016). "Immunological aspects of intestinal mucus and mucins." Nat Rev Immunol **16**(10): 639-649.

Johansson, M. E., J. M. Larsson and G. C. Hansson (2011). "The two mucus layers of colon are organized by the MUC2 mucin, whereas the outer layer is a legislator of host-microbial interactions." Proc Natl Acad Sci U S A **108 Suppl 1**: 4659-4665.

Johansson, M. E., M. Phillipson, J. Petersson, A. Velcich, L. Holm and G. C. Hansson (2008). "The inner of the two Muc2 mucin-dependent mucus layers in colon is devoid of bacteria." Proc Natl Acad Sci U S A **105**(39): 15064-15069.

Johnson, A. J., P. Vangay, G. A. Al-Ghalith, B. M. Hillmann, T. L. Ward, R. R. Shields-Cutler, A. D. Kim, A. K. Shmagel, A. N. Syed, S. Personalized Microbiome Class, J. Walter, R. Menon, K. Koecher and D. Knights (2019). "Daily Sampling Reveals Personalized Diet-Microbiome Associations in Humans." Cell Host Microbe **25**(6): 789-802 e785.

Jones, S. E., M. L. Paynich, D. B. Kearns and K. L. Knight (2014). "Protection from intestinal inflammation by bacterial exopolysaccharides." J Immunol **192**(10): 4813-4820.

Jost, T., C. Lacroix, C. Braegger and C. Chassard (2015). "Impact of human milk bacteria and oligosaccharides on neonatal gut microbiota establishment and gut health." Nutr Rev **73**(7): 426-437.

Jouvet, N. and J. L. Estall (2017). "The pancreas: Bandmaster of glucose homeostasis." Exp Cell Res **360**(1): 19-23.

Juárez-Fernández, M., D. Porras, P. Petrov, S. Román-Sagüillo, M. V. García-Mediavilla, P. Soluyanova, S. Martínez-Flórez, J. González-Gallego, E. Nistal, R. Jover and S. Sánchez-Campos (2021). "The synbiotic combination of akkermansia muciniphila and quercetin ameliorates early obesity and NAFLD through gut microbiota reshaping and bile acid metabolism modulation." Antioxidants **10**(12).

Juraskova, D., S. C. Ribeiro and C. C. G. Silva (2022). "Exopolysaccharides Produced by Lactic Acid Bacteria: From Biosynthesis to Health-Promoting Properties." Foods **11**(2).

Kageyama, A., Y. Benno and T. Nakase (1999). "Phylogenetic and phenotypic evidence for the transfer of Eubacterium aerofaciens to the genus Collinsella as Collinsella aerofaciens gen. nov., comb. nov." Int J Syst Bacteriol **49 Pt 2**: 557-565.

Kamada, N., G. Y. Chen, N. Inohara and G. Nunez (2013). "Control of pathogens and pathobionts by the gut microbiota." Nat Immunol **14**(7): 685-690.

Kanehisa, M., Y. Sato and K. Morishima (2016). "BlastKOALA and GhostKOALA: KEGG tools for functional characterization of genome and metagenome sequences." J. Mol. Biol. **428**(4): 726-731.

Kang, C. S., M. Ban, E. J. Choi, H. G. Moon, J. S. Jeon, D. K. Kim, S. K. Park, S. G. Jeon, T. Y. Roh, S. J. Myung, Y. S. Gho, J. G. Kim and Y. K. Kim (2013). "Extracellular vesicles derived from gut microbiota, especially Akkermansia muciniphila, protect the progression of dextran sulfate sodium-induced colitis." PLoS One **8**(10): e76520.

Karcher, N., E. Nigro, M. Puncochar, A. Blanco-Miguez, M. Ciciani, P. Manghi, M. Zolfo, F. Cumbo, S. Manara, D. Golzato, A. Cereseto, M. Arumugam, T. P. N. Bui, H. L. P. Tytgat, M. Valles-Colomer, W. M. de Vos and N. Segata (2021). "Genomic diversity and ecology of human-associated Akkermansia species in the gut microbiome revealed by extensive metagenomic assembly." Genome Biol **22**(1): 209.

Karkaria, B. D. M. A. F. A. J. B. C. P. (2021). "Chaos in small microbial communities." bioRxiv.

Karlsson, C. L., J. Onnerfalt, J. Xu, G. Molin, S. Ahrne and K. Thorngren-Jerneck (2012). "The microbiota of the gut in preschool children with normal and excessive body weight." Obesity (Silver Spring) **20**(11): 2257-2261.

Kassambara, A. (2018). "ggpubr:"ggplot2" based publication ready plots." R package version 0.1 **7**.

Kearney, S. M., S. M. Gibbons, S. E. Erdman and E. J. Alm (2018). "Orthogonal dietary niche enables reversible engraftment of a gut bacterial commensal." Cell Rep **24**(7): 1842-1851.

Keates, A. C., D. P. Nunes, N. H. Afdhal, R. F. Troxler and G. D. Offner (1997). "Molecular cloning of a major human gall bladder mucin: complete C-terminal sequence and genomic organization of MUC5B." Biochem J **324 (Pt 1)**: 295-303.

Kemperman, R. A., G. Gross, S. Mondot, S. Possemiers, M. Marzorati, T. Van de Wiele, J. Doré and E. E. Vaughan (2013). "Impact of polyphenols from black tea and red wine/grape juice on a gut model microbiome." Food Research International **53**(2): 659-669.

Kilpatrick, A. and A. Ives (2003). "Species interactions can explain Taylor's power law for ecological time series." Nature **422**(6927): 65.

Kim, H. J., D. Huh, G. Hamilton and D. E. Ingber (2012). "Human gut-on-a-chip inhabited by microbial flora that experiences intestinal peristalsis-like motions and flow." Lab Chip **12**(12): 2165-2174.

Kim, H. J., H. Li, J. J. Collins and D. E. Ingber (2016). "Contributions of microbiome and mechanical deformation to intestinal bacterial overgrowth and inflammation in a human gut-on-a-chip." Proc Natl Acad Sci U S A **113**(1): E7-15.

Kim, J. S., S. W. Kang, J. H. Lee, S. H. Park and J. S. Lee (2022). "The evolution and competitive strategies of Akkermansia muciniphila in gut." Gut Microbes **14**(1): 2025017.

Kim, S., Y. Lee, Y. Kim, Y. Seo, H. Lee, J. Ha, J. Lee, Y. Choi, H. Oh and Y. Yoon (2020). "Akkermansia muciniphila Prevents Fatty Liver Disease, Decreases Serum Triglycerides, and Maintains Gut Homeostasis." Appl Environ Microbiol **86**(7).

Kim, S., Y. C. Shin, T. Y. Kim, Y. Kim, Y. S. Lee, S. H. Lee, M. N. Kim, E. O, K. S. Kim and M. N. Kweon (2021). "Mucin degrader Akkermansia muciniphila accelerates intestinal stem cell-mediated epithelial development." Gut Microbes **13**(1): 1-20.

Kirmiz, N., K. Galindo, K. L. Cross, E. Luna, N. Rhoades, M. Podar and G. E. Flores (2020). "Comparative genomics guides elucidation of vitamin B12 biosynthesis in novel human associated Akkermansia strains." bioRxiv: 587527.

Kopylova, E., L. Noé and H. Touzet (2012). "SortMeRNA: fast and accurate filtering of ribosomal RNAs in metatranscriptomic data." Bioinformatics **28**(24): 3211-3217.

Korcz, E. and L. Varga (2021). "Exopolysaccharides from lactic acid bacteria: Techno-functional application in the food industry." Trends in Food Science & Technology **110**: 375-384.

Koropatkin, N. M., E. A. Cameron and E. C. Martens (2012). "How glycan metabolism shapes the human gut microbiota." Nat Rev Microbiol **10**(5): 323-335.

Korpela, K., A. Salonen, L. J. Virta, R. A. Kekkonen, K. Forslund, P. Bork and W. M. de Vos (2016). "Intestinal microbiome is related to lifetime antibiotic use in Finnish pre-school children." Nat Commun **7**: 10410.

Kostopoulos, I., S. Aalvink, P. Kovatcheva-Datchary, B. Nijsse, F. Backhed, J. Knol, W. M. de Vos and C. Belzer (2021). "A Continuous Battle for Host-Derived Glycans Between a Mucus Specialist and a Glycan Generalist in vitro and in vivo." Front Microbiol **12**: 632454.

Kostopoulos, I., J. Elzinga, N. Ottman, J. T. Klievink, B. Blijenberg, S. Aalvink, S. Boeren, M. Mank, J. Knol, W. M. de Vos and C. Belzer (2020). "Akkermansia muciniphila uses human milk oligosaccharides to thrive in the early life conditions in vitro." Scientific Reports **10**(1).

Kovatcheva-Datchary, P., S. Shoaie, S. Lee, A. Wahlstrom, I. Nookaew, A. Hallen, R. Perkins, J. Nielsen and F. Backhed (2019). "Simplified Intestinal Microbiota to Study Microbe-Diet-Host Interactions in a Mouse Model." Cell Rep **26**(13): 3772-3783 e3776.

Koziolek, M., M. Grimm, D. Becker, V. Iordanov, H. Zou, J. Shimizu, C. Wanke, G. Garbacz and W. Weitschies (2015). "Investigation of pH and Temperature Profiles in the GI Tract of Fasted Human Subjects Using the Intellicap((R)) System." J Pharm Sci **104**(9): 2855-2863.

Krause, J. L., S. S. Schaepe, K. Fritz-Wallace, B. Engelmann, U. Rolle-Kampczyk, S. Kleinsteuber, F. Schattenberg, Z. Liu, S. Mueller, N. Jehmlich, M. Von Bergen and G. Herberth (2020). "Following the community development of SIHUMIx - a new intestinal in vitro model for bioreactor use." Gut Microbes **11**(4): 1116-1129.

Kumar, R., H. Kane, Q. Wang, A. Hibberd, H. M. Jensen, H. S. Kim, S. Y. Bak, I. Auzanneau, S. Bry, N. Christensen, A. Friedman, P. Rasinkangas, A. C. Ouwehand, S. D. Forssten and O. Hasselwander (2022). "Identification and Characterization of a Novel Species of Genus Akkermansia with Metabolic Health Effects in a Diet-Induced Obesity Mouse Model." Cells **11**(13).

Lagesen, K., P. Hallin, E. A. Rødland, H. H. Stærfeldt, T. Rognes and D. W. Ussery (2007). "RNAmmer: Consistent and rapid annotation of ribosomal RNA genes." Nucleic Acids Research **35**(9): 3100-3108.

Lahti, L. and S. A. Shetty (2018). "Tools for microbiome analysis in R."

Langmead, B. and S. L. Salzberg (2012). "Fast gapped-read alignment with Bowtie 2." Nature Methods **9**(4): 357-359.

Le Chatelier, E., T. Nielsen, J. Qin, E. Prifti, F. Hildebrand, G. Falony, M. Almeida, M. Arumugam, J. M. Batto, S. Kennedy, P. Leonard, J. Li, K. Burgdorf, N. Grarup, T. Jorgensen, I. Brandslund, H. B. Nielsen, A. S. Juncker, M. Bertalan, F. Levenez, N. Pons, S. Rasmussen, S. Sunagawa, J. Tap, S. Tims, E. G. Zoetendal, S. Brunak, K. Clement, J. Dore, M. Kleerebezem, K. Kristiansen, P. Renault, T. Sicheritz-Ponten, W. M. de Vos, J. D. Zucker, J. Raes, T. Hansen, H. I. T. c. Meta, P. Bork, J. Wang, S. D. Ehrlich and O. Pedersen (2013). "Richness of human gut microbiome correlates with metabolic markers." Nature **500**(7464): 541-546.

Le Poul, E., C. Loison, S. Struyf, J. Y. Springael, V. Lannoy, M. E. Decobecq, S. Brezillon, V. Dupriez, G. Vassart, J. Van Damme, M. Parmentier and M. Detheux (2003). "Functional characterization of human receptors for short chain fatty acids and their role in polymorphonuclear cell activation." J Biol Chem **278**(28): 25481-25489.

Leake, S. L., M. Pagni, L. Falquet, F. Taroni and G. Greub (2016). "The salivary microbiome for differentiating individuals: proof of principle." Microbes Infect **18**(6): 399-405.

Leal-Lopes, C., F. J. Velloso, J. C. Campopiano, M. C. Sogayar and R. G. Correa (2015). "Roles of Commensal Microbiota in Pancreas Homeostasis and Pancreatic Pathologies." J Diabetes Res **2015**: 284680.

Lee, A., J. Fox and S. Hazell (1993). Pathogenicity of Helicobacter pylori: A perspective. Infection and Immunity, American Society for Microbiology (ASM). **61:** 1601-1610.

Leth, M. L., M. Ejby, C. Workman, D. A. Ewald, S. S. Pedersen, C. Sternberg, M. I. Bahl, T. R. Licht, F. L. Aachmann, B. Westereng and M. Abou Hachem (2018). "Differential bacterial capture and transport preferences facilitate co-growth on dietary xylan in the human gut." Nat Microbiol **3**(5): 570-580.

Ley, R. E., F. Backhed, P. Turnbaugh, C. A. Lozupone, R. D. Knight and J. I. Gordon (2005). "Obesity alters gut microbial ecology." Proc Natl Acad Sci U S A **102**(31): 11070-11075.

Ley, R. E., M. Hamady, C. Lozupone, P. J. Turnbaugh, R. R. Ramey, J. S. Bircher, M. L. Schlegel, T. A. Tucker, M. D. Schrenzel, R. Knight and J. I. Gordon (2008). "Evolution of mammals and their gut microbes." Science **320**(5883): 1647-1651.

Ley, R. E., C. A. Lozupone, M. Hamady, R. Knight and J. I. Gordon (2008). "Worlds within worlds: evolution of the vertebrate gut microbiota." Nat Rev Microbiol **6**(10): 776-788.

Li, B. and C. N. Dewey (2011). "RSEM: Accurate transcript quantification from RNA-Seq data with or without a reference genome." BMC Bioinformatics **12**(1): 323-323.

Li, E., C. M. Hamm, A. S. Gulati, R. B. Sartor, H. Chen, X. Wu, T. Zhang, F. J. Rohlf, W. Zhu, C. Gu, C. E. Robertson, N. R. Pace, E. C. Boedeker, N. Harpaz, J. Yuan, G. M. Weinstock, E. Sodergren and D. N. Frank (2012). "Inflammatory bowel diseases phenotype, C. difficile and NOD2 genotype are associated with shifts in human ileum associated microbial composition." PLoS One **7**(6): e26284.

Li, G., M. Yang, K. Zhou, L. Zhang, L. Tian, S. Lv, Y. Jin, W. Qian, H. Xiong, R. Lin, Y. Fu and X. Hou (2015). "Diversity of Duodenal and Rectal Microbiota in Biopsy Tissues and Luminal Contents in Healthy Volunteers." J Microbiol Biotechnol **25**(7): 1136-1145.

Li, J., H. Jia, X. Cai, H. Zhong, Q. Feng, S. Sunagawa, M. Arumugam, J. R. Kultima, E. Prifti, T. Nielsen, A. S. Juncker, C. Manichanh, B. Chen, W. Zhang, F. Levenez, J. Wang, X. Xu, L. Xiao, S. Liang, D. Zhang, Z. Zhang, W. Chen, H. Zhao, J. Y. Al-Aama, S. Edris, H. Yang, J. Wang, T. Hansen, H. B. Nielsen, S. Brunak, K. Kristiansen, F. Guarner, O. Pedersen, J. Dore, S. D. Ehrlich, H. I. T. C. Meta, P. Bork, J. Wang and H. I. T. C. Meta (2014). "An integrated catalog of reference genes in the human gut microbiome." Nat Biotechnol **32**(8): 834-841.

Li, M., B. Wang, M. Zhang, M. Rantalainen, S. Wang, H. Zhou, Y. Zhang, J. Shen, X. Pang, M. Zhang, H. Wei, Y. Chen, H. Lu, J. Zuo, M. Su, Y. Qiu, W. Jia, C. Xiao, L. M. Smith, S. Yang, E. Holmes, H. Tang, G. Zhao, J. K. Nicholson, L. Li and L. Zhao (2008). "Symbiotic gut microbes modulate human metabolic phenotypes." Proceedings of the National Academy of Sciences of the United States of America **105**(6): 2117-2122.

Ligthart, K., C. Belzer, W. M. de Vos and H. L. P. Tytgat (2020). "Bridging Bacteria and the Gut: Functional Aspects of Type IV Pili." Trends Microbiol **28**(5): 340-348.

Linden, S. K., P. Sutton, N. G. Karlsson, V. Korolik and M. A. McGuckin (2008). "Mucins in the mucosal barrier to infection." Mucosal Immunol **1**(3): 183-197.

Liu, C., S. M. Finegold, Y. Song and P. A. Lawson (2008). "Reclassification of *Clostridium coccoides*, *Ruminococcus hansenii*, *Ruminococcus hydrogenotrophicus*, *Ruminococcus luti*, *Ruminococcus productus* and *Ruminococcus schinkii* as *Blautia coccoides* gen. nov., comb. nov., *Blautia hansenii* comb. nov., *Blautia hydrogenotrophica* comb. nov., *Blautia luti* comb. nov., *Blautia producta* comb. nov., *Blautia schinkii* comb. nov. and description of *Blautia wexlerae* sp. nov., isolated from human faeces." Int J Syst Evol Microbiol **58**(8): 1896-1902.

Liu, Q., W. Lu, F. Tian, J. Zhao, H. Zhang, K. Hong and L. Yu (2021). "Akkermansia muciniphila Exerts Strain-Specific Effects on DSS-Induced Ulcerative Colitis in Mice." Front Cell Infect Microbiol **11**: 698914.

Liu, Z., N. Cichocki, F. Bonk, S. Günther, F. Schattenberg, H. Harms, F. Centler and S. Müller (2018). "Ecological stability properties of microbial communities assessed by flow cytometry." mSphere **3**(1): e00564-00517.

Lopez-Siles, M., T. M. Khan, S. H. Duncan, H. J. Harmsen, L. J. Garcia-Gil and H. J. Flint (2012). "Cultured representatives of two major phylogroups of human colonic Faecalibacterium prausnitzii can utilize pectin, uronic acids, and host-derived substrates for growth." Appl Environ Microbiol **78**(2): 420-428.

Lopez-Siles, M., M. Martinez-Medina, D. Busquets, M. Sabat-Mir, S. H. Duncan, H. J. Flint, X. Aldeguer and L. J. Garcia-Gil (2014). "Mucosa-associated Faecalibacterium prausnitzii and Escherichia coli co-abundance can distinguish Irritable Bowel Syndrome and Inflammatory Bowel Disease phenotypes." Int J Med Microbiol **304**(3-4): 464-475.

Louis, P. and H. J. Flint (2017). "Formation of propionate and butyrate by the human colonic microbiota." Environ. Microbiol. **19**(1): 29-41.

Lowe, T. M. and S. R. Eddy (1997). "tRNAscan-SE: A Program for Improved Detection of Transfer RNA Genes in Genomic Sequence." Nucleic Acids Research **25**(5): 955-964.

Lu, Z., X. Luan and G. Li (2021). A novel encapsulating method of pasteurized Akkermansia muciniphila with double-network hydrogel microstructures by a digital mask printing system. 2021 IEEE 11th Annual International Conference on CYBER Technology in Automation, Control, and Intelligent Systems, CYBER 2021.

Ludwig, W., O. Strunk, R. Westram, L. Richter, H. Meier, A. Yadhukumar, A. Buchner, T. Lai, S. Steppi, G. Jacob, W. Förster, I. Brettske, S. Gerber, A. W. Ginhart, O. Gross, S. Grumann, S. Hermann, R. Jost, A. König, T. Liss, R. Lüßbmann, M. May, B. Nonhoff, B. Reichel, R. Strehlow, A. Stamatakis, N. Stuckmann, A. Vilbig, M. Lenke, T. Ludwig, A. Bode and K. H. Schleifer (2004). "ARB: A software environment for sequence data." Nucleic Acids Research **32**(4): 1363-1371.

Lukovac, S., C. Belzer, L. Pellis, B. J. Keijser, W. M. de Vos, R. C. Montijn and G. Roeselers (2014). "Differential modulation by Akkermansia muciniphila and Faecalibacterium prausnitzii of host peripheral lipid metabolism and histone acetylation in mouse gut organoids." MBio **5**(4).

Luna, E., S. G. Parkar, N. Kirmiz, S. Hartel, E. Hearn, M. Hossine, A. Kurdian, C. Mendoza, K. Orr, L. Padilla, K. Ramirez, P. Salcedo, E. Serrano, B. Choudhury, M. Paulchakrabarti, C. T. Parker, S. Huynh, K. Cooper and G. E. Flores (2022). "Utilization Efficiency of Human Milk Oligosaccharides by Human-Associated Akkermansia Is Strain Dependent." Appl Environ Microbiol **88**(1): e0148721.

Lyra, A., S. Forssten, P. Rolny, Y. Wettergren, S. J. Lahtinen, K. Salli, L. Cedgard, E. Odin, B. Gustavsson and A. C. Ouwehand (2012). "Comparison of bacterial quantities in left and right colon biopsies and faeces." World J Gastroenterol **18**(32): 4404-4411.

Mabwi, H. A., E. Kim, D. G. Song, H. S. Yoon, C. H. Pan, E. V. G. Komba, G. Ko and K. H. Cha (2021). "Synthetic gut microbiome: Advances and challenges." Comput Struct Biotechnol J **19**: 363-371.

Macfarlane, G. T., S. Hay, S. Macfarlane and G. R. Gibson (1990). "Effect of different carbohydrates on growth, polysaccharidase and glycosidase production by Bacteroides ovatus, in batch and continuous culture." J Appl Bacteriol **68**(2): 179-187.

Macfarlane, G. T. and S. Macfarlane (2007). "Models for intestinal fermentation: association between food components, delivery systems, bioavailability and functional interactions in the gut." Curr Opin Biotechnol **18**(2): 156-162.

Machado, D., J. C. Barbosa, D. Almeida, J. C. Andrade, A. C. Freitas and A. M. Gomes (2022). "Insights into the Antimicrobial Resistance Profile of a Next Generation Probiotic Akkermansia muciniphila DSM 22959." Int J Environ Res Public Health **19**(15).

Madsen, J. L. (1992). "Effects of gender, age, and body mass index on gastrointestinal transit times." Dig Dis Sci **37**(10): 1548-1553.

Maier, L., C. V. Goemans, J. Wirbel, M. Kuhn, C. Eberl, M. Pruteanu, P. Muller, S. Garcia-Santamarina, E. Cacace, B. Zhang, C. Gekeler, T. Banerjee, E. E. Anderson, A. Milanese, U. Lober, S. K. Forslund, K. R. Patil, M. Zimmermann, B. Stecher, G. Zeller, P. Bork and A. Typas (2021). "Unravelling the collateral damage of antibiotics on gut bacteria." Nature **599**(7883): 120-124.

Makki, K., E. C. Deehan, J. Walter and F. Backhed (2018). "The Impact of Dietary Fiber on Gut Microbiota in Host Health and Disease." Cell Host Microbe **23**(6): 705-715.

Mallon, C. A., F. Poly, X. Le Roux, I. Marring, J. D. van Elsas and J. F. Salles (2015). "Resource pulses can alleviate the biodiversity–invasion relationship in soil microbial communities." Ecology **96**(4): 915-926.

Marcial-Coba, M. S., T. Cieplak, T. B. Cahu, A. Blennow, S. Knochel and D. S. Nielsen (2018). "Viability of microencapsulated Akkermansia muciniphila and Lactobacillus plantarum during freeze-drying, storage and in vitro simulated upper gastrointestinal tract passage." Food Funct **9**(11): 5868-5879.

Marcial-Coba, M. S., L. Saaby, S. Knochel and D. S. Nielsen (2019). "Dark chocolate as a stable carrier of microencapsulated Akkermansia muciniphila and Lactobacillus casei." FEMS Microbiol Lett **366**(2).

Marcial, G., J. Villena, G. Faller, A. Hensel and G. F. de Valdez (2017). "Exopolysaccharide-producing Streptococcus thermophilus CRL1190 reduces the inflammatory response caused by Helicobacter pylori." Benef Microbes **8**(3): 451-461.

Marcotte, H. and M. C. Lavoie (1998). "Oral microbial ecology and the role of salivary immunoglobulin A." Microbiol Mol Biol Rev **62**(1): 71-109.

Marsh, P. D., D. A. Head and D. A. Devine (2015). "Ecological approaches to oral biofilms: control without killing." Caries Res **49 Suppl 1**: 46-54.

Martens, E. C., H. C. Chiang and J. I. Gordon (2008). "Mucosal glycan foraging enhances fitness and transmission of a saccharolytic human gut bacterial symbiont." Cell Host Microbe **4**(5): 447-457.

Marti, J. M., D. Martinez-Martinez, T. Rubio, C. Gracia, M. Pena, A. Latorre, A. Moya and P. G. C (2017). "Health and disease imprinted in the time variability of the human microbiome." mSystems **2**(2).

Mateo Anson, N., R. van den Berg, R. Havenaar, A. Bast and G. R. M. M. Haenen (2009). "Bioavailability of ferulic acid is determined by its bioaccessibility." Journal of Cereal Science **49**(2): 296-300.

McDougall, C. J., R. Wong, P. Scudera, M. Lesser and J. J. DeCosse (1993). "Colonic mucosal pH in humans." Dig Dis Sci **38**(3): 542-545.

McFall-Ngai, M., M. G. Hadfield, T. C. G. Bosch, H. V. Carey, T. Domazet-Lošo, A. E. Douglas, N. Dubilier, G. Eberl, T. Fukami, S. F. Gilbert, U. Hentschel, N. King, S. Kjelleberg, A. H. Knoll, N. Kremer, S. K. Mazmanian, J. L. Metcalf, K. Nealson, N. E. Pierce, J. F. Rawls, A. Reid, E. G. Ruby, M. Rumpho, J. G. Sanders, D. Tautz and J. J. Wernegreen (2013). Animals in a bacterial world, a new imperative for the life sciences. Proceedings of the National Academy of Sciences of the United States of America, National Academy of Sciences. **110:** 3229-3236.

McHardy, I. H., M. Goudarzi, M. Tong, P. M. Ruegger, E. Schwager, J. R. Weger, T. G. Graeber, J. L. Sonnenburg, S. Horvath, C. Huttenhower, D. P. McGovern, A. J. Fornace, Jr., J. Borneman and J. Braun (2013). "Integrative analysis of the microbiome and metabolome of the human intestinal mucosal surface reveals exquisite inter-relationships." Microbiome **1**(1): 17.

McMurdie, P. J. and S. Holmes (2013). "Phyloseq: an R package for reproducible interactive analysis and graphics of microbiome census data." PloS one **8**(4): e61217.

Memba, R., S. N. Duggan, H. M. Ni Chonchubhair, O. M. Griffin, Y. Bashir, D. B. O'Connor, A. Murphy, J. McMahon, Y. Volcov, B. M. Ryan and K. C. Conlon (2017). "The potential role of gut microbiota in pancreatic disease: A systematic review." Pancreatology **17**(6): 867-874.

Meng, X., J. Zhang, H. Wu, D. Yu and X. Fang (2020). "Akkermansia muciniphila Aspartic Protease Amuc_1434* Inhibits Human Colorectal Cancer LS174T Cell Viability via TRAIL-Mediated Apoptosis Pathway." Int J Mol Sci **21**(9).

Mennigen, R. and M. Bruewer (2009). "Effect of probiotics on intestinal barrier function." Ann N Y Acad Sci **1165**: 183-189.

Merchant, H. A., E. L. McConnell, F. Liu, C. Ramaswamy, R. P. Kulkarni, A. W. Basit and S. Murdan (2011). "Assessment of gastrointestinal pH, fluid and lymphoid tissue in the guinea pig, rabbit and pig, and implications for their use in drug development." Eur J Pharm Sci **42**(1-2): 3-10.

Milani, C., S. Duranti, S. Napoli, G. Alessandri, L. Mancabelli, R. Anzalone, G. Longhi, A. Viappiani, M. Mangifesta and G. A. Lugli (2019). "Colonization of the human gut by bovine bacteria present in parmesan cheese." Nat. Commun. **10**(1): 1-12.

Miller, R. S. and L. C. Hoskins (1981). "Mucin degradation in human colon ecosystems. Fecal population densities of mucin-degrading bacteria estimated by a "most probable number" method." Gastroenterology **81**(4): 759-765.

Mohd Nadzir, M., R. W. Nurhayati, F. N. Idris and M. H. Nguyen (2021). "Biomedical Applications of Bacterial Exopolysaccharides: A Review." Polymers (Basel) **13**(4).

Molly, K., M. Vande Woestyne and W. Verstraete (1993). "Development of a 5-step multi-chamber reactor as a simulation of the human intestinal microbial ecosystem." Appl Microbiol Biotechnol **39**(2): 254-258.

Momozawa, Y., V. Deffontaine, E. Louis and J. F. Medrano (2011). "Characterization of bacteria in biopsies of colon and stools by high throughput sequencing of the V2 region of bacterial 16S rRNA gene in human." PLoS One **6**(2): e16952.

MOORE, W. E. C., J. L. JOHNSON and L. V. HOLDEMAN (1976). "Emendation of Bacteroidaceae and Butyrivibrio and Descriptions of Desulfomonas gen. nov. and Ten New Species in the Genera Desulfomonas, Butyrivibrio, Eubacterium, Clostridium, and Ruminococcus." International Journal of Systematic and Evolutionary Microbiology **26**(2): 238-252.

Moran, A. P., A. Gupta and L. Joshi (2011). Sweet-talk: Role of host glycosylation in bacterial pathogenesis of the gastrointestinal tract. Gut, Gut. **60:** 1412-1425.

Morikawa, M., S. Tsujibe, J. Kiyoshima-Shibata, Y. Watanabe, N. Kato-Nagaoka, K. Shida and S. Matsumoto (2016). "Microbiota of the Small Intestine Is Selectively Engulfed by Phagocytes of the Lamina Propria and Peyer's Patches." PLoS One **11**(10): e0163607.

Mosele, J. I., A. Macia and M. J. Motilva (2015). "Metabolic and Microbial Modulation of the Large Intestine Ecosystem by Non-Absorbed Diet Phenolic Compounds: A Review." Molecules **20**(9): 17429-17468.

Mouillot, D., W. Stubbs, M. Faure, O. Dumay, J. A. Tomasini, J. B. Wilson and T. Do Chi (2005). "Niche overlap estimates based on quantitative functional traits: a new family of non-parametric indices." Oecologia **145**(3): 345-353.

Muegge, B. D., J. Kuczynski, D. Knights, J. C. Clemente, A. González, L. Fontana, B. Henrissat, R. Knight and J. I. Gordon (2011). "Diet drives convergence in gut microbiome functions across mammalian phylogeny and within humans." Science **332**(6032): 970-974.

Nasidze, I., D. Quinque, J. Li, M. Li, K. Tang and M. Stoneking (2009). "Comparative analysis of human saliva microbiome diversity by barcoded pyrosequencing and cloning approaches." Anal Biochem **391**(1): 64-68.

Newburg, D. S. (2000). "Oligosaccharides in human milk and bacterial colonization." J Pediatr Gastroenterol Nutr **30 Suppl 2**: S8-17.

Nguyen, P.-T., T.-T. Nguyen, D.-C. Bui, P.-T. Hong, Q.-K. Hoang and H.-T. Nguyen (2020). "Exopolysaccharide production by lactic acid bacteria: the manipulation of environmental stresses for industrial applications." AIMS microbiology **6**(4): 451-469.

Nielsen, P. A., E. P. Bennett, H. H. Wandall, M. H. Therkildsen, J. Hannibal and H. Clausen (1997). "Identification of a major human high molecular weight salivary mucin (MG1) as tracheobronchial mucin MUC5B." Glycobiology **7**(3): 413-419.

Nikolic, M., P. Lopez, I. Strahinic, A. Suarez, M. Kojic, M. Fernandez-Garcia, L. Topisirovic, N. Golic and P. Ruas-Madiedo (2012). "Characterisation of the exopolysaccharide (EPS)-producing Lactobacillus paraplantarum BGCG11 and its non-EPS producing derivative strains as potential probiotics." Int J Food Microbiol **158**(2): 155-162.

Nilsson, N. E., K. Kotarsky, C. Owman and B. Olde (2003). "Identification of a free fatty acid receptor, FFA2R, expressed on leukocytes and activated by short-chain fatty acids." Biochem Biophys Res Commun **303**(4): 1047-1052.

Nishiyama, H., T. Nagai, M. Kudo, Y. Okazaki, Y. Azuma, T. Watanabe, S. Goto, H. Ogata and T. Sakurai (2018). "Supplementation of pancreatic digestive enzymes alters the composition of intestinal microbiota in mice." Biochem Biophys Res Commun **495**(1): 273-279.

Nugent, S. G., D. Kumar, D. S. Rampton and D. F. Evans (2001). "Intestinal luminal pH in inflammatory bowel disease: possible determinants and implications for therapy with aminosalicylates and other drugs." Gut **48**(4): 571-577.

Oliphant, K., V. R. Parreira, K. Cochrane and E. Allen-Vercoe (2019). "Drivers of human gut microbial community assembly: coadaptation, determinism and stochasticity." ISME J **13**(12): 3080-3092.

On, S. L. W., W. G. Miller, K. Houf, J. G. Fox and P. Vandamme (2017). "Minimal standards for describing new species belonging to the families Campylobacteraceae and Helicobacteraceae: Campylobacter, Arcobacter, Helicobacter and Wolinella spp." Int J Syst Evol Microbiol **67**(12): 5296-5311.

Ottman, N., M. Davids, M. Suarez-Diez, S. Boeren, P. J. Schaap, V. A. P. Martins Dos Santos, H. Smidt, C. Belzer and W. M. de Vos (2017). "Genome-Scale Model and Omics Analysis of Metabolic Capacities of Akkermansia muciniphila Reveal a Preferential Mucin-Degrading Lifestyle." Appl Environ Microbiol **83**(18).

Ottman, N., S. Y. Geerlings, S. Aalvink, W. M. de Vos and C. Belzer (2017). "Action and function of Akkermansia muciniphila in microbiome ecology, health and disease." Best Practice & Research Clinical Gastroenterology.

Ottman, N., L. Huuskonen, J. Reunanen, S. Boeren, J. Klievink, H. Smidt, C. Belzer and W. M. de Vos (2016). "Characterization of Outer Membrane Proteome of Akkermansia muciniphila Reveals Sets of Novel Proteins Exposed to the Human Intestine." Front Microbiol **7**: 1157.

Ottman, N., J. Reunanen, M. Meijerink, T. E. Pietila, V. Kainulainen, J. Klievink, L. Huuskonen, S. Aalvink, M. Skurnik, S. Boeren, R. Satokari, A. Mercenier, A. Palva, H. Smidt, W. M. de Vos and C. Belzer (2017). "Pili-like proteins of Akkermansia muciniphila modulate host immune responses and gut barrier function." PLoS One **12**(3): e0173004.

Ottman, N. A. (2015). Host immunostimulation and substrate utilization of the gut symbiont Akkermansia muciniphila, Wageningen University.

Ouwerkerk, J. P. (2016). *Akkermansia* species - phylogeny, physiology and comparative genomics.

Ouwerkerk, J. P., S. Aalvink, C. Belzer and W. M. de Vos (2016). "Akkermansia glycaniphila sp. nov., an anaerobic mucin-degrading bacterium isolated from reticulated python faeces." Int J Syst Evol Microbiol **66**(11): 4614-4620.

Ouwerkerk, J. P., S. Aalvink, C. Belzer and W. M. De Vos (2017). "Preparation and preservation of viable Akkermansia muciniphila cells for therapeutic interventions." Benef Microbes **8**(2): 163-169.

Ouwerkerk, J. P., J. J. Koehorst, P. J. Schaap, J. Ritari, L. Paulin, C. Belzer and W. M. de Vos (2017). "Complete Genome Sequence of Akkermansia glycaniphila Strain PytT, a Mucin-Degrading Specialist of the Reticulated Python Gut." Genome Announc **5**(1).

Ouwerkerk, J. P., H. L. P. Tytgat, J. Elzinga, J. Koehorst, P. Van den Abbeele, B. Henrissat, M. Gueimonde, P. D. Cani, T. Van de Wiele, C. Belzer and W. M. de Vos (2022). "Comparative Genomics and Physiology of Akkermansia muciniphila Isolates from Human Intestine Reveal Specialized Mucosal Adaptation." Microorganisms **10**(8).

Ouwerkerk, J. P., K. C. van der Ark, M. Davids, N. J. Claassens, T. Robert Finestra, W. M. de Vos and C. Belzer (2016). "Adaptation of Akkermansia muciniphila to the oxic-anoxic interface of the mucus layer." Appl Environ Microbiol.

Overmann, J. (2006). "Principles of enrichment, isolation, cultivation and preservation of prokaryotes." The prokaryotes **1**: 80-136.

Ovesen, L., F. Bendtsen, U. Tage-Jensen, N. T. Pedersen, B. R. Gram and S. J. Rune (1986). "Intraluminal pH in the stomach, duodenum, and proximal jejunum in normal subjects and patients with exocrine pancreatic insufficiency." Gastroenterology **90**(4): 958-962.

Page, A. J., C. A. Cummins, M. Hunt, V. K. Wong, S. Reuter, M. T. G. Holden, M. Fookes, D. Falush, J. A. Keane and J. Parkhill (2015). "Roary: rapid large-scale prokaryote pan genome analysis." Bioinformatics **31**(22): 3691-3693.

Parada Venegas, D., M. K. De la Fuente, G. Landskron, M. J. Gonzalez, R. Quera, G. Dijkstra, H. J. M. Harmsen, K. N. Faber and M. A. Hermoso (2019). "Short Chain Fatty Acids (SCFAs)-Mediated Gut Epithelial and Immune Regulation and Its Relevance for Inflammatory Bowel Diseases." Front Immunol **10**: 277.

Pasolli, E., L. Schiffer, P. Manghi, A. Renson, V. Obenchain, D. T. Truong, F. Beghini, F. Malik, M. Ramos and J. B. Dowd (2017). "Accessible, curated metagenomic data through ExperimentHub." Nat. Methods **14**(11): 1023.

Patel, A. G., M. T. Toyama, C. Alvarez, T. N. Nguyen, P. U. Reber, S. W. Ashley and H. A. Reber (1995). "Pancreatic interstitial pH in human and feline chronic pancreatitis." Gastroenterology **109**(5): 1639-1645.

Patrascu, O., F. Beguet-Crespel, L. Marinelli, E. Le Chatelier, A. L. Abraham, M. Leclerc, C. Klopp, N. Terrapon, B. Henrissat, H. M. Blottiere, J. Dore and C. Bera-Maillet (2017). "A fibrolytic potential in the human ileum mucosal microbiota revealed by functional metagenomic." Sci Rep **7**: 40248.

Peng, Y., H. C. M. Leung, S. M. Yiu and F. Y. L. Chin (2012). "IDBA-UD: A de novo assembler for single-cell and metagenomic sequencing data with highly uneven depth." Bioinformatics **28**(11): 1420-1428.

Pereira, F. C. and D. Berry (2017). "Microbial nutrient niches in the gut." Environ. Microbiol. **19**(4): 1366-1378.

Pereira, P., V. Aho, J. Arola, S. Boyd, K. Jokelainen, L. Paulin, P. Auvinen and M. Farkkila (2017). "Bile microbiota in primary sclerosing cholangitis: Impact on disease progression and development of biliary dysplasia." PLoS One **12**(8): e0182924.

Perelman, P., W. E. Johnson, C. Roos, H. N. Seuánez, J. E. Horvath, M. A. M. Moreira, B. Kessing, J. Pontius, M. Roelke, Y. Rumpler, M. P. C. Schneider, A. Silva, S. J. O'Brien and J. Pecon-Slattery (2011). "A Molecular Phylogeny of Living Primates." PLoS Genetics **7**(3): e1001342-e1001342.

Pierre, J. F., K. B. Martinez, H. Ye, A. Nadimpalli, T. C. Morton, J. Yang, Q. Wang, N. Patno, E. B. Chang and D. P. Yin (2016). "Activation of bile acid signaling improves metabolic phenotypes in high-fat diet-induced obese mice." Am J Physiol Gastrointest Liver Physiol **311**(2): G286-304.

Pigny, P., V. Guyonnet-Duperat, A. S. Hill, W. S. Pratt, S. Galiegue-Zouitina, M. C. d'Hooge, A. Laine, I. Van-Seuningen, P. Degand, J. R. Gum, Y. S. Kim, D. M. Swallow, J. P. Aubert and N. Porchet (1996). "Human mucin genes assigned to 11p15.5: identification and organization of a cluster of genes." Genomics **38**(3): 340-352.

Plichta, D. R., A. S. Juncker, M. Bertalan, E. Rettedal, L. Gautier, E. Varela, C. Manichanh, C. Fouqueray, F. Levenez and T. Nielsen (2016). "Transcriptional interactions suggest niche segregation among microorganisms in the human gut." Nat. Microbiol. **1**(11): 16152.

Plovier, H., A. Everard, C. Druart, C. Depommier, M. Van Hul, L. Geurts, J. Chilloux, N. Ottman, T. Duparc, L. Lichtenstein, A. Myridakis, N. M. Delzenne, J. Klievink, A. Bhattacharjee, K. C. van der Ark, S. Aalvink, L. O. Martinez, M. E. Dumas, D. Maiter, A. Loumaye, M. P. Hermans, J. P. Thissen, C. Belzer, W. M. de Vos and P. D. Cani (2017). "A purified membrane protein from Akkermansia muciniphila or the pasteurized bacterium improves metabolism in obese and diabetic mice." Nat Med **23**(1): 107-113.

Plugge, C. M. (2005). "Anoxic media design, preparation, and considerations." Methods Enzymol **397**: 3-16.

Png, C. W., S. K. Linden, K. S. Gilshenan, E. G. Zoetendal, C. S. McSweeney, L. I. Sly, M. A. McGuckin and T. H. Florin (2010). "Mucolytic bacteria with increased prevalence in IBD mucosa augment in vitro utilization of mucin by other bacteria." Am J Gastroenterol **105**(11): 2420-2428.

Possemiers, S., S. Bolca, W. Verstraete and A. Heyerick (2011). "The intestinal microbiome: a separate organ inside the body with the metabolic potential to influence the bioactivity of botanicals." Fitoterapia **82**(1): 53-66.

Pruesse, E., J. Peplies and F. O. Glöckner (2012). "SINA: Accurate high-throughput multiple sequence alignment of ribosomal RNA genes." Bioinformatics **28**(14): 1823-1829.

Qian, K., S. Chen, J. Wang, K. Sheng, Y. Wang and M. Zhang (2022). "A beta-N-acetylhexosaminidase Amuc_2109 from Akkermansia muciniphila protects against dextran sulfate sodium-induced colitis in mice by enhancing intestinal barrier and modulating gut microbiota." Food Funct **13**(4): 2216-2227.

Qin, J., Y. Li, Z. Cai, S. Li, J. Zhu, F. Zhang, S. Liang, W. Zhang, Y. Guan, D. Shen, Y. Peng, D. Zhang, Z. Jie, W. Wu, Y. Qin, W. Xue, J. Li, L. Han, D. Lu, P. Wu, Y. Dai, X. Sun, Z. Li, A. Tang, S. Zhong, X. Li, W. Chen, R. Xu, M. Wang, Q. Feng, M. Gong, J. Yu, Y. Zhang, M. Zhang, T. Hansen, G. Sanchez, J. Raes, G. Falony, S. Okuda, M. Almeida, E. LeChatelier, P. Renault, N. Pons, J. M. Batto, Z. Zhang, H. Chen, R. Yang, W. Zheng, S. Li, H. Yang, J. Wang, S. D. Ehrlich, R. Nielsen, O. Pedersen, K. Kristiansen and J. Wang (2012). "A metagenome-wide association study of gut microbiota in type 2 diabetes." Nature **490**(7418): 55-60.

Qin, N., F. Yang, A. Li, E. Prifti, Y. Chen, L. Shao, J. Guo, E. Le Chatelier, J. Yao, L. Wu, J. Zhou, S. Ni, L. Liu, N. Pons, J. M. Batto, S. P. Kennedy, P. Leonard, C. Yuan, W. Ding, Y. Chen, X. Hu, B. Zheng, G. Qian, W. Xu, S. D. Ehrlich, S. Zheng and L. Li (2014). "Alterations of the human gut microbiome in liver cirrhosis." Nature **513**(7516): 59-64.

Qu, S., L. Fan, Y. Qi, C. Xu, Y. Hu, S. Chen, W. Liu, W. Liu and J. Si (2021). "Akkermansia muciniphila Alleviates Dextran Sulfate Sodium (DSS)-induced acute colitis by NLRP3 activation." Microbiology Spectrum **9**(2).

Quast, C., E. Pruesse, P. Yilmaz, J. Gerken, T. Schweer, P. Yarza, J. Peplies and F. O. Glöckner (2013). "The SILVA ribosomal RNA gene database project: Improved data processing and web-based tools." Nucleic Acids Research **41**(D1): D590-D590.

Raftar, S. K. A., F. Ashrafian, A. Yadegar, A. Lari, H. R. Moradi, A. Shahriary, M. Azimirad, H. Alavifard, Z. Mohsenifar, M. Davari, F. Vaziri, A. Moshiri, S. D. Siadat and M. R. Zali (2021). "The protective effects of live and pasteurized akkermansia muciniphila and its extracellular vesicles against HFD/CCl4-induced liver injuryS." Microbiology Spectrum **9**(2).

Rajilic-Stojanovic, M., A. Maathuis, H. G. Heilig, K. Venema, W. M. de Vos and H. Smidt (2010). "Evaluating the microbial diversity of an in vitro model of the human large intestine by phylogenetic microarray analysis." Microbiology **156**(Pt 11): 3270-3281.

Rajilic-Stojanovic, M., F. Shanahan, F. Guarner and W. M. de Vos (2013). "Phylogenetic analysis of dysbiosis in ulcerative colitis during remission." Inflamm Bowel Dis **19**(3): 481-488.

Ramirez-Farias, C., K. Slezak, Z. Fuller, A. Duncan, G. Holtrop and P. Louis (2009). "Effect of inulin on the human gut microbiota: stimulation of Bifidobacterium adolescentis and Faecalibacterium prausnitzii." Br J Nutr **101**(4): 541-550.

Ramiro-Garcia, J., G. D. A. Hermes, C. Giatsis, D. Sipkema, E. G. Zoetendal, P. J. Schaap and H. Smidt (2016). "NG-Tax, a highly accurate and validated pipeline for analysis of 16S rRNA amplicons from complex biomes." F1000Res **5**: 1791.

Randal Bollinger, R., A. S. Barbas, E. L. Bush, S. S. Lin and W. Parker (2007). "Biofilms in the large bowel suggest an apparent function of the human vermiform appendix." J Theor Biol **249**(4): 826-831.

Ranjan, K. (2010). Verrucomicrobia: A model phylum to study the effects of deforestation on microbial diversity in the Amazon forest.

Reichardt, N., S. H. Duncan, P. Young, A. Belenguer, C. M. Leitch, K. P. Scott, H. J. Flint and P. Louis (2014). "Phylogenetic distribution of three pathways for propionate production within the human gut microbiota." ISME J **8**(6): 1323.

Relman, D. A. (2012). "The human microbiome: ecosystem resilience and health." Nutr Rev **70 Suppl 1**: S2-9.

Reunanen, J., V. Kainulainen, L. Huuskonen, N. Ottman, C. Belzer, H. Huhtinen, W. M. de Vos and R. Satokari (2015). "Akkermansia muciniphila Adheres to Enterocytes and Strengthens the Integrity of the Epithelial Cell Layer." Appl Environ Microbiol **81**(11): 3655-3662.

Riaz Rajoka, M. S., M. Jin, Z. Haobin, Q. Li, D. Shao, C. Jiang, Q. Huang, H. Yang, J. Shi and N. Hussain (2018). "Functional characterization and biotechnological potential of exopolysaccharide produced by Lactobacillus rhamnosus strains isolated from human breast milk." LWT **89**: 638-647.

Richter, M. and R. Rossello-Mora (2009). "Shifting the genomic gold standard for the prokaryotic species definition." Proc Natl Acad Sci U S A **106**(45): 19126-19131.

Rigler, F. (1975). The concept of energy flow and nutrient flow between trophic levels. Unifying concepts in ecology, Springer**:** 15-26.

Riley, L. A. and A. M. Guss (2021). "Approaches to genetic tool development for rapid domestication of non-model microorganisms." Biotechnol Biofuels **14**(1): 30.

Rios-Covian, D., I. Cuesta, J. R. Alvarez-Buylla, P. Ruas-Madiedo, M. Gueimonde and C. G. de Los Reyes-Gavilan (2016). "Bacteroides fragilis metabolises exopolysaccharides produced by bifidobacteria." BMC Microbiol **16**(1): 150.

Riviere, A., M. Gagnon, S. Weckx, D. Roy and L. De Vuyst (2015). "Mutual Cross-Feeding Interactions between Bifidobacterium longum subsp. longum NCC2705 and Eubacterium rectale ATCC 33656 Explain the Bifidogenic and Butyrogenic Effects of Arabinoxylan Oligosaccharides." Appl Environ Microbiol **81**(22): 7767-7781.

Roager, H. M., L. B. Hansen, M. I. Bahl, H. L. Frandsen, V. Carvalho, R. J. Gobel, M. D. Dalgaard, D. R. Plichta, M. H. Sparholt, H. Vestergaard, T. Hansen, T. Sicheritz-Ponten, H. B. Nielsen, O. Pedersen, L. Lauritzen, M. Kristensen, R. Gupta and T. R. Licht (2016). "Colonic transit time is related to bacterial metabolism and mucosal turnover in the gut." Nat Microbiol **1**(9): 16093.

Robinson, M. D., D. J. McCarthy and G. K. Smyth (2010). "edgeR: a Bioconductor package for differential expression analysis of digital gene expression data." Bioinformatics **26**(1): 139-140.

Rodriguez-Daza, M. C. (2020). Prebiotic-like effects of berry polyphenols on the gut microbiota: Akkermansia muciniphila and its molecular adaptation mechanisms to phenolics, Université Laval.

Roelofs, K. G., M. J. Coyne, R. R. Gentyala, M. Chatzidaki-Livanis and L. E. Comstock (2016). "Bacteroidales Secreted Antimicrobial Proteins Target Surface Molecules Necessary for Gut Colonization and Mediate Competition In Vivo." mBio **7**(4).

Rogers, M. B., V. Aveson, B. Firek, A. Yeh, B. Brooks, R. Brower-Sinning, J. Steve, J. F. Banfield, A. Zureikat, M. Hogg, B. A. Boone, H. J. Zeh and M. J. Morowitz (2017). "Disturbances of the Perioperative Microbiome Across Multiple Body Sites in Patients Undergoing Pancreaticoduodenectomy." Pancreas **46**(2): 260-267.

Rossen, N. G., S. Fuentes, K. Boonstra, G. R. D'Haens, H. G. Heilig, E. G. Zoetendal, W. M. de Vos and C. Y. Ponsioen (2015). "The mucosa-associated microbiota of PSC patients is characterized by low diversity and low abundance of uncultured Clostridiales II." J Crohns Colitis **9**(4): 342-348.

Rossi, O., M. T. Khan, M. Schwarzer, T. Hudcovic, D. Srutkova, S. H. Duncan, E. H. Stolte, H. Kozakova, H. J. Flint, J. N. Samsom, H. J. Harmsen and J. M. Wells (2015). "Faecalibacterium prausnitzii Strain HTF-F and Its Extracellular Polymeric Matrix Attenuate Clinical Parameters in DSS-Induced Colitis." PLoS One **10**(4): e0123013.

Ruas-Madiedo, P., M. Gueimonde, F. Arigoni, C. G. de los Reyes-Gavilan and A. Margolles (2009). "Bile affects the synthesis of exopolysaccharides by Bifidobacterium animalis." Appl Environ Microbiol **75**(4): 1204-1207.

Ryan, P. M., R. P. Ross, G. F. Fitzgerald, N. M. Caplice and C. Stanton (2015). "Sugar-coated: exopolysaccharide producing lactic acid bacteria for food and human health applications." Food Funct **6**(3): 679-693.

Salazar, N., M. Gueimonde, A. M. Hernandez-Barranco, P. Ruas-Madiedo and C. G. de los Reyes-Gavilan (2008). "Exopolysaccharides produced by intestinal Bifidobacterium strains act as fermentable substrates for human intestinal bacteria." Appl Environ Microbiol **74**(15): 4737-4745.

Salazar, N., A. M. Neyrinck, L. B. Bindels, C. Druart, P. Ruas-Madiedo, P. D. Cani, C. G. de Los Reyes-Gavilan and N. M. Delzenne (2019). "Functional Effects of EPS-Producing Bifidobacterium Administration on Energy Metabolic Alterations of Diet-Induced Obese Mice." Front Microbiol **10**: 1809.

Salazar, N., A. Prieto, J. A. Leal, B. Mayo, J. C. Bada-Gancedo, C. G. de los Reyes-Gavilan and P. Ruas-Madiedo (2009). "Production of exopolysaccharides by Lactobacillus and Bifidobacterium strains of human origin, and metabolic activity of the producing bacteria in milk." J Dairy Sci **92**(9): 4158-4168.

Salo, M., N. Marungruang, B. Roth, T. Sundberg, P. Stenstrom, E. Arnbjornsson, F. Fak and B. Ohlsson (2017). "Evaluation of the microbiome in children's appendicitis." Int J Colorectal Dis **32**(1): 19-28.

Salonen, A. and W. M. de Vos (2014). "Impact of diet on human intestinal microbiota and health." Annu Rev Food Sci Technol **5**: 239-262.

Saltykova, I. V., V. A. Petrov, M. D. Logacheva, P. G. Ivanova, N. V. Merzlikin, A. E. Sazonov, L. M. Ogorodova and P. J. Brindley (2016). "Biliary Microbiota, Gallstone Disease and Infection with Opisthorchis felineus." PLoS Negl Trop Dis **10**(7): e0004809.

Salyers, A. A., S. E. West, J. R. Vercellotti and T. D. Wilkins (1977). "Fermentation of mucins and plant polysaccharides by anaerobic bacteria from the human colon." Appl Environ Microbiol **34**(5): 529-533.

Sanapareddy, N., R. M. Legge, B. Jovov, A. McCoy, L. Burcal, F. Araujo-Perez, T. A. Randall, J. Galanko, A. Benson, R. S. Sandler, J. F. Rawls, Z. Abdo, A. A. Fodor and T. O. Keku (2012). "Increased rectal microbial richness is associated with the presence of colorectal adenomas in humans." ISME J **6**(10): 1858-1868.

Sanders, J. G., S. Powell, D. J. Kronauer, H. L. Vasconcelos, M. E. Frederickson and N. E. Pierce (2014). "Stability and phylogenetic correlation in gut microbiota: lessons from ants and apes." Mol Ecol **23**(6): 1268-1283.

Santacruz, A., M. C. Collado, L. Garcia-Valdes, M. T. Segura, J. A. Martin-Lagos, T. Anjos, M. Marti-Romero, R. M. Lopez, J. Florido, C. Campoy and Y. Sanz (2010). "Gut microbiota composition is associated with body weight, weight gain and biochemical parameters in pregnant women." Br J Nutr **104**(1): 83-92.

Santiago, A., M. Pozuelo, M. Poca, C. Gely, J. C. Nieto, X. Torras, E. Roman, D. Campos, G. Sarrabayrouse, S. Vidal, E. Alvarado-Tapias, F. Guarner, G. Soriano, C. Manichanh and C. Guarner (2016). "Alteration of the serum microbiome composition in cirrhotic patients with ascites." Sci Rep **6**: 25001.

Sarkar, A., M. Stoneking and M. R. Nandineni (2017). "Unraveling the human salivary microbiome diversity in Indian populations." PLoS One **12**(9): e0184515.

Savage, D. C. (1977). "Microbial ecology of the gastrointestinal tract." Annu Rev Microbiol **31**: 107-133.

Schape, S. S., J. L. Krause, B. Engelmann, K. Fritz-Wallace, F. Schattenberg, Z. Liu, S. Muller, N. Jehmlich, U. Rolle-Kampczyk, G. Herberth and M. von Bergen (2019). "The Simplified Human Intestinal Microbiota (SIHUMIx) shows high structural and functional resistance against changing transit times in *in vitro* bioreactors." Microorganisms **7**(12).

Scheithauer, B. K., M. L. Wos-Oxley, B. Ferslev, H. Jablonowski and D. H. Pieper (2009). "Characterization of the complex bacterial communities colonizing biliary stents reveals a host-dependent diversity." ISME J **3**(7): 797-807.

Schmid, J. (2018). "Recent insights in microbial exopolysaccharide biosynthesis and engineering strategies." Curr Opin Biotechnol **53**: 130-136.

Schmid, J., V. Sieber and B. Rehm (2015). "Bacterial exopolysaccharides: biosynthesis pathways and engineering strategies." Front Microbiol **6**: 496.

Schmid, J., N. Sperl and V. Sieber (2014). "A comparison of genes involved in sphingan biosynthesis brought up to date." Appl Microbiol Biotechnol **98**(18): 7719-7733.

Schmidt, T. S., M. R. Hayward, L. P. Coelho, S. S. Li, P. I. Costea, A. Y. Voigt, J. Wirbel, O. M. Maistrenko, R. J. Alves and E. Bergsten (2019). "Extensive transmission of microbes along the gastrointestinal tract." Elife **8**: e42693.

Schmidt, T. S. B., S. S. Li, O. M. Maistrenko, W. Akanni, L. P. Coelho, S. Dolai, A. Fullam, A. M. Glazek, R. Hercog, H. Herrema, F. Jung, S. Kandels, A. Orakov, R. Thielemann, M. von Stetten, T. Van Rossum, V. Benes, T. J. Borody, W. M. de Vos, C. Y. Ponsioen, M. Nieuwdorp and P. Bork (2022). "Drivers and determinants of strain dynamics following fecal microbiota transplantation." Nat Med **28**(9): 1902-1912.

Schneeberger, M., A. Everard, A. G. Gomez-Valades, S. Matamoros, S. Ramirez, N. M. Delzenne, R. Gomis, M. Claret and P. D. Cani (2015). "Akkermansia muciniphila inversely correlates with the onset of inflammation, altered adipose tissue metabolism and metabolic disorders during obesity in mice." Sci Rep **5**: 16643.

Schwiertz, A., D. Taras, K. Schafer, S. Beijer, N. A. Bos, C. Donus and P. D. Hardt (2010). "Microbiota and SCFA in lean and overweight healthy subjects." Obesity (Silver Spring) **18**(1): 190-195.

Scott, K. P., J. C. Martin, S. H. Duncan and H. J. Flint (2014). "Prebiotic stimulation of human colonic butyrate-producing bacteria and bifidobacteria, in vitro." FEMS Microbiol Ecol **87**(1): 30-40.

Seemann, T. (2014). "Prokka: rapid prokaryotic genome annotation." Bioinformatics **30**(14): 2068-2069.

Seemann, T. (2018). barrnap 0.9 : rapid ribosomal RNA prediction.

Segura Munoz, R. R., S. Mantz, I. Martinez, F. Li, R. J. Schmaltz, N. A. Pudlo, K. Urs, E. C. Martens, J. Walter and A. E. Ramer-Tait (2022). "Experimental evaluation of ecological principles to understand and modulate the outcome of bacterial strain competition in gut microbiomes." ISME J **16**(6): 1594-1604.

Sender, R., S. Fuchs and R. Milo (2016). "Revised Estimates for the Number of Human and Bacteria Cells in the Body." PLoS Biol **14**(8): e1002533.

Shah, P., J. V. Fritz, E. Glaab, M. S. Desai, K. Greenhalgh, A. Frachet, M. Niegowska, M. Estes, C. Jager, C. Seguin-Devaux, F. Zenhausern and P. Wilmes (2016). "A microfluidics-based in vitro model of the gastrointestinal human-microbe interface." Nat Commun **7**: 11535.

Shanahan, E. R., L. Zhong, N. J. Talley, M. Morrison and G. Holtmann (2016). "Characterisation of the gastrointestinal mucosa-associated microbiota: a novel technique to prevent cross-contamination during endoscopic procedures." Aliment Pharmacol Ther **43**(11): 1186-1196.

Sharp, C., C. Boinett, A. Cain, N. G. Housden, S. Kumar, K. Turner, J. Parkhill and C. Kleanthous (2019). "O-Antigen-Dependent Colicin Insensitivity of Uropathogenic Escherichia coli." J Bacteriol **201**(4).

Shaw, L., A. L. R. Ribeiro, A. P. Levine, N. Pontikos, F. Balloux, A. W. Segal, A. P. Roberts and A. M. Smith (2017). "The Human Salivary Microbiome Is Shaped by Shared Environment Rather than Genetics: Evidence from a Large Family of Closely Related Individuals." MBio **8**(5).

Sheehan, D., C. Moran and F. Shanahan (2015). "The microbiota in inflammatory bowel disease." J Gastroenterol **50**(5): 495-507.

Shen, H., F. Ye, L. Xie, J. Yang, Z. Li, P. Xu, F. Meng, L. Li, Y. Chen, X. Bo, M. Ni and X. Zhang (2015). "Metagenomic sequencing of bile from gallstone patients to identify different microbial community patterns and novel biliary bacteria." Sci Rep **5**: 17450.

Sheng, L., P. K. Jena, H. X. Liu, Y. Hu, N. Nagar, D. N. Bronner, M. L. Settles, A. J. Baumler and Y. Y. Wan (2018). "Obesity treatment by epigallocatechin-3-gallate-regulated bile acid signaling and its enriched Akkermansia muciniphila." FASEB J: fj201800370R.

Sheridan, P. O., P. Louis, E. Tsompanidou, S. Shaw, H. J. Harmsen, S. H. Duncan, H. J. Flint and A. W. Walker (2021). "Distribution, organization and expression of genes concerned with anaerobic lactate-utilization in human intestinal bacteria." bioRxiv: 2021.2004.2004.438253.

Shetty, S. A., S. Boeren, T. P. Bui, H. Smidt and W. M. de Vos (2020). "Unravelling lactate-acetate and sugar conversion into butyrate by intestinal *Anaerobutyricum* and *Anaerostipes* species by comparative proteogenomics." Environ. Microbiol. **22**(11): 4863-4875.

Shetty, S. A., F. Hugenholtz, L. Lahti, H. Smidt and W. M. de Vos (2017). "Intestinal microbiome landscaping: insight in community assemblage and implications for microbial modulation strategies." FEMS Microbiol Rev **41**(2): 182-199.

Shetty, S. A., I. Kostopoulos, S. Y. Geerlings, H. Smidt, W. M. de Vos and C. Belzer (2022). "Dynamic metabolic interactions and trophic roles of human gut microbes identified using a minimal microbiome exhibiting ecological properties." ISME J.

Shetty, S. A., B. Kuipers, S. Atashgahi, S. Aalvink, H. Smidt and W. M. de Vos (2022). "Inter-species Metabolic Interactions in an In-vitro Minimal Human Gut Microbiome of Core Bacteria." NPJ Biofilms Microbiomes **8**(1): 21.

Shetty, S. A., H. Smidt and W. M. de Vos (2019). "Reconstructing functional networks in the human intestinal tract using synthetic microbiomes." Curr Opin Biotechnol **58**: 146-154.

Shetty, S. A., S. Zuffa, T. P. N. Bui, S. Aalvink, H. Smidt and W. M. De Vos (2018). "Reclassification of *Eubacterium hallii* as *Anaerobutyricum hallii* gen. nov., comb. nov., and description of *Anaerobutyricum soehngenii* sp. nov., a butyrate and propionate-producing bacterium from infant faeces." Int J Syst Evol Microbiol.

Shi, M., Y. Yue, C. Ma, L. Dong and F. Chen (2022). "Pasteurized Akkermansia muciniphila Ameliorate the LPS-Induced Intestinal Barrier Dysfunction via Modulating AMPK and NF-kappaB through TLR2 in Caco-2 Cells." Nutrients **14**(4).

Shin, N. R., J. C. Lee, H. Y. Lee, M. S. Kim, T. W. Whon, M. S. Lee and J. W. Bae (2014). "An increase in the Akkermansia spp. population induced by metformin treatment improves glucose homeostasis in diet-induced obese mice." Gut **63**(5): 727-735.

Shukla, A., K. Mehta, J. Parmar, J. Pandya and M. Saraf (2019). "Depicting the exemplary knowledge of microbial exopolysaccharides in a nutshell." European Polymer Journal **119**: 298-310.

Silverman, J. D., H. K. Durand, R. J. Bloom, S. Mukherjee and L. A. David (2018). "Dynamic linear models guide design and analysis of microbiota studies within artificial human guts." Microbiome **6**(1): 202.

Smith, H. F., W. Parker, S. H. Kotzé and M. Laurin (2013). "Multiple independent appearances of the cecal appendix in mammalian evolution and an investigation of related ecological and anatomical factors." Comptes Rendus Palevol **12**(6): 339-354.

Smits, S. A., J. Leach, E. D. Sonnenburg, C. G. Gonzalez, J. S. Lichtman, G. Reid, R. Knight, A. Manjurano, J. Changalucha, J. E. Elias, M. G. Dominguez-Bello and J. L. Sonnenburg (2017). "Seasonal cycling in the gut microbiome of the Hadza hunter-gatherers of Tanzania." Science **357**(6353): 802-806.

Sommer, F., M. Stahlman, O. Ilkayeva, J. M. Arnemo, J. Kindberg, J. Josefsson, C. B. Newgard, O. Frobert and F. Backhed (2016). "The Gut Microbiota Modulates Energy Metabolism in the Hibernating Brown Bear Ursus arctos." Cell Rep **14**(7): 1655-1661.

Soneson, C., M. I. Love and M. D. Robinson (2016). "Differential analyses for RNA-seq: Transcript-level estimates improve gene-level inferences [version 2; referees: 2 approved]." F1000Research **4**.

Sonnenburg, E. D., H. Zheng, P. Joglekar, S. K. Higginbottom, S. J. Firbank, D. N. Bolam and J. L. Sonnenburg (2010). "Specificity of polysaccharide use in intestinal bacteroides species determines diet-induced microbiota alterations." Cell **141**(7): 1241-1252.

Sonoyama, K., R. Fujiwara, N. Takemura, T. Ogasawara, J. Watanabe, H. Ito and T. Morita (2009). "Response of gut microbiota to fasting and hibernation in Syrian hamsters." Appl Environ Microbiol **75**(20): 6451-6456.

Soto-Martin, E. C., I. Warnke, F. M. Farquharson, M. Christodoulou, G. Horgan, M. Derrien, J. M. Faurie, H. J. Flint, S. H. Duncan and P. Louis (2020). "Vitamin biosynthesis by human gut butyrate-producing bacteria and cross-feeding in synthetic microbial communities." mBio **11**(4).

Stearns, J. C., M. D. Lynch, D. B. Senadheera, H. C. Tenenbaum, M. B. Goldberg, D. G. Cvitkovitch, K. Croitoru, G. Moreno-Hagelsieb and J. D. Neufeld (2011). "Bacterial biogeography of the human digestive tract." Sci Rep **1**: 170.

Steidler, L., S. Neirynck, N. Huyghebaert, V. Snoeck, A. Vermeire, B. Goddeeris, E. Cox, J. P. Remon and E. Remaut (2003). "Biological containment of genetically modified Lactococcus lactis for intestinal delivery of human interleukin 10." Nat Biotechnol **21**(7): 785-789.

Storz, G., L. A. Tartaglia, S. B. Farr and B. N. Ames (1990). "Bacterial defenses against oxidative stress." Trends in Genetics **6**(C): 363-368.

Sundin, O. H., A. Mendoza-Ladd, M. Zeng, D. Diaz-Arevalo, E. Morales, B. M. Fagan, J. Ordonez, P. Velez, N. Antony and R. W. McCallum (2017). "The human jejunum has an endogenous microbiota that differs from those in the oral cavity and colon." BMC Microbiol **17**(1): 160.

Sung, J., S. Kim, J. J. T. Cabatbat, S. Jang, Y. S. Jin, G. Y. Jung, N. Chia and P. J. Kim (2017). "Global metabolic interaction network of the human gut microbiota for context-specific community-scale analysis." Nat Commun **8**: 15393.

Sungur, T., B. Aslim, C. Karaaslan and B. Aktas (2017). "Impact of Exopolysaccharides (EPSs) of Lactobacillus gasseri strains isolated from human vagina on cervical tumor cells (HeLa)." Anaerobe **47**: 137-144.

Susin, M. F., R. L. Baldini, F. Gueiros-Filho and S. L. Gomes (2006). "GroES/GroEL and DnaK/DnaJ have distinct roles in stress responses and during cell cycle progression in Caulobacter crescentus." Journal of Bacteriology **188**(23): 8044-8053.

Sutherland, I. W. (1994). "Structure-function relationships in microbial exopolysaccharides." Biotechnology Advances **12**(2): 393-448.

Sutor, D. J. and L. I. Wilkie (1976). "Diurnal variations in the pH of pathological gallbladder bile." Gut **17**(12): 971-974.

Suzek, B. E., H. Huang, P. McGarvey, R. Mazumder and C. H. Wu (2007). "UniRef: Comprehensive and non-redundant UniProt reference clusters." Bioinformatics **23**(10): 1282-1288.

Suzuki, M. T., L. T. Taylor and E. F. DeLong (2000). "Quantitative analysis of small-subunit rRNA genes in mixed microbial populations via 5'-nuclease assays." Applied and Environmental Microbiology **66**(11): 4605-4614.

Swidsinski, A., Y. Dorffel, V. Loening-Baucke, F. Theissig, J. C. Ruckert, M. Ismail, W. A. Rau, D. Gaschler, M. Weizenegger, S. Kuhn, J. Schilling and W. V. Dorffel (2011). "Acute appendicitis is characterised by local invasion with Fusobacterium nucleatum/necrophorum." Gut **60**(1): 34-40.

Symons, C. C. and S. E. Arnott (2014). "Timing is everything: priority effects alter community invasibility after disturbance." Ecol. Evol. **4**(4): 397-407.

Tailford, L. E., E. H. Crost, D. Kavanaugh and N. Juge (2015). "Mucin glycan foraging in the human gut microbiome." Front Genet **6**: 81.

Tan, G. D. (2014). "The pancreas." Anaesthesia & Intensive Care Medicine **15**(10): 485-488.

Tanner, S. A., A. Z. Berner, E. Rigozzi, F. Grattepanche, C. Chassard and C. Lacroix (2014). "In vitro continuous fermentation model (PolyFermS) of the swine proximal colon for simultaneous testing on the same gut microbiota." PloS one **9**(4): e94123.

Tap, J., M. Derrien, H. Tornblom, R. Brazeilles, S. Cools-Portier, J. Dore, S. Storsrud, B. Le Neve, L. Ohman and M. Simren (2017). "Identification of an Intestinal Microbiota Signature Associated With Severity of Irritable Bowel Syndrome." Gastroenterology **152**(1): 111-123 e118.

Taylor, L. R. (1961). "Aggregation, variance and the mean." Nature **189**(4766): 732-735.

Taylor, L. R. and I. P. Woiwod (1980). "Temporal Stability as a Density-Dependent Species Characteristic." Journal of Animal Ecology **49**(1): 209-224.

Thornton, D. J., N. Khan, R. Mehrotra, M. Howard, E. Veerman, N. H. Packer and J. K. Sheehan (1999). "Salivary mucin MG1 is comprised almost entirely of different glycosylated forms of the MUC5B gene product." Glycobiology **9**(3): 293-302.

Tims, S., C. Derom, D. M. Jonkers, R. Vlietinck, W. H. Saris, M. Kleerebezem, W. M. de Vos and E. G. Zoetendal (2013). "Microbiota conservation and BMI signatures in adult monozygotic twins." ISME J **7**(4): 707-717.

Tottey, W., D. Feria-Gervasio, N. Gaci, B. Laillet, E. Pujos, J. F. Martin, J. L. Sebedio, B. Sion, J. F. Jarrige, M. Alric and J. F. Brugere (2017). "Colonic Transit Time Is a Driven Force of the Gut Microbiota Composition and Metabolism: In Vitro Evidence." J Neurogastroenterol Motil **23**(1): 124-134.

Trabelsi, I., N. Ktari, S. Ben Slima, M. Triki, S. Bardaa, H. Mnif and R. Ben Salah (2017). "Evaluation of dermal wound healing activity and in vitro antibacterial and antioxidant activities of a new exopolysaccharide produced by Lactobacillus sp.Ca6." International Journal of Biological Macromolecules **103**: 194-201.

Traykova, D., B. Schneider, M. Chojkier and M. Buck (2017). "Blood Microbiome Quantity and the Hyperdynamic Circulation in Decompensated Cirrhotic Patients." PLoS One **12**(2): e0169310.

Trosvik, P. and E. J. Muinck (2015). "Ecology of bacteria in the human gastrointestinal tract—identification of keystone and foundation taxa." Microbiome **3**(1): 1.

Turck, D., T. Bohn, J. Castenmiller, S. De Henauw, K. I. Hirsch-Ernst, A. Maciuk, I. Mangelsdorf, H. J. McArdle, A. Naska, C. Pelaez, K. Pentieva, A. Siani, F. Thies, S. Tsabouri, M. Vinceti, F. Cubadda, T. Frenzel, M. Heinonen, R. Marchelli, M. Neuhäuser-Berthold, M. Poulsen, M. Prieto Maradona, J. R. Schlatter, H. van Loveren, R. Ackerl, H. K. Knutsen, N. F. Efsa Panelon Nutrition and A. Food (2021). "Safety of pasteurised Akkermansia muciniphila as a novel food pursuant to Regulation (EU) 2015/2283." EFSA Journal **19**(9).

Turnbaugh, P. J., M. Hamady, T. Yatsunenko, B. L. Cantarel, A. Duncan, R. E. Ley, M. L. Sogin, W. J. Jones, B. A. Roe, J. P. Affourtit, M. Egholm, B. Henrissat, A. C. Heath, R. Knight and J. I. Gordon (2009). "A core gut microbiome in obese and lean twins." Nature **457**(7228): 480-484.

Urbaniak, C., J. Cummins, M. Brackstone, J. M. Macklaim, G. B. Gloor, C. K. Baban, L. Scott, D. M. O'Hanlon, J. P. Burton, K. P. Francis, M. Tangney and G. Reid (2014). "Microbiota of human breast tissue." Appl Environ Microbiol **80**(10): 3007-3014.

Valdivia, R. M., P.; Davey, L. (2019). Systems and methods for genetic manipulation of akkermansia species. D. University. United States. **WO2019222359**.

Van de Wiele, T., P. Van den Abbeele, W. Ossieur, S. Possemiers and M. Marzorati (2015). The Simulator of the Human Intestinal Microbial Ecosystem (SHIME((R))). The Impact of Food Bioactives on Health: in vitro and ex vivo models. K. Verhoeckx, P. Cotter, I. Lopez-Exposito et al. Cham (CH): 305-317.

Van den Abbeele, P., C. Belzer, M. Goossens, M. Kleerebezem, W. M. De Vos, O. Thas, R. De Weirdt, F. M. Kerckhof and T. Van de Wiele (2013). "Butyrate-producing Clostridium cluster XIVa species specifically colonize mucins in an in vitro gut model." ISME J **7**(5): 949-961.

Van den Abbeele, P., C. Grootaert, M. Marzorati, S. Possemiers, W. Verstraete, P. Gérard, S. Rabot, A. Bruneau, S. El Aidy, M. Derrien, E. Zoetendal, M. Kleerebezem, H. Smidt and T. Van de Wiele (2010). "Microbial Community Development in a Dynamic Gut Model Is Reproducible, Colon Region Specific, and Selective for Bacteroidetes and Clostridium Cluster IX." Applied and Environmental Microbiology **76**(15): 5237-5246.

Van den Abbeele, P., S. Roos, V. Eeckhaut, D. A. MacKenzie, M. Derde, W. Verstraete, M. Marzorati, S. Possemiers, B. Vanhoecke, F. Van Immerseel and T. Van de Wiele (2012). "Incorporating a mucosal environment in a dynamic gut model results in a more representative colonization by lactobacilli." Microb Biotechnol **5**(1): 106-115.

Van den Abbeele, P., T. Van de Wiele, W. Verstraete and S. Possemiers (2011). "The host selects mucosal and luminal associations of coevolved gut microorganisms: a novel concept." FEMS Microbiol Rev **35**(4): 681-704.

van der Ark, K. C. H. (2018). Metabolic characterization and viable delivery of Akkermansia muciniphila for its future application, Wageningen University.

van der Ark, K. C. H., S. Aalvink, M. Suarez-Diez, P. J. Schaap, W. M. de Vos and C. Belzer (2018). "Model-driven design of a minimal medium for Akkermansia muciniphila confirms mucus adaptation." Microb Biotechnol.

van der Ark, K. C. H., A. D. W. Nugroho, C. Berton-Carabin, C. Wang, C. Belzer, W. M. de Vos and K. Schroen (2017). "Encapsulation of the therapeutic microbe Akkermansia muciniphila in a double emulsion enhances survival in simulated gastric conditions." Food Res Int **102**: 372-379.

van der Hoeven, J. S., C. W. van den Kieboom and P. J. Camp (1990). "Utilization of mucin by oral Streptococcus species." Antonie Van Leeuwenhoek **57**(3): 165-172.

van der Lugt, B., A. A. van Beek, S. Aalvink, B. Meijer, B. Sovran, W. P. Vermeij, R. M. C. Brandt, W. M. de Vos, H. F. J. Savelkoul, W. T. Steegenga and C. Belzer (2019). "Akkermansia muciniphila ameliorates the age-related decline in colonic mucus thickness and attenuates immune activation in accelerated aging Ercc1 (-/Delta7) mice." Immun Ageing **16**: 6.

Van Herreweghen, F., P. Van den Abbeele, T. De Mulder, R. De Weirdt, A. Geirnaert, E. Hernandez-Sanabria, R. Vilchez-Vargas, R. Jauregui, D. H. Pieper, C. Belzer, W. M. De Vos and T. Van de Wiele (2017). "In vitro colonisation of the distal colon by Akkermansia muciniphila is largely mucin and pH dependent." Benef Microbes **8**(1): 81-96.

van Passel, M. W., R. Kant, E. G. Zoetendal, C. M. Plugge, M. Derrien, S. A. Malfatti, P. S. Chain, T. Woyke, A. Palva, W. M. de Vos and H. Smidt (2011). "The genome of Akkermansia muciniphila, a dedicated intestinal mucin degrader, and its use in exploring intestinal metagenomes." PLoS One **6**(3): e16876.

Vandekerckhove, T. T., A. Coomans, K. Cornelis, P. Baert and M. Gillis (2002). "Use of the Verrucomicrobia-specific probe EUB338-III and fluorescent in situ hybridization for detection of "Candidatus Xiphinematobacter" cells in nematode hosts." Appl Environ Microbiol **68**(6): 3121-3125.

Vandeputte, D., L. De Commer, R. Y. Tito, G. Kathagen, J. Sabino, S. Vermeire, K. Faust and J. Raes (2021). "Temporal variability in quantitative human gut microbiome profiles and implications for clinical research." Nat Commun **12**(1): 6740.

Vellend, M. (2010). "Conceptual synthesis in community ecology." Q Rev Biol **85**(2): 183-206.

Venema, K. (2015). The TNO In Vitro Model of the Colon (TIM-2). The Impact of Food Bioactives on Health: in vitro and ex vivo models. K. Verhoeckx, P. Cotter, I. Lopez-Exposito et al. Cham (CH): 293-304.

Venema, K. and P. van den Abbeele (2013). "Experimental models of the gut microbiome." Best Practice & Research Clinical Gastroenterology **27**(1): 115-126.

Venturelli, O. S., A. C. Carr, G. Fisher, R. H. Hsu, R. Lau, B. P. Bowen, S. Hromada, T. Northen and A. P. Arkin (2018). "Deciphering microbial interactions in synthetic human gut microbiome communities." Mol Syst Biol **14**(6): e8157.

Verdu, E. F., H. J. Galipeau and B. Jabri (2015). "Novel players in coeliac disease pathogenesis: role of the gut microbiota." Nat Rev Gastroenterol Hepatol **12**(9): 497-506.

Verma, R., C. Lee, E. J. Jeun, J. Yi, K. S. Kim, A. Ghosh, S. Byun, C. G. Lee, H. J. Kang, G. C. Kim, C. D. Jun, G. Jan, C. H. Suh, J. Y. Jung, J. Sprent, D. Rudra, C. De Castro, A. Molinaro, C. D. Surh and S. H. Im (2018). "Cell surface polysaccharides of Bifidobacterium bifidum induce the generation of Foxp3(+) regulatory T cells." Sci Immunol **3**(28).

Vieira-Silva, S., G. Falony, Y. Darzi, G. Lima-Mendez, R. G. Yunta, S. Okuda, D. Vandeputte, M. Valles-Colomer, F. Hildebrand and S. Chaffron (2016). "Species–function relationships shape ecological properties of the human gut microbiome." Nat. Microbiol. **1**(8): 16088.

Vital, M., A. Karch and D. H. Pieper (2017). "Colonic Butyrate-Producing Communities in Humans: an Overview Using Omics Data." mSystems **2**(6).

Volkmer, B. and M. Heinemann (2011). "Condition-dependent cell volume and concentration of Escherichia coli to facilitate data conversion for systems biology modeling." PLoS One **6**(7): e23126.

Walker, A. W., J. D. Sanderson, C. Churcher, G. C. Parkes, B. N. Hudspith, N. Rayment, J. Brostoff, J. Parkhill, G. Dougan and L. Petrovska (2011). "High-throughput clone library analysis of the mucosa-associated microbiota reveals dysbiosis and differences between inflamed and non-inflamed regions of the intestine in inflammatory bowel disease." BMC Microbiol **11**: 7.

Wang, F., K. Cai, Q. Xiao, L. He, L. Xie and Z. Liu (2022). "Akkermansia muciniphila administration exacerbated the development of colitis-associated colorectal cancer in mice." Journal of Cancer **13**(1): 124-133.

Wang, J., W. Xu, R. Wang, R. Cheng, Z. Tang and M. Zhang (2021). "The outer membrane protein Amuc_1100 of: Akkermansia muciniphila promotes intestinal 5-HT biosynthesis and extracellular availability through TLR2 signalling." Food and Function **12**(8): 3597-3610.

Wang, L., C. T. Christophersen, M. J. Sorich, J. P. Gerber, M. T. Angley and M. A. Conlon (2011). "Low relative abundances of the mucolytic bacterium Akkermansia muciniphila and Bifidobacterium spp. in feces of children with autism." Appl Environ Microbiol **77**(18): 6718-6721.

Wang, M., S. Ahrne, B. Jeppsson and G. Molin (2005). "Comparison of bacterial diversity along the human intestinal tract by direct cloning and sequencing of 16S rRNA genes." FEMS Microbiol Ecol **54**(2): 219-231.

Wang, Q., G. M. Garrity, J. M. Tiedje and J. R. Cole (2007). "Naive Bayesian classifier for rapid assignment of rRNA sequences into the new bacterial taxonomy." Appl. Environ. Microbiol. **73**(16): 5261-5267.

Wang, T., A. Goyal, V. Dubinkina and S. Maslov (2019). "Evidence for a multi-level trophic organization of the human gut microbiome." PLoS Comput. Biol. **15**(12).

Wang, Z., P. Bie, J. Cheng, L. Lu, B. Cui and Q. Wu (2016). "The ABC transporter YejABEF is required for resistance to antimicrobial peptides and the virulence of Brucella melitensis." Scientific Reports **6**(1): 31876.

Weisburg, W. G., S. M. Barns, D. A. Pelletier and D. J. Lane (1991). "16S ribosomal DNA amplification for phylogenetic study." Journal of Bacteriology **173**(2): 697-703.

Weiss, A. S., A. G. Burrichter, A. C. Durai Raj, A. von Strempel, C. Meng, K. Kleigrewe, P. C. Munch, L. Rossler, C. Huber, W. Eisenreich, L. M. Jochum, S. Going, K. Jung, C. Lincetto, J. Hubner, G. Marinos, J. Zimmermann, C. Kaleta, A. Sanchez and B. Stecher (2021). "In vitro interaction network of a synthetic gut bacterial community." ISME J **16**(4): 1095-1109.

Wertz, J. T., E. Kim, J. A. Breznak, T. M. Schmidt and J. L. Rodrigues (2012). "Genomic and physiological characterization of the Verrucomicrobia isolate Geminisphaera colitermitum gen. nov., sp. nov., reveals microaerophily and nitrogen fixation genes." Appl Environ Microbiol **78**(5): 1544-1555.

Westreich, S. T., M. L. Treiber, D. A. Mills, I. Korf and D. G. Lemay (2018). "SAMSA2: a standalone metatranscriptome analysis pipeline." BMC Bioinform. **19**(1): 175.

Whitfield, C. (2006). "Biosynthesis and assembly of capsular polysaccharides in Escherichia coli." Annu Rev Biochem **75**: 39-68.

Wickham, H. (2011). "ggplot2." Wiley Interdiscip. Rev. Comput. Stat. **3**(2): 180-185.

Wilke, C. O. (2018). "Ggridges: Ridgeline plots in'ggplot2'." R package version 0.5 **1**.

Willis, C. L., J. H. Cummings, G. Neale and G. R. Gibson (1996). "In VitroEffects of Mucin Fermentation on the Growth of Human Colonic Sulphate-Reducing Bacteria: ECOLOGY." Anaerobe **2**(2): 117-122.

Wittebolle, L., M. Marzorati, L. Clement, A. Balloi, D. Daffonchio, K. Heylen, P. De Vos, W. Verstraete and N. Boon (2009). "Initial community evenness favours functionality under selective stress." Nature **458**(7238): 623.

Wu, F., X. Guo, M. Zhang, Z. Ou, D. Wu, L. Deng, Z. Lu, J. Zhang, G. Deng, S. Chen, S. Li, J. Yi and Y. Peng (2020). "An Akkermansia muciniphila subtype alleviates high-fat diet-induced metabolic disorders and inhibits the neurodegenerative process in mice." Anaerobe **61**: 102138.

Wu, M.-H., T.-M. Pan, Y.-J. Wu, S.-J. Chang, M.-S. Chang and C.-Y. Hu (2010). "Exopolysaccharide activities from probiotic bifidobacterium: Immunomodulatory effects (on J774A.1 macrophages) and antimicrobial properties." International Journal of Food Microbiology **144**(1): 104-110.

Wu, T., Z. Zhang, B. Liu, D. Hou, Y. Liang, J. Zhang and P. Shi (2013). "Gut microbiota dysbiosis and bacterial community assembly associated with cholesterol gallstones in large-scale study." BMC Genomics **14**: 669.

Wu, W., L. Lv, D. Shi, J. Ye, D. Fang, F. Guo, Y. Li, X. He and L. Li (2017). "Protective Effect of Akkermansia muciniphila against Immune-Mediated Liver Injury in a Mouse Model." Front Microbiol **8**: 1804.

Wust, P. K., M. A. Horn and H. L. Drake (2011). "Clostridiaceae and Enterobacteriaceae as active fermenters in earthworm gut content." ISME J **5**(1): 92-106.

Xiao, M., X. Ren, Y. Yu, W. Gao, C. Zhu, H. Sun, Q. Kong, X. Fu and H. Mou (2022). "Fucose-containing bacterial exopolysaccharides: Sources, biological activities, and food applications." Food Chem X **13**: 100233.

Xie, Y., W. Yang, F. Tang, X. Chen and L. Ren (2015). "Antibacterial activities of flavonoids: structure-activity relationship and mechanism." Curr Med Chem **22**(1): 132-149.

Xu, Q., P. Abdubek, T. Astakhova, H. L. Axelrod, C. Bakolitsa, X. Cai, D. Carlton, C. Chen, H. J. Chiu, T. Clayton, D. Das, M. C. Deller, L. Duan, K. Ellrott, C. L. Farr, J. Feuerhelm, J. C. Grant, A. Grzechnik, G. W. Han, L. Jaroszewski, K. K. Jin, H. E. Klock, M. W. Knuth, P. Kozbial, S. S. Krishna, A. Kumar, W. W. Lam, D. Marciano, M. D. Miller, A. T. Morse, E. Nigoghossian, A. Nopakun, L. Okach, C. Puckett, R. Reyes, H. J. Tien, C. B. Trame, H. van den Bedem, D. Weekes, T. Wooten, A. Yeh, J. Zhou, K. O. Hodgson, J. Wooley, M. A. Elsliger, A. M. Deacon, A. Godzik, S. A. Lesley and I. A. Wilson (2010). "Structure of a membrane-attack complex/perforin (MACPF) family protein from the human gut symbiont Bacteroides thetaiotaomicron." Acta Crystallogr Sect F Struct Biol Cryst Commun **66**(Pt 10): 1297-1305.

Yachi, S. and M. Loreau (1999). "Biodiversity and ecosystem productivity in a fluctuating environment: the insurance hypothesis." Proc. Natl. Acad. Sci. **96**(4): 1463-1468.

Yaghoubfar, R., A. Behrouzi, F. Ashrafian, A. Shahryari, H. R. Moradi, S. Choopani, S. Hadifar, F. Vaziri, S. A. Nojoumi, A. Fateh, S. Khatami and S. D. Siadat (2020). "Modulation of serotonin signaling/metabolism by Akkermansia muciniphila and its extracellular vesicles through the gut-brain axis in mice." Scientific Reports **10**(1): 22119.

Yassour, M., M. Y. Lim, H. S. Yun, T. L. Tickle, J. Sung, Y.-M. Song, K. Lee, E. A. Franzosa, X. C. Morgan, D. Gevers, E. S. Lander, R. J. Xavier, B. W. Birren, G. Ko and C. Huttenhower (2016). "Sub-clinical detection of gut microbial biomarkers of obesity and type 2 diabetes." Genome Medicine **8**(1): 17-17.

Ye, F., H. Shen, Z. Li, F. Meng, L. Li, J. Yang, Y. Chen, X. Bo, X. Zhang and M. Ni (2016). "Influence of the Biliary System on Biliary Bacteria Revealed by Bacterial Communities of the Human Biliary and Upper Digestive Tracts." PLoS One **11**(3): e0150519.

Yilmaz, M., G. Y. Celik, B. Aslim and D. Onbasili (2012). "Influence of Carbon Sources on The Production and Characterization of The Exopolysaccharide (EPS) by Bacillus sphaericus 7055 Strain." Journal of Polymers and the Environment **20**(1): 152-156.

Yoo, K. S., H. S. Choi, D. W. Jun, H. L. Lee, O. Y. Lee, B. C. Yoon, K. G. Lee, S. S. Paik, Y. S. Kim and J. Lee (2016). "MUC Expression in Gallbladder Epithelial Tissues in Cholesterol-Associated Gallbladder Disease." Gut Liver **10**(5): 851-858.

Yoon, H. S., C. H. Cho, M. S. Yun, S. J. Jang, H. J. You, J.-h. Kim, D. Han, K. H. Cha, S. H. Moon, K. Lee, Y.-J. Kim, S.-J. Lee, T.-W. Nam and G. Ko (2021). "Akkermansia muciniphila secretes a glucagon-like peptide-1-inducing protein that improves glucose homeostasis and ameliorates metabolic disease in mice." Nature Microbiology **6**(5): 563-573.

Ze, X., S. H. Duncan, P. Louis and H. J. Flint (2012). "*Ruminococcus bromii* is a keystone species for the degradation of resistant starch in the human colon." ISME J **6**(8): 1535.

Zeidan, A. A., V. K. Poulsen, T. Janzen, P. Buldo, P. M. F. Derkx, G. Oregaard and A. R. Neves (2017). "Polysaccharide production by lactic acid bacteria: from genes to industrial applications." FEMS Microbiol Rev **41**(Supp_1): S168-S200.

Zhai, R., X. Xue, L. Zhang, X. Yang, L. Zhao and C. Zhang (2019). "Strain-Specific Anti-inflammatory Properties of Two Akkermansia muciniphila Strains on Chronic Colitis in Mice." Front Cell Infect Microbiol **9**: 239.

Zhang, J., K. Kobert, T. Flouri and A. Stamatakis (2013). "PEAR: a fast and accurate Illumina Paired-End reAd mergeR." Bioinformatics **30**(5): 614-620.

Zhang, X., D. Shen, Z. Fang, Z. Jie, X. Qiu, C. Zhang, Y. Chen and L. Ji (2013). "Human gut microbiota changes reveal the progression of glucose intolerance." PLoS One **8**(8): e71108.

Zhang, Z., J. Geng, X. Tang, H. Fan, J. Xu, X. Wen, Z. S. Ma and P. Shi (2014). "Spatial heterogeneity and co-occurrence patterns of human mucosal-associated intestinal microbiota." ISME J **8**(4): 881-893.

Zhong, D., R. Brower-Sinning, B. Firek and M. J. Morowitz (2014). "Acute appendicitis in children is associated with an abundance of bacteria from the phylum Fusobacteria." J Pediatr Surg **49**(3): 441-446.

Zhong, H., H. Ren, Y. Lu, C. Fang, G. Hou, Z. Yang, B. Chen, F. Yang, Y. Zhao, Z. Shi, B. Zhou, J. Wu, H. Zou, J. Zi, J. Chen, X. Bao, Y. Hu, Y. Gao, J. Zhang, X. Xu, Y. Hou, H. Yang, J. Wang, S. Liu, H. Jia, L. Madsen, S. Brix, K. Kristiansen, F. Liu and J. Li (2019). "Distinct gut metagenomics and metaproteomics signatures in prediabetics and treatment-naive type 2 diabetics." EBioMedicine **47**: 373-383.

Zhou, J. and D. Ning (2017). "Stochastic community assembly: does it matter in microbial ecology?" Microbiol. Mol. Biol. Rev. **81**(4): e00002-00017.

Zhou, X., T. Hong, Q. Yu, S. Nie, D. Gong, T. Xiong and M. Xie (2017). "Exopolysaccharides from Lactobacillus plantarum NCU116 induce c-Jun dependent Fas/Fasl-mediated apoptosis via TLR2 in mouse intestinal epithelial cancer cells." Sci Rep **7**(1): 14247.

Zisu, B. and N. P. Shah (2003). "Effects of pH, temperature, supplementation with whey protein concentrate, and adjunct cultures on the production of exopolysaccharides by Streptococcus thermophilus 1275." J Dairy Sci **86**(11): 3405-3415.

Zivkovic, A. M., J. B. German, C. B. Lebrilla and D. A. Mills (2011). "Human milk glycobiome and its impact on the infant gastrointestinal microbiota." Proc Natl Acad Sci U S A **108 Suppl 1**: 4653-4658.

Zoetendal, E. G., J. Raes, B. van den Bogert, M. Arumugam, C. C. Booijink, F. J. Troost, P. Bork, M. Wels, W. M. de Vos and M. Kleerebezem (2012). "The human small intestinal microbiota is driven by rapid uptake and conversion of simple carbohydrates." ISME J **6**(7): 1415-1426.

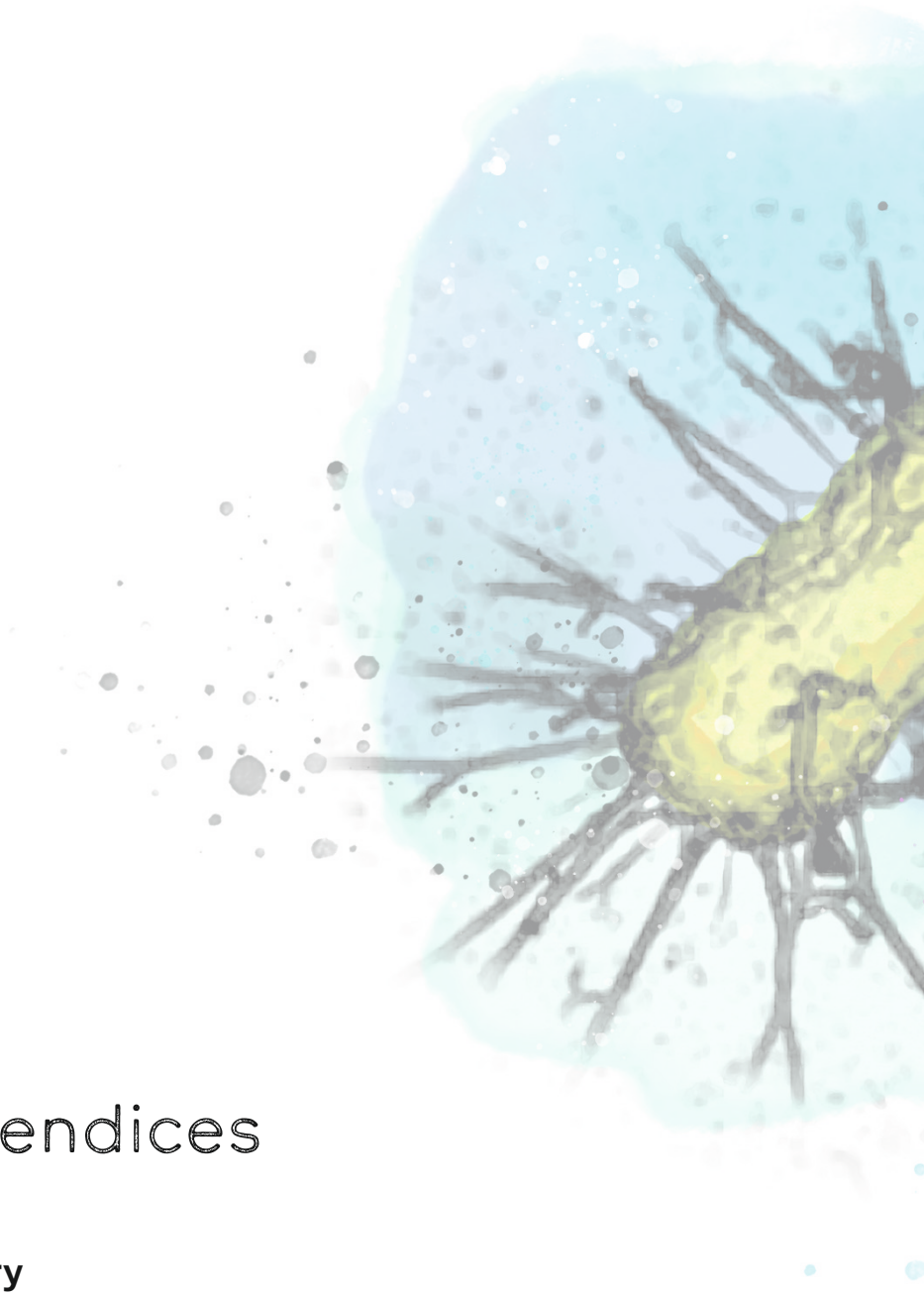

Appendices

Summary

A. muciniphila is a fascinating member of the gut microbiota, which has received considerable attention since its isolation in 2004 due to its mechanisms of action to improve host health. Not only is the abundance of this bacterium inversely correlated to several disease states, *A. muciniphila* administration in mice and humans also demonstrated its positive effects on host health. A. *muciniphila* was first described to reside in the mucus layer of the large intestine. We explored the presence of *Akkermansia*-like spp. in the human body, based on their 16S rRNA sequence and metagenomic signatures, to understand their colonization pattern in time and space. The presence of *Akkermansia*-like sequences (including Verrucomicrobia phylum and/or *Akkermansia* spp. sequences found in the literature) was detected in several locations apart from the colon, including the oral cavity, human milk, the pancreas, the biliary system, the small intestine, and the appendix. In this review we propose hypothetical functions of *A. muciniphila* in these anatomical sites.

Next to humans, *Akkermansia* spp. were suggested to be widely spread in the gut throughout the animal kingdom which may be indicating co-evolution with its host. Therefore, we studied the presence and genomic divergence of Verrucomicrobia and *Akkermansia* spp. within different mammalian hosts. We detected *A. muciniphila*-like bacteria in the gut of animals belonging to 15 out of 16 mammalian orders and isolated 10 new *A. muciniphila* strains from the feces of chimpanzee, siamang, mouse, pig, reindeer, horse and elephant. Low genomic divergence and considerable conservation of mucin degradation genes was observed among the new strains and the type strain *A. muciniphila* Muc^T. This may indicate that *A. muciniphila* favors mucosal colonization independent of the differences in hosts.

For human interventions with *A. muciniphila* cells, industrial-scale fermentations are needed and hence the used cultivation media should be free of animal-derived components, food-grade, non-allergenic and allow for efficient growth to high densities. The growth of *A. muciniphila* on a newly developed food-grade and plant-based medium supplemented with different ratios of GlcNAc and glucose was compared to its growth on mucin-containing medium, using a multi-omics approach. Comparison between growth on medium supplemented with GlcNAc and glucose in different ratios and mucin revealed differences in the expression of glycosyltransferases, signaling proteins and genes involved in stress-response. Our data suggests that the food-grade medium composition described here could be used to produce *A. muciniphila* in high yields for therapeutic purposes.

The cultivation of *A. muciniphila* in food-grade medium indicated exopolysaccharide production by this bacterium. An increasing interest has been observed for EPS produced by beneficial microbes. Revealing information regarding the structure of EPS may lead to uncovering mechanisms involved in microbe-microbe and host-microbe interactions and its therapeutic and food applications. Bioinformatic analysis led to the identification of a complete and partly inducible EPS production pathway in *A. muciniphila*. Our results indicate that that a higher GlcNAc concentration in the medium results in an increased production of EPS. Further characterization showed that the main monosaccharides present in *A. muciniphila* EPS are fucose, galactose, glucose and N-Acetylglucosamine (GlcNAc). In addition, the production of sialic acids was detected in medium supplemented with glucose and GlcNAc. In conclusion, these results indicate that *A. muciniphila* may produce EPS using the Wzx/Wzy-dependent pathway in variable amounts depending on the culturing conditions that are used.

The high complexity of the gut microbiome poses a major challenge for unravelling the metabolic interactions and trophic roles of key microbes. We assembled a synthetic gut microbiota community in bioreactors consisting of 16 different species including *A. muciniphila*. We aimed to investigate microbe-microbe interactions in this synthetic community. The bioreactors were continuously supplied with mucus, while a mixture of dietary fibers was added three times a day to mimic a dietary regimen. The synthetic community showed resistance and resilience to temporal perturbations. Furthermore, four trophic guilds were identified, driven by nutrient availability. *A. muciniphila* was one of the most abundant species in this synthetic community.

Generally, the functions of *A. muciniphila* are studied by using many different *in vitro* and *in vivo* approaches. Therefore, transcriptional landscape of *A. muciniphila* in different environmental conditions was studied. The environmental conditions included complexity of the community, diet, medium composition, and experimental design. We assessed the key functions of *A. muciniphila* throughout these environmental conditions, focusing on mucus degradation, pili production and EPS production. Even though the overall transcriptional response was altered under different environmental conditions, the key functions of *A. muciniphila* were stable throughout different ecosystems and were independent of environmental conditions.

To conclude, in this thesis we assessed the presence and functions of *A. muciniphila* throughout the human body and different mammalian hosts, not only showing the stable role of this mucin-degrading bacterium in different mammalian hosts, independent of host physiology, but also suggesting that *A. muciniphila* may play a role in other parts of the human gastrointestinal tract besides the colon. Furthermore, we have identified a novel physiological characteristic, namely the production of fuc-

EPS by *A. muciniphila*. In addition, the set-up of a 16-species synthetic community in fermentors revealed the ability of *A. muciniphila* to survive in a complex in vitro ecosystem, relying on mucin-utilization pathways, where it was found to be one of the two most abundant species in the community. Lastly, a comparison between the different models used to study *A. muciniphila* showed the main function of this bacterium remain stable in different ecosystems. Future research should focus on elucidating the mechanisms behind the health effects of *A. muciniphila* in different forms and its components, including live and pasteurized cells, extracellular vesicles and fuc-EPS. In addition, being able to genetically modify *A. muciniphila* can help elucidate the mechanism behind important functions (e.g. mucus degradation, EPS production, pili production and adaptation to stress factors in the human gut) via deletions or overexpression of genes involved in these processes. Altogether, this information may be useful for future therapeutic use of *A. muciniphila*.

Co-author affiliations

Clara Belzer
Laboratory of Microbiology, Wageningen University & Research, Wageningen, The Netherlands

Willem M. de Vos
Laboratory of Microbiology, Wageningen University & Research, Wageningen, The Netherlands
Human Microbiome Research Program, Faculty of Medicine, University of Helsinki, Helsinki, Finland

Mark C.M. van Loosdrecht
Department of Biotechnology, Delft University of Technology, Delft, the Netherlands

Bärbel Stecher
Max von Pettenkofer Institute of Hygiene and Medical Microbiology, Faculty of Medicine, LMU Munich, Germany

Bart Nijsse
Laboratory of Systems and Synthetic Biology, Wageningen University & Research, Wageningen, The Netherlands

Hauke Smidt
Laboratory of Microbiology, Wageningen University & Research, Wageningen, The Netherlands

Henk Schols
Laboratory of Food Chemistry, Wageningen University & Research, Wageningen, The Netherlands

Ioannis Kostopoulos
Laboratory of Microbiology, Wageningen University & Research, Wageningen, The Netherlands
Danone Nutricia Research, Utrecht, The Netherlands

Jan Knol
Laboratory of Microbiology, Wageningen University & Research, Wageningen, The Netherlands
Danone Nutricia Research, Utrecht, The Netherlands.

Janneke P. Ouwerkerk
Laboratory of Microbiology, Wageningen University & Research, Wageningen, The Netherlands

Jarmo Ritari
Finnish Red Cross Blood Service, Helsinki, Finland

Jasper J. Koehorst
Laboratory of Systems and Synthetic Biology, Wageningen University & Research, Wageningen, The Netherlands

Kees van der Ark
Laboratory of Microbiology, Wageningen University & Research, Wageningen, The Netherlands
Centre of Infectious Disease Control, National Institute for Public Health and the Environment (RIVM), Bilthoven, the Netherlands

Lars Paulin
Institute of Biotechnology, University of Helsinki, Helsinki, Finland

Madelon Logtenberg
Laboratory of Food Chemistry, Wageningen University & Research, Wageningen, The Netherlands

Maria-Carolina Rodriguez-Daza
Laboratory of Microbiology, Wageningen University & Research, Wageningen, The Netherlands

Martin Pabst
Department of Biotechnology, Delft University of Technology, Delft, the Netherlands

Peter J. Schaap
Laboratory of Systems and Synthetic Biology, Wageningen University & Research, Wageningen, The Netherlands

Sjef Boeren
Laboratory of Biochemistry, Wageningen University & Research, Wageningen, The Netherlands

Steven Aalvink
Laboratory of Microbiology, Wageningen University & Research, Wageningen, The Netherlands

Sudarshan A. Shetty
Laboratory of Microbiology, Wageningen University & Research, Wageningen, The Netherlands
University Medical Center Groningen, Groningen, The Netherlands.

Yuemei Lin
Department of Biotechnology, Delft University of Technology, Delft, the Netherlands

Acknowledgements

They say it takes a village to raise a child, and I would argue it takes a village to raise a PhD candidate. Through my years in this PhD I have been through many challenges. I could not have done this without the help and support of many people. Therefore, I would like to acknowledge everyone that has helped me on this journey.

Clara, first of all I want to thank you for giving me the opportunity to do my MSc thesis, minor thesis and then also a PhD in your group. I really appreciate the scientific discussions we have had over the years to lift the projects to the next level. This has especially helped me to improve as a scientist, and will definitely continue to help me in my future career. Your door was always open for both work related and unrelated topics and you have always been very supportive over the years. I really enjoyed working with you and could not have asked for better guidance during my PhD journey! **Willem,** thank you for giving me the opportunity to work on this project. Your efficient way of working and fast responses to all of my questions helped me to be able to continue my projects rapidly. The discussions we had and the feedback you have given me on the projects have improved the work significantly and have also helped me see things from different perspectives. **Mark,** thank you for giving me the opportunity to work on this project. I appreciate the fruitful collaborations that resulted from our meetings in Delft and your input in my PhD projects.

Members of the thesis committee, thank you for taking the time to evaluate my thesis and for your critical assessment.

Hauke, Erwin and Detmer, I've enjoyed the discussions we've had about my projects in MolEco meetings. **Hauke**, thank you for your input and collaboration on one of the chapters. It was a pleasure working with you. I would also like to thank the chair of MIB, **Thijs Ettema**, thank you for your support, you made sure your door was always open for everyone.

I would like to thank the technicians of MIB: **Ineke, Hans, Ton, Iame, Laura, Rob, Philippe, Merlijn and Tom** and **Steven** who is now lab manager. All of you have helped me on many occasions during my PhD. **Steven**, we have had many brainstorming sessions over the years with which you helped me greatly in setting up experiments in the lab for different projects. In addition, I really enjoyed working together with you on our EV project! **Ineke** you were always available for questions, giving explanations and nice small talk while working in the lab. **Laura** it was always fun working in the lab at the same time. **Phillippe,** your advices in teaching during the first year definitely

helped me improve my teaching skills in a fun way. **Anja and Heidi,** thank you for your help with the questions I had throughout the years.

I also want to thank my MSc thesis supervisor and minor thesis supervisors **LooWee, Kees** and **Yifan**. Working with you during both thesis periods helped me realize the great interest I have for studying gut bacteria. Working together with you, getting your advices, instructions, support, and your confidence in my work abilities played a big role my decision to try to obtain a PhD position in the MolEco group.

Next, I would like to thank the master students that have worked with me on different projects. I enjoyed working with all of you and, at the same time also learned a lot from working with you. **Mathieu**, you were the first student I supervised shortly after I started my PhD and it has taught me a lot. You are very creative and persistent, and that really showed during your MSc thesis. **Floriane**, you are a very hard-working and kind person. You worked on two projects, for both me and Carrie and put a lot of effort and dedication in both projects, wanting to learn as much as possible and while also being willing to help with other laboratory experiments. **David**, you are a very smart and hard-working person. During your project you were very dedicated, came with many new ideas and you were actively asking for feedback to continuously improve yourself. Even though the project you were working on did not become a chapter, your work still had a great impact on my thesis.

Furthermore, it was my pleasure to be a part of the SIAM council together with **Melvin**, **Nicolas** and **Jeroen**. It was a lot of fun to organize and be part of the SIAM events with you, from career events to team-building days in Texel!

PhD survivors - **Belèn, Enrique, Jannie, Joep, Carrie, Janneke, Max, Patrick, Thijs, Catarina, Isma** and **Ivette** – thank you for all the lunches, Thursday Fries and talks that have made our PhD time a lot of fun! **Carrie,** whether we were playing videogames, watching movies or having dinners with Isma and Mathijs, it was always nice to hang out with you. You have helped me on numerous occasions. Not only with work related matters but you also helped me improve on a personal level with your advice and knowledge. I value our friendship a lot and I hope we will continue to be friends far beyond our PhD journeys. **Jannie**, we have shared many moments together already starting from our MSc thesis at MolEco continuing into our PhDs. I enjoyed the activities we did together during this time –going to parties, Christmas shopping, dinners and many coffee breaks to catch up! These times spend together were an important contribution to my time in Wageningen, and I'm very glad to have been able to share this journey with you. **Patrick**, I appreciate your recommendations in horror movies (which were always very good), I enjoyed our talks about the videogames we

were playing or should be playing and of course also our work-related discussions. You are a very kind and hardworking person, but you are also always there to help and answer all of my questions. Thank you for everything! **Janneke**, we met already during our master thesis and I was very happy when you told me you would also continue with a PhD in the Laboratory of Microbiology. You are very thoughtful and kind, writing nice wishes and leaving small gifts on my desk. I always enjoyed talking to you about work-related and personal topics, and was very excited to start a project together with you for our PhDs. Unfortunately, it is not a part of my thesis, but let's continue to work on this and have it ready for yours! **Ivette** and **Enrique**, thank you for all the fun times during parties, Spanish lessons and talks whenever we would run into each other in the hallways of Helix.

I feel very lucky having been part of office 5034, now 6029, with you **Marina, Maryse, Chen, Tatsuro, Marjet, Hikma, Taojun and Valentina**. Our many office dinners, karaoke sessions, coffee breaks and talks in the office have been very nice! And of course let's not forget our yearly office Christmas cards! I hope you will keep our office traditions alive for the next generations to come! A special thanks to **Taojun** – it was nice to start our PhD adventure on the same day in office 5034. We have shared many fun moments in the office and you were always there to help. I also appreciate our shared interest in food, and your recommendations in trying spicy Chinese snacks that you then even ordered for me! **Maryse**, we met later on but have had many fun and long talks in the office since then. I wish you all the best! **Tatsuro**, it was fun to have you in the office while you were in Wageningen for your post-doc. I enjoyed talking with you, having work-related discussions about *Akkermansia* as well as discussing the anime shows we were watching at the time. **Chen**, thank you for always being kind, checking in on everyone and often bringing snacks to the office or organizing a tea tasting after dinner. **Marjet**, you may not have been working in the office for the entire duration of my PhD, but you never really left! Thank you for keeping in touch and staying part of the office dinners and karaoke sessions! **Hikma**, thank you for all the advices early on in my PhD and the fun we've had in the office! **Valentina**, it was very nice to have you join the office and have talks about our dogs!

Breakfast club – **Clara, Diana, Jannie, Carrie, Nancy, Maryse, Kate, Prokopis, Kelly, Anna, Sofie and Patrick** – thank you for all the Friday morning and Monday morning breakfasts, while discussing a variety of (science-related) topics to catch up with the whole group.

Of course there are more people that have been a part of this journey over the years. **Kate**, thank you for the nice chats we've had and for the productive discussions about *Akkermansia*. **Hanne**, your input and discussions on *Akkermansia* projects has helped

me a lot. I also want to thank you for all the fun times we have had in (online) coffee breaks and dinners. I'm happy to have had you as my colleague! Lastly, thank you for taking the SEM picture of *Akkermansia muciniphila*, together with **Steven**, that was now used as the basis for my PhD thesis cover. **Nikolas**, thank you for the late night coffee breaks early on in my PhD, teaching me how to play heroes of the storm and of course also for the work-related discussions we've had in which you have helped me a lot to get started with my project. **Wasin**, I got to know you more during the PhD trip, thank you for the fun times and the nice talks after we got back! **Ran**, thank you for your kindness throughout the years and it was a lot of fun to prepare the proteomics samples with you. **Diana and Raymond**, thank you for supervising the PhD trip to Boston and New York, it was very nice to get to know you more. Also, **Martha, Costas, Nancy, Prokopis, Zhuang, Yangwenshan, Marie-Luise, Annelies, Emmy, Hugo, Caifang, Despoina, Lyon, Maria, Felix, Gerben** and probably many more colleagues of MIB, thank you for your support and being a part of my PhD journey.

Now I would like to thank everyone I have collaborated with throughout the chapters in my thesis. **Giannis**, I'm happy to have collaborated on so many projects for our PhDs. I really enjoyed working with you, it always went smoothly and I have learned a lot from you during this process. We managed to do many experiments in the lab for our projects, while also having fun. You are very kind and always there to help out when I would come to you for advice. You have contributed greatly to my thesis and I'm very glad to have shared this adventure with you. I wish you all the best for the future! **Janneke O.**, thank you for the great collaboration on our project in chapter 3, I enjoyed working with you. **Sudarshan**, I have learned a lot from you and our collaboration working on the synthetic minimal microbiome. Your creativity in terms of data analysis and experiment ideas have greatly impacted our paper. **Carolina**, you started working in MolEco towards the end of my PhD, but helped me greatly with chapter 5. Thank you for performing the viscosity measurements and for having discussions with me to improve the manuscript further. **Yuemei,** your input and FTIR analysis were very valuable. Thank you for thinking along with the project and the many meetings we have had about the results. **Martin**, thank you for your input on the proteomics data analysis. **Bart**, I value the effort you have made to process the raw transcriptome data and set up an initial R script to start analysing the data for multiple chapters of my PhD thesis. Furthermore, you have helped me tremendously by answering all of my questions about further transcriptome data analysis. **Jasper**, thank you for your input in the bioinformatics analysis, your explanations of the process and your help in the final stages of submitting the manuscript in chapter 3. **Henk and Madelon**, thank you for your input in the monosaccharide analysis. Your expertise on this analysis and effort into optimizing the methods for the EPS isolates and data analysis have resulted in a great contribution to chapter 5. **Sjef**, thank you

for teaching me the ropes of the proteomics sample preparation and performing the proteome analysis of my samples for chapter 4 and 5. **Daan and Menia**, thank you for your insight and expertise in phylogenetic analysis. You have helped me a lot with answering all of my questions when I first started conducting phylogenetic analysis. This information has been valuable for multiple projects within my PhD.

Next, I would like to thank my paranymphs, Marina and Manouk, who have both been by my side during my PhD and showed me tremendous support.

Marina – My dear paranymph – I am so happy to have had you on my side these past years. Your kindness, support and of course all the funny moments we've shared at work and outside have made my time during the PhD even better! Already since the first day you arrived to Wageningen to start your PhD, we got along super well. We started talking a lot in the office (sometimes even a bit too much for our other officemates), meeting for coffee, planning dinners and more. You are such a good friend and made sure that I know I can come to you for advice or help with anything! I'm confident we will keep being friends for a very long time. It's my honor to have you as my paranymph.

Manouk – My dear paranymph – We met each other during our bachelor in Forensic Laboratory Science. In the first year we were placed together in a project, since then we have been inseparable for the rest of the time in our bachelor. I am happy that we have continued to stay such close friends, if not even closer, now years after our bachelor studies ended and for many years to come. Whether we plan trips to Pinkpop, weekends away, holidays or just visit each other at home, I always have the best time with you, full of laughter, good conversations and of course wine. I'm so happy to have you in my life. Thank you for all your help, advices, sweet messages, your enthusiasm and also your directness. It's my honor to have you as my paranymph.

Next to my colleagues, friends I met at work and my paranymphs, I would like to thank my friends and family who have been part of this journey with me.

Room 21 – **Kruno, Petra, Inga, Dunja, Pedro, Marieke, Monika, Matija** and **Dusan** I had an amazing time teaching in the Summer School of Science with all of you. We've kept in touch since then with reunions, some of your PhD defenses and of course the updates and jokes in the Room 21 WhatsApp group. Meeting with you is always a lot of fun and I hope we will keep in touch for many more years to come. Thank you all for your support and PhD-related advice these last years!

Loly y **Manolo**, ¡gracias por vuestro apoyo! Disfruto mucho pasando tiempo con vosotros, mejorando poco a poco mi español, aprendiendo a jugar a juegos como el Rummikub o el Remigio, y por supuesto aprendiendo a cocinar todos los platos típicos españoles. Siempre me habéis hecho sentir bienvenida y sois los suegros más atentos que hubiese podido pedir. **Silvia, Vanessa, Javi** y **Jose**, gracias a todos por los buenos momentos que hemos compartido en España, desde esos domingos de paella, pasando por las vacaciones en familia y hasta esas fiestas de cumpleaños sorpresa. Me habéis hecho sentir parte de la familia desde el primer momento.

Hans, dankjewel voor al je steun de afgelopen jaren. Je hebt me door stressvolle periodes heen geholpen en staat altijd voor me klaar. Het is altijd gezellig om met je af te spreken en onze passie voor lekker eten te delen! **Jeroen**, dankjewel voor alle leuke weekendjes en in het bijzonder natuurlijk alle Harry Potter activiteiten die we samen hebben gedaan. Je brengt altijd positieve energie met je mee en maakt me vaak aan het lachen, dankjewel! **Oma**, je hebt me tijdens mijn hele PhD tijd gesteund, maar kan nu helaas niet meer bij het laatste deel aanwezig zijn. Dankjewel oma, voor al je lieve woorden, dat je me altijd liet weten hoe trots je op me bent en dat je deur altijd voor me open stond. **Papa**, ondanks dat je mijn PhD tijd niet meer mee hebt kunnen maken, heb ik alles wat je me hebt geleerd meegenomen, zoals je advies om een stapje terug te doen wanneer ik gestrest of gefrustreerd raakte, even een pauze te nemen en het later nog eens te proberen (wat je me vaak hebt moeten vertellen). Ik mis je, maar weet dat je toch dichtbij bent en trots zou zijn, zoals je altijd was. **Mama**, je hebt me op deze wereld gezet en hebt sindsdien altijd in mij geloofd. Elke keer dat ik een nieuw doel had wat ik wilde bereiken was jij daar om me te vertellen dat ik het kan. Dankjewel voor alle momenten waarin je mij hebt aangemoedigd terwijl ik zelf twijfelde of het me ging lukken. Dit heeft me enorm geholpen om mijn doelen te bereiken. **Alicia**, jouw energie, grapjes en vrolijkheid zorgen altijd voor veel leuke momenten om zelfs de meest stressvolle periodes wat minder stressvol te maken. **Mandy**, dankjewel dat je er altijd voor me bent. Wij delen alles met elkaar, de goede en de minder goede momenten. We doen altijd veel leuke dingen samen, waaronder de weekendjes die we samen doorbrachten om te relaxen, series te kijken, te gamen en nieuwe recepten uit te proberen. Je ben ook altijd bereidt om gezellig te kletsen of om mijn verhalen aan te horen wanneer ik gestrest ben en advies te geven om me weer verder te helpen. Het maakt me heel blij om te zien dat je nu je eigen dromen achterna gaat en je eigen bedrijf hebt opgezet. Ik ben super trots op je en ik weet zeker dat het een groot succes wordt! **Tiffany**, ondanks dat je ver weg woont voelt het voor mij altijd alsof je heel dichtbij bent. Ik vind het superfijn om tijd door te brengen bij jou thuis, natuurlijk ook met **Claudio**, **Giordano** en **Mikey**! Als we samen zijn hebben we de grootste lol en langste lachbuien. Maar ook als we niet samen zijn en dezelfde series kijken terwijl we elkaar spraakberichtjes sturen. Bovenal, dankjewel dat je altijd

voor me klaar staat! Ik wil ook mijn **oma**, al mijn **ooms** en **tantes**, en mijn **neven** en **nichten** bedanken voor jullie steun, alle fijne gesprekken die we hebben gehad en jullie interesse in mijn projecten.

Ismael, thank you for being my rock ever since we have been together and for your unconditional love and support. One of the things I love most about our relationship is that we always manage to make each other laugh. I feel very lucky to have met you when I did, right before you were actually about to leave the Netherlands. Thank you for joining me in this PhD journey, always offering a helping hand, taking the time to talk and even to have brainstorm sessions about my projects when I needed a different perspective. I have learned a lot from you on work-related topics, but you especially helped me grow as a person. You have played a big role in helping me get out of my shell with your patience, kindness and caring and I can't thank you enough for this. I am looking forward to spend many more years together with you, while not being so occupied anymore with my PhD, in which we can focus even more on making great memories. I love you.

About the author

Sharon Yvonne Geerlings was born on the 4th of May 1994 in Vianen (Utrecht), the Netherlands. Sharon was raised in Vianen and obtained her HAVO-degree at Cals College Nieuwegein, after which she continued studying her bachelor in Biology and Medical Laboratory Research with a major in Forensic Laboratory Research at Avans University of Applied Sciences. During her bachelor, Sharon obtained an internship at KWR where she worked on the development of qPCR methods to detect fecal contamination in recreational lakes, under the supervision of Leo Heijnen and Bart Wullings. Her second bachelor internship took place at Alterra at Wageningen University and Research. At Alterra she worked on the development of environmental DNA markers for the detection of fish species under the supervision of dr. Arjen de Groot. Here, she decided to obtain a MSc degree in Biotechnology at Wageningen University and Research. During her Masters, she got fascinated by research concerning the human gut microbiota. Therefore, she performed her MSc thesis at the Laboratory of Microbiology of Wageningen University and Research where she investigated a co-occurrence model of infant-associated bifidobacteria under the supervision of dr. LooWee Chia and dr. Clara Belzer. Then, Sharon had the opportunity to stay for her minor thesis, where she worked on the transformation of *Akkermansia muciniphila* under the supervision of dr. Kees van der Ark, dr. Yifan Zhu and dr. Clara Belzer. After finishing her master in Biotechnology, Sharon started her PhD in 2017 at the Laboratory of Microbiology under the supervision of dr. Clara Belzer, prof. Willem M. de Vos and prof. Mark C.M. van Loosdrecht. During her PhD she studied several aspects of next-generation therapeutic microbe *Akkermansia muciniphila*, as described in this thesis. Currently, Sharon works as a postdoctoral researcher at the Laboratory of Microbiology.

List of publications

Ottman, N., **Geerlings, S. Y**., Aalvink, S., de Vos, W. M., & Belzer, C. (2017). Action and function of *Akkermansia muciniphila* in microbiome ecology, health and disease. Best practice & research Clinical gastroenterology, 31(6), 637-642.

Geerlings, S. Y., Kostopoulos, I., De Vos, W. M., & Belzer, C. (2018). *Akkermansia muciniphila* in the human gastrointestinal tract: when, where, and how? Microorganisms, 6(3), 75.

Wegh, C. A., **Geerlings, S. Y**., Knol, J., Roeselers, G., & Belzer, C. (2019). Postbiotics and their potential applications in early life nutrition and beyond. International journal of molecular sciences, 20(19), 4673.

Hagi, T., **Geerlings, S. Y.**, Nijsse, B., & Belzer, C. (2020). The effect of bile acids on the growth and global gene expression profiles in *Akkermansia muciniphila*. Applied microbiology and biotechnology, 104(24), 10641-10653.

Geerlings, S. Y.*, Ouwerkerk, J. P.*, Koehorst, J. J., Ritari, J., Aalvink, S., Stecher, B., ... & Belzer, C. (2021). Genomic convergence between *Akkermansia muciniphila* in different mammalian hosts. BMC microbiology, 21(1), 1-13.

Shetty, S. A.*, Kostopoulos, I.*, **Geerlings, S. Y.***, Smidt, H., de Vos, W. M., & Belzer, C. (2022). Dynamic metabolic interactions and trophic roles of human gut microbes identified using a minimal microbiome exhibiting ecological properties. The ISME journal, 16(9), 2144-2159.

Overview of completed training activities

Discipline specific activities	Organizing institute	Year
Microbiology centennial symposium	WUR	2017
Gut day	WUR	2018
SIAM symposium	SIAM	2018
KNVM fall meeting	KNVM	2018
SIAM summer retreat	SIAM	2018
KNVM spring meeting	KNVM	2019
SIAM symposium	SIAM	2019
Intestinal Microbiome in Humans and Animals	VLAG	2019
SIAM symposium	SIAM	2021
Microbiome Interactions in Health and Disease	Wellcome Genome Campus	2021

General courses	Organizing institute	Year
PhD week	VLAG	2018
Research data management	WGS	2018
How to keep the editor happy	VLAG	2018
PhD workshop carousel	WGS	2018
Scientific publishing	WGS	2018
Illustrator for scientists	MIB	2018
Reviewing a scientific paper	WGS	2018
Applied statistics	VLAG	2020
Scientific writing	WGS	2020

Other activities	Organizing institute	Year
Preparation of research proposal	VLAG	2017
Workgroup meetings MolEco	MIB	2017-2022
Journal club	MIB	2018
AIO/Postdoc meeting	MIB	2017-2022
SIAM council	SIAM	2017-2019
SIAM meeting	MIB	2017-2021
PhD Trip	MIB	2019

Colophon
The research described in this thesis was financially supported by the Soehngen Institute of Anaerobic Microbiology.
Financial support from the Laboratory of Microbiology, Wageningen University, for printing this thesis is gratefully acknowledged.

Cover design and layout by Erwin Timmerman, persoonlijkproefschrift.nl
Printed by Ridderprint, The Netherlands